

A microscopic image showing a dense field of cells, likely from a tissue sample, with numerous cells exhibiting bright red fluorescence. The background is dark, making the red-stained cells stand out prominently. The overall appearance is that of a complex, interconnected network of cells.

# **Radiotherapy-induced oral mucositis**

**The host-microbe interactions come into play**

**Tine De Ryck**

**Nothing in life is to be feared,  
it is only to be understood.**

Marie Curie

ISBN: 978-94-6197-286-6

Printed by University press, Zelzate, Belgium

Copyright ©: Tine De Ryck, Department of Radiotherapy and Experimental Cancer Research, Faculty of Medicine and health sciences, 2015. All rights reserved. No part of the dissertation may be reproduced in any form by print, photoprint, microfilm or any other means without written permission from the copyright holder.

The research reported in this dissertation was funded by the Research Foundation-Flanders (FWO Vlaanderen – G.0712.10 N)



Faculty of Medicine and Health Sciences  
2015

# Radiotherapy-induced oral mucositis

## The host-microbe interactions come into play

**Ir. Tine De Ryck**

Dissertation submitted in accordance with the requirements for the degree of Doctor  
in Medical Sciences



**Supervisors**

Prof. Dr. Marc Bracke

*Ghent University*

Prof. Dr. Ir. Tom Van de Wiele

*Ghent University*

Dr. Barbara Vanhoecke

*Ghent University*

**President of the Examination Committee**

Prof. Dr. Ir. Carlos De Wagter

*Ghent University*

**Members of the Reading Committee**

Prof. Dr. Mark De Ridder

*VUB/UZ Brussels*

Prof. Dr. Sarah Baatout

*SCK-CEN/ Ghent University*

Prof. Dr. Tom Coenye

*Ghent University*

Prof. Dr. Geert Claeys

*Ghent University Hospital*

**Remaining members of the Examination Committee**

Dr. Frédéric Duprez

*Ghent University Hospital*

Dr. Peter Vanhoenacker

*ActoGenix NV*

# CONTENTS

---

<b>Woord vooraf</b>	<b>III</b>
<b>Samenvatting</b>	<b>VII</b>
<b>Summary</b>	<b>IX</b>
<b>Abbreviations</b>	<b>XI</b>
<b>1. Introduction</b>	<b>1</b>
1.1. <i>Oral mucositis</i>	1
1.2. <i>Pathobiology of mucositis</i>	2
1.3. <i>The potential role of microbiota in the pathobiology of oral mucositis</i>	3
1.4. <i>Treatment strategies</i>	14
1.5. <i>Microbe – epithelial interactions: no need for physical contact</i>	15
1.6. <i>Research questions</i>	22
1.7. <i>Outline of the dissertation</i>	23
<b>2. Development of an oral mucosa model to study host-microbe interactions</b>	<b>25</b>
2.1. <i>Abstract</i>	25
2.2. <i>Introduction</i>	25
2.3. <i>Materials and methods</i>	27
2.4. <i>Results</i>	35
2.5. <i>Discussion</i>	45
<b>3. Microbial inhibition of oral epithelial wound healing</b>	<b>49</b>
3.1. <i>Abstract</i>	49
3.2. <i>Introduction</i>	49
3.3. <i>Material and methods</i>	51
3.4. <i>Results</i>	55
3.5. <i>Discussion</i>	63
<b>4. Irradiation affects the host-microbe crosstalk</b>	<b>67</b>
4.1. <i>Abstract</i>	67
4.2. <i>Introduction</i>	67
4.3. <i>Materials and methods</i>	68
4.4. <i>Results and discussion</i>	70
<b>5. Irradiation affects the functional behaviour of the oral microbiota</b>	<b>75</b>
5.1. <i>Abstract</i>	75
5.2. <i>Introduction</i>	75
5.3. <i>Materials and methods</i>	78
5.4. <i>Results</i>	81
5.5. <i>Discussion</i>	87

<b>6. Dynamic shifts in the oral microbiome during radiotherapy</b>	<b>91</b>
6.1. Abstract	91
6.2. Introduction	91
6.3. Patients, materials and methods	92
6.4. Results and discussion	95
6.5. Conclusion	99
<b>7. Microbial shifts in the context of radiotherapy-induced oral mucositis</b>	<b>101</b>
7.1. Abstract	101
7.2. Introduction	101
7.3. Patients, materials and methods	102
7.4. Results	104
7.5. Discussion	113
<b>8. E-cadherin as salivary biomarker of mucositis</b>	<b>117</b>
8.1. Abstract	117
8.2. Introduction	117
8.3. Patients, material and methods	118
8.4. Results and discussion	120
<b>9. E-cadherin as therapeutic target</b>	<b>125</b>
9.1. Abstract	125
9.2. Introduction	125
9.3. Material and methods	127
9.4. Results	130
9.5. Discussion	134
<b>10. General discussion</b>	<b>137</b>
10.1. Research objectives	137
10.2. Validation of the model in the context of radiotherapy-induced oral mucositis	140
10.3. Oral radiotherapy-induced mucositis: taking into account the oral microbiota	142
<b>11. General conclusion</b>	<b>145</b>
<b>References</b>	<b>147</b>
<b>Addendum 1</b>	<b>171</b>
A1.1. Material and methods	171
A1.2. Figures and tables	173
<b>Addendum 2</b>	<b>179</b>
A2.1. Figures and tables	180
<b>Curriculum Vitae</b>	<b>185</b>
<b>Scientific Curriculum Vitae</b>	<b>187</b>
Publications	187
Posters & presentations	188

## WOORD VOORAF

---

Juni 2015. Het boekje is af, het definitieve einde komt nu heel dichtbij... Tijd dus om even terug te blikken op een periode van hard werken met de onoverkomelijke ups-and-downs, maar zeker ook met vele fantastische momenten en ervaringen. Het zou nooit hetzelfde geweest zijn zonder de hulp van vele mensen, waarvan ik er hier enkele extra in de verf wil zetten.

Vooreerst wil ik mijn promotoren bedanken.

In het labo van Prof. Marc Bracke was ik welkom om mijn onderzoek uit te voeren. Ik kon steeds rekenen op zijn steun en blindelings vertrouwen in mijn werk.

Prof. Tom Van de Wiele zijn agenda is meestal goed gevuld, maar toch maakte hij steeds tijd om mijn resultaten te overlopen, te luisteren naar mijn problemen en oplossingen te zoeken waar nodig. Vooral de laatste jaren heb ik hier veel kracht uit geput!

Een dikke dank u wel gaat naar Dr. Barbara Vanhoecke. Zonder haar zou ik aan dit onderzoek niet gestart zijn. Ook al was ze letterlijk het verst van mij verwijderd, toch stond ze in mijn onderzoek vlak naast mij. Het eindeloos vertrouwen, de vele skype-gesprekken en mails toonden dat de wereld niet zo groot is als het op het eerste zicht lijkt.

Ik wil ook een woordje van dank richten aan alle leden van de lees- en examencommissie en aan alle co-auteurs en reviewers van mijn artikels voor hun feedback en leerrijke gesprekken.

Uiteraard wil ik ook alle mensen danken met wie ik de afgelopen jaren heb mogen samenwerken.

Het personeel van LabMET: ook al was ik maar af en toe in jullie labo's, ik voelde mij steeds welkom. Een extra likje verf voor iedereen van de HAM-cluster, Frederiek-Maarten, Jana, Tim en ex-LabMETter Charlotte.

Peter en Annemie van ActoGenix: tijdens onze verschillende fijne vergaderingen kon ik kennismaken met het onderzoeksleven binnen een bedrijf.

Alle dokters van OP7 met wie ik in contact kwam, met dan voornamelijk Prof. Boterberg voor het bestralen van mijn culturen en Dr. Duprez voor het aanbrengen van de nodige patiënten voor mijn studie.

Prof. Stevens, Bart, Dominic en Tom: ons verhaal begon reeds in mijn masterjaar en is ondertussen uitgegroeid tot een boek, waarin ik veel heb bijgeleerd en verplicht werd mijn focus breed te houden.

De thesisstudenten die ik onder mijn vleugels kreeg: Laura, Eline, Kevin, Dave, Michelle, Liselot, Eleanor en Karlijne. Ook al was het de bedoeling dat ik jullie dingen aanleerde, toch hebben jullie mij ook veel bijgebracht!

De voorbije vijf jaar zouden zeker niet hetzelfde geweest zijn zonder alle medewerkers van het LECR.

Het technisch personeel mag hierbij niet vergeten worden. Zij zorgden ervoor dat we steeds voldoende materiaal hadden om mee te werken. Extra dank voor Karlien, die mij begeleid heeft bij mijn eerste praktische stapjes in het labo en bij wie ik daarna ook steeds terecht kon.

Elly, Lynn, Glenn, Mieke, Liselot, Quentin en Stephanie wil ik bedanken voor de steun, de vele babbels (al dan niet wetenschappelijk) en de leuke sfeer binnen onze bureaumuren. Een pluim voor Glenn, die er met zijn Senseo-machine in slaagde mij de smaak van koffie te leren appreciëren tijdens mijn laatste schrijfmaanden. Ook een extra woordje van dank voor Lynn. Reeds als thesisstudenten zaten we in hetzelfde team. We hebben samen dan ook veel watertjes doorzwommen en zijn nu klaar voor een nieuwe start in het bedrijfsleven. Nog heel veel succes met de laatste loodjes en in de verdere toekomst!

Dorien en Zuza, ook al zaten we niet in dezelfde bureau, de afstand was gelukkig niet groot! Als TNF B vormden we ook een onklopbaar flow-team ;). Dziękuję bardzo za wszystko!

Maar de boog kon niet altijd gespannen staan. Bedankt aan iedereen die tijd maakte voor de TGIF-drinks, voor het opvrolijken van de kerstfeestjes en voor de verschillende activiteiten buiten de muren van het UZ. De hoofdprijs gaat hierbij naar Lore: onze citytrips waren onvergetelijk!

Voor de nodige ontspanning kon ik de voorbije jaren ook steeds terecht bij Nele, Caroline, Tara, Isabel, Nathalie VdB, Nathalie DZ, Madelena, Sofie, Iris, Kaat, Katrien, Ann, Nathalie VH, Sven en Joris.

Bij dringende nood aan beweging stonden Tori, Tessa, Lieve en Dirk ook altijd klaar om eens op een balletje te slaan. Bedankt!

And last, but not least, wil ik zeker mijn familie bedanken!

Tante Rita, voor de niet-aflatende steun in alles wat ik doe.

Leen, voor de belangrijkste en moeilijkste levenslessen die ik kon krijgen en die mij steeds helpen om, ook in moeilijke momenten, door te zetten met een glimlach.

Marijke en Wim, een dikke merci voor de steun, het begrip, de leuke ritten van en naar Gent en de hulp waar nodig.

Jasper en Linde om het kind in mij levend te houden en mij te verplichten mijn computer even aan de kant te schuiven.

Mama en papa, de dank voor jullie is niet in enkele woorden te vatten. Bedankt voor de steun, het vertrouwen, de vrijheid en om er steeds voor te zorgen dat ik echt kon thuiskomen!

Een zachte blik, een blij gelaat,  
een vriendelijk woord, een goede raad.

Al lijkt het simpel wat je schenkt,  
toch is het meer waard dan je denkt!

Bedankt!





## SAMENVATTING

---

Orale mucositis is een ontstekingsreactie van de orale mucosa die vaak optreedt ten gevolge van bestraling als behandeling voor hoofd- en halstumoren. Deze complicatie leidt tot een verlaagde levenskwaliteit van de patiënt, een verhoogde kans op hospitalisatie en in het ergste geval zelfs tot het stopzetten van de behandeling. De pathobiologie van mucositis is reeds uitvoerig besproken in de literatuur, maar de mogelijke rol van de bacteriën in deze aandoening werd nauwelijks beschouwd. Daarom ligt de focus in deze thesis op de microbe-gastheer interacties in de context van orale mucositis en werd de invloed van bestraling op de microbiële orale gemeenschap zowel *in vitro* als in een patiëntenstudie onderzocht.

Vooreerst werd een nieuw *in vitro* model ontwikkeld dat het mogelijk maakt om de microbe-epitheel interacties op te volgen gedurende minimaal 72 h. Met behulp van dit model werd een inhiberend effect aangetoond van de orale bacteriën ten opzichte van de epitheliale wondheling. Dit effect bleek species-afhankelijk, aangezien pure culturen van bijvoorbeeld *Klebsiella oxytoca*, een bacterie die voornamelijk teruggevonden wordt in de mondholte van patiënten met hoofd- en halstumoren na bestraling, de wondheling inhibeerden, terwijl bijvoorbeeld *Streptococcus oralis*, een veelvoorkomende orale bacterie, de wondheling stimuleerde. Verder onderzoek wees op een mogelijke rol van de *quorum sensing* moleculen in deze microbiële inhibitie van de wondheling, wat het belang aantoont van de inter-kingdom communicatie in het onderzoek van microbe-gastheer interacties.

Door bestraling van het model konden we vervolgens aantonen dat het inhiberend effect van de bacteriën op de epitheliale wondheling na bestraling voornamelijk bepaald wordt door de samenstelling van het microbiële inoculum, de bacteriën die gebruikt worden om het model op te starten. Sequenceringsanalyses wezen op lichte toenames in het aantal *Rothia*, *Granulicatella* and *Gemella* bacteriën na bestraling. Bovendien werd aangetoond dat bestraling van pure microbiële culturen kan resulteren in een verhoogde biofilmvorming en pathogeniciteit van de bacteriën.

Aangezien therapeutische bestralingsdosissen dus kunnen leiden tot verschuivingen in een microbiële gemeenschap *in vitro*, werd er onderzocht of er ook in de orale microbiële gemeenschap van patiënten met hoofd- en halskanker verschuivingen voorkomen ten gevolge van de radiotherapeutische behandeling. Na twee tot drie bestralingsweken werden duidelijk verschuivingen waargenomen met behulp van denaturerende gradiënt gel elektroforese. Deze verschuivingen konden gerelateerd worden aan een verstoring van de normale orale functies van de patiënten zoals het

opnemen van vast voedsel. Verder werd ook aangetoond dat er meer bacteriën aanwezig waren van *Lachnospiraceae\_incertainae\_sedis* en een niet-geclassificeerde groep *Prevotellaceae*, terwijl de hoeveelheid *Abiotrophia* afnam door de bestraling. Bovendien werden bepaalde genera geïdentificeerd, zoals de *Prevotella*, *Porphyromonas* en *Parvimonas* die konden gelinkt worden met de graad van mucositis. Enkele genera, zoals de *Atopobium*, werden zelfs geïdentificeerd als potentiële merkers voor een ernstige vorm van mucositis.

Ten slotte werd de mogelijkheid bestudeerd om E-cadherine, een belangrijke cel-cel adhesie molecule, aan te wenden als een biologische merker of als therapeutisch doel ter preventie van orale mucositis. Het E-cadherine niveau in het speeksel van de hoofd- en halskankerpatiënten daalde ten gevolge van de bestraling reeds na twee weken. Dit was tevens het tijdstip waarop de eerste klinische effecten van orale mucositis zichtbaar werden. Bovendien werd het potentieel aangetoond om de relatieve E-cadherine concentratie in het speeksel na één bestralingsweek aan te wenden als een predictieve merker voor de ernst van mucositis bij patiënten met orofarynxkanker. Bij de patiënten met een ernstige graad van mucositis, was de E-cadherine concentratie in het speeksel na één week toegenomen in tegenstelling tot de patiënten die een milde vorm van mucositis ontwikkelden.

Aangezien de epitheliale barrière verbroken wordt bij de ontwikkeling van mucositis, werd geprobeerd om deze barrière te versterken ter preventie van orale mucositis. Orale mondspoelingen met tamoxifen en 8-prenylnaringenine slaagden er in om de eerste tekens van orale mucositis uit te stellen in een muismodel, hetgeen hoogst waarschijnlijk een gevolg was van een reductie in epitheliale afschilfering ten gevolge van de bestralingstherapie.

Algemeen wijzen de verschillende resultaten op belangrijke verschuivingen in de orale microbiële gemeenschap ten gevolge van radiotherapie, die mogelijk de ernst van mucositis beïnvloeden. Deze verschuivingen kunnen in de toekomst aangewend worden als biomerker of mogelijk zelf als therapeutisch doel. Een nieuwe onderzoeksstrategie voor orale mucositis dringt zich op, waarbij er naast de effecten van bestraling op de humane mucosa, ook naar de rol van de orale bacteriën en de microbe-gastheer interacties gekeken wordt. Dit kan wellicht leiden tot nieuwe behandelingen voor de hoofd- en halskankerpatiënten die behandeld worden met radiotherapie en dus een groot risico hebben op het ontwikkelen van mucositis.

## SUMMARY

---

Oral mucositis is an important inflammatory side effect of radiotherapy in head and neck cancer patients, resulting in a decreased quality of life, hospitalization and at worst in the interruption of the anticancer therapy. While the pathobiology of mucositis has already been extensively described, research on the potential role of the oral microbiota is still limited. Hence, this dissertation focused on the host-microbe interactions in the context of oral mucositis by investigating the influence of irradiation on the microbiota both *in vitro* and in patients.

As a first objective, a new model was developed, which enables the study of microbe-epithelial crosstalks *in vitro* up to 72 h. Using this model, an inhibitory effect of the oral microbiota towards epithelial wound healing was identified. Interestingly, this effect was found to be species dependent as monocultures of *Klebsiella oxytoca*, mainly isolated from the oral cavity after irradiation for head and neck cancer, exerted an inhibitory effect, while *Streptococcus oralis*, a common oral habitant, was found to stimulate the epithelial wound healing. Further mechanistic work suggested the role of quorum sensing molecules in the delayed wound healing, pointing to the importance to study interkingdom signalling in the context of human diseases.

When applying the model in a radiotherapeutic setting, the impact of irradiation on the mucosal healing was shown to be largely dependent on the composition of the microbial inoculum. Sequencing analysis of the *in vitro* reconstituted oral biofilm further pointed to a slight increase in the abundances of *Rothia*, *Granulicatella* and *Gemella* due to irradiation. Furthermore, irradiation of microbial monocultures with a single dose of 10 Gy showed that biofilm formation and pathogenicity of microbiota could be affected by irradiation.

Since our results showed that therapeutic irradiation doses were able to generate shifts in the microbial community *in vitro*, the shifts due to radiotherapy in the oral microbial community of head and neck cancer patients were further investigated. After two to three weeks of therapy, the microbial community was shifted as shown with denaturing gradient gel electrophoresis. These shifts could be correlated with the patients' normal oral functioning (pain, nutrition). Moreover, the abundances of an unclassified group of *Prevotellaceae* and *Lachnospiraceae\_incertae\_sedis* were shown to increase, while the number of *Abiotrophia* decreased following radiotherapy. Higher abundances of certain genera like *Prevotella*, *Porphyromonas* and *Parvimonas* could be linked with the severity of mucositis and some particular genera like *Atopobium* could play a role as predictive marker for the development of severe mucositis.

Furthermore, the potential use of E-cadherin, an important cell-cell adhesion molecule, as a salivary biomarker or therapeutic target was evaluated. The salivary levels of the soluble extracellular fragment of E-cadherin were shown to decrease after two weeks of irradiation, the time point at which first signs of mucositis appear. In patients diagnosed with oropharynxcarcinoma, patients known to be at high risk for developing mucositis, the relative concentration of soluble E-cadherin after the first week of treatment was shown to be predictive for the severity of mucositis developed during the therapy. When the salivary levels increased, the patients were at high risk to develop severe mucositis.

In a therapeutic setting, an increased activity of the E-cadherin/catenin complex was aimed in an attempt to strengthen the epithelial barrier. Oral rinses with tamoxifen or 8-prenylnaringenin were able to delay the onset of mucositis in an established mouse model, most probably by reducing the shedding of the irradiated epithelial cells.

Altogether, our data point to important shifts in the oral microbiota due to radiotherapy, which could affect the severity of mucositis. In the future, these shifts can be used as a biomarker or as therapeutic target. Further research on oral mucositis should not only focus on the host mucosa, but should include the microbial component and the host-microbe interactions. This new research strategy may lead to new treatments for radiotherapy patients at risk of developing mucositis.

## ABBREVIATIONS

---

8-PN	8-prenylnaringenin
AB	antibiotics
AHL	N-acyl-homoserine lactone
AMP	adenosine monophosphate
AP-1	activator protein 1
BHI	brain heart infusion
bp	base pair
BSA	bovine serum albumin
CFU	colony forming units
COX-2	cyclooxygenase 2
CRAMP	chemotherapy or radiation associated molecular pattern
CRT	conventional radiotherapy
CT	chemotherapy
CUP	cancer of unknown primary origin
DAPI	4',6-diamidino-2-phenylindole
DGGE	denaturing gradient gel electrophoresis
DMEM	Dulbecco's modified Eagle's Medium
DMSO	Dimethyl sulphoxide
DNA	deoxyribonucleic acid
dNTP	deoxynucleotide triphosphates
EGFR	epidermal growth factor receptor
ELISA	enzyme-linked immunosorbent assay
EMA	European medicines agency
EORTC	European Organization for Research and Treatment of Cancer
f	female
FBS	foetal bovine serum
FDA	U.S. food and drug administration
FS	forward scatter
GPR	G-protein coupled receptor
H&E	haematoxylin & eosin staining
HECD-1	Human anti-E-cadherin antibody
HMP	human microbiome project
HSCT	hematopoietic stem cell transplantation

IGFBP	insulin-like growth factor binding protein
IgG	immunoglobulin G
IL	interleukin
IMRT	intensity-modulated radiotherapy
LDH	lactate dehydrogenase
LPS	lipopolysaccharide
m	male
MALDI-TOF	matrix-assisted laser desorption/ionization Time-of Flight
MAP	mitogen-activated protein
MEM	minimal essential medium
MID	multiplex identifiers
MMP	matrix metalloproteinase
MS	mass spectrometry
MTT	3-(4,5-dimethylthiazol-2-yl)-2,5-diphenyl-tetrazolium bromide
n	number of samples/observations
NA	not affected
ND	not determined
N.D.	not detected
NF- $\kappa$ B	nuclear factor kappa-B
NOD	nucleotide-binding oligomerization domain protein receptors
NOF	normal oral functioning
OD	optical density
OddHL	N-(3-oxododecanoyl) homoserine lactone
OSCC	oral squamous cell carcinoma
OTU	operational taxonomic unit
PAMP	pathogen-associated molecular pattern
PARP	poly-adenosine-di-phosphate-ribose polymerase
PBS	phosphate buffered saline
PCA	principal component analysis
PCR	polymerase chain reaction
PI	propidium iodide
PLC	phospholipase C
PRR	pathogen recognition receptors
R	richness
RDP	Ribosomal database project
ROS	reactive oxygen species

rRNA	ribosomal ribonucleic acid
RT	radiotherapy
RTOG	Radiation Therapy Oncology Group
SCFA	short chain fatty acid
SD	standard deviation
SE	standard error
sE-cadherin	soluble extracellular fragment of E-cadherin
spp.	species
SRA	sequence read archive
SRB	sulforhodamine B
SS	side scatter
SSU	small subunit
TAM	tamoxifen
TBS	tris-buffered saline
TCA	trichloroacetic acid
THY	Todd-Hewitt broth with yeast extract
TLR	Toll-like receptor
TNF	tumour necrosis factor
UPGMA	unweighted pair group method with arithmetic mean





# 1. INTRODUCTION

---

## 1.1. Oral mucositis

Oral mucositis is a severe side effect of cancer therapy and the conditioning treatment for hematopoietic stem cell transplantation (HSCT). For this dissertation, we will focus on oral mucositis in patients with head and neck cancer treated with radiotherapy. Nevertheless, also other side effects like xerostomia, dysphagia, fatigue, radiation dermatitis and weight loss will occur in those patients. In Belgium, 2 624 new incidences of head and neck cancer were reported in 2012. Most of these patients (~65 %) are treated with radiotherapy, with or without concurrent surgery or chemotherapy (Belgian Cancer Registry, 2012, 2015). Current prevalence is higher in men compared to women, probably due to their higher alcohol and tobacco use, the most important risk factors for developing head and neck tumours (Hashibe et al., 2009; Simard et al., 2014).

Eighty-five per cent of the patients treated with radiotherapy for head and neck tumours will develop oral mucositis. When radiotherapy is combined with chemotherapy, this percentage even rises up to 98 % (Elting et al., 2007). Clinically, oral mucositis is characterised by mucosal erythema and ulcerations, by which patients' quality of life will significantly decrease. Apart from lots of pain, also patients' ability to speak and nutritional intake is altered, sometimes resulting in the need for total parenteral nutrition or feeding tubes and in the worst case oral mucositis will result in an interruption of the therapy. All this will result in higher treatment costs and can cause decreased cancer survival for patients developing mucositis (Pico et al., 1998; Elting et al., 2007).

The severity of mucositis is described using different grading scales, of which that of the World Health Organisation is commonly used (Table 1-1). Here, the score of mucositis is determined by the combination of clinical observations and the patients' ability to eat. Grade 1 and 2 mucositis are recognized as mild or moderate mucositis, while grade 3 and 4 are considered to be severe (Treister and Sonis, 2007).

**Table 1-1: World Health Organisation mucositis grading scale**

Grade	Clinical features
0	No mucositis present
1	Pain, erythema
2	Erythema, ulcerations; Able to eat solids
3	Ulcerations; Unable to eat solids, liquid diet possible
4	Severe ulcerations; Oral alimentation not possible

Due to fractionated irradiation, ulcerations appear after a cumulative dose of 20 Gy (the end of the second week of therapy), while the first adverse mucosal effects already arise after a cumulative dose of 10 Gy (the end of the first week of therapy) (Van der Schueren et al., 1990; Sonis, 2007; Treister and Sonis, 2007). Potential risk factors to develop ulcerative oral mucositis can be subdivided in 2 groups. The therapy-related variables comprise the dose and treatment schedule, while the patient-related variables incorporate the age and gender of the patient, the nutritional stage, salivary function and, of most interest for this dissertation, the oral microbiota (Barasch and Peterson, 2003).

## **1.2. Pathobiology of mucositis**

The pathobiology of mucositis was extensively described by Sonis (2004, 2007, 2009) and can be subdivided in 5 phases. During the initiation phase, irradiation of the oral epithelium will cause direct damage to DNA, resulting in clonogenic cell death (Ross, 1999). Yet, this embraces only a minor part of the ultimate damage, since irradiation will also generate reactive oxygen species (ROS). These ROS can induce direct damage or trigger different pathways such as the nuclear factor kappa-B (NF- $\kappa$ B) and ceramide pathway (Andrieu-Abadie et al., 2001; Gloire et al., 2006). Of these, NF- $\kappa$ B will regulate the production of pro-inflammatory cytokines like tumour necrosis factor (TNF), interleukin-6 (IL-6) or interleukin-1 $\beta$  (IL-1 $\beta$ ), which are important mediators of injury. Moreover, NF- $\kappa$ B will also impact on genes of the BCL-2 family, resulting in cellular apoptosis (Sonis, 2007; Dewson and Kluck, 2010). Furthermore, the activation of sphingomyelinases and ceramide synthases of the ceramide pathway will also lead to apoptosis (Haimovitz-Friedman et al., 1997; Andrieu-Abadie et al., 2001; Sonis, 2007). Apart from the epithelium, also the fibroblasts in the submucosa will be damaged by irradiation. This injury is often mediated by another transcription factor, AP-1, which is known to regulate the genes of the matrix metalloproteinases, disrupting the integrity of the submucosa and epithelium (Sonis, 2004, 2007; Treister and Sonis, 2007). Recently Sonis (2010) proposed the involvement of Chemotherapy or Radiation Associated Molecular Patterns (CRAMPs). These endogenous molecules

are released from the damaged oral mucosa and might be recognized by pathogen recognition receptors (PRRs) like Toll-like receptors. Due to binding of these CRAMPs to PRRs, the NF- $\kappa$ B-pathway is activated, resulting in an increased progression of mucositis.

During the upregulation and signal amplification phase, the proteins produced in the primary damage response will stimulate additional damage. For example TNF is known to activate NF- $\kappa$ B and sphingomyelinase (Schütze et al., 1995). Hereby, the tissue injury is increased and prolonged, which will eventually result in the ulceration phase characterised by deep and painful ulcers. A lot of these ulcers are covered with pseudomembranes composed of death cells and fibrin, which creates an ideal environment for microbial colonization (Sonis, 2007). When these microbiota reach the blood vessels, bacteraemia or sepsis can occur.

At last, the healing phase will start spontaneously after completion of the therapy. Cyclooxygenase-2 (COX-2), produced by fibroblasts and vascular endothelium, may play a role in the rebuilding of the submucosa, as a burst of angiogenic activity was seen five days following peak COX-2 expression (Sonis et al., 2004). Moreover, cells present in the submucosa will provide signals to the epithelium to increase migration, proliferation and differentiation. However, the structure of the healed mucosa will never be identical to its original state (Denham and Hauer-jensen, 2002; Sonis, 2007).

### **1.3. The potential role of microbiota in the pathobiology of oral mucositis**

*Modified from: Vanhoecke B, De Ryck T, Stringer A, Van de Wiele T, Keefe D (2015) Microbiota and their role in the pathogenesis of oral mucositis. Oral diseases 21(1), 17-30.*

#### **1.3.1 Introduction**

The introduction of the pathobiology model of mucositis by Sonis in 2004 (updated in 2007, 2009, 2010) has tremendously improved our understanding. Within this model, colonization of the damaged mucosa by bacteria, fungi and viruses is thought to occur mainly at the ulceration phase and superimpose secondary infections (Rand et al., 1982). In an established hamster model of radiation-induced mucositis, there is a higher abundance of microbiota in the ulcerated epithelium compared to the intact epithelium and microbial colonization peaked synchronously with the mucositis score (at day 21), suggesting that the ulcerated mucosa represents a desirable colonization site (Sonis, 2009). Based on recent scientific evidence, van Vliet et al. (2010) proposed a modified version of the model for intestinal mucositis whereby commensal microbiota potentially interfere at many different stages of the process. They show a

potential impact of the intestinal commensals on (i) the process of inflammation and oxidative stress, (ii) intestinal permeability, (iii) the composition of the mucus layer, (iv) the resistance to harmful stimuli and modulation of epithelial repair and (v) the production and release of immune effector molecules. Unfortunately, evidence for a similar effect of microbiota during the course of oral mucositis is still missing and will therefore be one of the topics of this dissertation. Starting with the present knowledge about the composition of a healthy oral core microbiome and its arrangement in habitat-dependent biofilms, we will further highlight what is known about the microbial shifts that occur during and after radiotherapy. Finally, we will discuss what dual role oral microbiota are able to play in the context of mucositis as both commensals and pathogenic species are constituents of the normal ecosystem.

### **1.3.2 Characteristics of the oral mucosa and its colonizing microbiota**

The normal oral mucosa consists of a lamina propria and an upper stratified squamous epithelial layer. On top of the oral epithelium, there is a salivary film with a thickness of 70–100 µm consisting of water, mucins, salts, lipids and proteins (Collins and Dawes, 1987; Strous and Dekker, 1992; Amado et al., 2010). This mucous layer acts as a selective barrier for nutrients and a defence system against mechanical, chemical and biological stresses (Forstner and Forstner, 1994; Deplancke and Gaskins, 2001; Thornton and Sheehan, 2004; Allen and Flemström, 2005).

In the oral cavity, mucins are released by the submandibular, sublingual and minor salivary glands and are subdivided into membrane-bound mucins, such as MUC1 and MUC4, or secretory mucins such as MUC2, 5B, 7 and 19 (Thornton et al., 1999; Derrien et al., 2010). As these mucins can serve as nutrient sources (Wickström and Svensäter, 2008), they were found to be important for the growth of microbiota (Wei et al., 2006). Moreover, they also initiate host–microbe interactions such as adhesion of microbiota (Ligtenberg et al., 1992; Thornton et al., 1999; Kesimer et al., 2009). Carbohydrate structures present on salivary mucins MUC5B and 7, for example, offer a wide range of binding sites for microbiota (Derrien et al., 2010); therefore, it can be assumed that when salivary production is restricted, which is the case during radiation-induced xerostomia, patients are more prone to develop infections. Inter-individual variation in glycosylation patterns has been described for salivary MUC5B and 7 and may be one of the reasons for having a unique microbiome based on a general core of shared organisms (Ligtenberg et al., 1992; Thornton et al., 1999; Kesimer et al., 2009).

Teeth, gingival sulcus, gingiva, tongue, cheek, lip, tonsils, hard and soft palate are all microbial habitats that are colonized by distinct microbial communities, which form biofilms of different complexities (Mager et al., 2003; Aas et al., 2005). Those biofilms protect the host against pathogens through mechanisms such as competition for

nutrients (Momose et al., 2008) or adhesion receptors (Servin and Coconnier, 2003), production of inhibitory metabolites or antimicrobial agents against pathogens (Servin, 2004), modulation of toxin production or action (Czerucka et al., 1994; Brandão et al., 1998) and modifying inflammatory responses (Starling and Balish, 1981; Mitsuyama et al., 1986; Ohkubo et al., 1990; Clarke et al., 2010; Fagundes et al., 2012).

Exhaustive surveys using pyrosequencing technologies have suggested that the diversity of microbiota may be around 500 species-level phylotypes (Zaura et al., 2009; Dewhirst et al., 2010). With regard to the composition of the oral microbiome, Segata et al. (2012) have recently published a paper as part of the Human Microbiome Project (HMP). The analysis of the HMP data set characterized the microbial communities of the mouth, tonsils, throat and stool from more than 200 healthy adults. With regard to the mouth, samples showed that the oral habitats formed three categories of microbial community types: Group 1: buccal mucosa, keratinized gingiva and hard palate; Group 2: saliva, tongue; and Group 3: sub- and supragingival plaque. At phylum level, the microbiota of Group 1 consisted mostly of *Firmicutes* (>55 %), followed by *Proteobacteria* (15–25 %), *Bacteroidetes* (10–15 %) and *Actinobacteria* (< 10 %) or *Fusobacteria* (< 5 %). Group 2 had a decreased relative abundance of *Firmicutes* (40–45 %), followed by *Bacteroidetes* (20– 25 %), *Proteobacteria* (20 %), *Fusobacteria* (5–10 %), *Actinobacteria* (5–10 %) and *TM7* (< 5 %). Finally, dental plaque taxa (Group 3) were more evenly distributed dominated by *Firmicutes*, *Bacteroidetes*, *Actinobacteria*, *Proteobacteria* and *Fusobacteria*. At the genus level, Group 1 showed a low diversity with an overall dominance of the single genus *Streptococcus*, while Group 2 and 3 were characterized with a more even distribution of the most abundant genera *Streptococcus*, *Veillonella*, *Prevotella*, *Neisseria*, *Fusobacteria*, *Actinomyces* and *Leptotrichia* (> 2 % on average in Group 2 and >3 % in Group 3) and *Capnocytophaga*, *Rothia* and *Porphyromonas* (present at > 3 % in Group 3). The composition as revealed by Segata et al. (2012) was generally in line with the results from earlier studies. Interestingly, the authors provided evidence that even in a non-diseased population, recognized pathogens are part of the commensal oral microbiome. The genera *Porphyromonas*, *Tannerella* and *Treponema* associated with periodontal disease are highly prevalent. Unfortunately, at this stage, no such cohort studies have been performed with a large group of patients with mucositis. These studies are important to identify specific microbial species or communities as potential risk factors for mucositis. Recent studies have demonstrated a shift to a more complex oral bacterial profile in patients undergoing cancer chemotherapy (Napeñas et al., 2010), while the opposite was found after radiation therapy (Hu et al., 2013a), which raised the question whether these shifts may trigger the development of local or systemic infections in the long term.

### 1.3.3 Microbial shifts during and after radiotherapy

Little is known about the role of oral commensals in the onset, development and duration of oral mucositis, although it is well documented that cytotoxic therapies like chemotherapy and radiotherapy are often complicated by local and even systemic infections. In 2007, Napeñas et al. systematically reviewed the role of oral microbial changes in the development of oral mucositis during chemotherapy. Thirteen prospective clinical trials were identified, involving 300 patients with 13 different cancer diagnoses. There was great variability in patient populations, bacterial sample collection methodology and oral sample sites. As a conclusion, no clear pattern regarding qualitative and quantitative oral microbiome changes emerged among these studies. The most frequent Gram-negative species isolated during chemotherapy were *Enterobacteriaceae* spp., *Pseudomonas* spp. and *E. coli*. The most common Gram-positive species isolated were *Staphylococcus* spp. and *Streptococcus* spp. Five studies assessed the role of oral microbial changes in the genesis of oral mucosal changes, with no consensus among them. Since then, a number of studies on the composition of the oral microbiome before/during/after cytotoxic therapies (chemotherapy, radiation and HSCT) have been executed and conclusions concerning radiotherapy are listed in Table 1-2. Again, there was great variability in patient populations, bacterial sample collection, culturing and identification procedures and sample sites. Only a few studies (Tong et al., 2003; Al-Nawas and Grötz, 2006; Napeñas et al., 2010; Sonalika et al., 2012a; Hu et al., 2013a) looked at the effect of radio- and/or chemotherapy on the composition of the oral microbiota and/or the abundance of individual species before and during/after treatment, making general conclusions on the impact of a specific therapy on the oral microbiome premature. With regard to irradiation therapy, studies by Shao et al. (2011) and Hu et al. (2013) suggest that the core oral microbiome is modulated over time. Of particular interest is the recent study of Hu et al. (2013) on the 'dynamic core microbiome' of plaque microbiota in the diseased condition after radiotherapy. Dental plaque samples of 8 subjects were collected before and weekly during radiotherapy and high-throughput pyrosequencing of the bacterial 16S rRNA genes was performed. Results showed a negative correlation between the number of operational taxonomic units (OTUs) and radiation dose (number of OTUs pretreatment >10, 20, 30 Gy >40, 50, 60 Gy). Moreover, in an attempt to define a general core microbiome for all irradiated head and neck cancer patients, the group found that 4 phyla (*Actinobacteria*, *Bacteroidetes*, *Firmicutes* and *Proteobacteria*) and 11 genera (*Streptococcus*, *Actinomyces*, *Veillonella*, *Capnocytophaga*, *Derxia*, *Neisseria*, *Rothia*, *Prevotella*, *Granulicatella*, *Luteococcus* and *Gemella*) were found in all subjects. Temporal variations in relative abundance of these major cores were also observed. Other studies indeed reported an increase in the abundance of Gram-negative species (Tong et al., 2003; Panghal et al., 2012;



Sonalika et al., 2012a) together with *Candida* spp. (Belazi et al., 2004; Almståhl et al., 2008; Guobis et al., 2011; Sonalika et al., 2012a) and *Lactobacillus* spp. (Tong et al., 2003; Almståhl et al., 2008; Guobis et al., 2011). With regard to resident *Lactobacillus* spp., three studies including >100 subjects in total, showed an increased number and proportion of *Lactobacillus* spp. in swabs of tongue, buccal mucosa, vestibulum, supragingival plaque and subgingival region and saliva after radiotherapy (Tong et al., 2003; Almståhl et al., 2008; Guobis et al., 2011). Given the conflicting results in the two studies performed and given the small number of subjects tested in both studies, no general conclusions could be made regarding the effect of radiotherapy on *Streptococcus* spp. (Tong et al., 2003; Almståhl et al., 2008). Overall, *Candida albicans* fungi seemed to be the most significant oral cavity pathogen in radiotherapy.

Gram negatives such as *Pseudomonas aeruginosa* and *Klebsiella pneumoniae* were observed as main pathogens isolated from the blood of radiotherapy-treated patients (Panghal et al., 2012). The table further indicates that only a few studies have been performed since the publication of the review of Napeñas et al. (2007). More extensive research is necessary to obtain a better understanding of a core microbiome in a diseased state like oral mucositis. With those insights it would be possible to predict community responses to interventions like chemo- and radiation therapy (Hu et al., 2013a). Furthermore, it can lead to early diagnosis of general diseases based on oral microbiome data (Goodson et al., 2009; Zaura et al., 2009; Ahn et al., 2012).

### **1.3.4 Microbiota as risk factors**

The risk for oral mucositis with or without concurrent infection is characterized by patient-related and treatment-related variables. Although not proven yet, it is highly likely that the composition of the individual oral microbiome is also an important risk factor.

Based on treatment procedures, Panghal et al. (2012) divided the patients in three groups; Group I (radiotherapy), Group II (chemotherapy) and Group III (combined radiochemotherapy) and scored for prevalent bacterial pathogens (i.e., *Staphylococcus aureus*, *Escherichia coli*, *Staphylococcus epidermidis*, *Pseudomonas aeruginosa*, *Klebsiella pneumonia*, *Proteus mirabilis*, *Proteus vulgaris*) and the fungal pathogens (*Candida albicans* and *Aspergillus fumigatus*). The predominant Gram-negative bacteria *Ps. aeruginosa* and *K. pneumonia* were isolated from the blood of Group I and the oral cavity of Group II. The predominance of Gram-positive bacteria *S. aureus* and *S. epidermidis* was observed in the blood of Group II and III and the oral cavity of Group I and III. *C. albicans* fungi were the most significant oral cavity pathogens in Group I and III (Panghal et al., 2012).

**Table 1-2: Clinical studies on the composition of oral microbiome before/during/after radiotherapy and their outcomes**

<b>Treatment</b>	<b>Subjects</b>	<b>Sample origin</b>	<b>Aim</b>
Radiotherapy	12 naso-pharyngeal carcinoma patients (25-68 y)	Local (oral rinse samples)	To study mutans and non-mutans streptococci in patients after radiotherapy of the head and neck
Radiotherapy	22 patients with head and neck cancer	Local (deepest periodontal pocket)	Evaluation of the long term change in oral pathogens following radiation therapy (prospective study)
Radiotherapy	13 dentate patients and 13 controls (42-70 y)	Local (swabs of the dorsum of the tongue, the buccal mucosa and the vestibulum)	Analysis of microbiome on the tongue, buccal mucosa, vestibulum, supragingival plaque and subgingival region 6-8 months after completed radiation therapy
Radiotherapy	61 oral squamous cell carcinoma patients and 72 age and sex matched controls	Local (saliva)	Evaluation of shifts in oral microbial population during the radiotherapy (comparative study)
Radiotherapy	13 patients with head and neck cancer treated with IMRT and 12 with conventional RT (>18 y)	Local (dental plaque samples)	Evaluation of the temporal variation of plaque profiles during IMRT or CRT

**Table 1-2 Continued**

<b>Microbial evaluation (time point)</b>	<b>Technique</b>	<b>Observations and conclusions</b>	<b>Reference</b>
before/after	cultivation and 16S rDNA sequence homology analysis	After irradiation, mutans streptococci were not isolated; the levels of <i>S. mitis</i> , <i>S. salivarius</i> and lactobacilli increased, while the level of <i>S. sanguis</i> decreased after irradiation	Tong et al. (2003)
before/after	cultivation and PCR	No microbiological evidence for radiation periodontitis	Al-Nawas and Grötz (2006)
after	cultivation	The number of <i>C. albicans</i> and enterococci were significantly higher in the radiotherapy group compared to controls. In supragingival plaque, <i>Lactobacillus</i> spp. were detected in 92% of the radiotherapy subjects and the number and proportion of <i>Lactobacillus</i> spp. were extremely high compared with the controls. The mean total microbial count and the numbers of streptococci, <i>S. salivarius</i> and <i>F. nucleatum</i> were significantly lower. <i>S. aureus</i> and enteric rods were rare in the radiotherapy group	Almståhl et al. (2008)
before/during	colony characteristics, gram staining and a series of standard biochemical reactions.	Radiotherapy resulted in a significant increase in <i>Candida</i> spp.. Candidal carriage was also promoted by the tumor but was more pronounced by radiation. Specific increase in <i>E. coli</i> , <i>Ps. aeruginosa</i> , <i>Enterobacter</i> species and <i>K. pneumoniae</i> could contribute to exacerbation of mucositis	Sonalika et al. (2012)
during	PCR-DGGE	DGGE profiles changed over time in individuals during treatment. The degree of change over time varied between the IMRT ( $69.96 \pm 7.82\%$ ) and CRT subjects ( $51.98 \pm 10.45\%$ ). Temporal stability of microbiota was significantly higher in the IMRT group than the CRT group	Shao et al. (2011)

**Table 1-2: Continued**

<b>Treatment</b>	<b>Subjects</b>	<b>Sample origin</b>	<b>Aim</b>
Radiotherapy	64 patients with complaints of oral dryness (due to radiotherapy to the maxillofacial area, Sjögren's syndrome, xerogenic medications, and tricyclic antidepressants).	Local (saliva)	Evaluation of the dependence of the condition of the microbiota of the oral cavity on the etiology of xerostomia, patients' sex, age, degree of hyposalivation, and duration of the sense of dryness.
Radiotherapy	8 patients with head and neck cancer (26-70 y)	Local (dental plaque samples)	Exploration of the dynamic core microbiome of plaque microbiota during radiotherapy
Radiotherapy, chemotherapy or combined	186 patients with oral squamous cell carcinoma (25-83 y)	Local (oral swabs of the labial mucosa, tongue and cancerous lesion)/ systemic (blood)	Identification of bacterial and fungal colonization from the oral cavity and blood of patients undergoing radiotherapy (62), chemotherapy (62) or radiochemotherapy (62) (prospective cohort analysis)

**Table 1-2: Continued**

<b>Microbial evaluation (time point)</b>	<b>Technique</b>	<b>Observations and conclusions</b>	<b>Reference</b>
after	bacteriological tests for <i>Streptococcus mutans</i> and <i>Lactobacillus</i> spp. and cultivation of fungi and <i>Candida</i>	The percentage of patients with high counts of <i>Candida</i> spp. was greater in the radiotherapy group. Radiation resulted in a pronounced hyposalivation, which is linked with a significantly greater percentage of <i>Lactobacillus</i> spp. Significantly greater percentages of patients with the clinical duration of xerostomia of up to 6 months had high counts of <i>Lactobacillus</i> spp. and <i>Candida</i> spp. colonies	Guobis et al. (2011)
before/during	pyrosequencing	Four phyla ( <i>Actinobacteria</i> , <i>Bacteroidetes</i> , <i>Firmicutes</i> and <i>Proteobacteria</i> ) were found in all subjects, supporting the concept of a core microbiome. Temporal variations in relative abundance of these major cores were observed, as well as a negative correlation between the number of operational taxonomic units and radiation dose	Hu et al. (2013)
during	cultivation of blood and standard microbiological and biochemical procedures for swabs	The predominant Gram-negative bacteria, <i>Ps. aeruginosa</i> and <i>K. pneumonia</i> were isolated from blood of radiotherapy and oral cavity of chemotherapy treated cases respectively. The predominance of Gram-positive bacteria ( <i>S. aureus</i> and <i>S. epidermidis</i> ) were observed in blood of chemotherapy, radio-chemotherapy treated cases and oral cavity of radiotherapy, radio-chemotherapy treated cases. <i>C. albicans</i> fungi are the most significant oral cavity pathogens in radiotherapy and radio-chemotherapy cases	Panghal et al. (2012)

Another study showed that the temporal stability of the oral plaque microbiota was significantly higher after intensity-modulated radiotherapy (IMRT) than after conventional radiotherapy (CRT) (Shao et al., 2011). As it is known that the prevalence of grade 3 or higher mucositis is lowered in IMRT – treated patients (Vergeer et al., 2009; Lambrecht et al., 2013), this further supports the hypothesis of the potential involvement of the oral microbiota in the course of oral mucositis. Although most research is focused on identifying general shifts in composition of the ‘core microbiome’ present in the vast majority of patients during and after treatment (Shao et al., 2011; Hu et al., 2013a), it is important to note that the overall inter-individual similarity between saliva samples, for example, displays only approximately 52 % concordance (Shao et al., 2011), which complicates the search for microbial biomarkers of mucositis.

It is well known that mucus secretion is highly impaired after radiotherapy by a depletion and dysfunction of the salivary glands. Hyposalivation after radiotherapy contributes considerably to disruption of the natural barrier of the oral mucous membranes (Scully et al., 1994; Ellepola and Samaranayake, 2000). Already in the 1970s, Brown and coworkers clearly demonstrated the impact of hyposalivation on the microbial population dynamics in various oral microenvironments. The most prominent changes were increases in *Streptococcus mutans*, *Lactobacillus* spp., *Candida albicans* and *Staphylococcus* spp. and decreases in *Streptococcus sanguis* and *Neisseria* spp. and *Fusobacterium* spp. (Brown et al., 1975). These shifts persist as long as the xerostomia and are probably due to a reduced clearing of microbiota due to a lower salivary flow (Guobis et al., 2011). The relationship between hyposalivation and a shift in the oral microbiome was further investigated by Shao et al. (2011) using IMRT or CRT. The data showed that preservation of the salivary flow and the stability of the oral microbiome were significantly higher after IMRT.

Apart from the direct effects of the anti-cancer therapies on the structure and functionality of the oral mucosal layer, excessive degradation of mucins by mucolytic microbiota may contribute to the severity of mucositis as it disturbs the protective function of the mucosa. Intestinal MUC1, for example, has been shown to be a critical element of the mucosal barrier to infection (McAuley et al., 2007). A number of mucolytic species have been identified in the oral cavity and include *Streptococcus anginosus*, *Streptococcus mitis*, *Streptococcus mutans*, *Streptococcus oralis*, *Streptococcus sanguinis* and *Streptococcus sobrinus* (Derrien et al., 2010). Recent clinical evidence suggests that mucolytic streptococci play a role during chemotherapy- (Olczak-Kowalczyk et al., 2012) and radiotherapy-induced mucositis (Tong et al., 2003). Mucin degradation requires the subsequent activities of microbial enzymes, mainly glycosidases, each having the specificity to degrade a specific glycoside linkage. *Streptococcus* spp. produce one, several, or all mucin-degrading

enzymes (Derrien et al., 2010). Although it is unclear at what stage and extent *Streptococcus* spp. play a role in the pathogenesis of mucositis, they have definitely the potential to have detrimental effects by targeting different types of mucins present in the mucus layer. Due to their high abundance on every surface in the oral cavity, it is likely that *Streptococcus* spp. have an impact on both the composition and thickness of the oral mucus layer and can easily cause infections. Indeed, commensal *Streptococcus* spp. have been shown to be able to shift to a pathogenic phenotype under certain circumstances. For example, *S. mitis*, a normal commensal of the human oropharynx, has been shown to cause a variety of infectious complications including infective endocarditis in vulnerable immune-compromised patients (reviewed by Mitchell, 2011).

Anti-cancer therapies might also affect other properties of the microbiota such as adherence and biofilm formation. An interesting *in vitro* study on the direct effects of ionizing radiation has shown that therapeutic doses can promote biofilm formation and adherence of *Streptococcus mutans* on dental restorative materials (Cruz et al., 2010). Given the high prevalence of mutans *Streptococcus* spp. in saliva of irradiated patients (Meca et al., 2009), these observations may have relevance for the development of therapies against biofilm-dependent infections.

It is now well accepted that pathogen-associated molecular patterns (PAMPs) expressed by microbiota, but not by host cells, are primary stimulants of inflammation. Well-known PAMPs are lipopolysaccharide (LPS), flagellins and bacterial lipopeptides and may be implicated in mucositis by increasing risk and severity. A study by Wells et al. (1987) showed that total body irradiation of rabbits damaged the gut mucosa and resulted into leakage of endotoxin or LPS into the systemic circulation. An intraperitoneal injection of anti-LPS plasma significantly protected the rabbits from Gram-negative bacteraemia and mucosal damage. PAMPs are recognized by RIG-I-like receptors, nucleotide-binding oligomerization domain-like receptors and Toll-like receptors (TLRs). Binding to the corresponding receptors results in the activation of signalling pathways like the NF- $\kappa$ B and the MAP-kinase pathways and will eventually result in a rapid upregulation of pro-inflammatory adhesion molecules, cytokines and chemokines. Well-known examples of PAMPs that are implicated in oral diseases are the *Treponema denticola* flagellin (Beklen et al., 2009) and *Porphyromonas gingivalis* LPS (Kocgozlu et al., 2009). Interestingly, both species have recently been associated with oral ulcerations in patients treated with high-dose chemotherapy (Laheij et al., 2012). Recently, the potential involvement of TLR signalling in chemotherapy-induced gastrointestinal mucositis has been critically reviewed (Thorpe et al., 2013). General conclusion was that although strong scientific evidence of a link between TLRs and alimentary mucositis is still missing, there are some elements to suggest their implication. Yet, it remains to be elucidated to what



extent – positively and/or negatively – microbial PAMPs contribute to TLR reactivity, given the fact that TLRs are also engaged in crosstalks between epithelial and immune cells like T cells and dendritic cells (Beklen et al., 2009; Bahri et al., 2010a, 2010b; Kim and Blanke, 2012). In that respect, it is interesting to report the findings of a recent mouse study by Burdelya et al. (2012) showing that PAMPs have the potential to modulate therapy-induced tissue responses. The use of a pharmacologically optimized flagellin significantly reduced the severity of mucositis and the extent of radiation-induced weight loss after a single dose of 15 or 20 Gy.

### **1.3.5 Conclusion**

Recent studies have provided more evidence for the potential role of individual species or their metabolites during oral mucositis induced by radiation and/or chemotherapy. In most of the studies, irradiation was shown to result in increased abundances of Gram-negative species and lactobacilli. As the overall functionality and dynamics rather than the composition of a biofilm might determine its properties (Ahn et al., 2012), further research should focus on both composition and functional aspects of the various oral biofilms. A functional approach to combat the complication might be the prevention of mucosal breakdown, suppression of microbial colonization and effective management of severe xerostomia to reduce the overall morbidity and mortality of oral mucosal infections that complicate mucositis. How exactly this can be achieved is still a big challenge, but recent promising studies with oral probiotics show that they may offer an alternative to the standard treatment with antibiotics. Further, more research should be focused on the establishment, composition and functionality of new oral biofilms that arise after anti-cancer therapy in order to avoid the risk to develop harmful biofilms and systemic infections post-treatment.

## **1.4. Treatment strategies**

Up to date, different guidelines exist to manage mucositis, including a good oral care. Nevertheless, a golden standard treatment or preventive agent is still unavailable (Rubenstein et al., 2004; Lalla et al., 2014). Different strategies, which can be subdivided in cytokines and growth factors, anti-inflammatory agents, antimicrobial agents, analgesics or miscellaneous compounds, are being tested for their ability to ameliorate or prevent the development of oral mucositis. One of the most investigated growth factors is keratinocyte growth factor-1 also known as Palifermin. This is the only FDA and EMA approved drug to treat oral mucositis as a consequence of whole body irradiation and high dose chemotherapy before HSCT. Today multiple clinical trials (Phase II- Phase III) are further exploring the use of Palifermin in other settings to determine the risks of stimulating the growth of tumour cells as well. Furthermore,

other compounds and treatment strategies, like recombinant human epidermal growth factor, benzydamine HCl, soluble beta 1,3/1,6 glucan, doxepin and morphine mouthwashes, amifostine, Manuka honey, CD2 *Lactobacillus brevis* lozenges and the use of low level laser therapy are currently investigated in clinical studies phase III or phase IV ([www.ClinicalTrials.gov](http://www.ClinicalTrials.gov) - March 2015). Furthermore, MuGard® and Prothelial™ recently became commercially available for their use in the combat against mucositis. Despite a lot of research that has been performed, due to inadequate and conflicting evidence for many of the investigated compounds, up to date these compounds were not included in the MASCC/ISOO clinical practice guidelines for oral mucositis as a consequence of radiotherapy in head and neck cancer patients (Lalla et al., 2014).

Of particular interest for this dissertation are the microbial strategies that are currently explored. Recently, the use of probiotic microbiota for the treatment of oral mucositis gained interest. Sharma et al. (2012) showed that *Lactobacillus brevis* CD2 lozenges reduce radiation- and chemotherapy-induced mucositis in patients with head and neck cancer in a randomized double-blind placebo-controlled study. Furthermore, the ActoBiotic AG013, a mouth rinse formulation of *Lactococcus lactis* secreting human trefoil factor 1 significantly reduced the severity and course of mucositis in a hamster model for radiation-induced oral mucositis (Caluwaerts et al., 2010). A clinical Phase 1b study with this compound reported a reduced ulcerative oral mucositis duration, which supports further clinical studies (Limaye et al., 2013). Concerning the use of antimicrobial agents to prevent or treat oral mucositis, Donnelly et al. (2003) reviewed 30 studies. Of these, 15 reported no benefit and one study even showed an unfavourable outcome of the use of chlorhexidine with an increase of oral mucositis and discomfort. Furthermore, recent reviews also recommend against the use of antimicrobial compounds like for example isegagan for mucositis prevention in head and neck cancer patients treated with radiotherapy due to insufficient and conflicting results (Saunders et al., 2013; Lalla et al., 2014). The conflicting results of the different antimicrobial studies point to the need to better understand the role of the microbiota in the development of oral mucositis, before effective antimicrobial compounds can be developed (Donnelly et al., 2003).

## **1.5. Microbe – epithelial interactions: no need for physical contact**

### **1.5.1 Introduction**

As described above, evidence for the potential role of oral microbiota in radiotherapy-induced oral mucositis is currently increasing. Also in other well-known illnesses like

inflammatory bowel disease and diabetes type 2, researchers gain new insights in the pathobiology of these diseases and try to identify new treatment options by unravelling the host-microbe interactions (Everard and Cani, 2013; Hold et al., 2014; Moreno-Indias et al., 2014). To this end, many researchers are focussing on microbial surface molecules or microbial invasion to study the direct effect of the microbiota on the epithelium. However, Shapiro and co-workers recently highlighted the impact of diet-dependent microbial metabolites on the development and function of the immune system. Short chain fatty acids, together with long chain fatty acids, bile acids, polysaccharides, amino acids and vitamins will all affect the inflammatory cells in the gut environment (Shapiro et al., 2014). As these microbial small molecules will not only affect the immune cells, a summary of the known indirect microbe-epithelial interactions is provided in this section.

### **1.5.2 Microbial metabolites**

#### ***Short chain fatty acids***

Short chain fatty acids (SCFA) are the most important microbial metabolites, known to exert multiple effects on epithelial cells. As many of these effects were already extensively reviewed previously in the gut environment, not all details were considered in this section (Scheppach, 1994; Scheppach et al., 1995; Hamer et al., 2008; Louis et al., 2014).

First of all, the SCFA are an important energy source for the epithelium. Butyrate, for example, will enhance oxidative phosphorylation in the colonocytes and is considered as the major energy substrate for these cells (Comalada et al., 2006; Donohoe et al., 2011). By providing energy, SCFA will stimulate the proliferation of normal colon epithelial cells (Scheppach et al., 1992, 1995). One exception appears to be valerate, as its presence was inversely correlated with the number of cells per crypt of the rat cecum (Lupton and Kurtz, 1993). Furthermore, SCFA inhibit cellular autophagy in the mammalian colon by reducing the levels of p27 phosphorylation and LCR-II (Donohoe et al., 2011).

In contrast with the normal epithelial cells, the growth of cancer cells will be significantly inhibited by butyrate and propionate (Scheppach et al., 1995; Milovic et al., 2000). Butyrate acts as a strongly differentiating and thus anti-proliferative agent for human colon cancer cell lines *in vitro* (Barnard, 1993), while acetate is found to induce growth arrest by downregulation of cyclin D1 (Matsuki et al., 2013). Propionate treatment of HT-29 cells will result in short-time swelling of the cells, due to increased Na<sup>+</sup> concentrations to compensate cellular acidification (Rowe et al., 1993). Moreover, due to SCFA treatment, different epithelial cell lines were shown to become apoptotic (Sakurazawa and Ohkusa, 2005).

Apart from their effect on cellular viability and proliferation, the migratory capacity of multiple colon cancer cell lines was described to be stimulated by short chain fatty acids in a concentration dependent manner (butyrate up to 4 mM, propionate up to 16 mM and acetate up to 24 mM), although this was only the case in gastro-intestinal epithelial cell lines (Wilson and Gibson, 1997). At higher concentrations, the epithelial migration was inhibited, most probably as a result of toxic effects, as was indicated by Wilson and Gibson (1997) by measuring lactate dehydrogenase leakage after treatment with high concentrations of SCFA. Also an anti-invasive effect of acetate, propionate and mainly butyrate was found in a colon cancer cell line, most probably due to inhibition of urokinase plasminogen activator and the stimulation of tissue inhibitor matrix metalloproteinases (Emenaker and Basson, 1998).

SCFAs will also exert a protective role. The epithelial barrier function for example will be altered by butyrate in physiological concentrations, as measured by increases in transepithelial electrical resistance (Rickard et al., 2000; Peng et al., 2007). An increased AMP-activated protein kinase activity after induction of Caco-2 cells with butyrate, results in an accelerated assembly of tight junctions, the major component of the epithelial barrier (Peng et al., 2009). Moreover, the permeability of the tight junctions is altered by butyrate via the upregulation of the lipoxygenase activity (Ohata et al., 2005). Furthermore, by a time and concentration dependent increase in hsp25, the rat intestinal epithelial cells are protected towards oxidant injury in presence of butyrate (Ren et al., 2001). The properties of the intestinal mucus gel and its protective function are also influenced by butyrate through the specific modulation of the Muc gene expression in intestinal goblet cells (Gaudier et al., 2004).

While butyrate usually has a predominant beneficial connotation when present in the gut, it can also exert negative effects on the colon epithelium. Zumbrun et al. recently showed an increased sensitivity of the gut epithelial cells towards Shiga toxins in presence of butyrate (Zumbrun et al., 2013). In contrast, acetate was shown to protect the gut epithelium from enteropathogenic infections (Fukuda et al., 2011).

At the molecular level, butyrate inhibits the histone-deacetylase activity, resulting in hyperacetylated histones and an increased susceptibility of histone H3 to phosphorylation by the Ca<sup>2+</sup> dependent kinase (Whitlock et al., 1980; Hinnebusch et al., 2002; Waldecker et al., 2008). Apart from apoptotic cell death, histone acetylation was significantly correlated with the secretion of the insulin-like growth factor binding protein-2 (IGFBP-2) (McBain et al., 1997; Nishimura et al., 1998). Indeed, short chain fatty acids and more particular butyrate will decrease the synthesis of IGFBP-3, while that of IGFBP-2 was increased in Caco-2 cells cultures (Nishimura et al., 1998).

Butyrate and propionate will also activate the AP-1 pathway and suppress NF- $\kappa$ B activation, regulating multiple cellular events (Inan et al., 2000; Yin et al., 2001;

Nepelska et al., 2012). Apart from this, SCFA are able to activate G-protein coupled receptors (GPR41 and GPR43) on intestinal cells, resulting in activated protein kinase signalling and production of chemokines and cytokines (Kim et al., 2013). Treatment of colon derived cell lines with propionate or butyrate also modulated the secretion of angiopoietin-like protein 4, investigated for its multifunctional actions in the human body (Grootaert et al., 2011a).

### **Lactate**

Apart from the production by microbiota, the epithelial cells will also secrete lactate. As a result, the provoked effects of the microbial lactate fraction are less pronounced compared to SCFA. In epithelial cells, lactate is reported to inhibit histone-deacetylase activity, although relatively weak in comparison with butyrate (Latham et al., 2012). L-lactate was also shown to function as a chemo-attractants, stimulating the migration and invasion of epithelial cancers cells (Bonuccelli et al., 2010). Furthermore, Matsuki et al. (2013) described a downregulation of cyclin E1 in Caco-2 cells, although this effect was mainly due to the change in pH.

### **1.5.3 Toxins**

Microbes are known to attack their host with different toxins, which can be subdivided in exotoxins, comprising secreted protein-like structures and endotoxins (Ovington, 2003). Exotoxins can be both narrow- and broad-spectrum and their concentrations needed to negatively affect the host will depend on the microbial virulence (Ovington, 2003). Interactions of bacterial toxins with the gut epithelial cells were previously reviewed by Nusrat *et al.* (2001a). As many toxins exist, only a few important toxins known to affect epithelial cells in the human host are described in this section.

In the gastro-intestinal tract, toxin A and B, both released by *Clostridium difficile*, are causing diarrhoea and colitis. Both exotoxins were shown to have cytotoxic properties (Tucker et al., 1990). They will compromise the epithelial gut barrier by affecting the tight junction proteins and by inducing an early release of pro-inflammatory cytokines (Pothoulakis, 2000; Nusrat et al., 2001b). Cholera toxin from *Vibrio cholerae* will also result in diarrhoea. By binding of the toxin to the enterocytes, intracellular adenylate cyclases are activated, resulting in increased cyclic AMP levels (Taylor-Papadimitriou et al., 1980). This will cause water-efflux from the epithelial cells leading to diarrhoea (McGee et al., 1993). At the other hand, the increased cyclic AMP levels also stimulate the growth of the human epithelial cells, probably due to an increased growth response to mitogens (Taylor-Papadimitriou et al., 1980). Similar to toxin A and B, also cholera toxin will enhance cytokine expression, more specifically the IL-6 secretion from IEL-6 intestinal epithelial cells, thereby enlarging the inflammatory response (McGee et al., 1993). Antibiotic-associated colitis was recently

shown to be correlated with the presence of tilivalline, the toxin produced by *Klebsiella oxytoca*. This toxin will cause apoptosis in cultured human epithelial cells (Schneditz et al., 2014). Apart from the intestinal epithelium, exotoxins will also affect other epithelia in the human host. Vacuolating cytotoxin (VacA) of *Helicobacter pylori* for example, will cause apoptosis via mitochondrial actions in the gastric epithelial cells (Kim and Blanke, 2012). In the lungs, the tracheal epithelial permeability was shown to increase after exposure to  $\alpha$ -toxin produced by *Staphylococcus aureus* (Phillips et al., 2006), while shiga-toxins were proven to cause apoptosis in pulmonary epithelium derived cells (Uchida et al., 1999).

The most important endotoxins are the lipopolysaccharides (LPS), originating from the cell wall of Gram-negative species. These compounds are not only released after microbial cell lysis, but also as part of the normal vesicle trafficking activity of Gram-negative bacteria (Kulp and Kuehn, 2010). These vesicles were shown to be a common mechanism by which microbiota interact with their host, as reviewed by Kuehn and Kesty (2005), and contain adhesins, toxins and immunomodulatory compounds. Via Toll-like receptors, LPS will stimulate IL-6 and IL-8 secretion of airlifted conjunctival epithelial cells (Li et al., 2014). In rat duodenal epithelial cells, the LPS produced by *Helicobacter pylori* will induce nitric oxide synthase, resulting in apoptosis of these cells (Lamarque et al., 2000). While high concentrations of LPS appeared to be toxic, low concentrations of LPS (10  $\mu\text{g}/\text{mL}$ ) accelerate wound repair of airway epithelial cells via an EGFR phosphorylation pathway (Koff et al., 2006). Moreover, in different colorectal carcinoma cell lines, LPS treatment will result in the upregulation of Hif-1 $\alpha$ , which can indirectly contribute to the establishment of a metastatic phenotype (Simiantonaki et al., 2008).

#### **1.5.4 Quorum sensing molecules**

More recently, quorum sensing molecules were described to be important in the host-microbe communication (Hughes and Sperandio, 2008; Pacheco and Sperandio, 2009). N-(3-oxododecanoyl) homoserine lactone (OdDHL), the quorum sensing molecule of *Pseudomonas aeruginosa*, is one of the quorum sensing molecules that was investigated for its interactions with the host. Induction of airway epithelial cells with 100  $\mu\text{M}$  OdDHL increased the production of MUC5A, the major mucin core protein, both on mRNA and protein level. Most probably, this was obtained via phosphorylation of I-kB and ERK-1/2 (Imamura et al., 2004). In the gut, OdDHL can disrupt the epithelial barrier integrity; transepithelial electrical resistance decreased, while paracellular transport increased. At protein level, the expression and distribution of ZO-1 and occludin, respectively an important cytoplasmatic and transmembrane protein of the tight junction, decreased and F-actin was reorganised

in Caco-2 epithelial cells due to activation of p38 and p42/44 kinases (Vikström et al., 2006). The inflammatory response is also affected in presence of quorum sensing molecules. 100  $\mu$ M OdDHL significantly increased IL-8 production in human bronchial epithelial cells, without being toxic (Smith et al., 2001).

Moreover, in diseases like cystic fibrosis, this compound appeared to be very important. Higher levels of IL-6 production due to OdDHL were found in cystic fibrotic bronchial epithelial cells in a calcium dependent manner (Mayer et al., 2011). Saleh et al. (1999) described the reduction of the ATP- and UTP-induced SLPI secretion by cystic fibrotic human submucosal tracheal gland serous cells, presumably due to the inhibited expression of P2Y2 and P2Y4 by oxo-AHLs.

In human breast cancer cell lines, 50-100  $\mu$ M OdDHL will inhibit the proliferation and induce apoptosis, most probably correlated with the inhibition of STAT3 phosphorylation (Li et al., 2004). Recently, the group of De Spiegeleer, described the potential use of quorum sensing molecules or analogues in oncology treatment (Wynendaele et al., 2012). Moreover, PhrG from *B. subtilis*, CSP from *S. mitis* and EDF from *E. coli* were found to promote breast cancer cell invasion in a collagen type I matrix (De Spiegeleer et al., 2015).

### 1.5.5 Other small molecules

Apart from SCFA, toxins and quorum sensing proteins, microbiota will also secrete other small molecules, which are able to affect the host epithelial cells.

Exposure of HCT-8 cells to indole, a small molecule secreted by commensal *E. Coli*, upregulated gene expression correlated with epithelial barrier functions such as the genes responsible for the organisation of tight junctions (Bansal et al., 2010, 2012). This was consistent with an increased transepithelial resistance, which was found in both colon epithelial cells and retinal pigment epithelium (Bansal et al., 2012). Also cytoskeleton genes and genes involved in the production of mucus were induced, while the expression of Toll-like receptor genes (TLR3 and 9) and different cytokines or chemokines were altered in HCT-8 cells. Also the TNF- $\alpha$ -mediated inflammation was attenuated by indole (Bansal et al., 2010).

The virulence factor phospholipase C (PLC) was isolated from the culture medium of different Gram-positive and Gram-negative bacteria (Titball, 1993). The broad-spectrum PLC of *Bacillus cereus* was shown to induce MMP-2, MMP-3 and MMP-9 expression (Firth et al., 1997). This will result in epithelium disruption and subepithelial destruction of infected tissues. Higher levels of MMP-9 are also correlated with increased epithelial cell migration (Firth et al., 2001). Moreover, PLC was shown to stimulate integrin expression, resulting in higher levels of  $\alpha_v$ ,  $\alpha_2$ ,  $\alpha_5$  and  $\beta_1$  integrins (Firth et al., 2001).

Protein fermentation by bacteria will give rise to different compounds of which many are toxic for the human cells (Windey et al., 2012). The viability of epithelial cells, when exposed to e.g. phenol will decrease significantly and the trans-epithelial resistance of Caco-2 cells will be reduced after treatment with p-cresol, phenol or NH<sub>3</sub> (Windey et al., 2012). Ammonia, maybe the best-known end-product of protein fermentation, was shown to stimulate cell proliferation (Ichikawa and Sakata, 1998). In the stomach, ammonia is produced from urea by the urease activity of *Helicobacter pylori* (Smoot et al., 1990) and appeared to be the main causative agent for the epithelial vacuolation due to *H. pylori* (Megraud et al., 1992; Ricci et al., 1993). Moreover, the presence of ammonia will accelerate TNF- $\alpha$  induced apoptosis in gastric epithelial cells (Smoot et al., 1990; Megraud et al., 1992; Igarashi et al., 2001). Also other peptides produced by the microbiota can influence the epithelial cells. *Listeria monocytogenes*, for example, produces a  $\beta$ -casein derived peptide, which stimulates the motility and invasion of HCT-8 colon cancer cells (Oliveira et al., 2003). The digestive processes will further result in the production of hydrogen sulphide (H<sub>2</sub>S). This gaseous molecule will increase the proliferation rate of rat intestinal crypt cells. Moreover it will modulate the expression of genes involved in cell-cycle progression, inflammation and DNA repair response. Apart from this, sulphide will also prevent the oxidation of butyrate in the epithelial cells, which will induce an energy deficient state. Furthermore the cellular respiration will be inhibited as H<sub>2</sub>S will inhibit cytochrome C (Windey et al., 2012; Linden, 2014).

Already in 1922, Mcleod and Gordon proved the presence of hydrogen peroxide (H<sub>2</sub>O<sub>2</sub>) in the supernatant of pneumococcal and streptococcal bacteria (Mcleod and Gordon, 1922). H<sub>2</sub>O<sub>2</sub> produced by *Streptococcus oralis* was capable of eliciting epithelial cell death and induces IL-6 production (Okahashi et al., 2014) Also the H<sub>2</sub>O<sub>2</sub> produced by a *Lactobacillus* strain was able to induce both apoptosis and necrosis in human epithelial cells (HT-29)(Strus et al., 2009). *L. crispatus* M247 uses H<sub>2</sub>O<sub>2</sub> as a signal transducing molecule to induce PPAR- $\gamma$  activation in intestinal epithelial cells, directly modulating epithelial cell responsiveness to inflammatory stimuli (Voltan et al., 2008).

### 1.5.6 Conclusion

In this section, it was highlighted how some important microbial compounds are able to affect the epithelium. While some compounds appear to be beneficial, others are detrimental or have a dual role. Hereby, the necessity is shown to further unravel the indirect host-microbe interactions to gain new insights in diseases and their treatments. Although most of the cited research is not focusing on the host-microbe interactions in the oral cavity, these data are still valuable. Some oral microbiota will produce similar compounds as described above, while it was also shown that some



microbiota are found in the oral cavity beyond expectations. *Staphylococcus aureus* for example, a well-known colonizer of the skin and respiratory tract, is frequently isolated from the oral cavity (Smith et al., 2003). Also in oral mucositis, a possible role for this microbe has already been described (Bagg et al., 1995).

Up to date, studies concerning the influence of irradiation on the production of the microbial metabolites and their effects on the epithelium are very limited. Although, taking into account the microbial shifts irradiation can cause, one should consider differential effects of the microbial metabolites on the host epithelium after irradiation.

## 1.6. Research questions

For this dissertation, we aimed to gain better insight in the potential role of oral microbiota in radiation-induced mucositis. Therefore, various research questions and objectives were set.

The first objective was to develop a model, which makes it possible to investigate microbe-epithelial crosstalk for longer time periods. Once this model was characterised, some research questions arose.

*RQ1:* which microbial species will affect the epithelial cells in a wound healing set-up and what is the underlying mechanism?

*RQ2:* what is the influence of irradiation on the host-microbe crosstalks?

*RQ3:* what is the influence of irradiation on the functional behaviour of the microbes?

Next, we aimed to gain better insight in the oral microbial shifts in patients with head and neck cancer treated with radiotherapy.

*RQ4:* how are the oral microbiota evolving during radiotherapy?

*RQ5:* is there a correlation between the microbiota present in the oral cavity and the severity of oral mucositis?

Finally, we explored the potential of E-cadherin, an important cell-cell adhesion molecule, for its use as a salivary marker for or as therapeutic target of oral mucositis.

This objective comprises 2 research questions:

*RQ6:* what is the potential of soluble E-cadherin as a salivary marker for mucositis?

*RQ7:* can we target E-cadherin molecules to prevent or ameliorate mucositis?

## 1.7. Outline of the dissertation

This dissertation is subdivided in different chapters compiling different research articles, which were accepted or submitted to international peer-reviewed journals. The outline of this dissertation is also summarized in Figure 1-1.

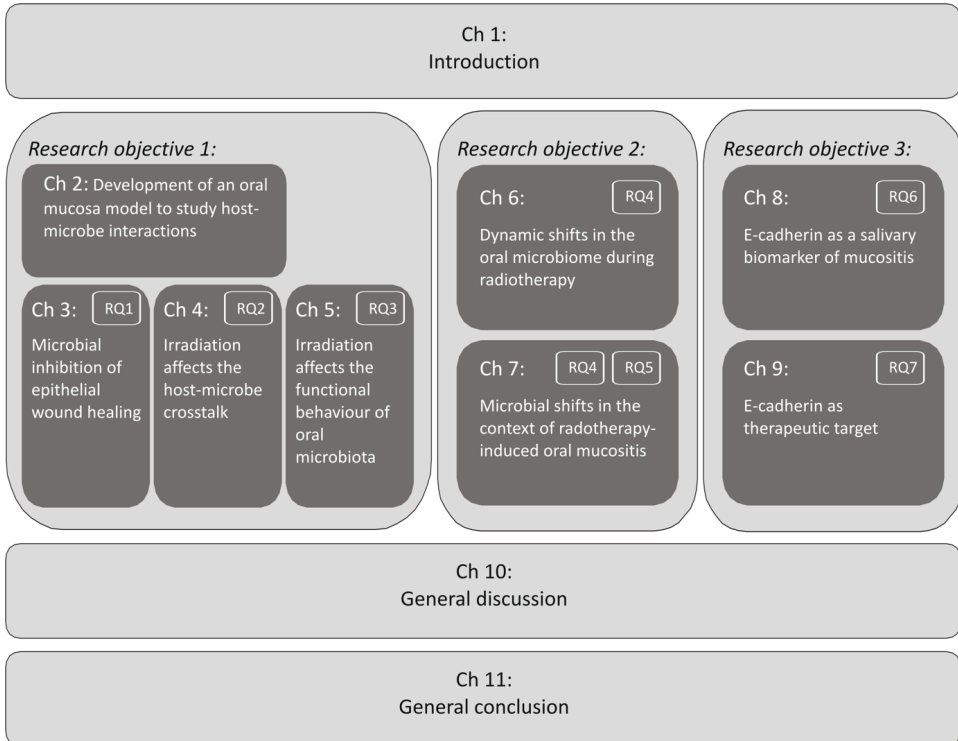


**Figure 1-1: Schematic outline of the dissertation**

The first part embraces the *in vitro* research on host microbe interactions. For this, a new *in vitro* model was developed in which we were able to co-culture microbiota and epithelial cells in non-infectious conditions for longer time periods (Chapter 2). In this chapter, the characterisation of the model is described and some important microbe-epithelial crosstalks were highlighted. For example the number, size and complexity of the microbiota will be influenced by the presence of the epithelial cells. On the other hand, oral microbiota will exert an inhibitory effect on wound healing. This chapter was published in Applied microbiology and biotechnology (De Ryck et al, 2014).

In Chapter 3, the *in vitro* model was used to investigate the inhibitory effect of different oral monocultures on the epithelial wound healing (RQ1). The selected oral

species could be subdivided in 3 groups, whether they were inhibiting, stimulating or not affecting the epithelial wound closure. Further mechanistic experiments were performed to investigate the inhibitory effect of different microbial small molecules on the epithelial wound healing process. All these data were published in *AMB express* (De Ryck et al., 2015a).

Chapter 4 is focussing on the second research question (RQ2) and was published in the *Journal of Nuclear medicine & Radiation Therapy* (De Ryck et al., 2015b). By irradiating the model, differential effects of the oral microbiota on the epithelial wound healing could be noticed after irradiation. 454-pyrosequencing analyses identified some microbial changes after irradiation. Unfortunately we were not able to fully unravel which microbiota were causing the differential effects in the *in vitro* model.

As irradiation of the model appeared to influence the microbial part of the oral mucosa model, we further investigated the effect of irradiation on some basic characteristics of oral microbes (RQ3). In cooperation with Dr. Vanhoecke, we showed alterations in viability and biofilm formation. Moreover, we also identified an increased pathogenicity of *Klebsiella oxytoca* due to irradiation. These results are described in Chapter 5 and were accepted for publication in *Experimental Biology and Medicine* (Vanhoecke et al., 2015a). Altogether, the results obtained *in vitro*, point to the necessity to include the oral microbes in the research of mucosal radiation effects in the context of mucositis.

In the second part of this dissertation, we first investigated the microbial shifts during radiotherapy on a small patient population using DGGE-analysis (RQ4; Chapter 6). The observed shifts could be correlated with the patients' ability to eat solid foods. These results were published in *Clinical Research in Infectious Diseases* (De Ryck et al., 2015c). Microbial 16S rDNA sequencing analysis was used to investigate the changes in the oral microbiota of 25 patients during radiotherapy (RQ4; Chapter 7). Moreover, we were able to identify some microbial genera, which could be significantly correlated with the severity of mucositis (RQ5).

For the third part of the dissertation, the potential of the epithelial cell-cell adhesion molecule E-cadherin to be used as a salivary marker for mucositis was investigated (RQ6; Chapter 8). In the last research chapter of this dissertation, which was published in *Strahlentherapie und Onkologie* (De Ryck et al., 2015d), we describe the potential of targeting the E-cadherin molecules to ameliorate mucositis (RQ7; Chapter 9).

In Chapter 10, all research objectives are recapitulated and the usefulness of the obtained results are critically discussed in the context of oral radiotherapy induced mucositis. At last, the general conclusion of this dissertation can be found in Chapter 11.

## 2. DEVELOPMENT OF AN ORAL MUCOSA MODEL TO STUDY HOST-MICROBE INTERACTIONS

---

*Modified from: De Ryck T, Grootaert C, Jaspert L, Kerckhof FM, Van Gele M, De Schrijver J, Van den Abbeele P, Swift S, Bracke M, Van de Wiele T, Vanhoecke B (2014). Development of an oral mucosa model to study host-microbiome interactions during wound healing. Applied microbiology and biotechnology 98 (15), 6831-6846.*

### 2.1. Abstract

Crosstalk between the human host and its microbiota is reported to influence various diseases such as mucositis. Fundamental research in this area is however complicated by the timeframe restrictions during which host-microbe interactions can be studied *in vitro*. The model proposed in this chapter, consisting of an oral epithelium and biofilm, can be used to study microbe-host crosstalk *in vitro* in non-infectious conditions up to 72 h. Microbiota derived from oral swabs were cultured on an agar/mucin layer and challenged with monolayers of keratinocytes grown on plastic or collagen type I layers embedded with fibroblasts. The overall microbial biofilm composition in terms of diversity remained representative for the oral microbiome, whilst the epithelial cell morphology and viability were unaffected. Applying the model to investigate wound healing revealed a reduced healing of 30 % in presence of microbiota, which was not caused by a reduction of the proliferation index (52.1–61.5) or a significantly increased number of apoptotic (1-1.13) or necrotic (32-30.5 %) cells. Since the model allows the separate study of the microbial and cellular exometabolome, the biofilm and epithelial characteristics after co-culturing, it is applicable for investigations within fundamental research and for the discovery and development of agents that promote wound healing.

### 2.2. Introduction

The various surfaces of the oral cavity are covered by a huge diversity of microbial species organized within the structure of a biofilm (Aas et al., 2005; Kolenbrander et al., 2010; Segata et al., 2012). Some of the species of this oral microbiome are the causative agents of oral diseases such as caries and periodontitis (Løe, 1981; Aas et al., 2008) or serious systemic infections like bacterial endocarditis and pneumonia (Scannapieco, 1999; Li et al., 2000; Paju and Scannapieco, 2007). It is now clear that

alterations in the composition and/or functionality of the oral microbiome may compromise the normal host-microbe crosstalk, thereby resulting in a higher risk for disease onset.

An important selective parameter in the colonization process of oral microorganisms is the nature of the contact surface. Despite the importance of epithelial cells in the oral cavity, all epithelial surfaces are covered with mucus. Therefore, the first important step for microbes to colonize the oral cavity is the adhesion to and migration across this mucus layer. After adhesion, the microbiota can develop into biofilm communities exhibiting specialized biofilm-specific activities, e.g. up-regulation of virulence factor expression (Costerton et al., 1987, 1995; van Loosdrecht et al., 1990; Mitchell et al., 2010). Local disturbances of the adhesion sites may have an impact on the normal host-microbe crosstalk eventually affecting the physiology of the whole micro-ecosystem. Moreover, without direct contact between microbiota and the epithelium, crosstalk occurs via signalling molecules (e.g. secreted proteins, soluble peptides, DNA, toxins, hormone like chemicals) and microbial metabolites (e.g. short chain fatty acids) (Scheppach, 1994; Letzelter et al., 1998; Hughes and Sperandio, 2008; Grootaert et al., 2011b).

Well-designed 3D tissue-engineered human skin and oral mucosa constructs are now available, and have been used for a wide variety of purposes including the examination of mucotoxicity and wound healing (Moharamzadeh et al., 2008a; K uchler et al., 2010). Recently these models have been applied to investigate bacterial infection, mostly of the skin (Dongari-Bagtzoglou and Kashleva, 2006; Shepherd et al., 2009; MacNeil et al., 2011). However, these models use planktonic bacterial cells instead of biofilm grown bacteria. In a clinical context, biofilms are relevant as a source of many chronic and life-threatening infections, where they are difficult to eradicate due to the diffusion-limited availability of antibiotics (Stewart and Costerton, 2001). A mechanistic understanding of the microbe-host interaction in healthy or diseased states is often complicated by the black-box environment in *in vivo* models, while many *in vitro* models are often restricted in terms of the timeframe (< 4 h) during which microbe-host interactions can be studied, due to the high cytotoxicity of microbiota for the host epithelial cells (Mempel et al., 2002; Wiegand et al., 2009; Marzorati et al., 2014).

The aim of this study was to design a new *in vitro* oral mucosa model where crosstalk between microbial biofilms and host epithelial cells can be studied in absence of direct microbe-epithelial contact for longer time periods, which are more relevant to the *in vivo* situation. Doubling time of oral epithelial cells goes up to 63 h (Thomson et al., 1999), which is a good estimate of the epithelial surface renewal following the concept of epithelial homeostasis and thus also approach the contact time between the microbiota and oral epithelial surface layers. The model is suitable for research on

biofilm architecture and composition, viability, activity and integrity of the oral mucosa and analysis of the microbial and cellular exometabolome. In this study, we applied the model in a wound healing setting in order to unravel host-microbe crosstalk during wound recovery. Furthermore, the model is suitable in other settings to investigate the effects of the presence of antibiotics, growth factors, biofilms of single/multiple bacterial and yeast strains, pro/prebiotics, upon cancer-derived, normal skin and oral keratinocytes.

## **2.3. Materials and methods**

### **2.3.1 Cell culture**

The TR146 cell line, obtained from Clare Hall Laboratories (Cancer Research UK), is an oral squamous cell carcinoma line derived from a local lymph node metastasis. The NIH-3T3 cell line is an immortalized fibroblast cell line derived from NIH swiss mice, kindly provided by Prof. Helmut Deissler (Institute of Cell Biology, Germany). TR146 and NIH-3T3 cells were cultured in Dulbecco's modified Eagle's Medium (DMEM) (Gibco, Merelbeke, Belgium) supplemented with 10 % heat-inactivated foetal bovine serum (FBS) (Greiner bio-one, Belgium), 100 IU/mL penicillin (Gibco, Merelbeke, Belgium), 100 µg/mL streptomycin (Gibco, Merelbeke, Belgium) and 2.5 µg/mL amphotericin B (Bristol-MyersSquibb, Braine-l'Alleud, Belgium). HaCaT cells are human keratinocytes derived from a spontaneously immortalized, non-tumorigenic cell line. The cell line was kindly provided by Dr. Norbert Fusenig (Institute of Biochemistry, Germany) (Boukamp et al., 1988) and cultured in DMEM supplemented with 2 mM L-glutamine (Gibco, Merelbeke, Belgium), 10 % serum and 1 % antibiotics/antimycotics. In the complex model, a mixture of DMEM and Ham F12 (7:1) supplemented with insulin (2.5 µg/mL), Epidermal Growth Factor (EGF) (1 ng/mL), hydrocortisone (0.2 µg/mL), adenine (50 nM), serine (5 µM), carnitine (5 µM), albumin (0.5 mg/mL), cholera toxin (50 nM), transferrin (25 µg/mL) and ascorbic acid (25 µg/mL) (Sigma, Diegem, Belgium) was used during the co-culturing of the HaCaT cells and the microbial biofilm. Human epidermal keratinocytes were isolated from neonatal foreskin derived from single donors with the appropriate informed consent and ethical committee approval. The keratinocytes were isolated according to Rheinwald and Green (1975) and were further grown in keratinocyte serum-free medium supplemented with recombinant epidermal growth factor and bovine pituitary extract (Life Technologies Europe, Belgium) to obtain monolayer cultures in the first or second passage. All cell lines were cultured at 37 °C in a humidified atmosphere at 10 % CO<sub>2</sub>. During co-culture with oral microbiota, all cell lines were cultured in serum-free medium (Gibco, Merelbeke, Belgium) without antibiotics at 37 °C and 5 % CO<sub>2</sub>.

### **2.3.2 Oral swab collection and preparation of oral biofilm**

Before sampling, the oral cavity of a healthy individual was flushed extensively with drinking water. A sterile spatula was gently wiped ten times along the inner cheek and inserted in a tube containing 2 mL Brain heart infusion (BHI) broth (Oxoid, Hampshire, UK). The inoculum was rigorously mixed for 30 s using a vortex mixer and incubated at 37 °C for 30 min (Figure 2-1(1)). In the meantime an agar/mucin layer (Figure 2-1 (2)) was prepared according to the method described by Van den Abbeele et al. (2009). Briefly, a Bacto-agar (BD, Erembodegem, Belgium) solution (0.8 g/100 mL) containing 5% (w/v) porcine mucin type III (Sigma-aldrich, Diegem, Belgium) was sterilized by autoclaving at 121 °C for 15 min. 75 µL of the agar/mucin solution was used to cover the apical side of the polycarbonate filter inserts (pore size of 0.4 µm) of 24-well plate Transwell® systems (Corning inc., NY, USA) and allowed to solidify at room temperature for 1 h. 20 µL of the microbiota inoculum was spotted on top of the agar/mucin layer, after which the insert was positioned on top of an epithelial monolayer (Figure 2-1 (4)).

### **2.3.3 Oral mucosa preparation and the oral scratch assay in the simplified and complex model**

For the preparation of oral epithelial monolayers, 250 000 epithelial cells (TR146, HaCaT or normal keratinocytes) were seeded in the lower compartment of the 24-well Transwell® plate (Figure 2-1 (4)). TR146 cells were labelled in suspension with Vybrant DiI cell labelling solution (Life technologies Europe, Gent, Belgium) before seeding. At the start of the assay, a wound was created in the cell monolayer with a sterile plastic pipette tip. Immediately thereafter, cells were washed with serum-free DMEM to remove floating cellular debris and reincubated in 1 mL serum-free antibiotics-free DMEM (Gibco, Merelbeke, Belgium) (Figure 2-1 (3)).

In the complex model, epithelial cells were seeded on a collagen type I layer containing NIH-3T3 fibroblasts (Figure 2-1 (5)). Briefly, 50 000 NIH-3T3 cells were suspended in 300 µL of a collagen type I solution (1 mg/mL). For this solution, 4 volumes of Rat tail collagen type I (BD, Erembodegem, Belgium) were mixed on ice with 5 volumes of calcium- and magnesium-free Hank's balanced salt solution, 1 volume of Minimal Essential Medium (MEM) (10x), 1 volume of 0.25 M NaHCO<sub>3</sub>, 0.3 volumes of 1 M NaOH and 2.7 volumes of DMEM with 10 % FBS without antibiotics. After 1 h of solidification at 37 °C, DMEM containing 10 % serum and a reduced (2/3<sup>rds</sup>) concentration of antibiotics was added to the wells. After 2 days of incubation, EtOH-sterilized plastic strips (1x1x12mm) were placed on top of the collagen gel before seeding the epithelial cells (250 000 TR146 or 400 000 HaCaT cells/well). Cells were allowed to attach and differentiate for 5 days. One day before the start of the experiment, medium was refreshed, using DMEM with 10 % FBS without antibiotics.

At the start of the wound healing assay, the strips were removed, the cells were washed twice with serum-free, antibiotics-free DMEM to remove cell debris and remnants of antibiotics and 1.2 mL serum-free, antibiotics-free DMEM (TR146) or a mixture of DMEM-Ham F12 (1:7) with additives (HaCaT) was added (Figure 2-1 (3)). We made use of a custom-made spacer plate to avoid direct contact between the bottom side of the insert and the oral mucosa.

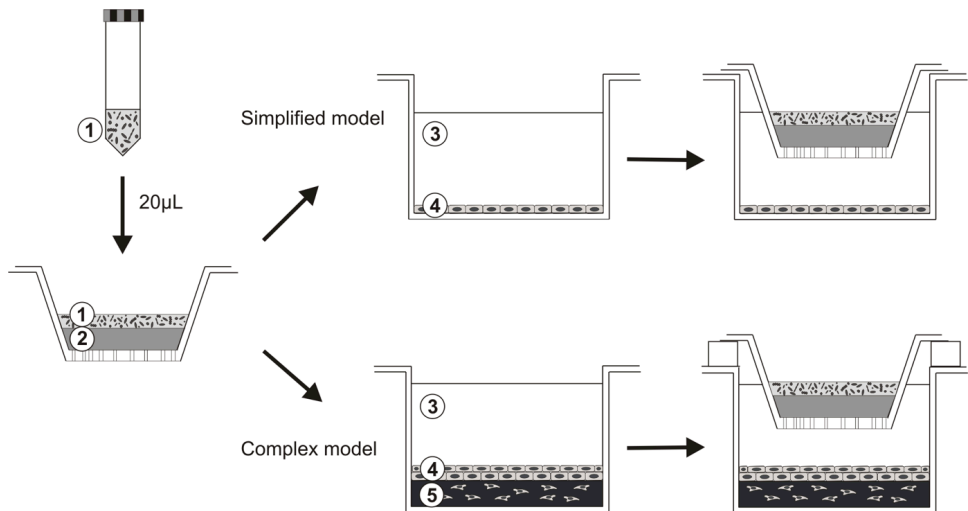


**Figure 2-1:** A schematic presentation of the *in vitro* model. Microbiota derived from a swab of the inner cheek (1) are grown on an agar/mucin layer (2). At the basolateral side, a monolayer of differentiated oral epithelium cells (4) is cultured on the bottom of the well (simplified model) or on top of a collagen type I layer embedded with fibroblasts (5) (complex model). The co-culture medium (3) between the 2 compartments comprises secretion products derived from both the cellular layer and the biofilm

Phase contrast pictures (Leica DMI 3000B) of unlabelled cells or fluorescent pictures (Zeiss Axiovert 200M) of DiI-labelled cells were taken on marked points along the wounded area at time 0. The inserts containing the oral biofilms were then transferred to the wells with the wounded monolayers and incubated at 37 °C and 5 % CO<sub>2</sub>. Dynamic experiments were carried out by putting the plates on a rotating shaker at 80 rpm for 24 h. Migration of the cells into the wounded area in the presence and absence of oral microbiota was assessed by comparing the micrographs after different time points of treatment. Each condition was tested at least three times. The relative distance (%) between the moving fronts of the wound was determined by calculating the difference between the non-recovered fronts after treatment time comparing with the initial fronts at time 0. For TR146 cells, relative wound surfaces (%) at different time points were calculated by use of a custom made macro in ImageJ.





30 s, 72 °C – 2 min) and a final extension at 72 °C for 10 min. For the DGGE, a 45-60 % gradient acrylamide gel was used. The DGGE profiles were analysed and clustered with the Bionumerics software 2.0. In brief, the calculation of similarities was based on the Pearson correlation coefficient. Clustering analysis was performed using the UPGMA to calculate the dendrograms of each DGGE gel.

### **2.3.6 Pyrosequencing**

For amplicon pyrosequencing, total DNA was extracted from the filters as described above. Barcoded amplicons were generated by using the FastStart High Fidelity Taq DNA Polymerase kit (Roche, Vilvoorde, Belgium), purified with the High Pure PCR Product Purification Kit (Roche, Vilvoorde, Belgium) and pooled equimolarly as determined by picogreen DNA concentration measurement. Emulsion PCR, emulsion breaking and sequencing were performed applying the GS FLX Titanium chemistry protocols and using a 454 GS FLX pyrosequencer (Roche, Vilvoorde, Belgium) as recommended by the manufacturer. The number of reads generated by pyrosequencing for each sample is listed in Table A1-1. The 454 pyrosequencing data were deposited to the European Nucleotide Archive (SRA) with accession number PRJEB5215. After processing the results, Operational taxonomic units (OTU) were classified using the RDP database. Details can be found in Addendum 1. To make sure technical variation in relative abundance of the samples is within acceptable range, duplicate analysis of the initial swab (0 h) was performed.

### **2.3.7 Live/dead staining and flow cytometry**

After 24, 48 and 72 h of incubation, the epithelial cells were collected together with the co-culture medium and centrifuged at 5000 rpm (Eppendorf Mini Spin) for 10 min. The entire supernatant was used for short chain fatty acid and lactate analysis. The cell pellets and the apical biofilms were suspended in 20 and 500 µL filtersterilized drinking water (Evian, local market), respectively. A live/dead staining of microbiota was performed with SYBR Green and propidium iodide as described before by Grootaert et al. (2011). Flow cytometry was carried out using a Cyan ADP flow cytometer (Dako, Glostrup, Denmark) with a laser emitting a fixed wavelength of 488 nm. Green fluorescence was collected at 530 nm, red fluorescence was collected at 670 nm. Measurement of the samples within one experiment was always done at the same speed and the amount of analysed sample volume was determined based on calibration with Dako Cytocount beads (Dako, Heverlee, Belgium).

### **2.3.8 Short chain fatty acid (SCFA) analysis**

After 24, 48 or 72 h, the co-culture medium (Figure 2-1 (3)) was removed between the apical and basal compartment (simplified model) and used for SCFA analysis. Acetate, propionate, butyrate, isobutyrate, valerate, isovalerate, caproate and

isocaproate concentrations were determined using a diethyl ether extraction as described before (Alander et al., 1999; De Boever et al., 2000). Briefly, 1 mL of the samples was acidified using 0.5 mL H<sub>2</sub>SO<sub>4</sub> after which 0.4 g of NaCl and an internal standard were added. SCFAs were extracted in 1 mL diethyl ether during 2 min by putting the closed tubes on a tumbling rotator (45 rpm). A GC-2014 (Shimadzu) with FID detector and split injector was used. The injection volume was 1 µL and the temperature profile was set from 110 to 160 °C, with a temperature increase of 6 °C/min. The column was a capillary fatty acid-free column (EC-1000 Econo-Cap column, Alltech, Belgium, 25 m × 0.53 mm; film thickness 1.2 µm). The carrier gas was nitrogen, and the temperature of the injector and detector were 200 and 220 °C respectively.

### **2.3.9 Lactate analysis**

L- and D-lactate concentrations of the co-culture media were determined by use of the D-lactic acid/L-lactic acid (UV method) kit of R-biofarm (Roche, Vilvoorde, Belgium). For this 100, 20 and 2 µL of respectively solution 1, 2 and 3 of the kit was brought in a 96 well plate and background absorbance at 340 nm was measured. D- and L-lactate dehydrogenase (2 µL) were allowed to react 45 min before measuring absorbance at 340 nm, after which concentrations could be calculated.

### **2.3.10 pH measurements**

pH estimations of low volumes of co-culture medium were done by an in-house developed spectrophotometric method based on phenol red discoloration of the medium. Over the pH range 6.8 - 8.2, a gradual colour transition from yellow to red (Abs<sub>max</sub> at 436 and 560 nm, respectively) can be observed. pH of the co-culture medium was estimated using a standard curve created by adding acetic acid to 200 µL DMEM medium followed by measuring pH and absorbance ratios at 436 and 560 nm (436 nm/560 nm) with a spectrophotometer (Paradigm, Molecular devices, United States).

### **2.3.11 MTT analysis**

Metabolic activity and viability of cells can be evaluated using a MTT assay (Mosmann, 1983). In short, 1 mg/mL of 3-(4,5-dimethylthiazol-2-yl)-2,5-diphenyl-tetrazolium bromide was added to each well and cells were incubated at 37 °C. After 2 h, all media was discarded and formazan crystals were dissolved in 1 mL DMSO. Absorbance at 570 nm was measured with a spectrophotometer (Paradigm, Molecular devices, United States).

### **2.3.12 SRB analysis**

Sulforhodamine B colorimetric assay (SRB) was used to determine the total cell number (Vichai and Kirtikara, 2006). After treatment, cells were fixed with 250  $\mu\text{L}$  50 % TCA for 1 h at 4 °C, rinsed with tap water and dried overnight. After staining with SRB (0.4 % in 1 % glacial acetic acid) for 0.5 h all wells were washed 5 times with 1 % glacial acetic acid to remove excess stain. After drying, cell-bound dye was dissolved in 100  $\mu\text{L}$  of 10  $\text{mmol}\cdot\text{L}^{-1}$  Tris buffer (pH 10.5). Absorbance values were measured at 490 nm with a spectrophotometer (Paradigm, Molecular devices, United States).

### **2.3.13 Lactate dehydrogenase (LDH) analysis**

By use of the CytoTox 96<sup>®</sup> Non-Radioactive Cytotoxicity Assay (Promega, Leiden, The Netherlands), the presence of lactate dehydrogenase in the co-culture medium was quantitatively measured to determine the percentage of necrotic cells. Cells of one well were lysed to determine the maximum amount of LDH release (100 %). Co-culture medium was collected, centrifuged at 270 g during 4 min and 50  $\mu\text{L}$  of the supernatant was transferred to a 96 well plate together with 50  $\mu\text{L}$  of substrate. After a 30 min incubation period protected from light, 50  $\mu\text{L}$  stopping solution was added and absorbance values were measured at 490 nm with a spectrophotometer (Paradigm, Molecular devices, United States).

### **2.3.14 Western Blot**

For Western blot analysis, cells were washed three times with Phosphate buffered solution (PBS) and lysed with 150  $\mu\text{L}$  of Laemmli 1x. After sonication, samples were centrifuged at 14 000 rpm for 5 min, the concentration of the supernatants was adjusted to 1  $\text{mg}/\text{mL}$  by adding sample buffer (Laemmli 1.5x, 5 % bromophenol blue and 5 %  $\beta$ -mercaptoethanol) and boiled for 5 min at 95 °C and 900 rpm. Proteins were separated on a 10 % or 16 % poly-acrylamide gel and transferred to a nitrocellulose membrane (GE Healthcare, Diegem, Belgium). For immunostaining, a 1:1000 dilution of the mouse monoclonal anti-PARP (Poly-adenosine-di-phosphate-ribose polymerase) antibody (BD, Erembodegem, Belgium) and a 1:200 dilution of the goat-polyclonal Caspase-3 p11 antibody (Santa Cruz, Texas, USA) were used as primary antibodies, followed by a horseradish peroxidase-labelled secondary anti-mouse (GE Healthcare, Diegem, Belgium) and anti-goat antibody (Santa Cruz, Texas, USA).

### **2.3.15 E-cadherin staining**

Prior to staining, cells seeded on glass coverslips in the Transwell® plate were fixed with ice-cold methanol. After blocking with 5 % Bovine Serum Albumin (BSA), cells were incubated for 1 h with 0.2  $\mu\text{g}/\text{mL}$  HECD-1 human anti-E-cadherin antibody

(Takara, Shiga, Japan) in a 1 % solution of BSA in Tris-Buffered saline (TBS) buffer. After washing with TBS, cells were incubated for 45 min with the secondary antibody (1/1000 Alexa-fluor®, anti-mouse 594 nm from goat IgG, Life technologies Europe, Gent, Belgium), 1 % BSA and 1/100 4'-6-diamidino-2-phenylindole (DAPI) in TBS. After washing, coverslips were mounted with glycergel and pictures were taken with the fluorescence microscope (Zeiss Axiovert 200M).

### **2.3.16 Ki67 staining**

For determination of the proliferation index, cells were stained for the Ki67 protein. After methanol fixation, coverslips were blocked with 5 % of BSA and incubated for 1 h with Ki67 ready to use solution (Thermo scientific, Erembodegem, Belgium). After washing the coverslips with TBS, 1/1000 secondary anti-rabbit antibody (Alexa-fluor® 594 nm) and 1/100 DAPI in TBS was added for 45 min. Next, coverslips were washed three times with PBS and mounted with Glycergel mounting medium (Dako, Heverlee, Belgium) after which pictures were taken with the fluorescence microscope (Zeiss Axiovert 200M).

### **2.3.17 Haematoxylin eosin (H&E) staining**

The oral mucosa layers were fixed with buffered formalin and embedded in paraffin. 8 µm slices of the paraffin embedded collagen gels were deparaffinized in xylene and rehydrated by transferring them sequentially to xylene/ethanol (1:1), 100 % ethanol or isopropanol, 96 % ethanol, 70 % ethanol and finally distilled water. For the haematoxylin-eosin staining, the slides were incubated in Harris' haematoxylin (Sigma-Aldrich, Diegem, Belgium) for 2 min and submerged briefly in 0.1 M HCl. After washing in running tap water for 10 min, they were incubated in eosin y Gurr® (0.1 % in water (w/v)) (VWR, Leuven, Belgium) for 1 min, dehydrated and mounted with fluoromount. Micrographs were made by use of a light microscope (Leitz Dialux 20).

### **2.3.18 Von Gieson staining**

After deparaffinization, collagen in the mucosa layer was visualized using the Von Gieson staining protocol. For this, slides were incubated for 5 min with Celestin blue solution (0.5 % Celestin blue, 5 % ammonium ferric sulphate)(Sigma-aldrich, Diegem, Belgium), rinsed in distilled water and stained with Mayer's haematoxylin solution (Sigma-aldrich, Diegem, Belgium). After washing in running tap water for 5 min, glasses were brought in Curtis stain (90 mL saturated aqueous picric acid solution, 10 mL glacial acetic acid, 10 mL 1 % Ponceau S (Sigma-Aldrich, Diegem, Belgium)) for 5 min. Quick dehydration in 95 %, 100 % EtOH and xylene was followed by fluoromount mounting. Micrographs were made by use of a light microscope (Leitz Dialux 20).

### 2.3.19 Alcian blue staining

To visualize the mucins, alcian blue staining was performed. For this the agar/mucin layers were fixed in paraformaldehyde and embedded in paraffin. 8  $\mu\text{m}$  sections of the gels were hydrated and stained for 0.5 h in 1 % alcian blue solution (3 % acetic acid, pH 2.5) with 1/100 dilution of DAPI. After rinsing in distilled water, slides were dehydrated and mounted with fluoromount. Images were obtained using a fluorescent light microscope (Leitz Dialux 20).

### 2.3.20 Statistics

SPSS Statistics 21 was used for statistical analysis of the results. Normality (Shapiro-Wilk test) and equality of variances (Levene test) was verified. Depending on those results, a Student's t-test or Wilcoxon rank sum test was performed.

## 2.4. Results

### 2.4.1 Characterization of the *in vitro* oral mucosa model

#### *Epithelial monolayer and oral mucosa*

The set-up of our simplified and complex oral mucosa model is shown in Figure 2-1. Preparation and co-culture of the two different compartments is described in the materials and methods section. The simplified model comprises an oral biofilm grown on a layer of agar/mucin and co-cultured for 24 h in presence of an epithelial monolayer. In the complex model, epithelial cells were seeded and allowed to differentiate on a collagen type I layer embedded with fibroblasts prior to challenge with the microbial compartment. In order to establish a differentiating epithelial monolayer in serum-free conditions, we first evaluated the effect of the agar/mucin insert (without microbiota) on the viability of TR146 and HaCaT monolayers. Viability of TR146 monolayers was not affected by the presence of the agar/mucin insert ( $p=0.06$ ), while a small, but significant decrease in metabolic activity of HaCaT monolayers could be observed ( $\sim 10\%$ ;  $p=0.001$ ) after 24 h (Figure A1-1a). Further, no phenotypical changes of the cells could be noticed and the expression and localisation of E-cadherin, as differentiation marker and important cell-cell adhesion molecule, remained unaffected (Figure A1-1b). Next, we evaluated the effect of the reconstituted oral biofilm grown on the agar/mucin insert on the morphology and differentiation status of the epithelial monolayers. Immunostaining showed no alteration in localisation and/or expression levels of E-cadherin in the presence of the oral biofilm (Figure A1-1c). Although cells remained morphologically intact, there was a minor reduction in epithelial viability of 15.6 % in presence of microbiota ( $p<0.001$ ) (data not shown).

In the complex model, the collagen layer embedded with fibroblasts was prepared 2 days prior to seeding of the TR146 cells. After 6 days of incubation and 2 days of biofilm co-culture, the collagen matrix was fixed, embedded in paraffin for sectioning and stained with H&E (Figure 2-2a). The fibroblasts were nicely spread and stretched within the collagen matrix (Figure 2-2c - arrowheads), which is covered by 1-2 layers of TR146 cells (Figure 2-2b - arrows). Von Gieson staining of the mucosa highlighted the network of collagen fibres, which was particularly concentrated at the epithelium-collagen interface (Figure 2-2d - arrows). The epithelial layer remained intact even after 48 h of co-culturing with microbiota in serum free conditions (Figure 2-2e).

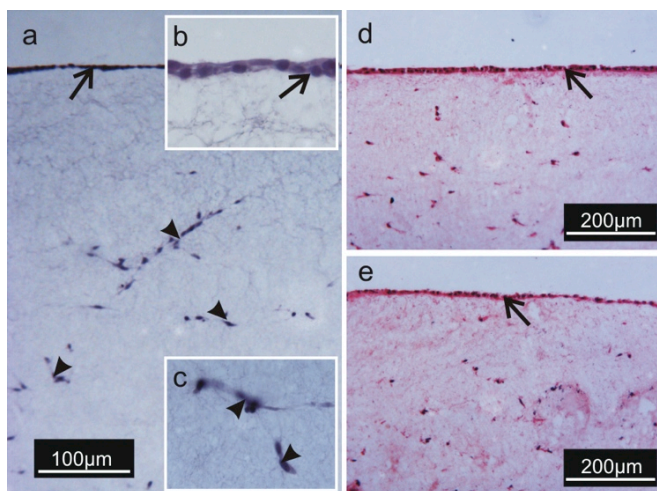


**Figure 2-2 a: H & E staining of the collagen layer covered with TR146 cells (arrows; b) and embedded with fibroblasts (arrowheads; c). d, e: Von Gieson staining on the collagen layer in absence (d) or presence (e) of microbiota. Arrows indicate a concentrated layer of collagen fibers**

### *Oral biofilm*

The oral biofilm was reconstituted as described in material and methods. To enumerate the correlation between the microbiota from the buccal swab and the reconstituted biofilm, 16S rDNA gene based DGGE profiling and pyrosequencing analysis were performed. First, a kinetic experiment was performed with microbiota separately derived from oral swabs of two healthy individuals. Microbiota were cultured in BHI or on an agar/mucin filter and samples were taken after 0, 6, 24 and 48 h in absence of epithelial cells. Figure 2-3a shows the results of the DGGE profiling and cluster analysis of oral microbiota.

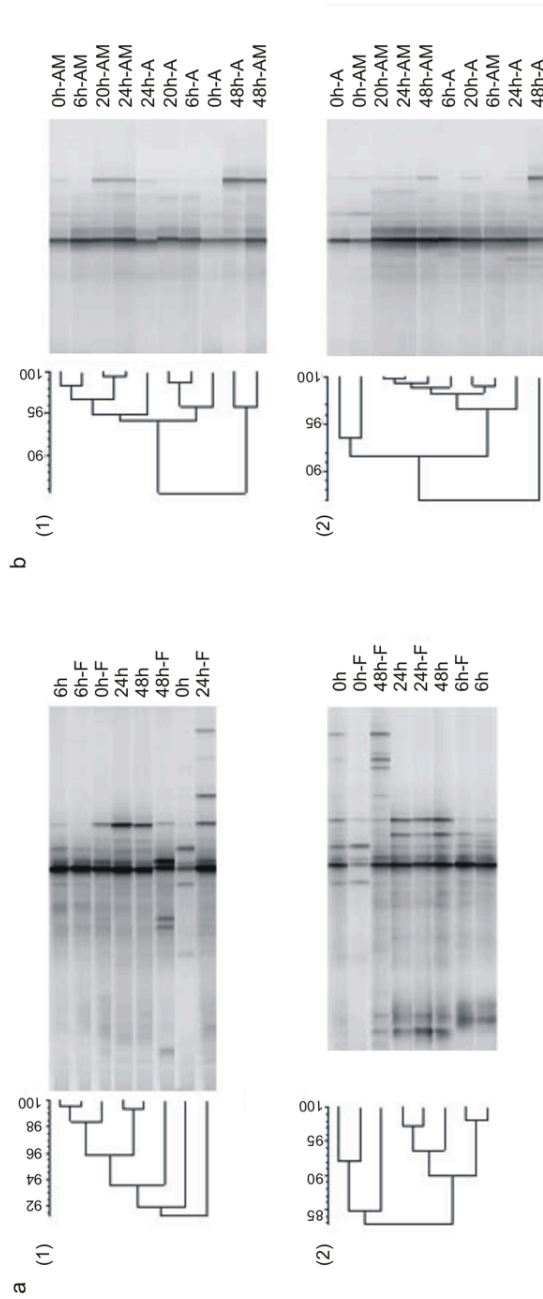


**Figure 2-3 a: DGGE profiling and cluster analysis of oral microbiota derived from buccal swabs of 2 healthy individuals cultured in BHI broth (0h, 6h, 24h, 48h) or on the agar/mucin filter (0h-F, 6h-F, 24h-F, 48h-F). b: Oral microbiota derived from buccal swabs of 2 healthy individuals cultured on an agar filter (A) or on an agar/mucin filter (AM) on different time periods (0, 6, 20, 24 and 48 h)**



The data suggest only minor shifts in microbial composition due to culturing (Pearson correlation > 83 %). By comparing DGGE profiling of oral microbiota of the same individuals cultured on a layer of agar (A) alone or in presence of mucins (AM), we observed > 90 % similarity in biofilm composition after 24 h between the initial oral swab composition and the biofilms cultured in presence of mucins (Figure 2-3b). With regard to the structure of the biofilm, alcian blue staining shows a homogeneous network of mucins in the agar-mucin layer (Figure 2-4). Aggregates of microbiota could be observed in the mucin matrix as evidenced by DAPI staining of a cross-section of the agar/mucin layer.

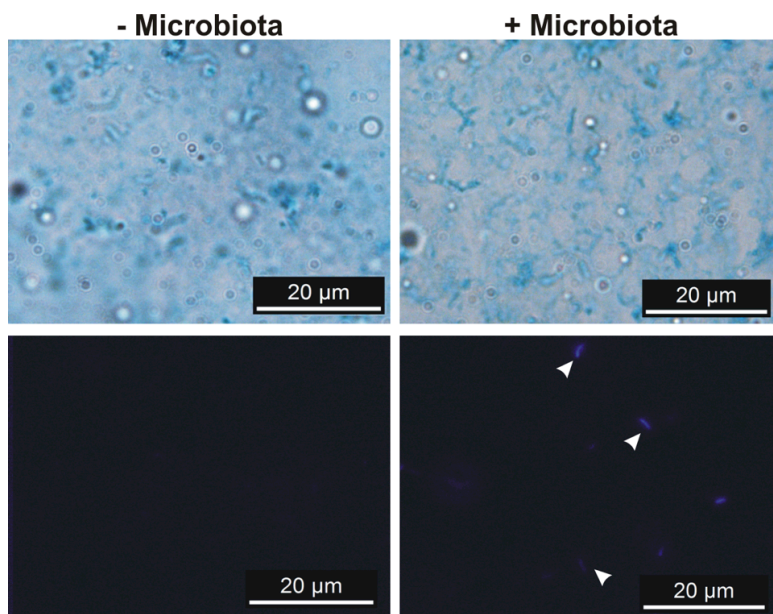


**Figure 2-4: Alcian blue and DAPI staining of a representative cross-section of the agar/mucin layer in presence or absence of microbiota (arrowheads).**

Next, we evaluated the effect of the epithelial cells on the viability and composition of the biofilm. To enumerate the microbiota in the biofilm (apical), flow cytometry was used after 24, 48 and 72 h. Table 2-1 shows that in absence of epithelial cells, ~7 log/mL microbial cells could be recovered from the apical side. Interestingly, significantly less microbiota (~5-6 log/mL) were counted in presence of an epithelial monolayer at the different time points ( $p_{24h} = 0.018$ ;  $p_{48h} = 0.002$ ;  $p_{72h} = 0.004$ ). We further counted the microbiota in the basal co-culture medium, however no microbial cells were observed above detection limit (< 3 log/mL) even after 3 days of co-culture. Microbial absence in the basal media was also confirmed by use of plating techniques.

This shows that the model is suitable for long-term host-microbiota co-culture studies in absence of direct microbe-epithelial contact.

**Table 2-1: The number of microbiota (log/mL) in the apical and basal compartment of the model after 24, 48 or 72 h of incubation (n= 3).**

Compartment	Time (h)	- Cells	+ Cells
Apical	24	6.9 ± 0.36*	5.9 ± 0.27*
	48	7.1 ± 0.04*	5.2 ± 0.44*
	72	7.2 ± 0.12*	6.0 ± 0.33*
Basal	24	N.D.	N.D.
	48	N.D.	N.D.
	72	N.D.	N.D.

N.D.: not detected; \*p < 0.05

Live/dead staining followed by flow cytometric analysis of the apical microbiota showed a clear shift in the microbial community in presence of epithelial cells (Figure 2-5). From the side scatter (SS) log/forward scatter (FS) log plot, it was clear that the microbiota have a larger size (FS) and complexity (SS) after 24 and 48 h of incubation when TR146 cells are present ((1) and (3) compared to (2) and (4)). At the same time, the community fingerprint showed more living microbiota when TR146 cells were absent, as indicated by the 670 log/530 log plots ((7) and (9) compared to (8) and (10)). Yet, at 72 h of incubation, the amount of live populations had increased again in the presence of TR146 cells, in both plot types ((5) and (11) compared to (6) and (12)), which may indicate the growth of those populations that adapted to the presence of TR146 cells. These results demonstrate a clear impact of the TR146 cells on the residing microbial community.

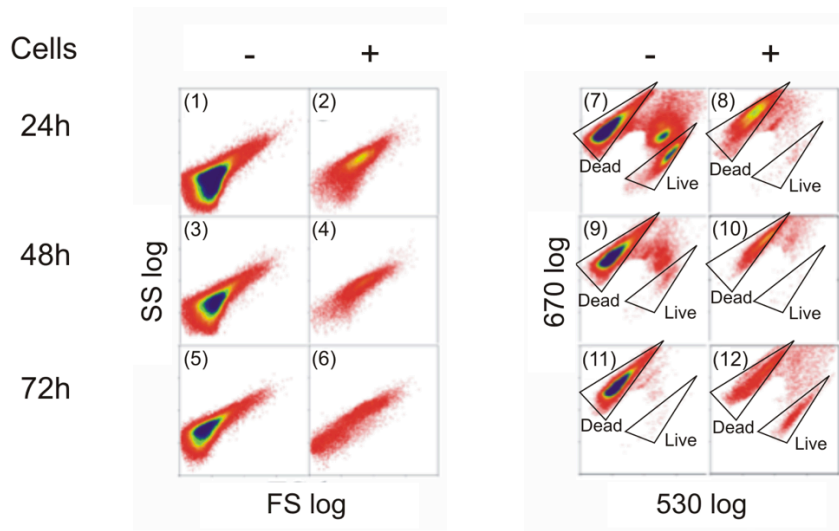


**Figure 2-5: Flow cytometric fingerprint of the microbial community in the apical compartment in absence or presence of TR146 cells after 24, 48 and 72 h of incubation**

Since epithelial cells appeared to have an important impact on the flow cytometric fingerprints, 454 pyrosequencing was performed to evaluate the composition of the biofilm in different model set-ups. Duplicate pyrosequencing analysis of the initial swab revealed only limited technical variation in relative abundances; all relevant families were detected on both filters, with *Streptococcaceae* as most abundant family (Figure A1-2). We compared the relative abundance of microbiota colonizing a layer of agar or agar/mucin without epithelial cells and on an agar/mucin insert in the simplified or complex model (Figure 2-6). After 24 and 48 h, *Firmicutes* are most abundantly present, irrespective of the set-up. The main shifts were found in the 5 % of non-streptococci species, although it should be noticed that these values concern relative abundances. Plating analysis of the inoculum (3-4 log CFU/filter) and the apical compartment after 24 h of incubation (~6 log CFU/filter) revealed a total growth of 2-3 log CFU/filter within 24 h. Taking this into account, the shift in relative abundance of non-streptococcal species from 5 to 0.5 % still implies a growth of these species of 1-2 log CFU/filter. Considering their absolute numbers, non-streptococcal species therefore manage to survive and grow during co-culture and are able to communicate and interact with the underlying mucosa. In general, 454 pyrosequencing results suggest good preservation of the oral microbiota, with shifts found in only 5 % of the total population.

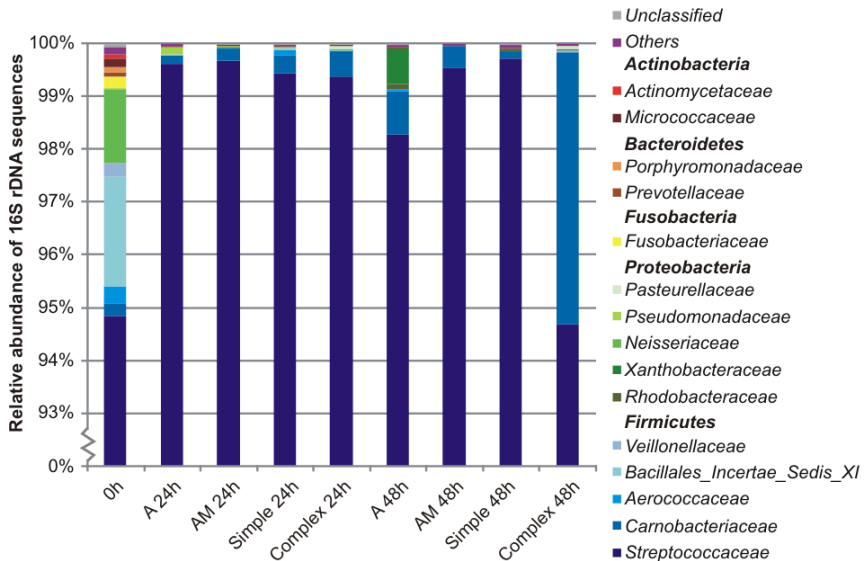


**Figure 2-6: Analysis of the microbiota cultured for 0, 24 or 48 h on an insert with agar (A) or with agar/mucin without cells (AM), in presence of a monolayer of TR146 cells (simple) or with cells cultured on a collagen type I matrix (complex). 454 pyrosequencing results of 16S rDNA assigned to family, grouped in the different phyla are shown**

## 2.4.2 Applications of the model

### Wound healing

The *in vitro* model was used for assessment of wound healing in presence or absence of oral microbiota. Different types of keratinocytes were tested, namely TR146 (oral squamous cell carcinoma cell line), HaCaT (immortalised keratinocyte cell line), and normal patient derived keratinocytes from the epidermis. First, the effect of oral microbiota on wound healing of a differentiated layer of keratinocytes was evaluated. Fluorescent images of the wounds (Figure A1-3a panel (1)) were taken at 0 and 24 h and analysed with a customized ImageJ macro (Figure A1-3a panel (2); see materials and methods), overlay pictures (Figure A1-3a panel (3)) were obtained to check the accuracy of the surface calculation. Green lines represent the edges of the wounds used to calculate the wound surface in the macro. Figure 2-7a shows that wound healing was significantly reduced by ~ 30 % ( $p < 0.001$ ) after 24 h in presence of microbiota. Although less pronounced, the same effect could be observed with the HaCaT cells after 24 h (~ 15 %;  $p = 0.009$ ) and normal keratinocytes after 65 h ( $p_{24h} = 0.925$ ; ~ 15 %,  $p_{65h} < 0.001$ ). These observations were also confirmed using our complex model with an epithelial layer covering a collagen type I gel. Wound healing was reduced with > 40 % in presence of microbiota, although only significantly after

48 h ( $p_{24h}=0.134$ ;  $p_{48h}=0.002$ ) for TR146 cells. Using HaCaT cells, we found a reduction of 30 % after 48 h, although this was not significant ( $p_{24h}=0.85$ ;  $p_{48h}=0.055$ ) (Figure 2-7b). Figure A1-3b and c represent schematic overviews of the wound scratch assay in the simplified and complex model.

We further aimed to mimic the dynamic environment of the oral cavity more closely by subjecting the model to continuous rotation at 80 rpm for 24 h. However, similar results for the wound scratch and MTT assay were obtained as in static conditions (Figure A1-4a and b). At the microbial side, shaking conditions resulted in a minimal increase in microbial diversity (mean variability within group 13 %; versus 14 % between groups) (Figure A1-4c).

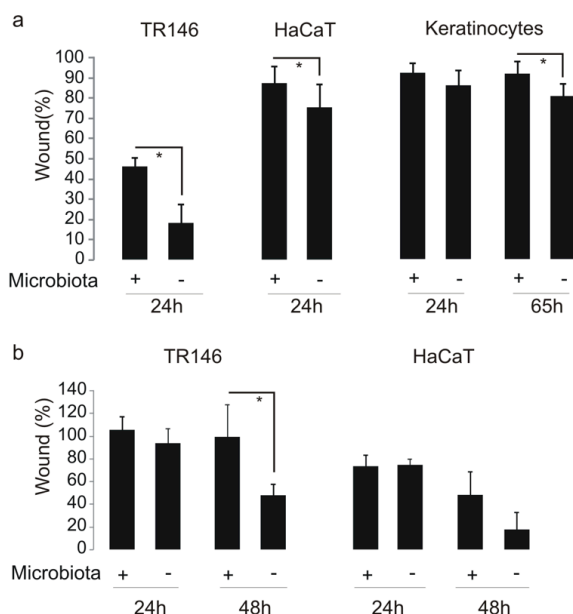


**Figure 2-7 a: Wound healing capacity of TR146 cells (n= 6), HaCaT cells (n= 12) or primary keratinocytes (n= 12) in absence or presence of oral microbiota in the simplified model (mean + SD; \* p< 0.05). b: Effect of microbiota on wound healing in the complex model after 24 and 48 h with TR146 (n= 6) and HaCaT cells (n= 4) (mean + SD; \* p<0.05)**

#### *Analysis of the co-culture medium*

Due to the modular design of the model, collection and analysis of the basal co-culture medium containing both host- and biofilm-derived metabolites is easy and straightforward. To discriminate the contribution of the microbiota on the release of metabolites of interest, experiments were performed in presence or absence of epithelial cells. Figure 2-8 shows the levels of D-, L-lactate and acetic acid in the co-culture medium collected after 24, 48 and 72 h in presence of microbiota. D-lactic acid

was only detected at low concentrations (< 200 µg/mL) and in absence of epithelial cells ( $p_{24h}=0.024$ ;  $p_{48h}<0.001$ ;  $p_{72h}=0.071$ ). A similar trend was observed for the short-chain fatty acid acetate, where higher levels were recovered in absence of epithelial cells ( $p_{24h}<0.001$ ;  $p_{48h}=0.001$ ;  $p_{72h}=0.122$ ). Presumably, the epithelial cells have an impact on the metabolism and/or secretion of D-lactate and acetate.

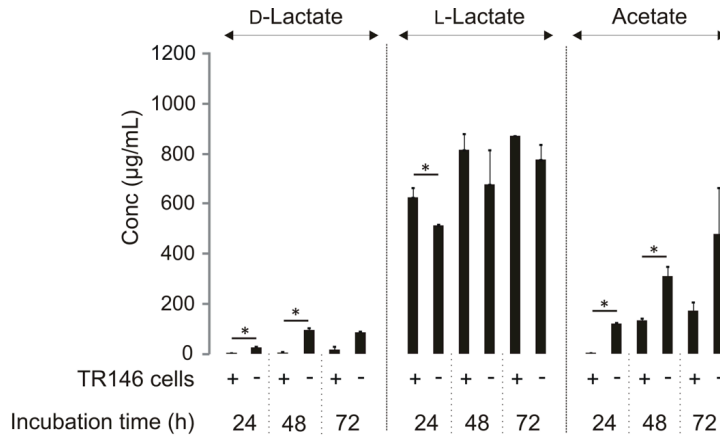


**Figure 2-8: Concentrations of D-, L-lactate and acetate in the co-culture medium after 24, 48 or 72 h in presence or absence of TR146 epithelial cells in the model (n = 8; mean + SD; \* p < 0.05).**

In contrast, an inverse trend was observed for L-lactic acid, where higher levels were detected in presence of epithelial cells ( $p_{24h}=0.005$ ;  $p_{48h}=0.193$ ;  $p_{72h}=0.119$ ). In general, high basal levels of L-lactate were present in the co-culture medium (600-1000 µg/mL) without microbiota pointing to the substantial secretion of L-lactate by TR146 cells.

pH estimations of a small volume of the co-culture medium can be performed via an in-house developed colorimetric method as described in materials and methods. Figure A1-5 shows the correlation between the absorbance ratios  $OD_{436nm}/OD_{560nm}$  and corresponding pH values of co-culture medium in presence or absence of microbiota and buffered with 0, 25 or 50 mM  $NaHCO_3$ . It is clear that, at buffering concentrations of 25 mM  $NaHCO_3$ , pH values were normalised to ~ 7.2 in presence of microbiota. Figure 2-9 shows that buffering of the co-culture medium resulted in partial, but non-significant ( $p_{0-25mM}=p_{0-50mM}=1$ ) recovery of wound healing, indicating that other factors contribute to the inhibitory effect of microbiota on wound healing.

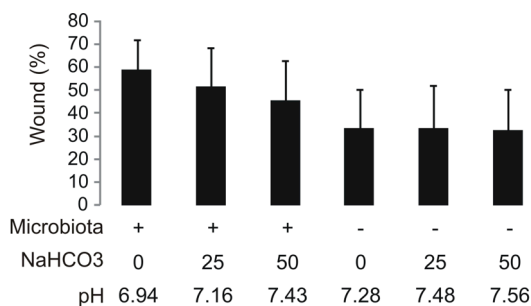


**Figure 2-9: Wound healing of TR146 cells in presence or absence of microbiota when buffered with different concentrations of NaHCO<sub>3</sub> together with their respective pH values (n = 4; mean + SD)**

When wound scratch assays were performed with lactate and acetate at similar concentrations as found in the co-culture medium in presence of microbiota, namely 10 mM (*i.e.* 900 and 600 µg/mL for lactate and acetate resp.), no effect on wound recovery was observed (Figure 2-10).

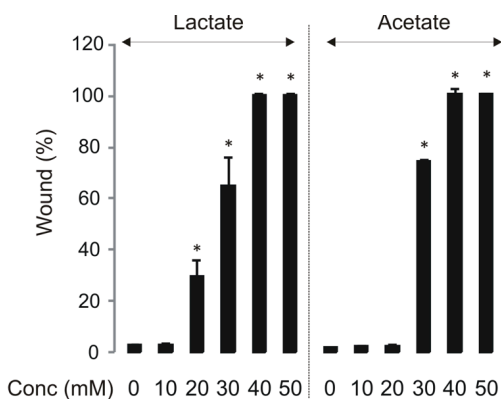
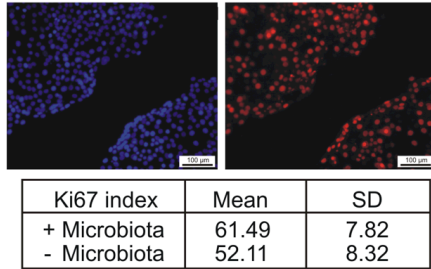


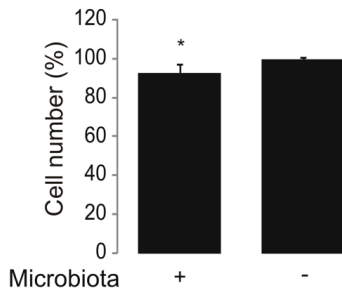
**Figure 2-10: Wound healing of TR146 cells in presence of different concentrations of acetate or lactate (n = 3; mean + SD; \* p < 0.05)**

We further investigated the hypothesis that microbiota might have an effect on the proliferation rate or might induce apoptosis or necrosis of epithelial cells and in that way reduce epithelial recovery. Figure 2-11a shows that the Ki67 staining revealed no significant difference between conditions with and without microbiota (p = 0.112). Also, although significant (p = 0.01), the protein content, measured by the SRB assay, decreased only slightly (7 %) in presence of microbiota (Figure 2-11b). Additionally, no significant increase in necrotic or apoptotic cells was observed when microbiota were present as evidenced by an LDH assay (p = 0.747) (Figure 2-11c) or the analysis of PARP cleavage (89 kD fragment) (p = 0.643) and caspase-3 activation (p11 subunit) (p = 0.492) (Figure 2-11d).

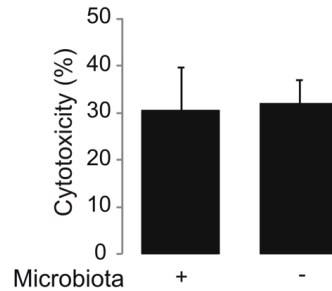
a



b



c



d

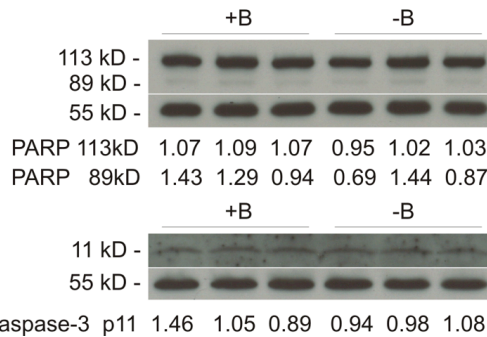


**Figure 2-11 a: Ki67 staining and index (n= 5), b: SRB analysis (n= 5), c: LDH analysis (n= 6) and d: Western blot analysis (n= 3) and relative intensities of PARP cleavage and caspase-3 activation of TR146 cells after culturing for 24 h in presence or absence of microbiota (mean + SD; \* p< 0.05)**

## 2.5. Discussion

We present a new *in vitro* model of the oral mucosal microenvironment including an *ex vivo* generated oral biofilm. Different models have been developed to mimic the oral mucosa *in vitro* (reviewed by Moharamzadeh et al. (2007, 2012)). However, none of the described models have incorporated a fully functional microbial biofilm. Our



aim was to develop an *in vitro* model to study the interactions between the oral mucosa and its associated biofilm in time frames representative for the *in vivo* situation. Technically, there are some advantages of the modular set-up of our model: i) the co-culture medium is easy to refresh and collect for further analysis; ii) the oral biofilm can be analysed separately from the epithelium; iii) the choice of the pore size of the semi-permeable membrane allows working in presence or absence of direct microbe-epithelial contact.

Our model is designed for the study of indirect host-microbe interactions by using a pore size that avoids microbial migration. As different regions of the oral cavity are colonised by their specific biofilms (Aas et al., 2005; Segata et al., 2012), it is important to have the potential to reconstitute a biofilm in the model representative to the preferred *in vivo* situation by defining the precise swab site or by manipulating the different starting inoculates of the species of interest. The observed shifts in microbial composition are unavoidable due to the transfer of microbiota from an *in vivo* to an artificial environment (Van den Abbeele et al., 2009). However, the overall similarity of the original composition was very high. Furthermore, we showed that the microbiota present in the reconstituted biofilm were dominated by the genera *Firmicutes* and *Proteobacteria* (Segata et al., 2012) similarly to what is found in the mouth. 454 pyrosequencing revealed shifts in abundances, mainly situated in the non-streptococcal regions. Although these values seem to point to a loss in non-streptococcal species, in absolute numbers the non-streptococcal species increased with 1-2 log CFU/filter, demonstrating their growth capability in the *in vitro* model. Further research is needed to quantify absolute growth rates of the different species in the model. The most abundant families present in the oral swab sustained in the model and genera like *Gemella*, *Abiotrophia*, *Veillonella*, *Granulicatella* and *Rothia*, which have been described to colonize the oral cavity, were also found on the filters (Table A1-2)(Aas et al., 2005; Bik et al., 2010; Chen et al., 2010; Dewhirst et al., 2010; Segata et al., 2012). Altogether, we have shown that our new model is an *in vivo* representation of the oral microbiome found in a non-diseased health state, though harbouring potential harmful species.

In terms of the applicability and functionality of our model, we were able to identify several crosstalks between the microbial biofilm and the epithelial cell layer. First, flow cytometry analysis showed that the presence of the epithelial layer had a negative impact on the number of microbiota residing within the biofilm. Moreover, the microbiota differ also in size, complexity and diversity of physiological states when cultured in presence of the epithelium. However, at this stage we can only speculate about a possible explanation and/or relevance of this observation, since it is the first time that an oral biofilm and its underlying mucosa have been successfully co-cultured in close proximity for > 24 h. The reduced number of microbial cells in

presence of host cells might be explained by the activation of host immune responses mediated by host pattern recognition receptors, like Toll-like receptors (TLR) and nucleotide-binding oligomerization domain protein receptors (NOD). Stimulation of these receptors is essential for the production of chemokines of which many possess an inherent antimicrobial activity (Dürr and Peschel, 2002; Ganz, 2003; Yang et al., 2003). Interestingly, Jiao et al. (2013) found an important role of NOD1 in periodontitis induced by *γ-proteobacteria*, belonging to the *Pasteurellaceae* family. Therefore, it is plausible that the *Pasteurellaceae* and possibly other microbiota present in our reconstituted biofilm trigger PRR-mediated responses, eventually leading to the reduced number of microbiota. Regarding the difference in composition of the oral biofilm when co-cultured with epithelial cells, one might speculate on a competition for nutrients. Glucose is the most important carbohydrate and nutrient source in the model and will be converted by both the epithelial cells as the microbiota. So plausibly, when cells are present, microbiota that are able to grow on other nutrient sources such as mucins are privileged.

On their turn, the biofilm microorganisms will ultimately have an effect on the epithelial cells as evidenced in this study by their effect on wound recovery. It has already been reported that low levels of bacterial cells may stimulate wound recovery, but once a critical level of bacteria is exceeded, the repair process will be prolonged (Bucknall, 1980; Edwards and Harding, 2004). Here, we show that acidification of the medium may be partly responsible for the reduced wound healing as buffering of the co-culture medium to pH 7 or 7.4 (= buffering capacity of saliva) only reduced but not completely abolished the microbial effect. Also, we have shown that acetate and lactate did not negatively influence wound healing capacity at concentration measured in our model. SCFAs are known to alter a whole range of host responses (Jeng et al., 1999; Grootaert et al., 2011b) and they have been shown to promote migration of colonic epithelial cells at concentrations (2-16 mM) comparable to those measured in our model (2-10 mM), however in other cell types this observation could not be confirmed (Wilson and Gibson, 1997). Since direct effects of the microbiota on epithelial cell proliferation or cell death by apoptosis or necrosis could also be excluded, we are currently following a proteomic approach to identify factors present in the co-culture medium that are important for wound healing.

In our model, we mainly used the human oral-derived squamous cell carcinoma cell line TR146, in analogy with the existing oral mucosa models (Jacobsen et al., 1995) or the reconstructed Human Oral Epithelium (HOE) designed by the SkinEthic Laboratories. Although these cells do not develop into a fully differentiated oral epithelium, they remain desirable for the use in screening models because they are easy to culture and the results have a high reproducibility and a low batch-to-batch variability (Moharamzadeh et al., 2008b, 2012). Furthermore, TR146 cells also

express E-cadherin at their cell surface, a molecule that is part of the adherent junctions of normal epithelial cells and which is instrumental in maintaining cell-cell adhesion (Lewis et al., 1995; Baum and Georgiou, 2011). Yet, we also considered the use of an epithelial cell line of non-cancer origin and proved the obtained results with HaCaT cells, an immortalized keratinocyte cell line, or primary keratinocytes similar to the ones with TR146 cells.

Additional development and optimization steps were followed to make the model more representative, reproducible and semi-high-throughput: i) addressing the fact that the oral mucosa is far more complex than a simple monolayer of epithelial cells and that interaction between keratinocytes and fibroblasts are important during wound healing (Werner et al., 2007), we optimized our model using a collagen matrix embedded with NIH-3T3 fibroblasts, inspired by the group of Dongari-bagtzoglou & Kashleva (2006), who developed a very similar and successful co-culture model of human epithelial cell lines with murine fibroblasts. Nevertheless, it would also be possible to use fibroblasts of the human, non-cancerous oral cavity, like it was described in the model of Rautava et al. (2012). ii) we developed an easy technique that created wounds at the level of the keratinocyte layer without intruding or harming the collagen matrix; iii) through a computerized automation step, wound healing could be evaluated in a high-throughput way both in absence or presence of a collagen matrix.

Although in this study we mainly focused on wound healing as an initial end point, the model also allows screening of other endpoints like biofilm architecture and composition, metabolic activity and phenotypic characteristics of the oral mucosa, and analysis of the microbial and/or cellular derived exometabolome. Moreover, the presented model can be used in a lot of different settings, such as the addition of antibiotics, growth factors, pro/prebiotics, using biofilms composed of single or multiple microbiota strains. This model will most certainly be helpful to identify factors important in host-microbe crosstalks.

## 3. MICROBIAL INHIBITION OF ORAL EPITHELIAL WOUND HEALING

---

*Modified from: De Ryck T, Vanlancker E, Grootaert C, Roman B, De Coen LM, Vandenberghe I, Stevens CV, Bracke M, Van de Wiele T, Vanhooecke B (2015). Microbial inhibition of oral epithelial wound recovery: potential role for quorum sensing molecules? AMB Express 5: 27.*

### 3.1. Abstract

Awareness of the impact of microbiota in both health and disease is growing. By use of our new *in vitro* oral mucosa co-culture model, we showed a clear inhibition of epithelial wound healing in the presence of an oral microbial community. In this chapter, we have used the same model in combination with specific oral microbial species to obtain a better insight into the role of the oral microbiota in wound healing. Monocultures of *Klebsiella oxytoca* and *Lactobacillus salivarius* significantly inhibited wound healing with ~20 %, whereas *Streptococcus mitis* and *Streptococcus oralis* enhanced the healing process with ~15 % in 24 h. Yet, neither *S. oralis* nor *S. mitis* were able to counteract the inhibitory effects from *K. oxytoca* on wound healing. Other tested microbial species had no effect on wound healing. Apart from this species-dependency, the inhibitory effect on wound healing depended on a microbial threshold concentration. Further mechanistic experiments with *K. oxytoca* suggest that quorum sensing molecules might play a role in the inter-kingdom signalling during wound healing, although further research is needed. These results are important for the development of new strategies for the management of wounds and ulcerations.

### 3.2. Introduction

Microbiota are omnipresent in the human body, where they are colonizing the skin, mouth, nose, ears, vagina and the intestinal tract, each with their particular community (Bik, 2009). Although awareness of the involvement of microbiota in human health and disease is growing, research in the area of non-infectious host-microbe interactions is complicated by the lack of suitable models due to the cytotoxicity of microbiota towards host cells in long-term experiments (Marzorati et

al., 2011). To circumvent this issue, most studies report the results of experiments with limited co-culture times (< 4h) or using microbial supernatant instead of living cultures. In this study, we applied our recently developed co-culture model to study host-microbe interactions during wound healing in absence of direct microbe-epithelial contact (De Ryck et al., 2014). By means of a semi-permeable membrane, microbiota and epithelial cells are physically separated, while metabolites and other secreted factors can pass the membrane. This enables the study of indirect crosstalks between the microbiota and the host epithelium for a timeframe up to 72h.

Wound healing and re-epithelisation are a set of complex processes that are initiated upon tissue injury. In many studies, oral wound healing is considered as a representative model for scarless and fast healing (Enoch and Stephens, 2009; Glim et al., 2013). Edwards and Harding (2004) reviewed the role of microbiota in chronic wounds, marking an important distinction between microbial colonization and infection. They showed that the presence of low numbers of microbiota in the injured tissue could improve the wound healing process, whereas lesions infected with large amounts of microbiota are characterised by poor healing. It is still largely unknown which microbial species, factors or activities have an impact on epithelial wound healing. Already in 1994, Okada showed that the healing of longitudinal skin incisions was enhanced in the presence of normal intestinal microbiota in comparison to wound healing in germ free mice. In contrast, Laheij et al. (2013) found that wounds infected with *Porphyromonas gingivalis*, *Prevotella nigrescens* and secretions of *P. gingivalis* strongly inhibited cell migration, whereas weaker inhibitory effects were found for *Prevotella intermedia*, *Tannerella forsythia* and *Streptococcus mitis*. These results confirm our previous observation that the oral microbiota may be involved in delayed wound healing (De Ryck et al., 2014).

Factors that have been shown to have an impact on wound healing are microbial cell wall components such as lipopolysaccharides (LPS) (Koff et al., 2006), microbial metabolites such as short chain fatty acids (SCFAs) (Wilson and Gibson, 1997) and other secreted factors such as the toxin C3-transferase from *Clostridium botulinum* (Aepfelbacher et al., 1997)

Previously, we showed an overall negative impact of oral microbiota derived from a buccal swab on wound healing of oral-derived epithelial cells (De Ryck et al., 2014). In this study, we aim to obtain a better understanding of the underlying mechanisms using mono- and mixed cultures of species known to be present in the oral cavity in healthy or diseased states.

### 3.3. Material and methods

#### 3.3.1 TR146 cell line

The TR146 cells, an oral squamous carcinoma cell line derived from a local lymph node metastasis, were kindly provided by Clare Hall Laboratories (Cancer Research UK). The cells were cultured in Dulbecco's modified Eagle's Medium (DMEM) (Gibco, Merelbeke, Belgium) supplemented with 10 % heat-inactivated fetal bovine serum (Greiner bio-one, Belgium), 22.8 µg/mL penicillin-streptomycin (5000 U/mL; Gibco, Merelbeke, Belgium) and 2.5 µg/ml amphotericin B (Bristol-MyersSquibb, Braine-l'Alleud, Belgium) at 37 °C and 10 % CO<sub>2</sub>. Cells were regularly checked for mycoplasma contamination (MycoAlert Mycoplasma Detection kit; Lonza, Rockland, USA).

#### 3.3.2 Microbial cultures

Different monocultures were obtained from the BCCM™/LMG bacteria collection (Ghent, Belgium). *Streptococcus salivarius* (LMG 11489), *S. oralis* (LMG 14553), *S. mitis* (LMG 14557), *S. pyogenes* (LMG 15868) and *Klebsiella Oxytoca* (LMG 3055) were cultured in BHI broth (Sigma-aldrich, Diegem, Belgium), *Lactobacillus salivarius* (LMG 9477), *L. oralis* (LMG 9848) and *L. plantarum* (LMG 9211) were cultured in MRS broth (Sigma-aldrich, Diegem, Belgium) and *Neisseria mucosa* (LMG 5136) was cultured in heart infusion broth (Sigma-aldrich, Diegem, Belgium).

*K. oxytoca* AHC-6 (WT), *K. oxytoca* AHC-6 Mut89 ( $\Delta$ nspB mutant) and *K. oxytoca* AHC-6 Mut89+nspB (pACYC184; complementation) were kindly provided by Prof. E. Zechner (Institute of Molecular Biosciences, University of Graz, Graz, Austria)(Schneditz et al., 2014). All strains were cultured in CASO broth (Sigma-aldrich, Diegem, Belgium) supplemented with 50 µg/mL kanamycin or 30 µg/mL chloramphenicol for the mutant and complementation strain respectively.

For microbial enumeration, suspensions were plated using the microdilution plating method, on BHI agar plates, MRS agar plates or CASO agar plates (BHI/MRS/CASO broth: Sigma-aldrich, Diegem, Belgium; 15 % agar: BD, Erembodegem, Belgium) and incubated at 37 °C. When plating mixed cultures, selective BHI agar plates with Listeria mono Selective Supplement I (Sigma-aldrich, Diegem, Belgium) were used for selectively culturing streptococci at 37 °C, whilst *K. oxytoca* was enumerated after incubating standard BHI plates at room temperature, as streptococci were not able to grow at room temperature.

#### 3.3.3 Chemicals

A filter-sterilized stock solution of 5 mg/mL sodium D-lactate (Sigma-aldrich, Diegem, Belgium) was prepared in serum-free, antibiotics-free DMEM, which was further

diluted in serum-free, antibiotics-free DMEM during the experiments to obtain the desired concentrations (100, 500, 1000, 5000 µg/mL).

The quorum sensing molecule N-(3-oxododecanoyl)-L-homoserine lactone (Sigma-aldrich, Diegem, Belgium) was dissolved in DMSO to obtain stock solutions of 15, 30, 45 and 60 mM. For experiments, further dilutions (1:500) in DMEM without serum and antibiotics were prepared.

For the synthesis of the pyrrolobenzodiazepine tilivalline, we followed the protocol described by Schneditz et al. (2014). However, we used the freeze-pump-thaw method (3x) instead of the vacuum/N<sub>2</sub> cycle (3x) for degassing the reaction. In this way a yield of 57 % was obtained compared to the previously reported 38 % (Schneditz et al., 2014).

For the *in vitro* experiments, stock solutions of 100, 50, 10, 5 and 1 mM tilivalline were prepared in DMSO, which were further diluted (1:1000) in DMEM without serum and antibiotics.

### **3.3.4 Co-culture model**

To co-culture microbiota and TR146 epithelial cells in absence of direct microbe-epithelial contact, we used our recently published model (De Ryck et al., 2014). Briefly, 75 µL of an agar/mucin solution (5 % porcine mucin type III (Sigma-aldrich, Diegem, Belgium), 0.8 % agar (BD, Erembodegem, Belgium)) was brought on the porous membrane (0.4 µm) of a 24-well plate Transwell® system (Corning inc., NY, USA) and allowed to solidify for at least 30 min after which 20 µL of a microbial suspension was spotted on top of this agar/mucin layer (apical compartment). In the basal compartment, a monolayer of epithelial cells was grown and a wound scratch assay was performed as described below. During co-culture, the inserts with the microbiota were transferred into the wells with the wounded epithelial cells. For experiments with pre-incubation, inserts with microbiota were incubated for 4 h in wells filled with serum-free, antibiotics-free DMEM without epithelial cells, prior to their transfer into the wells with wounded epithelial cells.

### **3.3.5 Wound scratch assay**

For the wound scratch assays, TR146 epithelial cells were seeded (300 000 cells/well) in a 24 well plate (in absence of microbiota; Nunc Thermo Scientific, Erembodegem, Belgium) or in a 24-well plate Transwell® system (co-culture model; Corning inc., NY, USA) after labelling with DiI cell labelling solution (Life technologies Europe, Ghent, Belgium). At the start of the experiment a scratch was created with a sterile plastic pipette tip, all medium was discarded to remove cellular debris and fresh serum-free, antibiotics-free DMEM was added on the cells. Micrographs of selected points along the wounds were taken with an automated fluorescence

microscope (Zeiss Axiovert 200M) at the start of the experiment and after 24 h of incubation at 37 °C and 5 % CO<sub>2</sub>.

In experiments using conditioned medium, the filter-sterile basal co-culture medium of experiments with *K. oxytoca* (inoculum concentration: 6 log colony forming units (CFU)/mL) was used and added on top of wounded epithelial layers. At the end of each experiment, cell viability was checked by use of an MTT assay, which was performed as described previously (De Ryck et al., 2014).

### **3.3.6 Cytokine analysis**

For cytokine analysis, we applied the Luminex platform (R&D Systems Europe, Abingdon, UK). By use of the multiplex kits (R&D Systems Europe, Abingdon, UK), concentrations of IL-1 $\beta$ , IL-6, TNF- $\alpha$  and Rantes in the basal conditioned medium of the co-culture model were determined following the manufacturer's protocol.

### **3.3.7 Lactate analysis**

For the determination of L- and D-lactate concentrations in the co-culture media, we used the D-lactic acid/L-lactic acid (UV method) kit of R-biofarm (Roche, Vilvoorde, Belgium) as described previously.

### **3.3.8 Glucose analysis**

By use of the CMA 600M Microdialysis Analyser (CMA Microdialysis AB, Solna, Sweden), glucose concentrations present in the basal conditioned medium were determined following the manufacturer's protocol using the glucose reagent (CMA Microdialysis AB, Solna, Sweden ; Barham and Trinder, 1972).

### **3.3.9 Effects of glucose on wound healing**

To test the effect of glucose on wound healing, different mixtures of serum-free, antibiotics-free DMEM with low glucose (1 g/L glucose; Gibco, Merelbeke, Belgium) and high glucose (4.5 g/L glucose; Gibco, Merelbeke, Belgium) were used.

### **3.3.10 Fractionated conditioned medium**

Basal medium of previous experiments in presence or absence of *K. oxytoca* was collected and sequentially fractionated using Amicon centrifugal filters (pore size: 3 and 10 kD; Merck Millipore, Overijse, Belgium) (Figure A2-1a). The wound healing capacity in presence of the control-conditioned medium (absence of *K. oxytoca*) was compared to the control-conditioned medium in which particular fractions ( $x > 10$  kD;  $10$  kD  $> x > 3$  kD) were interchanged with the same fraction of *K. oxytoca*-conditioned medium. For the fraction below 3 kD, the control-conditioned fraction  $< 3$  kD was compared to the *K. oxytoca*-conditioned fraction  $< 3$  kD (Figure A2-1b).



### **3.3.11 Proteinase K treatment of conditioned medium**

Conditioned medium of *K. oxytoca*-exposed cells was treated with proteinase K (200 µg/mL; Sigma-aldrich, Diegem, Belgium) during 1 h at 37 °C. After cooling down on ice for 5 min, the medium was boiled at 98 °C for 10 min and centrifuged during 10 min at maximum speed to inactivate the enzyme. The supernatant was further filter-sterilised before use in a wound scratch assay. Proteinase activity and subsequent inactivation were checked using bovine serum albumin (Sigma-aldrich, Diegem, Belgium) dissolved in DMEM as a control protein.

### **3.3.12 Matrix-assisted laser desorption/ionization Time-of Flight (MALDI-TOF) analysis**

For MALDI-TOF analysis of the conditioned medium fraction < 3 kD, samples of control-conditions and *K. Oxytoca*-exposed cells (< 3 kD) were treated with SPE STRATA X (Phenomex, Utrecht, The Netherlands). Different fractions (drain, washing steps of 5, 10 and 50 % methanol and the eluate with 50/50 ACN/MeOH) were concentrated using a vacuum centrifuge (Speedvac SC110 concentrator, NY, USA). MS and tandem MS spectra were acquired on a 4800 Plus MALDI TOF/TOF analyzer (ABSCIEX, Framingham, USA), using the delayed extraction and reflector technologies in the positive ion mode. Instrument calibration was performed using the 4700 mass standard kit from Applied Biosystems (Life Technologies, Ghent, Belgium).

### **3.3.13 Tris-Tricine gel analysis**

The medium fraction < 3 kD of control conditions and *K. oxytoca*-exposed cells was concentrated (10X) by lyophilisation followed by dissolving in loading buffer (200 mM Tris-HCl (pH 6.8), 2 % SDS, 40 % glycerol, 0.04 % Coomassie brilliant blue, 2 % β-mercapto-ethanol). Peptides were separated on a Mini protean® Tris-Tricine precast gel (Bio-Rad laboratories, Eke, Belgium) as described in the manufacturers protocol. After fixation in 50 % methanol and 10 % acetic acid during 30 min, the gel was stained for 1 h in a Coomassie Brilliant blue R-250 staining solution (Bio-Rad laboratories, Eke, Belgium). Destaining of the gel was performed in a 5 % methanol/7 % acetic acid/H<sub>2</sub>O solution until the desired background was obtained.

### **3.3.14 Statistics**

For statistical analysis of the different experiments, Shapiro-Wilk analysis was used to check normality of the data. Depending of the normality and the experiment student's t-tests, ANOVA, Kruskal Wallis or Mann Whitney U analyses were performed. Bonferroni correction was used when performing multiple comparisons. All analyses were performed using the SPSS Statistics 22 software package and differences were considered significant at the  $p < 0.05$  level.

## 3.4. Results

### 3.4.1 Microbial effects on wound healing: mono- and mixed cultures

Wounded TR146 epithelial cells were exposed to 5.5–6 log CFU of *S. salivarius*, *S. oralis*, *S. mitis*, *S. pyogenes*, *L. salivarius*, *L. oralis*, *L. plantarum*, *N. mucosa* or *K. oxytoca* monocultures for 24 h (no pre-incubation). These microbiota are all known to be present in the oral cavity, with streptococci as most important habitant. *S. salivarius*, *S. oralis* and *S. mitis* are frequently isolated from the healthy oral cavity. *S. pyogenes* was added to the test panel as a known virulent *Streptococcus* spp. causing for example pharyngitis. *Lactobacillus* spp. are less abundant in the oral cavity (< 1%), but were chosen for their ability to induce acidification. Furthermore, *N. mucosa* is a microbe known to colonize the mucosal surfaces within the oral cavity and *K. oxytoca* is mainly isolated from the oral cavity after irradiation for head and neck cancer (Marsh and Martin, 1999). Remarkably, wound healing was only significantly reduced in the presence of *L. plantarum* (-20 %; p= 0.003) and *K. oxytoca* (-26 %; p= 0.007). In contrast, *S. oralis* significantly enhanced wound closure after 24 h (+15 %; p= 0.022) and *S. mitis* showed a similar trend (+13 %; p= 0.054) (Figure 3-1; black bars). All p-values are listed in Table A2-1a.

The different outcome depending on the type of species could be explained by the fact that some species grew better on the agar/mucin substrate during co-culture than others. Enumeration of the microbiota after 24 h of co-culture with TR146 cells indeed revealed important differences in survival between the test species. The number of streptococci was strongly reduced to ~1 log CFU during co-culture, whereas lactobacilli and *K. oxytoca* grew steadily with another 2-3 log units (Figure 3-1, Table A2-1b).

In order to evaluate whether immediate confrontation of the microbiota with TR146 cells was detrimental for the establishment of a biofilm on an agar/mucin substrate, monocultures of test species were added to the substrate 4 h prior to confrontation with the wounded TR146 monolayers (4 h pre-incubation). When we included this pre-incubation step, also *S. salivarius* (-33 %) and *L. salivarius* (-27 %) had a significant negative impact on wound healing (p< 0.001). In contrast, *S. oralis* consistently and significantly stimulated wound closure after 24 h (+22.5 %; p= 0.029), while *S. mitis* displayed a trend to enhance wound healing (+22 %; p= 0.081; Table A2-1a) (Figure 3-1; white bars). All streptococci were at least present at 3 log CFU/filter after 4 h of pre-incubation (Figure 3-1, Table A2-1b). From these experiments, we can conclude that i) the effect of wound recovery is species-dependent and ii) there seems to be a strong correlation between the number of *S. salivarius* and the effect on wound healing.

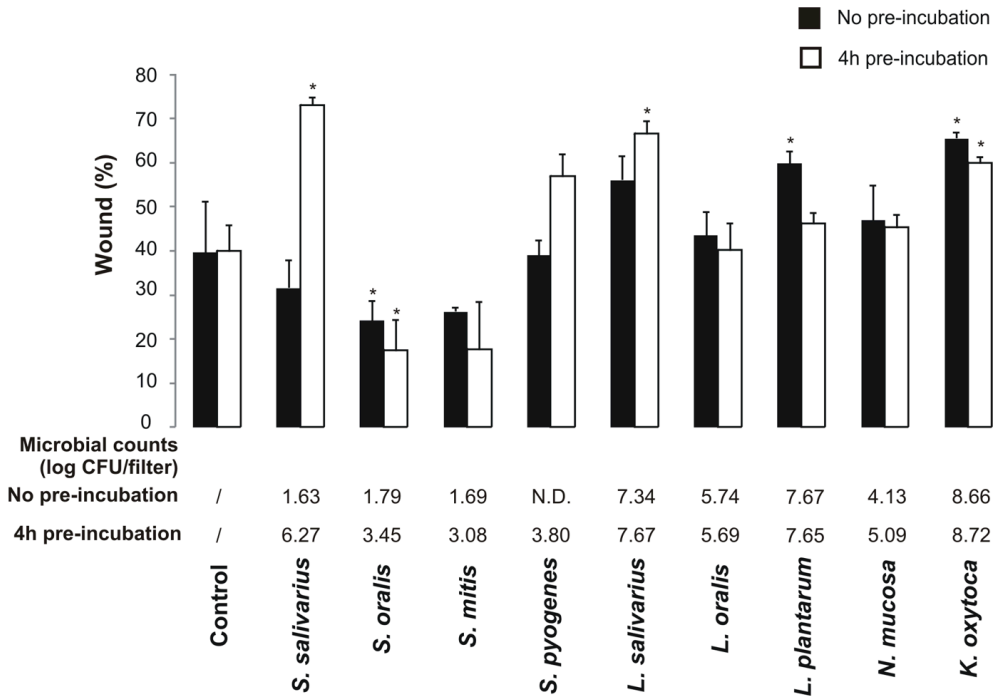


**Figure 3-1: Wound healing capacity of TR146 epithelial cells confronted with inserts containing 5.5-6 log CFU of monocultures of different oral species. The relative area of the wound after 24 h is plotted (n= 3; mean + SD; \*p< 0.05). The black bars represent data from experiments performed without pre-incubation of the microbial cells on the insert, the white bars represent data from experiments with a 4 h pre-incubation step of the microbiota before confrontation with the epithelial cells. Mean microbial counts of the different species present on the filters after 24 h of co-culture with TR146 epithelial cells are depicted (n= 3; N.D. = not detected)**

Cytokine analysis of the basal medium collected after 24 h of co-culture revealed no direct link between the type and concentration of cytokines released and the effects on wound healing. While a significant increase of IL-1 $\beta$  was observed for *S. oralis* (p= 0.008), no significant changes as compared to levels in the control conditions could be noticed for the other test species. Rantes was significantly reduced in presence of *S. oralis*, *S. mitis* and *S. pyogenes* (p= 0.017; p= 0.020; p= 0.016 resp.) but not in presence of the other species (Figure 3-2, Table A2-2). TNF- $\alpha$  and IL-6 levels remained largely unchanged. Overall, the microbiota-induced release of cytokines in TR146 is low in our model, which is probably due to the absence of direct microbe-epithelial contact.

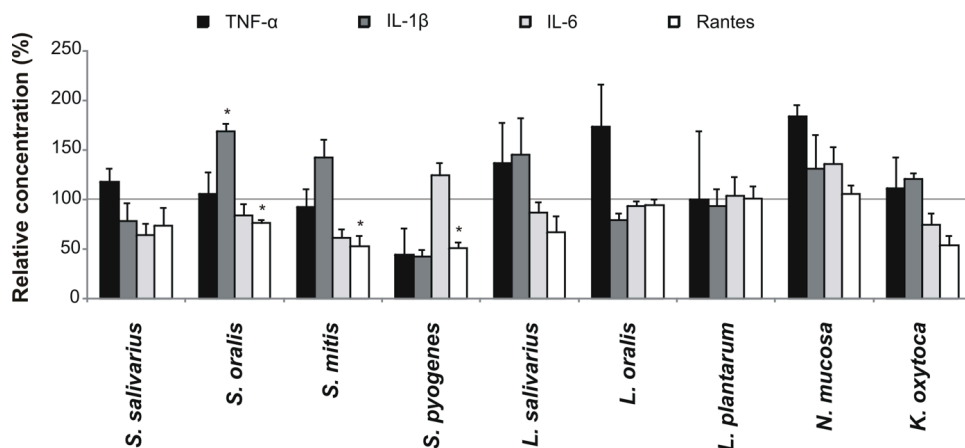


**Figure 3-2: Cytokine analysis of the basal conditioned medium. The microbial monocultures of different oral species were pre-incubated for 4 h before confrontation with the TR146 cells for 24 h. Relative concentrations are shown (n= 3; mean + SD; \*p< 0.05)**

As microbial growth requires energy, microbial metabolism will reduce the glucose concentrations present in the co-culture medium (with pre-incubation). The glucose concentration in the co-culture medium of *K. oxytoca*-exposed cells was significantly decreased to 2.238 mg/mL (p= 0.009) (Table 3-1), whereas a non-significant drop was noticed with *S. salivarius* and *L. salivarius* (p= 0.081). However, further experiments using glucose concentrations ranging from 1 g/L to 4.5 g/L (standard cell culture medium), showed no differences in wound healing (p= 0.148; Figure 3-3a). This made us conclude that glucose-depletion by microbial activity is probably not the underlying mechanism for wound healing inhibition.

**Table 3-1: Concentrations of glucose, L- and D-Lactate found in the basal cell culture medium after 24 h of co-culture of the TR146 cells with different oral microbial species (n= 3; mean ± SD; \*p< 0.05). Microbiota were pre-incubated for 4 h on the insert, before they were exposed to the wounded TR146 cells**

	Glucose (mg/mL)	L-Lactate (µg/mL)	D-Lactate (µg/mL)
<i>Control</i>	3.374 ± 0.388	619.51 ± 66.64	2.89 ± 7.34
<i>S. salivarius</i>	2.498 ± 0.140	930.13 ± 53.90*	3.17 ± 1.91
<i>S. oralis</i>	3.523 ± 0.153	568.29 ± 9.40	3.76 ± 6.76
<i>S. mitis</i>	3.744 ± 0.100	543.57 ± 26.44	-0.79 ± 4.50
<i>S. pyogenes</i>	3.440 ± 0.061	680.60 ± 9.89	9.11 ± 0.69
<i>L. salivarius</i>	2.658 ± 0.034	817.63 ± 6.82*	239.49 ± 15.72*
<i>L. oralis</i>	3.610 ± 0.085	636.80 ± 11.66	18.22 ± 2.99
<i>L. plantarum</i>	3.041 ± 0.023	522.31 ± 27.73	408.86 ± 40.25*
<i>N. mucosa</i>	3.445 ± 0.047	608.82 ± 23.53	5.15 ± 6.86
<i>K. oxytoca</i>	2.238 ± 0.218*	343.48 ± 26.22	215.13 ± 72.28

We further questioned if the release of acids like L- and D- lactic acid in the co-culture medium (with pre-incubation) could explain the inhibiting effect of certain species on wound healing (Table 3-1). At least for *S. salivarius* and *L. salivarius* higher levels of L-lactate (930.1  $\mu\text{g}/\text{mL}$ ,  $p= 0.027$ ; 817.6  $\mu\text{g}/\text{mL}$ ,  $p= 0.027$  resp.) were found compared to the control condition (without microbiota; 619.5  $\mu\text{g}/\text{mL}$ ). However, no elevated levels were observed for *K. oxytoca*. D-lactic acid concentrations were dramatically increased in presence of *L. salivarius* and *L. plantarum* (239.5  $\mu\text{g}/\text{mL}$ ,  $p= 0.027$ ; 408.9  $\mu\text{g}/\text{mL}$ ,  $p= 0.027$  resp.) and, although not significantly, also in presence of *K. oxytoca* (215.1  $\mu\text{g}/\text{mL}$ ,  $p= 0.153$ ). Exogenous D-lactic acid only showed inhibiting effects on wound healing at concentrations starting from 5000  $\mu\text{g}/\text{mL}$  (Figure 3-3b). Previously, lactic and acetic acid were found to inhibit wound healing starting at 1800  $\mu\text{g}/\text{mL}$  and thus not at concentrations that were found in the model (De Ryck et al., 2014). Together, these results indicate that acids do not play a major role in the effect on wound healing.

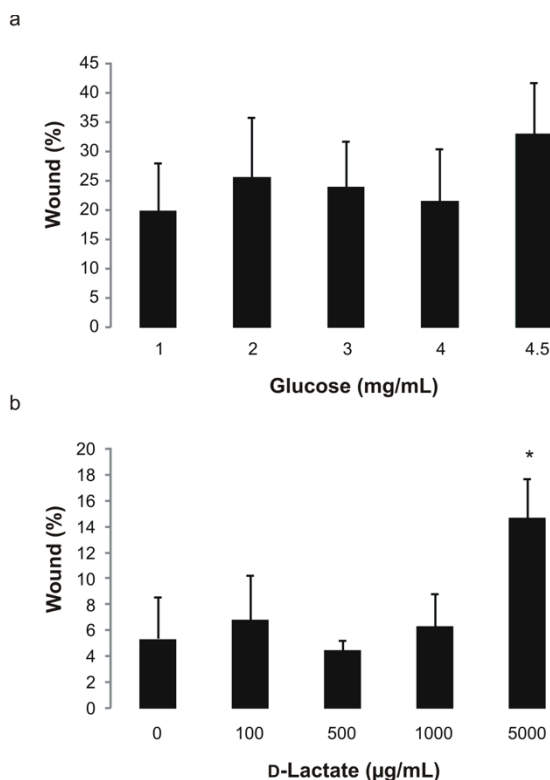
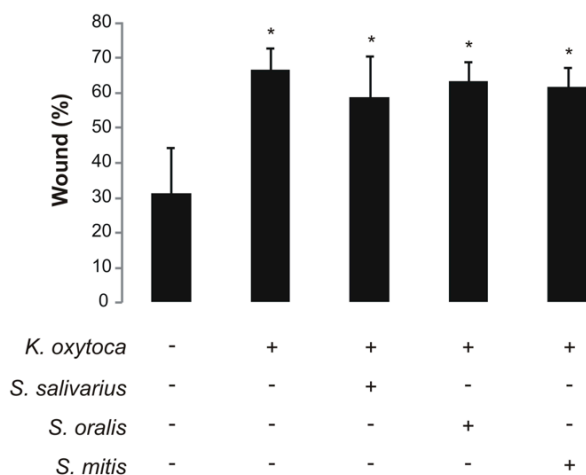


**Figure 3-3 a: Wound healing capacity of TR146 cells in cell culture medium with different glucose concentrations (n= 7; mean + SD; \* $p < 0.05$ ). b: Wound healing capacity of TR146 cells treated with different D-lactic acid concentrations (n= 4; mean + SD; \* $p < 0.05$ )**

In addition to monocultures, we also evaluated the effect of mixed cultures of *S. salivarius*, *S. oralis* or *S. mitis* with *K. oxytoca* (no pre-incubation) on the wound healing of TR146 cells. Overall, we found a dominant negative effect on wound healing, probably due to the presence of *K. oxytoca*. Whereas monocultures of *S. oralis* and *S. mitis* had a stimulating effect on wound healing, these two strains were completely unable to counteract the inhibitory effect of *K. oxytoca* towards wound healing (Figure 3-4a). This may be explained by the 5 log higher microbial counts for *Klebsiella* compared to streptococci after 24 h (Figure 3-4b).

a



b

	0 h (log CFU/filter)		24 h (log CFU/filter)	
	<i>Klebsiella</i>	<i>Streptococci</i>	<i>Klebsiella</i>	<i>Streptococci</i>
<i>K. oxytoca</i>	4.38	/	8.50	/
<i>K. oxytoca</i> + <i>S. salivarius</i>	4.62 ± 0.12	5.03 ± 0.05	8.67 ± 0.05	3.97 ± 0.02
<i>K. oxytoca</i> + <i>S. oralis</i>	4.05 ± 0.04	5.13 ± 0.26	8.56 ± 0.05	3.65 ± 0.22
<i>K. oxytoca</i> + <i>S. mitis</i>	4.26 ± 0.18	5.79 ± 0.02	8.49 ± 0.04	3.76 ± 0.57

**Figure 3-4 a: Wound healing capacity of TR146 epithelial cells confronted with *K. oxytoca* alone or mixed with *S. salivarius*, *S. oralis* or *S. mitis* (n= 6; mean + SD; \*p< 0.05). b: Microbial counts of *K. oxytoca* or mixtures of *K. oxytoca* with *S. salivarius*, *S. oralis* or *S. mitis* present on the insert at time 0 and after 24 h of co-culture with TR146 epithelial cells (n= 6; mean ± SD)**

### 3.4.2 The involvement of small microbial molecules in wound healing

Due to its dominating negative effect and its well-known virulence, we chose *K. oxytoca* as a model organism to further elucidate the mechanism underlying its effects on wound healing.

As shown in Figure 3-5, the basal conditioned medium collected after 24 h of co-culture of TR146 cells and *K. oxytoca*, was also able to exert inhibitory effects on wound healing. This suggests an inhibitory effect of a cellular or microbial factor present in the co-culture medium. Treatment of the conditioned medium with leupeptin (a protease inhibitor) or proteinase K (a broad-spectrum serine protease) did not significantly alter this inhibitory effect ( $p_{\text{control-K.oxytoca}} < 0.001$  in all 3 cases) indicating that the effect is probably not due to the activity of a protease or a protein (Figure 3-5).

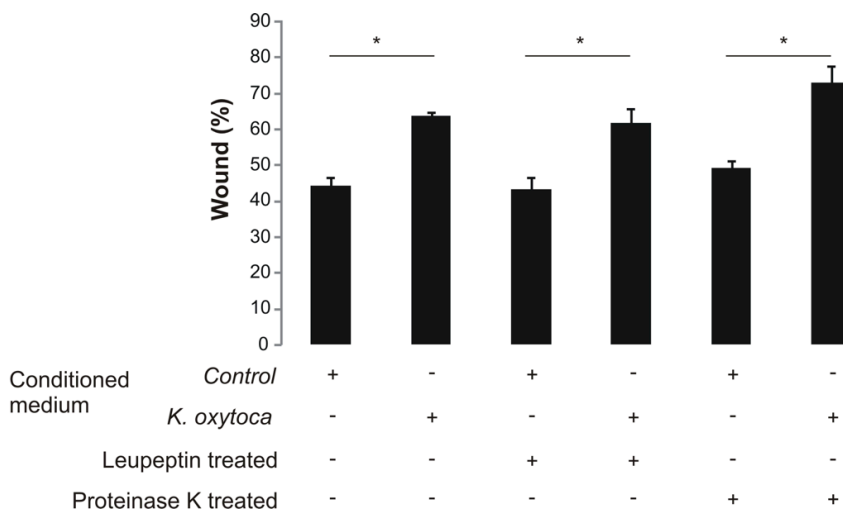


**Figure 3-5: Wound healing capacity of TR146 epithelial cells in presence of the conditioned medium of *K. oxytoca*-exposed TR146 cells (n=4; mean + SD; \*p < 0.05). Leupeptin- or proteinase K-treatment of the conditioned medium was performed as described in Materials and methods**

Next, we tested 3 different fractions of the *K. oxytoca*-conditioned medium. Whilst the protein fraction > 10 kD and the fraction between 3 and 10 kD of the *K. oxytoca*-conditioned medium showed no inhibitory effect ( $p = 1$ ), fully *K. oxytoca*-conditioned medium (unfractionated) and the fraction < 3 kD caused a significant reduction in wound healing ( $p < 0.001$ ) (Figure 3-6, Figure A2-1). We therefore concluded that a small molecule or peptide present in the fraction < 3 kD of the *K. oxytoca*-conditioned medium is likely to be responsible for the effect on wound healing. Unfortunately, separation on a tris-glycine gel and visualisation by Coomassie staining of the < 3 kD fraction of both the control- and *K. oxytoca*-conditioned medium did not reveal clear differences (data not shown). Using MALDI-TOF analysis, we could identify one peptide that was less abundant in the control sample compared to the eluate of the

*K. oxytoca*-conditioned sample (\* in Table A2-3). Yet, further MS/MS analysis of this peptide pointed to background artefacts or medium compounds.

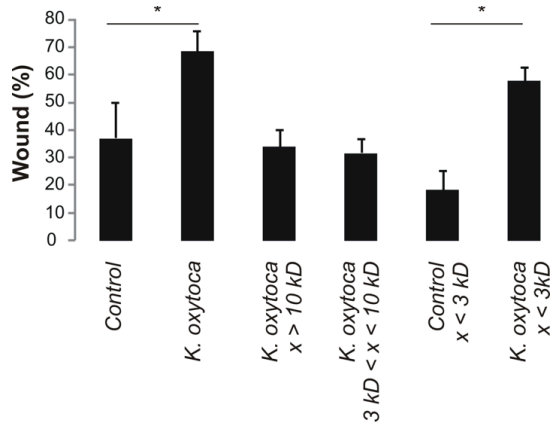


**Figure 3-6: Wound healing capacity of TR146 epithelial cells in presence of different fractions of the *K. oxytoca*-conditioned medium (n= 4; mean + SD; \*p< 0.05). Full conditioned medium was tested together with 3 different fractions > 10 kD, 3 kD < x < 10 kD and < 3 kD**

Altogether, these results indicate that at least for *K. oxytoca* the inhibitory factor is likely to be a small molecule different from an acid or a small peptide. One such molecule produced by *K. oxytoca* and recently reported to be toxic for epithelial cells is tilivalline (Schneditz et al., 2014). Therefore, we studied the epithelial wound healing capacity in the presence of synthetic tilivalline and found a significant inhibition when tilivalline was present at concentrations starting from 5  $\mu\text{M}$  ( $p_{0-1\mu\text{M}}= 0.325$ ,  $p_{0-5\mu\text{M}}= 0.01$ ,  $p_{0-10\mu\text{M}}= 0.01$ ,  $p_{0-50\mu\text{M}}= 0.01$ ,  $p_{0-100\mu\text{M}}= 0.01$ ; Figure 3-7).

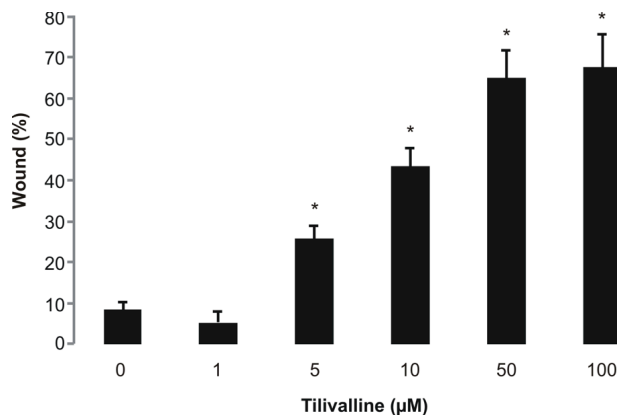


**Figure 3-7: Wound healing capacity of TR146 cells treated with different concentrations of tilivalline (n= 6; mean + SD; \*p< 0.05)**



At these concentrations a higher amount of death, floating cells was observed, although the viability of the adherent cells was not affected (data not shown). To further investigate the potential of tilivalline, we performed co-culture experiments with different tilivalline-mutant *K. oxytoca* strains. Unlike the AHC-6 wild type and Mut89+nspB strain, the Mut89 strain is unable to produce tilivalline (Schneditz et al., 2014). Unfortunately, all 3 tested *K. oxytoca* strains (AHC-6, Mut89 and Mut89+nspB) inhibited epithelial wound healing significantly ( $p < 0.001$ ), showing no differences between the 3 strains ( $p = 1$ ) (Figure 3-8 a, b). These results exclude the involvement of tilivalline in the microbial effects on epithelial wound healing in our model.

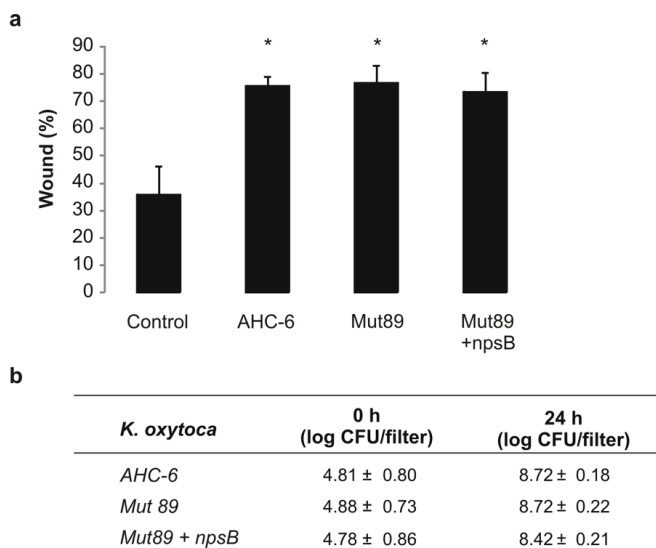


**Figure 3-8 a: Wound healing capacity of TR146 cells exposed to *K. oxytoca* AHC-6 wild type, the  $\Delta$ npsB mutant Mut89 unable to produce tilivalline and the Mut89 with npsB complementation (n= 6; mean + SD; \* $p < 0.05$ ). b: Microbial counts of the different *K. oxytoca* strains (AHC-6, Mut 89, Mut89+npsB) present on the insert at time 0 and after 24 h of co-culture with TR146 epithelial cells (n= 6; mean ± SD)**

Last, we tested the hypothesis that quorum sensing molecules might be involved in the inhibition of wound healing. We chose to test N-(3-oxododecanoyl)-L-homoserine lactone as this molecule has been shown to induce apoptosis in epithelial breast cancer cells (Li et al., 2004). Starting from 90  $\mu$ M, a significant decrease in wound healing capacity was observed ( $p_{90\mu M} = 0.012$ ;  $p_{120\mu M} = 0.02$ ; Figure 3-9).

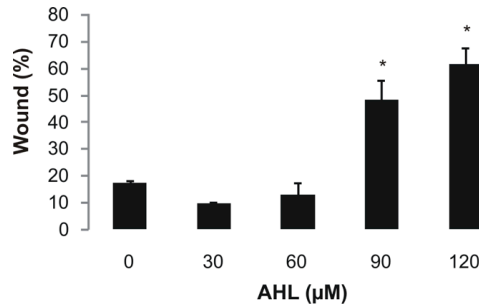


**Figure 3-9: Wound healing capacity of TR146 cells treated with different concentrations of N-(3-oxododecanoyl)-L-homoserine lactone (AHL) (n= 2; mean + SD; \*p< 0.05)**

### 3.5. Discussion

The human epithelium is the most important barrier for all physical, chemical or biological attacks on the human body. In case of acute damage, wound healing processes are very important to protect the inner tissues. Pathogenic infections of the wound are known to delay wound healing (Edwards and Harding, 2004). Here we show that indirect host-microbe interactions are also able to modulate the epithelial wound healing process. Indirect exposure of epithelial cells to *K. oxytoca* has a significant negative effect on the healing process whereas no influence or an improvement of the healing was found after co-culture with e.g. *N. mucosa* and *S. oralis*, respectively. Inhibition of cellular migration without the direct exposure of epithelial cells to microbiota has previously been shown by the use of *Pseudomonas aeruginosa* or peptostreptococcal supernatants (de Bentzmann et al., 2000; Stephens et al., 2003). In contrast, supernatant of *Escherichia coli* (strain DH5 $\alpha$ ) or *Citrobacter diversus* did not reveal pronounced effects on epithelial wound healing (de Bentzmann et al., 2000; Stephens et al., 2003), confirming our findings of a species-specific effect.

The microbial density in the wound seems to be a very important parameter. A low grade inflammatory response as a consequence of low concentrations of microbiota have been shown to accelerate wound healing (Häkkinen et al., 2000). Low numbers ( $10^2$ ) of *Staphylococcus aureus*, for example, have been shown to enhance local blood flow, while its enterotoxin A induces the accumulation of collagen hydroxyproline, both contributing to accelerated healing (Laato et al., 1990). Also microbial factors like phospholipase C and LPS have been found to modulate cell migration (Firth et al., 1997; Häkkinen et al., 2000; Koff et al., 2006). At 10  $\mu\text{g/mL}$ , LPS stimulates wound healing, whereas higher concentrations appeared to be toxic (Koff et al., 2006), which was also confirmed in our model (data not shown). However, all these compounds have a size > 3 kD and could be excluded as modulating factors from *K. oxytoca* in this study. The importance of the number of microbiota required to induce inhibitory

effects on wound healing also became clear in our study. Without pre-incubation, *S. salivarius* was unable to grow sufficiently on the agar/mucin substrate in order to obtain a negative effect on wound healing. However, after a pre-incubation period of 4 h, enough viable microbiota were present to exert an inhibitory effect on wound healing.

Since microbial growth appeared important in order to observe effects on wound healing, a time-lapse experiment with *K. oxytoca* was performed monitoring both microbial growth and epithelial wound healing after 8, 12 and 16 h. While microbial cultures in the apical compartment were fully grown after 8 h, the effect on wound healing was only seen after more than 12 h of incubation (data not shown). These results indicate that accumulation of (a) microbial metabolite(s) or molecule(s) is needed before wound healing is affected. SCFA and lactic acid are the most important microbial metabolites in carbon-rich environments. Although SCFA have been described to affect cellular migration of colon epithelial cells (Wilson and Gibson, 1997), we previously showed that reduced healing was only found at concentrations higher than those detected in our model (De Ryck et al., 2014). Another metabolite that can negatively impact health when accumulated is lactic acid. The combination of high levels of D-lactic acid and low pH has been shown to increase epithelial inflammation (Hanstock et al., 2010). Although inflammatory reactions have been demonstrated to impair wound recovery *in vivo*, D-lactic acid supplementation in our model did not reduce wound healing up to 10-fold higher concentrations than those found in the co-culture model. Finally, reduced concentrations of glucose, the most important source of carbohydrates in our model, did not explain the effects on wound healing. McDermott et al. (1998) have previously shown reduced migration when glucose concentrations in the media were raised. No reports of reduced healing due to glucose-shortage were found, thus eliminating the predominant role of glucose in reduced wound healing.

Specific proteins have been reported to affect epithelial migration or wound healing. Elastase for example, a serine proteinase produced by *Ps. aeruginosa*, has previously been reported as the causing agent for the reduction of airway epithelial wound repair (de Bentzmann et al., 2000). However, in our study, treatment with the serine proteinase inhibitor leupeptin did not restore the inhibitory effect of *K. oxytoca* on wound healing. Further, experiments with proteinase K showed no evidence for the involvement of a particular protein or peptide in the underlying mechanism. Our observations are supported by Halper et al. (2003), who also excluded proteins or peptides present in the supernatant of *Lactobacillus* as causing factors for the effect on wound healing.

Although it was already described in 1982 that *K. oxytoca* produces the pyrrolobenzodiazepine cytotoxin tilivalline (Mohr and Budzikiewicz, 1982), only

recently a direct link between tilivalline and antibiotic-associated haemorrhagic colitis has been described (Schneditz et al., 2014). In our study, tilivalline significantly inhibited the wound healing capacity of TR146 epithelial cells. However, no differences in the effects on wound healing were observed between the *K. oxytoca* tilivalline mutant strain, the wild type and the complementation strain. This suggests that its concentration present in the co-culture medium is probably too low to exert any effect and thus excludes this molecule from being responsible for *K. oxytoca*'s inhibitory effect on wound healing in our model.

Many microbiota use quorum sensing molecules to coordinate processes that are microbial concentration-dependent such as biofilm formation and virulence. Common classes of quorum sensing molecules are oligopeptides produced by Gram-positive bacteria and N-acyl-homoserine lactones (AHL) produced by Gram-negative bacteria (Miller and Bassler, 2001). Recently, researchers proposed a role for quorum sensing molecules in the communication between microbiota and their host (Hughes and Sperandio, 2008; Pacheco and Sperandio, 2009). Due to the clear similarities between the bacterial quorum-sensing mechanisms and the metastatic process initiated by tumour cells, the use of quorum-sensing signalling peptides in oncology is now being investigated (Wynendaele et al., 2012). For example, N-3-oxo-dodecanoyl-homoserine lactone, a quorum sensing molecule secreted by *Ps. aeruginosa*, induces apoptosis in several breast cancer cell lines and enhances the production of interleukins (IL-6, IL-8) in bronchial epithelial cells (Smith et al., 2001; Li et al., 2004; Mayer et al., 2011). Our data indicate that this molecule also inhibits the wound healing capacity of the TR146 cells at physiologically relevant concentrations. Although the most common quorum sensing molecules found in the oral cavity are the oligopeptides and auto-inducer-2 molecules produced by Gram positive bacteria, Yin et al. (2012) recently isolated N-octanoyl-homoserine lactone and N-3-dodecanoyl-L-homoserine lactone, produced by *K. pneumoniae* residing on the dorsal surface of the tongue. Also, *K. oxytoca* isolated from patient blood samples was found to produce high amounts of AHL when grown in stationary conditions (Wang et al., 2006). Taken together, these data indicate that quorum-sensing molecules produced by *Klebsiella* may contribute significantly to the inhibitory effect on epithelial wound healing.

In conclusion, we show a species-, and concentration-dependent effect on epithelial wound healing in our *in vitro* oral mucosa model. In our search for molecules involved in the crosstalk between microbiota and host cells during wound healing, we were unable to fully unravel the mechanism underlying the inhibitory effect of *K. oxytoca*. However, our preliminary results suggest that quorum sensing molecules might play a role in this process. This opens new thoughts in the field of the host-microbe interactions, which need to be addressed in the future.



## 4. IRRADIATION AFFECTS THE HOST-MICROBE CROSSTALK

---

*Modified from: De Ryck T, Boterberg T, Kerckhof FM, De Schrijver J, Bracke M, Van de Wiele T, Vanhoecke B (2015). Effects of irradiation on epithelial wound healing and microbial diversity in an in vitro oral mucosa model. Journal of Nuclear medicine & Radiation Therapy 6: 218.*

### 4.1. Abstract

The impact of irradiation on host-microbe crosstalk is still underexplored. By use of our *in vitro* oral mucosa model, we show an impact of irradiation on epithelial wound healing depending on the microbial composition and functionality. 454-pyrosequencing analyses pointed to a slight increase in abundance of *Rothia*, *Granulicatella* and *Gemella* in our model after irradiation. Further research is needed to unravel the effects of irradiation on the oral microbiota and the host-microbe interactions more in detail.

### 4.2. Introduction

Oral mucositis is an important side effect of cancer therapies. In 91 % of the patients with head and neck cancer, radiotherapy results in the development of mucositis (Elting et al., 2007). The pathobiological process of mucositis can be subdivided in 5 phases: the initiation phase, the primary damage response followed by signal amplification, the ulceration and the healing phase (Sonis, 2004, 2007). From these, the healing phase is highly variable between patients and is probably the least understood (Sonis, 2007; Wygoda et al., 2012). Although differences in treatment schedules, irradiation doses and individual radiation sensitivity may be responsible for the differences in wound healing, the composition of the oral microbiome is also thought to be one of the determining factors. An oral core microbiome has been described for healthy individuals with *Streptococcus* being a predominant genus; yet, genera like *Neisseria*, *Prevotella*, *Veillonella* or *Haemophilus* can also become highly abundant. At species level, this interindividual variation is even larger (Bik et al., 2010). A recent review describes important shifts in the core oral microbiome due to radiotherapy, with an increased abundance of Gram-negative species and

*Lactobacillus* spp. (Vanhoecke et al., 2015b). While irradiation thus has a clear impact on the host, eliciting mucositis, and on the oral microbiome, it is not known to what extent irradiation impacts the host-microbe crosstalk, particularly during the wound healing phase. Here, we used an *in vitro* oral mucosa model (De Ryck et al., 2014) to study the impact from oral microbes on the dynamics of the wound healing process following irradiation more in detail.

## **4.3. Materials and methods**

### **4.3.1 Epithelial cell line**

TR146 cells, an oral squamous carcinoma cell line derived from a local lymph node metastasis was obtained from Clare Hall Laboratories (Cancer Research UK). The Dulbecco's modified Eagle's cell culture Medium (DMEM) (Gibco, Belgium) was supplemented with 10 % heat-inactivated fetal bovine serum (Greiner bio-one, Belgium), 22.8 µg/mL penicillin-streptomycin (5000 U/mL; Gibco, Belgium) and 2.5 µg/mL amphotericin B (Bristol-MyersSquibb, Belgium). Cells were cultured at 37 °C and 10 % CO<sub>2</sub> and regularly controlled to be mycoplasma free (MycoAlert Mycoplasma Detection kit; Lonza, USA).

### **4.3.2 Irradiation**

A single 6 MV photon beam was generated using a linear accelerator (SLi-18, Elekta, UK). The 24-well plates were placed on top of a 1.5 cm Perspex (polymethylmethacrylate) plate to compensate for the build-up effect and irradiated from below. The model was irradiated with a total dose of 10 Gy at an instantaneous dose rate of 430 cGy/min.

### **4.3.3 Oral swab collection**

Before sampling, the oral cavity of a healthy volunteer was extensively flushed with drinking water. A sterile cotton swab was used to rub the buccal mucosa 10 times before submersion in 2 mL of synthetic saliva buffer. Briefly, an organic buffer (500 mg/L ureum), an inorganic buffer (2.987 g/L KCl, 2.96 g/L NaH<sub>2</sub>PO<sub>4</sub>, 0.667 g/L KSCN, 1.9 g/L Na<sub>2</sub>SO<sub>4</sub>, 0.993 g/L NaCl and 10.8 mM NaOH) and an additive buffer (483 mg/L amylase, 167 mg/L mucin and 50 mg/L uric acid) were autoclaved and mixed (4:3:3) immediately before use. After incubating the oral swabs for 15 min at 37 °C, the microbial suspensions were snap frozen in liquid nitrogen and stored at -80 °C until the experiments were performed. For all experiments, a different oral swab was taken from the same healthy volunteer.

#### **4.3.4 Oral mucosa model**

To co-culture microbiota and TR146 epithelial cells in absence of direct microbe-epithelial contact, we used our recently published oral mucosa model (De Ryck et al., 2014). Briefly, 75  $\mu$ L of an agar/mucin solution was spotted on the porous membrane of a 24-well plate Transwell® system (Corning inc., USA) and allowed to solidify for at least 30 min. After thawing at room temperature, 20  $\mu$ L of the microbial samples ( $\sim$  3.2 log/filter) were brought on top of the agar/mucin layer. In the basal compartment, a confluent layer of TR146 cells was generated by seeding 300 000 TR146 cells into a well after labelling with DiI cell labelling solution (Life technologies Europe, Belgium). Cells were allowed to attach and grow for 3 days prior to wounding.

#### **4.3.5 Wound healing assay**

TR146 monolayers were scratched using a sterile plastic pipette tip. Floating cells were removed by replacing the medium with fresh serum-free, antibiotics-free DMEM. Filters containing the microbiota and the agar/mucin layer were placed on top of the wounded cells prior to irradiation. By means of an automated fluorescence microscope (Zeiss Axiovert 200M), pictures of selected points along the wounds were taken immediately after irradiation (0 h) and 24 h after incubation at 37 °C and 5 % CO<sub>2</sub>. Migration of the cells into the wounded area in the presence and absence of oral microbiota was assessed by comparing the micrographs after 0 and 24 h. The relative surface (%) of the wound was determined by dividing the wound surface after 24 h by the wound surface at time 0. For this we made use of a custom-made macro in ImageJ (De Ryck et al., 2014). For each well, the mean value of the wound surface was calculated (n=1) and used for further analysis. In total, 5 independent experiments were performed, each with 2 to 4 wells per condition.

#### **4.3.6 Microbial enumeration**

To enumerate the microbiota at the start of the experiment, 10-fold dilutions of the oral swab suspension were prepared in sterile PBS and plated on BHI agar plates (Sigma, Belgium) using the microdilution plating technique.

After 24 h of co-culture, microbiota in the apical compartment were suspended in 200  $\mu$ L of sterile PBS before plating 10-fold dilutions as described above.

#### **4.3.7 PCR-DGGE**

A nested PCR strategy was applied as described previously (Bakke et al., 2011; De Ryck et al., 2014). For the external PCR reaction, we made use of EUB8F (5'-agagtttgatcmtggctcag-3') and 984 $\gamma$ R (5'-gtaaggttcytcgcgt -3') primers during 35 PCR cycles (95 °C, 30 s; 50 °C, 30 s and 72 °C, 1 min). A 1:3000 dilution of the first PCR-product was added in the internal PCR, for which the primers PRBA338GC (5'-



cgcccccgcgcgcgggcgggcgggggcgggggcacggggggactcctacgggaggcagcag-3') and 518R (5'-attaccgcggtgctgg-3') were used for 25 cycles (95 °C, 30 s; 53 °C, 30 s and 72 °C, 1 min). In this way, 16S rDNA gene fragments of 180 bp were obtained, which are suitable for denaturing gradient gel electrophoresis. The master mix used for these PCR reactions was the TaKaRa Ex Taq™ kit (Westburg, Leusden, The Netherlands). Each reaction consisted of 2.5 µL Ex Taq buffer (10x), 2 µL dNTPs, 0.125 µL Ex Taq enzyme, 0.2 µM of each primer, 17.375 µL of PCR water (Sigma-Aldrich, Diegem, Belgium) and 1 µL of DNA. The reaction mixtures were incubated in a Biometra thermocycler (Westburg, Leusden, The Netherlands) at 94 °C for 5 min, followed by 35 or 25 cycles and a final extension at 72 °C for 10 min. For the DGGE analysis, a 45-60 % gradient acrylamide gel was used to separate the DNA fragments (Callewaert et al., 2013).

#### **4.3.8 Pyrosequencing**

DNA extraction and 454 pyrosequencing analysis of the apical compartment was performed as described in Chapter 2 (De Ryck et al., 2014). On average, 12 907 number of reads were generated by pyrosequencing for each sample. After processing the results, operational taxonomic units were classified using the RDP database.

#### **4.3.9 Statistics**

Statistical analyses were performed with *SPSS statistics 22*. After normality check with the Shapiro-Wilk assay, an ANOVA, Student's T, Kruskal Wallis or Mann Whitney-U test was used. Bonferroni correction was performed to correct for multiple comparisons.

All other techniques used for this study are described in detail in Chapter 2 (De Ryck et al., 2014).

### **4.4. Results and discussion**

In patients suffering from oral mucositis, the healing phase starts spontaneously two to three weeks after completion of radiotherapy. Signals originating from the extracellular matrix promote wound healing by stimulating migration, proliferation and differentiation of the epithelium (Sonis, 2007). We previously showed our in vitro oral mucosa model to be useful for the study of effects of oral microbiota on the wound healing capacity of different oral-derived cell lines (De Ryck et al., 2014). In non-irradiated conditions, epithelial recovery was significantly reduced with 12-16 % in the presence of microbiota (Figure 4-1, 0 Gy;  $p < 0.001$ ). After irradiation however, our experimental data could be categorized in 2 different sets. In 3 of the 5

independent experiments (set 1) the inhibitory effect of the microbiota on wound healing was more pronounced after irradiation as compared to the non-irradiated condition (Figure 4-1a, set 1;  $p < 0.001$ ). In contrast, no effect of the microbiota after irradiation could be noticed in the other 2 independent experiments (Figure 4-1c, set 2;  $p = 1$ ). Interestingly, plate counts revealed a lower number of microbiota in set 2 after 24h of co-culture compared to set 1 ( $p = 0.053$ ). While the difference in microbial concentrations between the 2 experimental datasets was not influenced by irradiation (Table 4-1;  $p_{\text{set1:0Gy-10Gy}} = 0.979$ ;  $p_{\text{set2:0Gy-10Gy}} = 0.800$ ), our data suggest that microbial growth is an important determining factor for the wound healing process after irradiation.

Irradiation has previously been shown to prolong the lag phase of foodborne pathogens delaying the stationary phase (Aguirre et al., 2011). As a consequence, microbial metabolites might be present at concentrations that are too low to have an effect on the epithelial cells. A microbial metabolite that was present in our *in vitro* model was D-lactic acid (De Ryck et al., 2014). In this study we can confirm that oral microbiota increase the levels of D-lactic acid after 24 h in both datasets (Figure 4-1b set 1:  $p_{0\text{Gy}} < 0.001$  and  $p_{10\text{Gy}} < 0.001$ ; Figure 4-1d set2:  $p_{0\text{Gy}} = 0.167$  and  $p_{10\text{Gy}} = 0.445$ ). Irradiation did not have an effect on this increase ( $p_{\text{set1}} = 0.308$ ;  $p_{\text{set2}} = 1$ ).

**Table 4-1: Microbial enumeration of the apical compartment after 24 h of co-culture with TR146 cells in irradiated (10 Gy) or non-irradiated (0 Gy) conditions (mean  $\pm$  SD)**

Microbial counts (log CFU/filter)	0 Gy	10 Gy
Set 1	7.29 $\pm$ 0.51	7.31 $\pm$ 0.74
Set 2	5.88 $\pm$ 1.55	5.77 $\pm$ 1.08

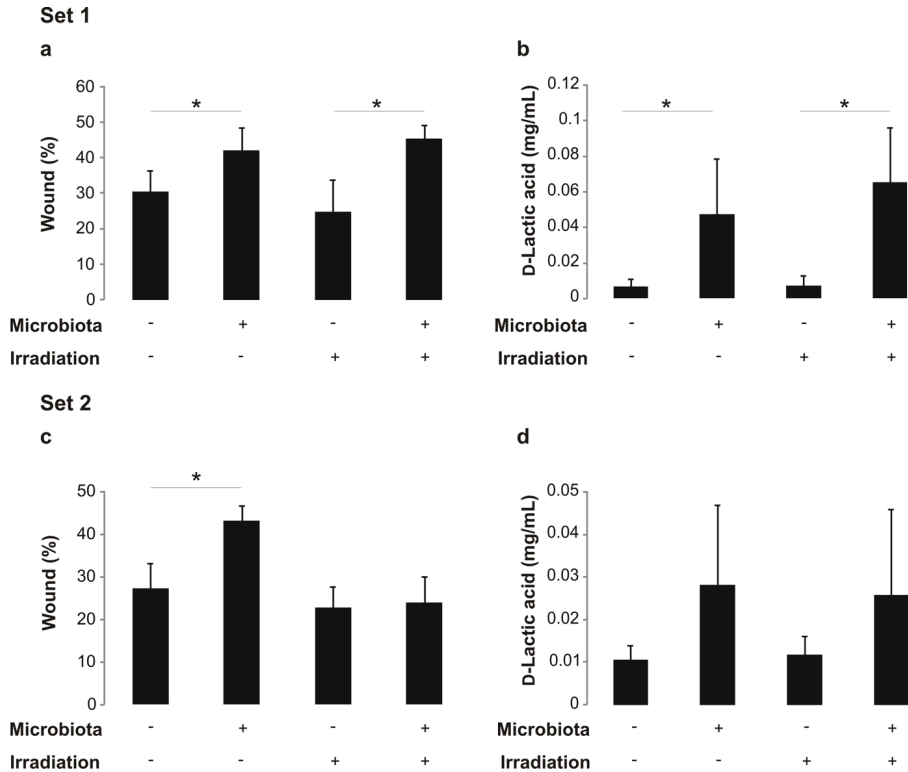


**Figure 4-1 a and c: Wound healing capacity of TR146 cells in the absence or presence of oral microbiota, both in irradiated (10 Gy) or non-irradiated (0 Gy) conditions. b and d: Concentrations of D-lactate in the co-culture medium in the absence or presence of oral microbiota, both in irradiated (10 Gy) or non-irradiated (0 Gy) conditions (mean + SD; \* $p < 0.05$ ). Data could be categorised in 2 sets ( $n_{set1} = 12$  (a and b),  $n_{set2} = 7$  (c and d)) depending on the experimental outcome of the wound healing experiments after irradiation**

Next, we evaluated to what extent irradiation induces shifts in the microbial composition of the oral biofilm after 24 h in our *in vitro* oral mucosa model. To this end, PCR-DGGE was used as a quick screening technique. While shifts in microbial composition were noted upon irradiation, this was only evident for 50 % of the experiments (Figure 4-2). In all samples, an identical GC-poor group of microbiota could be detected (arrow-marked on Figure 4-2), most probably representing the oral core microbiome.



**Figure 4-2: DGGGE profiling of the oral microbiota present in the apical compartment after 24 h of co-culture with TR146 epithelial cells in irradiated (10 Gy) or non-irradiated (0 Gy) conditions. Indicated (arrow) is a group of GC-poor bacteria present in all samples (n= 24)**

454 pyrosequencing analysis of the microbiota co-incubated with an epithelial monolayer for 24 or 48 h, showed that irradiation induces a small increase (< 1 %) in *Rothia*, *Granulicatella* and *Gemella* species (Figure 4-3;  $p_{Rothia-24h} = 0.174$ ,  $p_{Granulicatella-24h} = 0.055$ ,  $p_{Gemella-24h} = 0.057$ ,  $p_{Rothia-48h} = 0.220$ ,  $p_{Granulicatella-48h} = 1$ ,  $p_{Gemella-48h} = 0.207$ ). Unlike *Granulicatella* and *Gemella* that are omnipresent in the oral cavity, *Rothia* is mostly linked with tooth surfaces (Aas et al., 2005). Interestingly, *Rothia* species were reported to become more abundant in head and neck cancer patients during radiotherapy, whereas *Granulicatella* species were shown to decrease after irradiation (Hu et al., 2013a, 2013b). Therefore *Granulicatella* species are not likely to be the causing agents of post-radiation diseases (Hu et al., 2013b). In contrast, different cases of *Rothia* bacteraemia have been reported of which 36 % could be linked with oral mucositis (Ramanan et al., 2014).

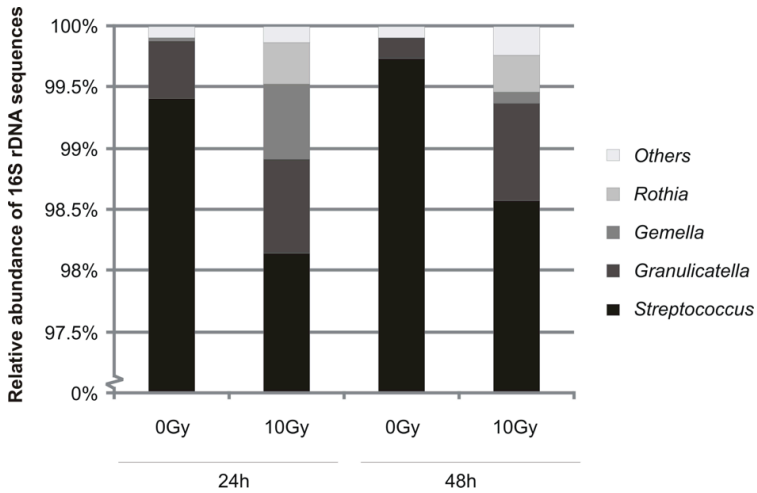


**Figure 4-3: Pyrosequencing analysis of the oral microbiota cultured for 24 or 48 h in co-culture with TR146 epithelial cells in irradiated or non-irradiated conditions (n= 3). Results of 454 pyrosequencing of 16S rDNA assigned to genus are shown**

In summary, our study shows that irradiation can affect the host-microbe crosstalk during wound healing, depending on the composition and functionality of the microbiota. A slight increase in abundance of *Rothia* after irradiation could be noticed in our *in vitro* system, which was correlated with mucositis-related local and/or systemic infections *in vivo*. Further research is necessary to determine which species are likely to have a negative impact on the recovery of the epithelium after irradiation and to develop new strategies to combat infections associated with radiotherapy-induced mucositis.

## 5. IRRADIATION AFFECTS THE FUNCTIONAL BEHAVIOUR OF THE ORAL MICROBIOTA

---

*Modified from: Vanhoecke B\*, De Ryck T\*, De boel K, Boterberg T, Wiles Siouxsie, Van de Wiele T, Swift S (2015). Effects of low dose irradiation on function behaviour of oral microbiota in the context of mucositis. Accepted for publication in Experimental Biology and Medicine (\*Equally contributing).*

### 5.1. Abstract

The role of host-microbe interactions in the pathobiology of oral mucositis is still unclear; therefore this study aimed to unravel the effect of irradiation on behavioural characteristics of oral microbial species in the context of mucositis. Using various experimental *in vitro* set-ups, the effects of irradiation on growth and biofilm formation of two *Candida* spp., *Streptococcus salivarius* and *Klebsiella oxytoca* in different culture conditions were evaluated. Irradiation did not affect growth of planktonic cells but reduced the number of *K. oxytoca* cells in newly formed biofilms cultured in static conditions. Biofilm formation of *K. oxytoca* and *C. glabrata* was affected by irradiation and depended on the culturing conditions. In the presence of mucins, these effects were lost, indicating the protective nature of mucins. Furthermore, the *Galleria melonella* model was used to study effects on microbial virulence. Irradiated *K. oxytoca* microbes were more virulent in *Galleria melonella* larvae compared to the non-irradiated ones. Our data indicate that low dose irradiation can have an impact on functional characteristics of microbial species. Further research should elaborate on these observations in search for new insights on the potential role of oral microbiota in the development of oral mucositis following radiation therapy.

### 5.2. Introduction

Alimentary mucositis is a severe side effect of both chemo- and radiotherapy and causes a range of symptoms throughout the gastrointestinal tract, including ulcers in the oral cavity, nausea, vomiting, diarrhoea and constipation. Accelerated fractionated schedules and concurrent chemotherapy have increased the incidence and severity of mucositis. Apart from being treatment limiting, the impacts on patient quality-of-life

and the economic costs of supportive therapies are of significant concern (Sonis, 2004, 2009, 2010). Limited therapeutic effects have been described for a variety of agents including radioprotectors, antibiotics, low-level laser therapy and growth factors, but the evidence gathered to date does not support the use of any of these agents as a standard treatment. Therefore, there is an urgent need for original strategies to prevent and/or treat oral mucositis. This would not only reduce the suffering of the patients involved but would also dramatically reduce hospital and management costs associated with this condition. Although reports regarding the oral microbiota as a risk factor are scarce, prescription of alkaline mouthwashes is standard practice in the prevention of overgrowth by pathogens such as *Candida albicans* or Gram-negative bacilli.

Recently, we extensively reviewed the scientific literature on the link between oral mucositis and the endogenous microbiota (Vanhoecke et al., 2015b). Overall, there is convincing data to conclude that irradiation changes the oral core microbiome over time (Shao et al., 2011; Hu et al., 2013a) with Gram-negative species becoming more abundant (Tong et al., 2003; Panghal et al., 2012; Sonalika et al., 2012a) together with *Candida* spp. (Belazi et al., 2004; Almståhl et al., 2008; Guobis et al., 2011; Sonalika et al., 2012a) and *Lactobacillus* spp. (Tong et al., 2003; Almståhl et al., 2008; Guobis et al., 2011). The number and proportion of *Lactobacillus* spp. were found to be increased in swabs of tongue, buccal mucosa, vestibulum, supragingival plaque and subgingival region and saliva after radiotherapy, while data on *Streptococcus* spp. were inconclusive (Tong et al., 2003; Almståhl et al., 2008; Guobis et al., 2011). *C. albicans* fungi seemed to be the most significant oral cavity pathogen in radiotherapy-induced mucositis patients, whereas Gram-negatives such as *Pseudomonas aeruginosa* and *Klebsiella pneumoniae* were observed as main pathogens isolated from the blood of radiotherapy-treated patients (Panghal et al., 2012).

Radiation therapy uses high-energy irradiation to shrink tumours and kill cancer cells. X-rays, gamma rays, and charged particles are types of irradiation used for cancer treatment. In this study we will mainly focus on the effect of gamma rays on microbial behaviour. Irradiation causes damage to nucleic acids and (phospho)lipids of the microbiota, whereas proteins, carbohydrates, and fats in food are not significantly affected by doses up to 10 kGy (Farkas, 1998). It has further been shown that irradiation significantly changes the expression of heat shock proteins, the 50S ribosomal protein, the transcriptional regulator (CtsR) and the enzyme formate acetyltransferase at doses >1 kGy (Caillet et al., 2008; Trudeau et al., 2012). Surprisingly, effects of low dose gamma irradiation on the viability, metabolic activity and other functional properties of microbiota are hardly investigated. Only a few studies show that doses <kGy might indeed induce some effect. Recently, a study by Parikka *et al.* (2012) showed that two doses of 25 Gy with a one month's interval was

sufficient to reactivate a latent *Mycobacterium marinum* infection in adult zebrafish. In the reactivation group, a steep drop in survival after 16 days concomitant with high bacterial loads was seen and histological analysis of the moribund zebra fish revealed vast areas of free microbiota outside granulomas. Although in the zebra fish model the dampened immune suppression of the host is likely to be the trigger for reactivation, gamma irradiation is likely to have direct effects on *Mycobacterium* as *in vitro* studies with doses above 1 Gy have previously shown that the viability of *M. tuberculosis* is adversely affected (Zack et al., 1974).

It is well known that gamma irradiation causes oxidative DNA damage and triggers oxidative stress responses and compromised DNA repair mechanisms can lead to increased risk of carcinogenesis. It is currently unknown if or to what extent microbiota play a role in regulating radiosensitivity. A recent study by Maier et al (2014) showed that the composition of the intestinal microbiome has an impact on the DNA repair response following irradiation. Mice with a conventional intestinal microbiota exhibited lower levels of acute chromosomal DNA lesions and  $\gamma$ -H2AX phosphorylation than mice with a restricted composition after total body irradiation (1 Gy). On the other hand, Crawford and Gordon (2005) showed that germ-free mice seem to be markedly resistant to lethal irradiation enteritis. Although limited, these studies indeed suggest a potential role for the microbiota in the host's response to irradiation.

In this study we wanted to determine whether radiation therapy might result in microbial dysfunction thereby providing a risk factor for developing or exacerbating oral mucositis. Therefore, the aim of this study was to unravel the effects of low dose irradiation on the functional behaviour of a panel of oral species, namely *Candida albicans*, *C. glabrata*, *Klebsiella oxytoca* and *Streptococcus salivarius*. *C. albicans* is found primarily in the intestines, colon, and the oral cavity and although it is a commensal, it can become pathogenic if a person's immunity is lowered or if there is a dysbiosis (Singh et al., 2014). *C. glabrata* is considered a relatively harmless commensal of mucosal tissues, however, with the increased use of immunosuppressive agents, mucosal and systemic infections caused by *C. glabrata* have increased significantly (Rodrigues et al., 2014). *K. oxytoca* is like other *Klebsiella* spp. an opportunistic pathogen and although it tends to colonize along the mucosal membranes, it can be found in all parts of the body. Infections often occur in patients with immunodeficient diseases and those being treated with antibiotics (Rodriguez and Bodey, 1973). *S. salivarius* is the principal commensal of the oral cavity in humans, the pioneer in colonizing dental plaque and infrequently pathogenic (Nyvad and Kilian, 1987).

To study the effect of irradiation on the pathogenicity of the microbes, we used an established model using larvae of *Galleria mellonella*, also known as the greater wax



moth (Fuchs and Mylonakis, 2006; Fuchs et al., 2010; Mukherjee et al., 2010; Lionakis, 2011; Navarro-Velasco et al., 2011). The major advantage of this model above other invertebrate models is the ability to grow these larvae at 37°C, the human body temperature. Furthermore, they can be inoculated via oral delivery, topical application or injection (Fuchs et al., 2010). In this study, the latter method was used, where the microbial suspension is injected directly into the hemocoel, which ensures a correct calculation of the received amount of microbes by the larvae (Fuchs et al., 2010). As in other insects, the *G. mellonella* larvae have a complex, multi-component innate immune system, similar to the human beings. Both in mammals and *Galleria*, pathogens are killed by use of enzymes, reactive oxygen species and antimicrobial peptides (Mukherjee et al., 2010). Furthermore, phagocytosis of the microbes by the insect hemocytes resembles the mechanism used by human neutrophils (Bergin et al., 2005).

To our knowledge, this type of study has not been performed so far but would provide information on specific microbiota as risk factors for developing or progressive oral mucositis following radiation therapy.

## 5.3. Materials and methods

### 5.3.1 Cells, chemicals and irradiation

*Candida albicans* (ATCC 10231), *C. glabrata* (ATCC 2001), *Klebsiella oxytoca* (ATCC 49131) and *Streptococcus salivarius* (ATCC 7073) were obtained from the New Zealand Reference Culture Collection (ESR, Porirua, New Zealand) and grown on horse blood agar plates (Fort Richard Laboratories, Auckland, New Zealand). For growth studies cells were cultured in Bacto Todd-Hewitt broth (*Candida* species) (Fort Richard Laboratories) supplemented with 0.5 % yeast extract (THY), Bacto Brain Heart Infusion (BHI) broth (*K. oxytoca* and *S. salivarius*), Dulbecco's Modified Eagle Medium (DMEM) (Life Technologies, Auckland, New Zealand) or DMEM supplemented with 5 % (w/v) mucins from porcine stomach type III (Sigma-Aldrich). The live/dead BacLight bacterial viability staining kit was purchased from Life Technologies, and crystal violet, Fluka Calcofluor white and 3-(4,5-dimethylthiazol-2-yl)-2,5-diphenyl-tetrazolium bromide (MTT) from Sigma-Aldrich. For the *in vitro* experiments, 60-cobalt irradiations were performed using an AECL Eldorado Model 'G' (Atomic Energy of Canada, Ltd., Commercial Products Division, Ottawa, Canada) at a dose rate of 0.5 Gy/min. For the experiments with *Galleria mellonella*, microbiota were irradiated with a single 6 MV photon beam that was generated using a linear accelerator SLi-18 (Elekta, Crawley, UK) at a dose rate of 430 cGy/min.

### **5.3.2 Determination of viability of test species**

In order to assess the effect of different media (THY, BHI, DMEM, DMEM supplemented with mucins) on the viability of all test bacterial species with or without irradiation (10 Gy), different assays were performed. First, growth curves for each test species were prepared in presence of the different media with or without irradiation. The tested species were inoculated in 10 mL of culture broth and grown overnight. A 1:1000 dilution (optical density (OD) at 600 nm ~0.03-0.05) was prepared in a 50 mL V-bottom polypropylene tube in presence of the different media and irradiation was performed prior to incubation at 37 °C and 200 rpm. Absorbance at 600 nm was measured spectrophotometrically every 30 min, using cuvettes with a path length of 1 cm, until cultures reached stationary phase (mQuant, Bio-Tek Instruments Inc., Winooski, Vermont, USA).

Second, to test the effect of irradiation upon biofilm formation, 200 µL of a 1:100 dilution of an overnight culture of all test species was transferred into sterile 24-well microtiter plates (Fisher Scientific, Pittsburgh, PA) and 800 µL of the different media was added to the culture prior to irradiation. Plates were incubated for 24 h at 37 °C either statically or shaking at 200 rpm in an atmosphere of air. After 24 h, planktonic cells were gently removed and the remaining biofilm cells of one plate were stained with the live/dead BacLight bacterial viability kit (Life Technologies) according to manufacturer's guidelines. Briefly, 3 µL of the dye mixture of SYTO9 and propidium iodide (PI) was added to the cells and incubated in the dark at room temperature. After 20 min, fluorescence was measured using a fluorimeter (EnSpire 2300 Multilabel Reader (Perkin Elmer, Waltham, Massachusetts, USA) at Ex480/Em500 nm for SYTO9 and Ex490/Em635 nm for PI. Metabolic activity and viability of the biofilm cells was evaluated using the MTT assay (Mosmann, 1983). In short, 1 mg/mL of 3-(4,5-dimethylthiazol-2-yl)-2,5-diphenyl-tetrazolium bromide was added to each well after removal of the medium (containing the planktonic cells) and biofilm cells were incubated at 37 °C. After 2 h, all media were discarded and formazan crystals were dissolved in 1 mL DMSO. Absorbance at 570 nm was measured spectrophotometrically (mQuant, Bio-Tek Instruments Inc., Winooski, Vermont, USA).

### **5.3.3 Determination of biofilm formation**

Biofilm formation of all test species was measured in 24-well plates and in 50 mL V-bottom tubes. For the set-up in plates, 200 µL of a 1:100 dilution of overnight culture was transferred into 24-well plates to which 800 µL of medium was added. For the set-up in tubes, 1 mL of a 1:100 dilution of an overnight culture of the test species was transferred into a sterile 50 mL V-bottom tube and 4 mL of the different test media was added. Subsequently, plates and tubes were subjected to irradiation or not (controls) and incubated statically for 24 h at 37 °C in air (plates) or in shaking

conditions (plates: 200 rpm – in air; tubes: 80 rpm – at 5 % CO<sub>2</sub>) at 37 °C. After 24 h, planktonic cells were gently removed. Biofilms grown on the bottom (plates) and sides of the wells (tubes: ring formation) were washed 3 times with tap water and stained with 0.2 % crystal violet for 30 min. Excess of staining solution was removed by 3 washing steps with tap water. After overnight drying of the plates and the tubes, the crystal violet was dissolved by adding a mixture of methanol:acetic acid (1:4) and the OD540 nm was measured spectrophotometrically (mQuant; Bio-Tek Instruments Inc., Winooski, Vermont, USA).

#### **5.3.4 Calcofluor white staining assay**

To test the influence of different media and irradiation on extracellular matrix components  $\beta$ -linked polysaccharides such as cellulose and chitin, a calcofluor white staining was performed on biofilm cells. Calcofluor white cannot penetrate intact cell membranes and does not stain viable cells (Mason et al., 1995). 200  $\mu$ L of the calcofluor white solution was added to the biofilms formed in 24-well plates (see above). Calcofluor staining of *C. albicans* and *C. glabrata* was enhanced by adding 1 drop of KOH to dissolve keratinized particles and to help emulsify solid, viscous material that may mask fungal elements. After 10 min incubation in the dark at room temperature, the dye was discarded and biofilms were thoroughly washed with filter-sterilized water to remove unbound dye. Fluorescence was measured using a fluorescence microplate reader with an excitation filter of 355 and an emission filter of 430 nm (EnSpire 2300 Multilabel Reader (Perkin Elmer, Waltham, Massachusetts, USA).

#### **5.3.5 *Galleria mellonella* larvae infection and survival assay**

*G. mellonella* larvae (also known as the wax worm) were purchased from a local supplier (De Papegaai, Sint-Niklaas, Belgium), maintained at room temperature in the dark, and used within 1 week. Overnight bacterial cultures were divided in two equal parts after which one part was irradiated (10 Gy). Cultures were washed 3 times and resuspended in sterile PBS at the desired concentration. Larvae were each injected with 20  $\mu$ l of inoculum at the site of the lower left proleg using an insulin syringe. Each group of 9 - 10 larvae was incubated at 37 °C in 9 cm petri dishes without food for up to 3 days.

For tests with supernatant, supernatant of irradiated and non-irradiated overnight cultures of *K. oxytoca* and *S. salivarius* was collected 4 h post-irradiation and cleared from remaining cells by centrifugation (10 min, 2200 g) and passing through a filter (0.2  $\mu$ m). Larvae were injected with 20  $\mu$ L of the supernatant or sterile broth as a control. For the experiments with dead bacteria, cells were fixed with ice-cold methanol during 10 min and washed with PBS prior to injection.

### 5.3.6 Statistics

Statistical testing was conducted using SPSS statistics 22. Normality of the data was checked using the Shapiro-Wilk assay. When normality could be assumed, statistical differences between the growth conditions was determined using Students t-tests or ANOVA. For non-parametric analyses Mann-Whitney U or Kruskal-Wallis tests were used. Pairwise post-hoc analysis was performed with Bonferroni correction. For the *G. mellonella* experiments the survival between the different groups was compared using the log rank assay. A 0.05 statistical significance level was used for all analyses.

## 5.4. Results

### 5.4.1 Effect of ionizing irradiation on growth of oral planktonic cells

We first investigated the effect of ionizing irradiation (10 Gy) on the growth of different oral species (*C. albicans*, *C. glabrata*, *S. salivarius* and *K. oxytoca*) under agitation. Growth curves were obtained by culturing planktonic cells in presence of rich culture broth (THY or BHI), glucose-rich DMEM and DMEM supplemented with mucins. As shown in Figure 5-1, a dose of 10 Gy did not affect subsequent outgrowth of test species.

### 5.4.2 Effect of ionizing irradiation on biofilm formation and viability of oral microbiota

Biofilm formation was assessed after irradiation of the inoculum. Biofilms were allowed to form in 1) static conditions, using 24-well plates, and 2) dynamic conditions, using 24-well plates or 50 mL V-bottom tubes, in the presence of the different test media during a period of 24 h following irradiation of the inoculum. Crystal violet staining of the biofilms was performed as a measure of biofilm material, including both cells and extracellular matrix components. Thicker biofilms will result in higher OD at 540 nm. The biofilm formation of *C. albicans* was found to be reduced after irradiation in dynamic conditions (tubes) in presence of mucins (not significant). This reduction was also observed for *C. glabrata* ( $p= 0.017$ ). Furthermore, a small, but significant increase in biofilm formation of *C. glabrata* was observed in static conditions in absence of mucins (DMEM;  $p= 0.029$ ) (Figure 5-2).

In case of microbial biofilm formation, no effect of irradiation was found for *S. salivarius*. Interestingly, we showed significantly reduced biofilm formation of *K. oxytoca* in static conditions in absence of mucins (DMEM;  $p= 0.002$ ). In contrast, thicker biofilms were observed for *K. oxytoca* cultured in dynamic (tubes; broth) conditions (not significant) (Figure 5-3).

In addition, there was often a stimulating effect of mucins on biofilm formation (0 Gy, DMEM compared to mucins), which was significant for *K. oxytoca* (static:  $p= 0.022$ ; dynamic-wells:  $p< 0.001$ ; dynamic-tubes:  $p< 0.001$ ), *C. albicans* (dynamic-wells:  $p= 0.012$ ) and *S. salivarius* (dynamic-wells:  $p< 0.001$ ).

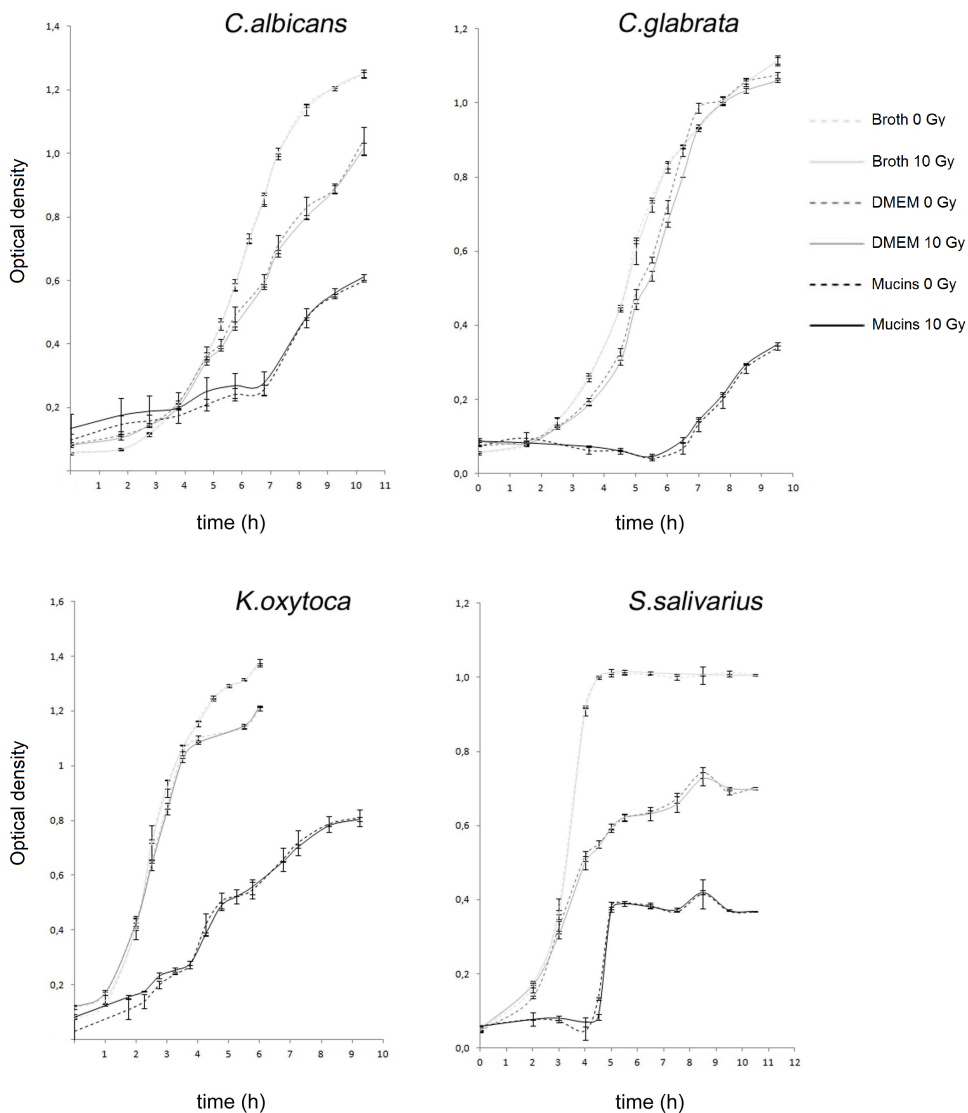


**Figure 5-1: Growth curves of irradiated (10 Gy) and non-irradiated *C. albicans*, *C. glabrata*, *K. oxytoca* and *S. salivarius* planktonic cells cultured in different media (broth, DMEM or DMEM + mucins): vertical axis represents the optical density (OD) of the cells measured at 600 nm using a spectrophotometer (n= 2)**

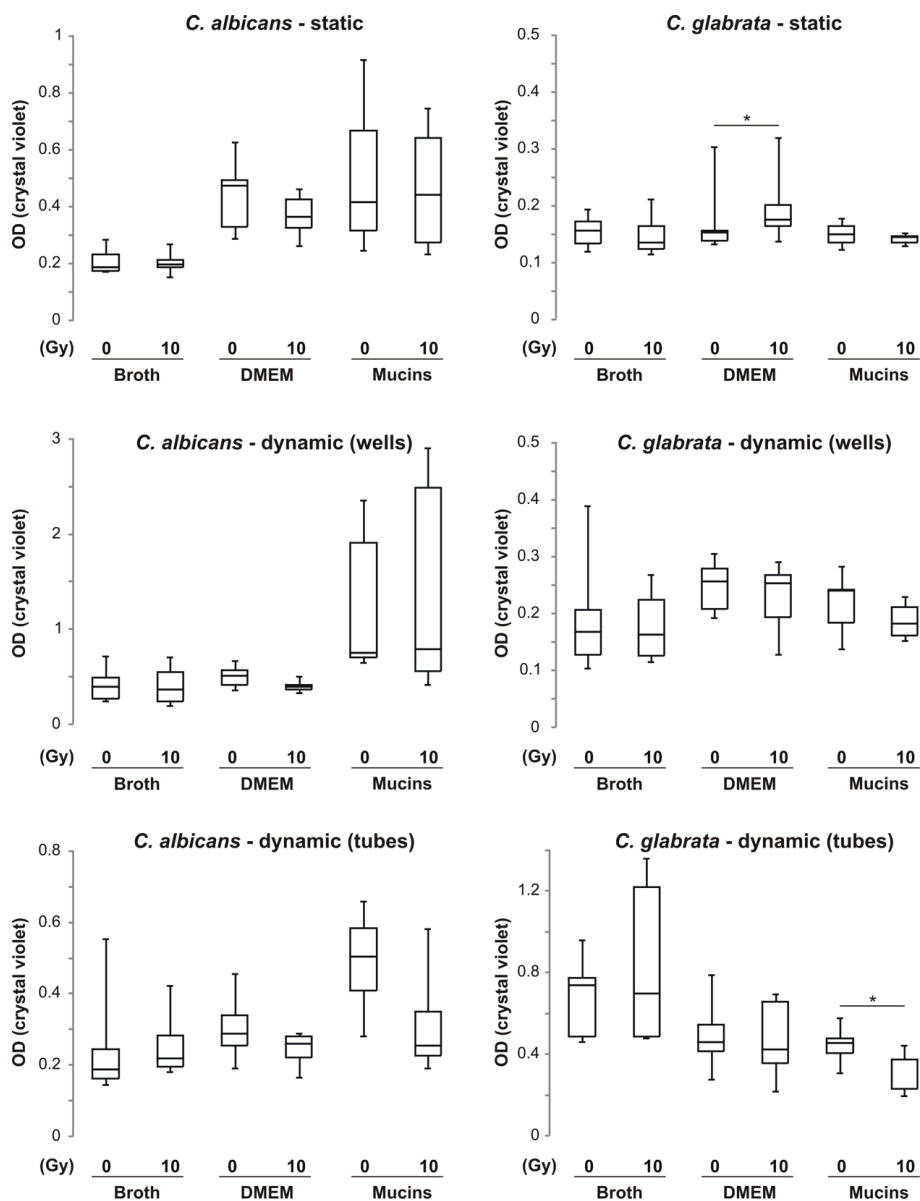


**Figure 5-2:** Box plot presentation of biofilms of irradiated (10 Gy) and non-irradiated *C. albicans*, *C. glabrata*, *K. oxytoca* and *S. salivarius* cells formed during 24 h of culture in different media (broth, DMEM or DMEM + mucins). The whiskers represent the minimum and maximum observed values. Biofilms were generated both in static (24-well plates, first column) and dynamic conditions (24-well plates, second column; tubes, third column). Vertical axis represents the optical density (OD) of dissolved crystal violet molecules measured at 540 nm using a spectrophotometer (n= 4-8; \* p< 0.05)

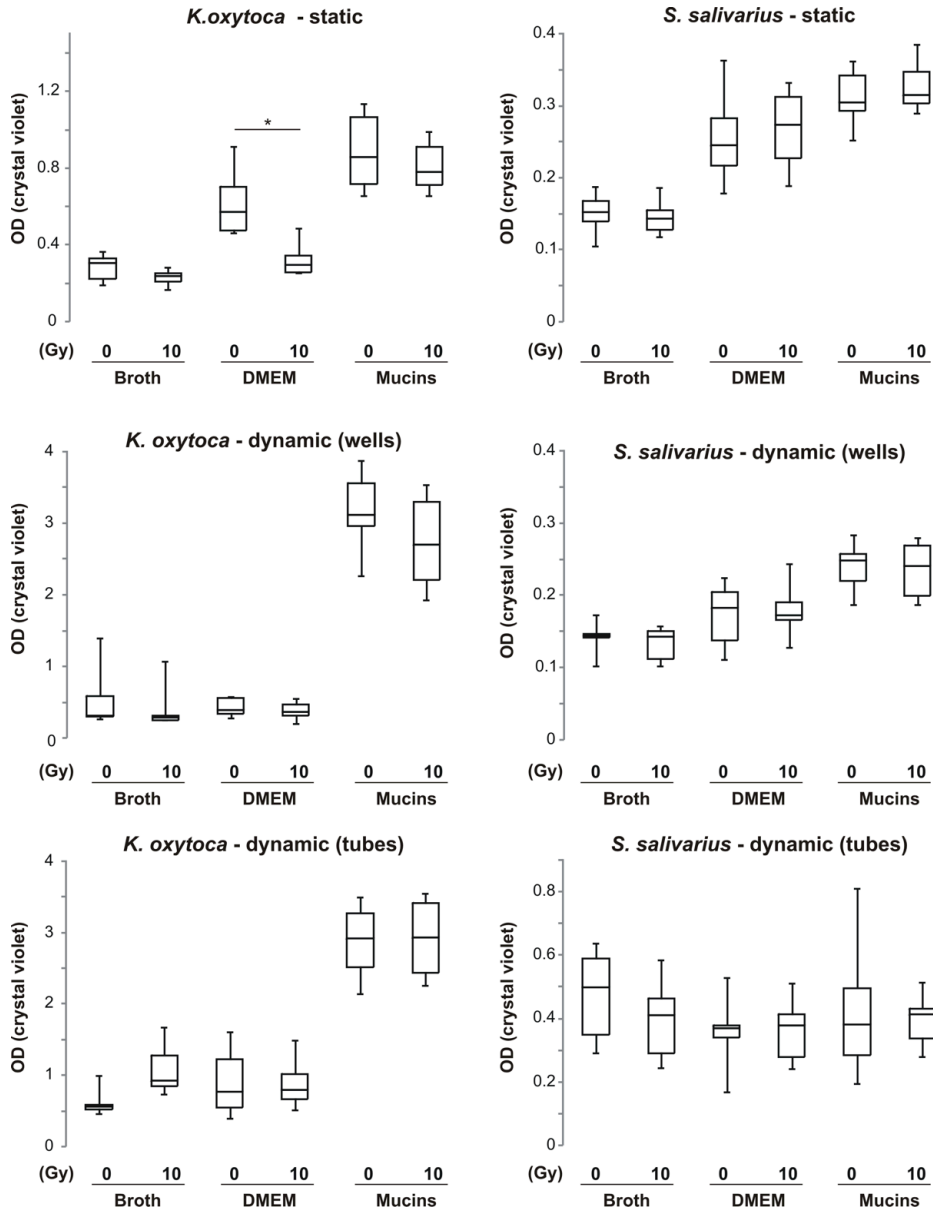
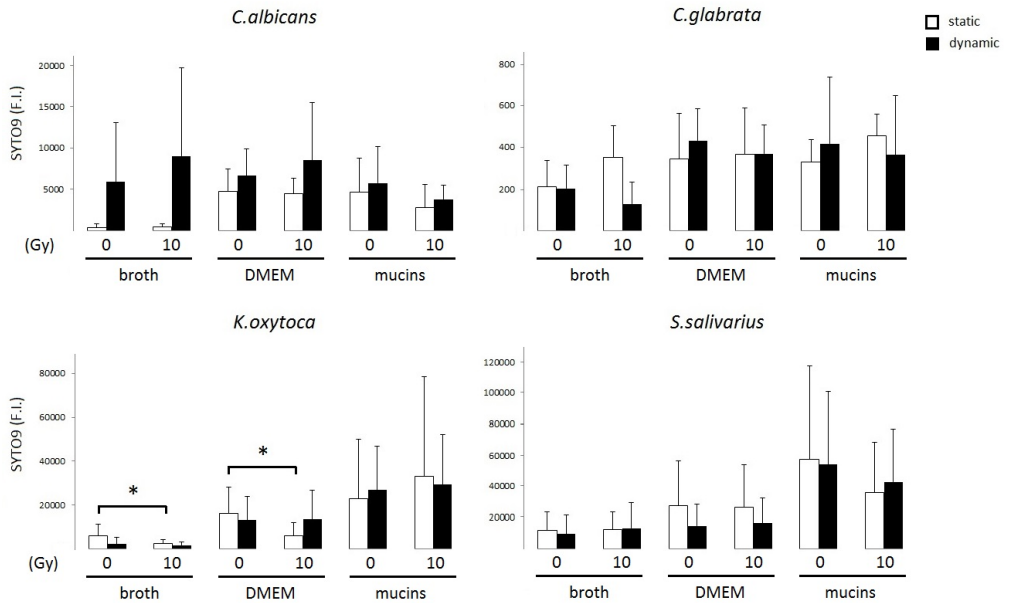


Figure 5-3: Box plot presentation of biofilms of irradiated (10 Gy) and non-irradiated *C. albicans*, *C. glabrata*, *K. oxytoca* and *S. salivarius* cells formed during 24 h of culture in different media (broth, DMEM or DMEM + mucins). The whiskers represent the minimum and maximum observed values. Biofilms were generated both in static (24-well plates, first column) and dynamic conditions (24-well plates, second column; tubes, third column). Vertical axis represents the optical density (OD) of dissolved crystal violet molecules measured at 540 nm using a spectrophotometer (n= 5-8; \* p< 0.05)

Next, we evaluated the number of cells in biofilms of all test species grown for 24 h after irradiation of the inoculum. To this end, we measured the fluorescence intensity of the biofilms after SYTO9 and PI staining. The SYTO9 stain generally labels all microbiota in a population, whereas PI penetrates only microbiota with damaged membranes, causing a reduction in the SYTO9 fluorescence when both dyes are present. We observed that irradiation significantly reduced the number of SYTO9-positive *K. oxytoca* cells, when the biofilms were grown in static conditions and in the absence of mucins (broth:  $p= 0.041$ ; DMEM:  $p= 0.008$ ) (Figure 5-4).



**Figure 5-4: SYTO9-positive cells present in irradiated and non-irradiated biofilms after 24 h in different culture media. Biofilms were generated both in static and dynamic conditions (24-well plates with or without shaking). SYTO9-positivity was assessed by measurement of fluorescence intensity (F.I.) at Ex480/Em500nm (vertical axis). (n= 9; mean + SD; \*  $p < 0.05$ )**

Furthermore, the metabolic activity, measured as MTT reduction, of the *K. oxytoca* biofilms was also reduced in those specific conditions (Figure 5-5). Figure 5-4 further illustrates that *Candida* biofilm formation on polystyrene plates is poor, irrespective of the type of medium used, whereas *K. oxytoca* and *S. salivarius* form dense biofilms in all media as was also obvious upon visual inspection. There was a trend for the presence of mucins to enhance biofilm formation by *K. oxytoca* and *S. salivarius*, although this difference was not statistically significant. We were unable to detect PI values that significantly differed from the detection limit, which indicates that the majority of the biofilm cells were alive and not affected by irradiation.



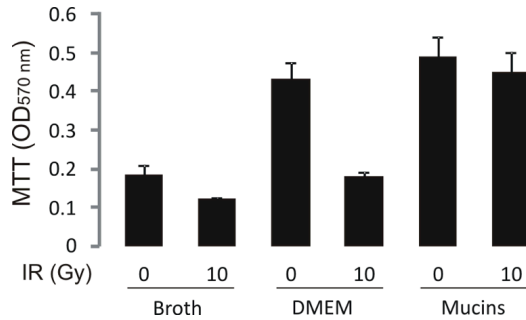


**Figure 5-5: Metabolic activity (MTT) of irradiated and non-irradiated biofilm cells of *K. oxytoca* after 24 h of culturing in different media (without agitation) as determined by measuring the optical density (OD) at 570 nm of the dissolved formazan crystals (n= 2; Mean + SD)**

We further examined if irradiation had an impact on the production of extracellular matrix components of biofilm cells. The cellulose content of the biofilms grown for 24 h after irradiation of the inoculum was evaluated by a calcofluor white staining. In our set-up, only *C. albicans* and *S. salivarius* produced an extracellular matrix that contained cellulose (Figure 5-6). Overall, no effect of irradiation on the cellulose content of the biofilm matrix could be observed.

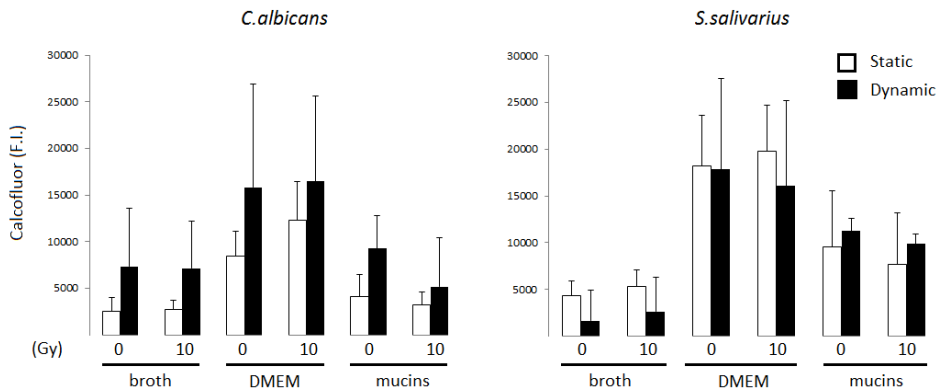


**Figure 5-6: Calcofluor staining of biofilms of irradiated (10 Gy) and non-irradiated *C. albicans* and *S. salivarius* formed within 24 h in static (white bars) or dynamic conditions (black bars) in 24-well plates and in presence of the 3 test media. Vertical axis represents the calcofluor fluorescence intensity (F.I.) at Ex355/Em430nm (n= 4; mean +SD, \* p< 0.05)**

### 5.4.3 Effect of ionizing irradiation on virulence of *K. oxytoca* and *S. salivarius*

We further questioned if irradiation had an impact on the virulence of the pathogen *K. oxytoca* and the commensal *S. salivarius*. To test this, we used larvae of the wax moth *G. mellonella* as a model host for examining the virulence potential of the species of interest. For survival assays, wax moth larvae were infected and mortality was monitored every 24 h for 4 days. At a dose of 10<sup>6</sup> CFU/mL, irradiated *K. oxytoca* were

significantly more virulent than non-irradiated cells ( $p= 0.027$ ;  $n= 20$ ) (Figure 5-7). At one day post-inoculation, the survival probability of the wax moth larvae infected with irradiated cells was lower than with non-irradiated cells. The time course of survival of the wax moth larvae depended on the pathogen load as injection of a dose of  $10^7$  or  $10^8$  CFU/mL resulted in a high mortality rate 24 h post-inoculation, while a dose of  $10^5$  CFU/mL was too low to cause infection (data not shown). In contrast to *K. oxytoca*, the virulence of *S. salivarius* at a dose of  $10^7$  CFU/mL did not significantly change upon irradiation (Figure 5-7). In order to find out if the increased virulence of *K. oxytoca* after irradiation was due to the secretion of particular factors, supernatants from non-irradiated and irradiated cells were collected and injected into the wax moth larvae. However, the supernatant of both groups had no effect on the overall survival of the wax larvae (data not shown). Also injection of dead cells had no influence on larval survival (data not shown), pointing to the need of living, metabolically active bacteria for virulence.

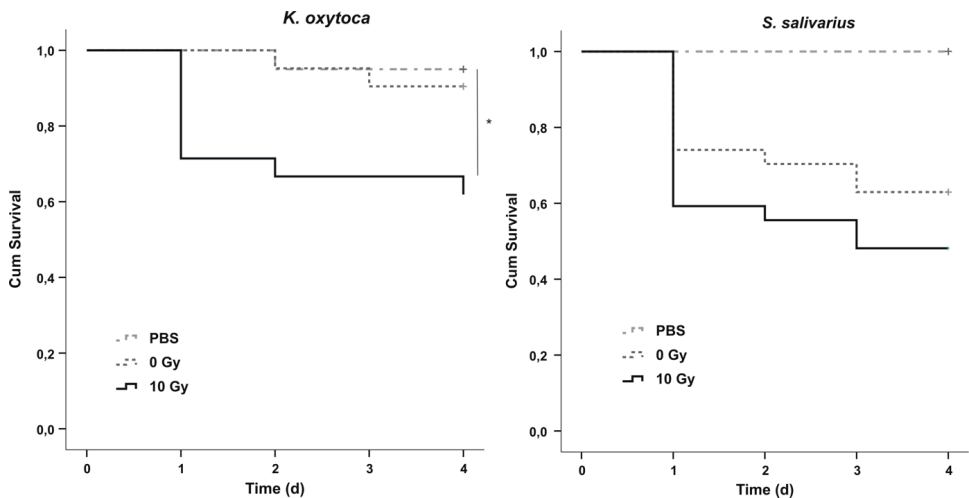


**Figure 5-7: Kaplan Meier survival curves of *Galleria mellonella* after inoculation with *K. oxytoca* ( $n= 20$ ) or *S. salivarius* ( $n= 27$ ). Test groups were PBS controls, non-irradiated (0 Gy) and irradiated (10 Gy) microbiota. Vertical axis represents the cumulative survival probability of the wax larvae during 4 days post-injection (\*  $p< 0.05$ )**

## 5.5. Discussion

Overall, our data indicate that ionizing irradiation can induce behavioural changes in specific oral species (Table 5-1). Of all species tested, only *K. oxytoca* was consistently affected. Most importantly, we showed that irradiation significantly increased the virulence of *K. oxytoca* *in vivo* using the *G. mellonella* model system. This model allows the study of bacterial and fungal infections at 37 °C and the immune system of the

larvae shares functional homology with the human innate immune system, possessing both humoral and cellular immunity (Hoffmann, 1995; Lionakis, 2011). This observation is important and relevant in the context of oral mucositis. Indeed, *K. pneumoniae* is a prevalent isolate in blood and oral cavity of cancer patients undergoing (chemo)radiation therapy (Gaetti-Jardim Júnior et al., 2011; Panghal et al., 2012) and pediatric patients undergoing high-dose chemotherapy or hematopoietic stem cell therapy (Kersun et al., 2005; Soares et al., 2011). Both groups have a very high incidence of developing oral mucositis. Due to their high incidence rate, *Klebsiella* spp. are considered one of the most significant infectious pathogens, causing urinary tract infections, pneumonia, wound infections, septicaemia, neonatal septicaemia and nosocomial infections (Sahly and Podschun, 1997; Podschun and Ullmann, 1998). As *K. pneumoniae* is frequently identified in individuals wearing removable maxillary prosthesis and are assumed to play important roles in denture stomatitis, wearing a removable prosthesis might be an important risk factor for developing mucositis and/or infections during or after radiation therapy (Pereira et al., 2013). It is therefore likely that the oral ulcerations are gateways for *Klebsiella* spp. and other opportunistic pathogens to penetrate the underlying damaged mucosa.

**Table 5-1: Overview of effect of irradiation on different behavioral characteristics of oral species**

		STATIC	DYNAMIC
<b>Growth planktonic cells</b>	<i>C.albicans</i>	-	NA
	<i>C.glabrata</i>	-	NA
	<i>K.oxytoca</i>	-	NA
	<i>S.salivarius</i>	-	NA
<b>Biofilm formation</b>	<i>C.albicans</i>	NA	NA
	<i>C.glabrata</i>	↑ (p <sub>DMEM</sub> =0.029);	↓ (p <sub>DMEM+mucins</sub> =0.017)
	<i>K.oxytoca</i>	↓ (p <sub>DMEM</sub> =0.002)	↑ (broth: trend)
	<i>S.salivarius</i>	NA	NA
<b>Number of biofilm cells</b>	<i>C.albicans</i>	NA	NA
	<i>C.glabrata</i>	NA	NA
	<i>K.oxytoca</i>	↓ (p <sub>broth</sub> =0.041; p <sub>DMEM</sub> =0.008)	NA
	<i>S.salivarius</i>	NA	NA
<b>Cellulose content</b>	<i>C.albicans</i>	NA	NA
	<i>C.glabrata</i>	NA	NA
	<i>K.oxytoca</i>	NA	NA
	<i>S.salivarius</i>	NA	NA
<b>Virulence</b>	<i>K.oxytoca</i>	↑ (p=0.027)	
	<i>S.salivarius</i>	NA	

- = not tested; NA = not affected

We further observed that irradiated *K. oxytoca* cells formed less biofilm in static conditions where oxygen transfusion is limited. In dynamic, oxygen-rich conditions, an opposite trend could be observed. Interestingly, these changes were not seen when mucins were present in the culture medium. Mucins exhibit protective effects on the alimentary tract through reducing mechanical and chemical stress, preventing bacterial overgrowth and penetration of the mucosa. During progressive mucositis, desquamation of the epithelium and its overlaying mucin layer results in severe ulcerations often associated with local infections. Moreover, mucin composition and expression have been shown to be altered by chemotherapy and this is thought to be associated with mucositis (Stringer et al., 2009a, 2009b, 2009c). Therefore, our *in vitro* observations provide biological clues as to why patients with a damaged mucosa have an increased risk of developing infections.

Our data suggest that the overall effect of irradiation on biofilm formation by *K. oxytoca* is dependent on factors such as oxygen availability and the shear stress. In the oral cavity, mucin-poor, static, oxygen-deprived conditions are found in the gingival crevice, which is a reservoir of opportunistic pathogens. *K. oxytoca* has been frequently isolated in biofilms of HIV-positive patients with plaque-associated gingivitis or periodontitis, indicating their ability to colonize oxygen-deprived mucin-poor niches in these patients (Zambon et al., 1990; Gaetti-Jardim Júnior et al., 2008) and after brace placement (Naranjo et al., 2006). Our data show that in oxygen-deprived conditions a lower number of *Klebsiella* cells were found in newly formed biofilms whereas in oxygen-rich conditions a higher number could be observed. This suggests that radiation therapy might lead to a lower number of potentially harmful cells in the gingival crevices after radiation therapy, whereas the opposite could happen on the teeth or gum line, where oxygen is abundantly available. Therefore, patients with a history of gingivitis/periodontitis might be able to manage their condition (gingivitis/ periodontitis) better after radiotherapy when maintaining good oral hygiene (as they are prone to develop denser *K. oxytoca* biofilms on the teeth surface). However, those patients might have an increased risk of developing infections related to *C. glabrata* as our data suggest that irradiation stimulates the biofilm formation of that species in static, oxygen-deprived conditions.

A potential relationship between radiation-induced mucositis and periodontitis has recently been suggested by Khaw et al. (2014) as both diseases are linked with chronic and systemic inflammation. This is clinically important, since the subgingival sites of patients with chronic periodontitis contain multi-resistant enterobacteria such as *Klebsiella* spp., which may contribute to tissue destruction and spreading (Gonçalves et al., 2007). Therefore, these patients may have a particular risk of developing oral mucositis complicated with systemic infections especially when they

are immunocompromised and hospitalized. Various *Candida* species are frequently identified in oral mucositis patients, especially after high-dose chemotherapy and radiotherapy (Belazi et al., 2004; Gaetti-Jardim Júnior et al., 2011; Laheij et al., 2012; Kurnatowski et al., 2014). In our study, no changes in biofilm formation of *C. albicans* were observed after irradiation. Therefore the mechanism by which *C. albicans* is able to overgrow the affected mucosa during mucositis might not be associated with effects on growth or biofilm formation.

Overall, the risk of developing an infection after irradiation will ultimately also depend on other factors like the virulence of the microbiota, the shift in tempo-regional attachment and colonization of the microbiota and the complexity of the composition of the biofilm. Recent data indicate that both chemo- and radiotherapy are associated with a decrease in microbial diversity (van Vliet et al., 2009; Shao et al., 2011; Hu et al., 2013a), which is believed to be correlated with a poor health prognosis. Our data indicate that apart from the composition, radiation therapy can also change the functional behaviour of the resident oral microbiome. Therefore, we hypothesize that local and systemic infections associated with mucositis are probably more likely to result from the cumulative effect of changes in composition, function and behaviour of the microbiome than solely from a compromised diversity. Therefore functional changes in the oral microbiome following chemo- and radiation therapy should be studied more in depth.

Although this work is relevant in the context of identifying microbial risk factors for the development of oral mucositis, it is important to highlight its limitations. Oral biofilms are highly complex multi-species structures and it is the delicate interaction between all its members that will ultimately determine their behaviour. Thus, further studies should address i) if similar observations can be made with other mucositis-associated pathogens besides *K. oxytoca* and in multi-species biofilms containing *K. oxytoca* and ii) what the underlying mechanism of this increased virulence potential of *K. oxytoca* is. Based on our preliminary results, we hope to further clarify if treatments like chemo- and radiotherapy are likely to modify the functional behaviour of the oral microbiome in a way that will eventually lead to dysbiosis, bacterial translocation and the overgrowth of pathogens during the progression phase of mucositis.

## 6. DYNAMIC SHIFTS IN THE ORAL MICROBIOME DURING RADIOTHERAPY

---

*Modified from: De Ryck T, Duprez F, Bracke M, Vanhoecke B\*, Van de Wiele T\*(2015). Dynamic shifts in the oral microbiome during radiotherapy. Clinical research in infectious diseases 2(1): 1013 (\* Equally contributing).*

### 6.1. Abstract

Awareness is growing concerning the potential role of the oral microbiota in radiotherapy-induced side effects like mucositis. In a small-scale patient study, we used denaturing gradient gel electrophoresis to visualize the shifts in the oral microbial community during radiotherapy. Samples of the first weeks of irradiation clustered together and towards the end of the therapy the richness decreased (-14 %) and the oral microbial community became dominated by a small fraction of species. The shifts at the level of the buccal mucosa and the tongue were correlated with different clinical parameters and a significant correlation between shifts in the buccal microbial community and the patients' normal oral functioning (pain, nutrition) was observed. By further monitoring the microbial shifts during therapy, the role of the microbiota can be elucidated and treatment regimes can be adapted, increasing patients' quality of life during therapy.

### 6.2. Introduction

Radiotherapy is still one of the most important treatment options for patients with head and neck cancer. Unfortunately, apart from the tumour, ionizing radiation also affects the healthy tissue surrounding the target, resulting in serious side effects and an overall decrease in the patients' quality of life. Irradiation of the oral cavity, for example, can have destructive effects on the salivary glands and often leads to hyposalivation (reduced salivary flow) and xerostomia (dry mouth syndrome) (Nutting et al., 2011; Tribius et al., 2013). This interruption of the salivary flow and associated xerostomia following radiation therapy have previously been linked with shifts in the oral microbiome with *Streptococcus mutans*, *Lactobacillus* spp., *Candida* and *Staphylococcus* spp. becoming more abundant whereas the number of *S. sanguis*, *Neisseria* spp. and *Fusobacterium* spp. tends to decrease (Brown et al., 1975; Almståhl

et al., 2008; Guobis et al., 2011). These microbial changes might trigger other side effects. The overgrowth of potential harmful species such as *Candida* spp. (mainly *C. albicans*) or cariogenic species will explain for example the higher prevalence of candidiasis and caries in patients treated with radiotherapy (Keene and Fleming, 1987; Farah et al., 2001; Su et al., 2011; Hu et al., 2013a).

Up to date, no data exist that correlate the shifts in the oral microbiome with the severity of mucositis. Nevertheless strong evidence exists that also in the context of mucositis the oral microbiota can be very important (van Vliet et al., 2010; Vanhoecke et al., 2015b). To enhance our current knowledge on the correlation between microbial shifts and particular radiation-related side effects like mucositis, a small-scale prospective study with 10 head and neck cancer patients was performed. To analyse their oral microbiome, we used 16S rRNA gene denaturing gradient gel electrophoresis (DGGE) profiling, a culture-independent approach, as over 30 % of the oral microbial species have not yet been cultivated (Dewhirst et al., 2010). Microbial shifts at the level of the buccal mucosa and the tongue were analysed and the correlation with different clinical parameters was investigated.

## **6.3. Patients, materials and methods**

### **6.3.1 Patients**

Ten patients treated with radiotherapy for head and neck cancer were enrolled in the study. All but one of the patients were male and the age ranged from 49-74 y, with a median of 60 y. All patients were treated with intensity-modulated radiotherapy (IMRT) at the department of Radiotherapy at Ghent University Hospital, Belgium (2011-2012). Five patients received concurrent chemotherapy. All patients had different treatment regimens due to the heterogeneity in their tumours and combined therapy modalities. Although the cumulative tumour doses were comparable for all patients (Table 1), the cumulative dose at the buccal and tongue mucosa differed from patient to patient depending on the location of the primary tumour. This resulted in more severe grades of mucositis in patients treated for cancer of the oropharynx or oral cavity.

The study was approved by the Medical Ethical Committee (Ghent University hospital, B670201110552) and all patients provided their written informed consent prior to the study.

### **6.3.2 Oral sampling**

To sample the oral microbial community, the oral cavity of the patients was flushed with drinking water before gently wiping the buccal and tongue mucosa ten times with a cotton swab. The upper part of the swab (cotton part) was stored in a sterile

eppendorf tube at -20 °C until DNA extraction. Samples were taken in the beginning of radiotherapy (before the fifth fraction) and weekly during the treatment (immediately after irradiation) until the end of the therapy. After the therapy, an extra sample was taken within the 2 first months after the therapy (follow-up appointment).

### 6.3.3 Clinical records

Weekly, all patients enrolled for the study consulted a radiotherapist. Their oral cavity and oropharynx were inspected and the severity of mucositis was scored according to the grading scale of the World Health Organization (Table 1-1).

At the time of sampling, patients were interrogated about their oral pain and their ability to eat solid foods. The time point during therapy when patients first suffered from severe pain and/or when they had difficulties to eat (only liquid food possible or the need for percutaneous endoscopic gastrostomy or total parenteral nutrition) was recorded. At this time point, the normal oral functioning (NOF) was considered to be significantly affected.

All patients' characteristics are listed in Table 6-1.

**Table 6-1: Overview of the patients' clinical characteristics**

Patient	Sex	Age (y)	Tumour site	Treatment	Number of RT fractions	Cummulative dose (Gy)	Mucositis (grade)	Hospitalization (*)	ΔNOF (*)
1	male	74	larynx	RT+CT	30	70.2	0	3	2
2	female	73	oral cavity	RT+AB	32	69.12	3	/	0
3	male	60	oral cavity	RT+CT	32	69.12	4	4	3
4	male	60	oropharynx	RT	32	69.12	3	/	3
5	male	66	oropharynx	RT+CT	32	69.12	3	6	3
6	male	56	oropharynx	RT+CT	30	69.12	3	/	2
7	male	65	CUP	RT	33	66	3	4	1
8	male	60	CUP	RT	32	69.12	2	/	3
9	male	58	CUP	RT+CT+AB	33	66	3	7	6
10	male	49	hypopharynx	RT	32	69.12	1	/	0

CUP= cancer of unknown primary origin; RT= radiotherapy; CT= chemotherapy; AB= antibiotics / = no hospitalization; ΔNOF= significant change in patients' normal oral functioning (NOF); \*= time during therapy (weeks after start) at which the patient was hospitalized or when the NOF was affected.

### 6.3.4 DNA-extraction

Total DNA extraction was performed as described earlier (De Ryck et al., 2014). Briefly, 500 µL Tris-HCl (10 mM, pH 9) and 1 mg lysozyme (VWR, Leuven, Belgium) was added to the cotton swab and the mixture was incubated at 37 °C on a rotary shaker for 10 min (250 rpm). 37.5 µL SDS (20 %) was added and the eppendorfs were gently mixed manually for 5 min. 500 µL chloroform-isoamyl alcohol (24:1 (v/v)) was added to extract the DNA. After homogenization of the suspension, the tubes were centrifuged at 7,000 g for 15 min at 4 °C and the water phase was recovered. 0.8 volumes of 100 % isopropanol were added and the DNA was allowed to precipitate during at least 1 h at -20 °C. By centrifugation at 7,000 g for 15 min at 4 °C the DNA



was pelleted. After drying the pellet, it was resuspended in polymerase chain reaction (PCR) water (250  $\mu$ L), and the DNA was purified with the Wizard® DNA Clean-Up System (Promega, Leiden, The Netherlands) according to the manufacturer's protocol. The purified DNA was stored at  $-20$  °C.

### 6.3.5 Nested PCR

A nested PCR strategy was applied as described previously (Bakke et al., 2011; De Ryck et al., 2014). For the external PCR reaction, we made use of EUB8F (5'-agagtttgatcmtggctcag-3') and 984 $\gamma$ R (5'-gtaagttctcgcgt -3') primers during 35 PCR cycles (95 °C, 30 s; 50 °C, 30 s and 72 °C, 1 min). For the internal PCR, the primers PRBA338GC (5'-cgcccgccgcgcggcgggcgggggcggggggcacggggggactcctacgggaggcagcag-3') and 518R (5'-attaccgcggctgctgg-3') were used for 25 cycles (95 °C, 30 s; 53 °C, 30 s and 72 °C, 1 min) to obtain 16S rDNA gene fragments of 180 bp suitable for DGGE analysis. The TaKaRa Ex Taq™ kit (Westburg, Leusden, The Netherlands) was used as master mix. Each reaction consisted of 2.5  $\mu$ L Ex Taq buffer (10x), 2  $\mu$ L dNTPs, 0.125  $\mu$ L Ex Taq enzyme, 0.2  $\mu$ M of each primer, 17.375  $\mu$ L of PCR water (Sigma-Aldrich, Diegem, Belgium) and 1  $\mu$ L of DNA. The PCR product of the external PCR was diluted 1:3000 and 1  $\mu$ L of this dilution was added to 24  $\mu$ L of mastermix for the internal PCR. The reaction mixtures were incubated in a Biometra thermocycler (Westburg, Leusden, The Netherlands) at 94 °C for 5 min, followed by 35 or 25 cycles and a final extension at 72 °C for 10 min.

### 6.3.6 DGGE analysis

For the DGGE analysis (Callewaert et al., 2013), the PCR-samples were mixed with loading buffer (4:1) before separation of the DNA fragments on an 8 % acrylamide gel with a denaturing gradient from 40 - 60 % (100 % denaturant contains 7 M urea and 40 % formamide). Electrophoresis was run for 16 h at 120 V, while the gel was maintained at 60 °C using the INGENYphorU System (Ingeny International BV, Middelburg, The Netherlands). DNA bands were visualized using SYBR Green (0.5x). The DGGE profiles were analysed and clustered with the BioNumerics software 5.10 (Applied Maths, Sint-Martens-Latem, Belgium). For this, the different lanes were defined, background was subtracted and the intensity of the lanes was normalized. The calculation of similarities was based on the Dice correlation coefficient. Clustering analysis was performed using Ward's method to calculate the dendrograms. The same homemade marker was used on every gel, allowing inter-gel (inter-patient) analysis.

### 6.3.7 Richness, Pareto-Lorenz curves and Gini coefficients

The richness (R) of a sample equals the number of bands that were detected on the DGGE profile. The Pareto-Lorenz curves were used to visualize the evenness of a certain microbial community and were constructed as described by Marzorati et al.

(2008). Higher evenness is characterized by a curve close to the 45° diagonal (the theoretical perfect evenness line). Lower evenness points to the dominance of a small fraction of species in the community. The Gini coefficient equals the normalized area between a given Pareto–Lorenz curve and the perfect evenness line.

For this study, the differences in richness and Gini coefficients between the samples at the end and at the start of the therapy were calculated. When the difference equals 0, no changes were found. Negative values point to a lower richness or evenness at the end compared to the start.

### **6.3.8 Statistics**

Statistical analysis was performed in SPSS statistics 22. Spearman's correlation coefficient was used to search for significant ( $p < 0.05$ ) correlations between the patients' normal oral functioning and the Dice-Ward clusters found after DGGE analysis. After a normality check using the Shapiro-Wilk assay, T-tests were used to evaluate if the differences in richness and Gini coefficients were significantly different from zero ( $p < 0.05$ ).

## **6.4. Results and discussion**

In this study, bandwise cluster analysis was performed after DGGE to gain insights into the microbial shifts that occurred during radiation therapy. In 6 out of 10 patients (patient 1, 2, 3, 4, 5 and 7), 2 main clusters could be observed, in which samples of the first weeks of treatment clustered together (Figure 6-1). Shao et al. also used DGGE analysis to study the shifts in the oral plaque microbiota during radiotherapy. Comparable to our results, they also reported low similarity of the DGGE profiles within one individual (Shao et al., 2011).

PCR-DGGE analysis was previously proven useful to investigate the microbial diversity in healthy or diseased states. For example, the microbial colonization of tumour tissue (oral squamous cell carcinoma, OSCC) and healthy tissue was studied using DGGE. In this way, 4 bands could be identified that were unique for tumour tissues and may be associated with different stages of OSCC (Pushalkar et al., 2012). Ahmed et al. (2012) used DGGE to compare the oral microbial profiles of healthy individuals with those obtained from patients suffering from caries or periodontitis. Although most of the samples of the periodontitis group clustered together, no strict separation was found in that study. The overall microbial composition was shown to be highly similar over time within one person (Tao et al., 2013). Moreover, moving window analysis from 1 day to 1 month in 3 healthy individuals, showed similarities between 80 and 100 % (data not shown). Therefore, DGGE analysis is a promising tool to identify shifts due to therapy.

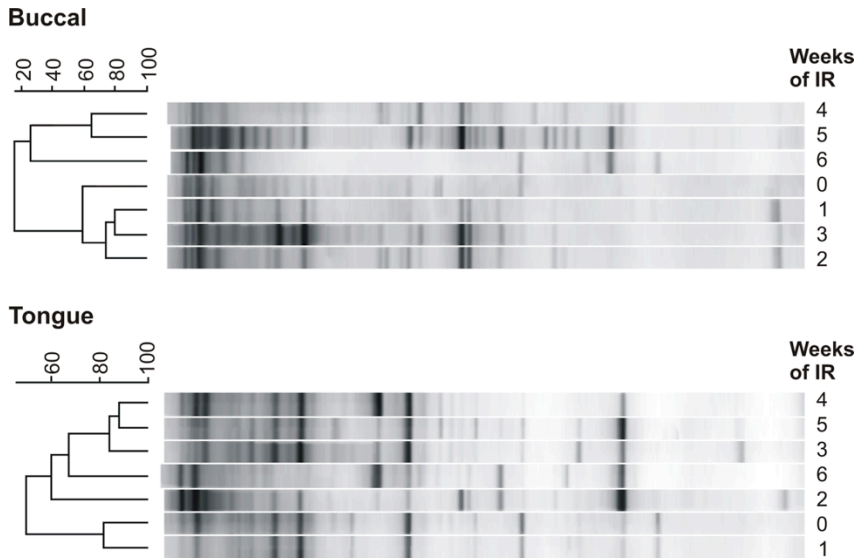


**Figure 6-1: DGGE cluster analysis (Dice-ward) of the buccal and tongue samples of one representative patient during radiotherapy (patient 5). Percentage of similarity is shown on the scale above the dendrogram**

For the buccal samples, microbial community shifts were mainly found after 3 weeks of irradiation (median cumulative dose of 32.94 Gy), whereas for the tongue, shifts could be noticed earlier (median= 2 weeks of IR; median cumulative dose= 23.76 Gy) (Table 6-2). Previously, pairwise similarity of plaque samples was also reported to decrease after 3 weeks of treatment (Shao et al., 2011). No significant differences could be noticed between the lowest similarity values of the buccal mucosa compared to the tongue (data not shown). Due to radiotherapy, the microbial richness (number of bands/sample, median  $R_{\text{buccal}}= 21$ ; median  $R_{\text{tongue}}= 20.5$  at start) was negatively impacted both on the buccal and tongue mucosa (median  $\Delta R_{\text{buccal}}= \text{median } \Delta R_{\text{tongue}} = -3$ ,  $p_{\text{buccal}}= 0.317$ ;  $p_{\text{tongue}}= 0.532$ ; Table 6-2). This decrease in richness confirmed the results of Hu et al. (2013), who observed a decrease in the number of operational taxonomic units after radiotherapy.

Marzorati et al. (2008) described how one could get more data from microbial fingerprints, making this technique more powerful. By use of Pareto-Lorenz curves for example, insights in the evenness can be obtained. A high evenness of a community means that all different species are present in similar amounts and the community is thus not dominated by a smaller fraction of species. As an uneven community is linked with a loss of functionality and an increased risk to get invaded by pathogens, it is important to evaluate this parameter. Pareto-Lorenz curves of the samples at the start and the end of the therapy were constructed and the differences in Gini coefficients

were calculated (Table 6-2). In 6 patients, the oral community remained stable or was dominated by a few species (uneven community), characterised with higher Gini coefficients at the end of the therapy (Figure 6-2 – left panel; Table 6-2 –  $\Delta\text{Gini} \geq 0$ ). However, in 4 patients (2, 8, 9 and 10) a higher evenness at the end of the therapy was observed (Figure 6-2 – right panel; Table 6-2 –  $\Delta\text{Gini} < 0$ ).

**Table 6-2: Overview of the patients’ microbial diversity characteristics**

Patient	First cluster buccal (*)	Cum. dose first cluster buccal (Gy)	First cluster tongue (*)	Cum. dose first cluster tongue (Gy)	$\Delta\text{R}$ (buccal)	$\Delta\text{R}$ (tongue)	$\Delta\text{Gini}$ (buccal)	$\Delta\text{Gini}$ (tongue)
1	3	35.64	1	16.2	-8	-9	0.120	0.158
2	1	12.96	2	23.76	ND	12	ND	-0.425
3	4	36.72	3	25.92	-4	-3	0.295	0.043
4	3	30.24	3	30.24	-1	-13	-0.002	0.117
5	3	36.72	1	12.96	-9	1	0.225	0.004
6	/	/	/	/	-8	-3	0.035	0.030
7	1	18	4	46	-3	-5	0.053	0.065
8	/	/	/	/	-2	7	-0.117	-0.216
9	/	/	/	/	6	-1	-0.106	-0.006
10	/	/	2	21.6	9	ND	-0.240	ND

IR= irradiation;  $\Delta\text{R}$ = richness(end)-richness(start);  $\Delta\text{Gini}$ = Gini(end)-Gini(start); ND= not determined; \*= Number of weeks after the start of radiotherapy that clustered together

The clinical records of these patients may give an indication why their oral microbial communities behave differently. Prior to the start of the radiotherapy, the tongue of patient 2 showed clear signs of infection for which the patient received antibiotics (clavulin). The microbial community was able to restore itself probably due to the antibiotics as evidenced by a higher richness and evenness of the community at the end of the treatment. Also patient 9 received antibiotics (glazidim and vancomycin) during radiation therapy, clarifying its deviant behaviour in our analysis. On the tongue surface of patient 8, a milky spot was observed at the start of the therapy and this was probably caused by a fungal infection. Oral rinses with the antifungal solution based on nystatin (5 times/day) were advised, which resulted in the successful elimination of the infection and the aberrant observations in the tongue microbial community. Patient 10 was the only patient who received a tracheostoma prior to the radiation therapy. In the course of the therapy, this patient was able to restart oral feeding. Moreover, this patient did not suffer from radiotherapy and had no clear signs of oral mucositis in his oral cavity or oropharynx. In all other patients no infection in the beginning of the therapy was noticed. As a preventive measure they were advised to maintain good oral hygiene and to rinse their oral cavity with an antifungal solution based on nystatin.

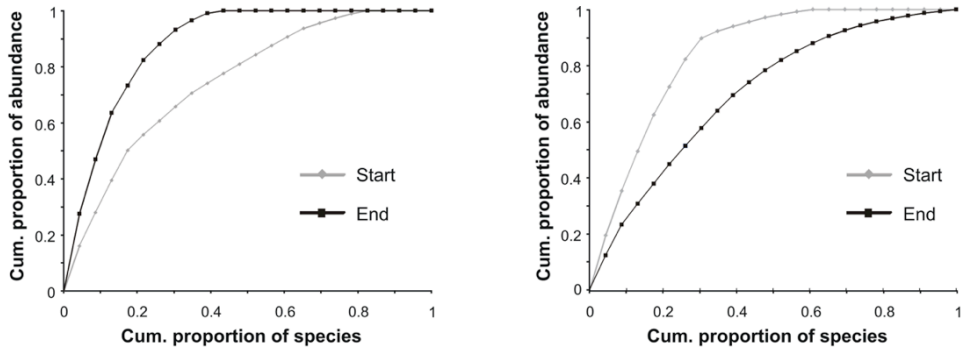


**Figure 6-2: Pareto-Lorenz curves of the buccal microbial community at the beginning and the end of the therapy of two representative patients (left panel= patient 5; right panel= patient 10)**

A significant correlation was found between the patients' normal oral functioning and the buccal clustering ( $p= 0.031$ ). When patients suffered from severe pain in the oral cavity or when they were unable to eat solids, their microbial population changed significantly. It was already shown before that diet and more specifically the protein and starch content influenced the oral microbial abundance of lactobacilli and streptococci (Blais and Lavoie, 1990). Also tube feeding will disrupt the indigenous oral microbiota, allowing other bacteria to become more dominant. This results in a higher number of opportunistic pathogens like *Corynebacterium striatum* and *Streptococcus agalacticae* in tube-fed patients (Takeshita et al., 2011). For the tongue samples, no significant correlations could be found.

There were no significant correlations between the severity of mucositis and the clustering or the changes in richness and evenness. Nevertheless, the microbial community of a mucosal lesion (inflammatory region) was found to be dominated by a few species (low evenness) compared to the community of a non-inflammatory region in the same patient at the same time point during therapy (Figure 6-3). The higher abundances of Gram-negative microbiota and lactobacilli due to radiotherapy are likely to cause this shift in evenness (Almståhl et al., 2008; Guobis et al., 2011; Sonalika et al., 2012b). After radiation therapy, the microbial community of the inflammatory region was restored (higher evenness; Figure 6-3).

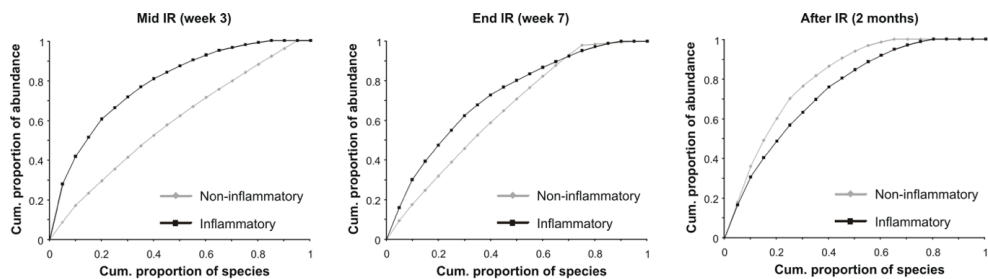


**Figure 6-3: Pareto-Lorenz curve of an inflammatory and non-inflammatory region in the oral cavity of patient 3 during the radiotherapy**

## 6.5. Conclusion

In this small-scale patient study we investigated the microbial shifts during radiotherapy. In patients who did not receive antibiotics during their treatment, the oral microbial community was shown to evolve to a more uneven community, similar to what was seen in the inflammatory regions. The shifts in the buccal microbiota were found to be significantly correlated with the patients' normal oral functioning. Although further research is necessary, when a certain therapy is affecting patients' ability to eat, doctors should be aware of possible important microbial shifts and they should monitor the presence of pathogens to avoid more undesirable side effects.



## 7. MICROBIAL SHIFTS IN THE CONTEXT OF RADIOTHERAPY-INDUCED ORAL MUCOSITIS

---

### 7.1. Abstract

Nowadays, researchers investigate host-microbe interactions to gain new insights in the pathobiology of different diseases in search for new treatment strategies. Also in case of oral mucositis, a severe side effect of cancer therapy, interest in the potential role of the oral microbiota is growing. By use of illumina sequencing analysis, we investigated the shifts in oral microbiota during radiotherapy. The relative abundances of *Bacteroidetes* and *Fusobacteria* spp. colonizing the buccal mucosa increased due to radiotherapy, while the tongue microbiota appeared to be more stable. Furthermore, microbiota like *Bifidobacterium*, *Fusobacterium*, *Peptostreptococcus*, *Porphyromonas* and *Prevotella* spp. were shown to increase with the severity of oral mucositis. Moreover, we were able to identify certain microbiota like *Atopobium* spp. which were significantly higher in the oral cavity of patients that would develop severe mucositis, pointing to its' potential use as a marker for severe mucositis. In the future, research should further elaborate on the potential role of oral microbiota in the context of oral mucositis in search for new markers or treatment strategies.

### 7.2. Introduction

During the last decade, the potential role of the microbiota in a plethora of diseases, including mucositis, has gained interest. Van Vliet et al. (2010) proposed an updated pathobiology model of chemotherapy-induced gastro-intestinal mucositis, which included the role of the microbiota. The commensal microbiota are shown to influence the inflammatory response, the intestinal permeability and the composition of the mucus layer. Also the epithelial resistance towards harmful stimuli, the epithelial repair mechanisms and the production of immune effector molecules are upregulated by the microbiota (van Vliet et al., 2010). All these factors are potential triggers to develop mucositis in the gut. Unfortunately, research on the role of the microbiota in radiotherapy-induced oral mucositis is still limited. Only a few studies focussed on the microbial shifts due to radiotherapy, which were recently reviewed by Vanhoecke et al. (2014). One of the studies used 454 pyrosequencing analysis to investigate



microbial shifts in eight head and neck cancer patients during radiotherapy (Hu et al., 2013a). Although these patients are prone to develop radiotherapy-induced oral mucositis, the authors did not take the severity of mucositis, developed by the patients during their treatment, into consideration.

In the previous chapter of this dissertation, it was shown that the shifts in the composition of the oral microbiome during radiotherapy were highly correlated with the patients' quality of life. Shifts in the buccal mucosa were found after a cumulative dose of 32.94 Gy, whereas in the tongue microbiota, shifts were observed slightly earlier (23.76 Gy). These shifts could be correlated with the pain and nutritional issues of the patients during radiotherapy. In this chapter, we aimed to identify microbial shifts during therapy and specific microbiota that could play a role in the pathobiology of mucositis. Therefore, the microbial communities derived from buccal and tongue swabs of 25 head and neck cancer patients were investigated using Illumina sequencing analysis.

## **7.3. Patients, materials and methods**

### **7.3.1 Patients**

For this study, 25 patients treated with radiotherapy for head and neck cancer were enrolled. Three of the included patients were female and the age of the patients ranged from 46-74 y, with a median of 63 y. All patients were treated with radiotherapy at the department of Radiotherapy at Ghent University Hospital, Belgium (2011-2012). Twelve patients received concurrent chemotherapy. All patients received the best possible treatment for their illness and therefore they all had different treatment regimens.

The study was approved by the Medical Ethical Committee (Ghent University hospital, B670201110552) and all patients provided their written informed consent prior to the study.

### **7.3.2 Oral sampling**

The oral cavity of the patients was flushed with drinking water before gently wiping the buccal and tongue mucosa with a cotton swab for ten times. The upper part of the swab (cotton part) was stored in a sterile eppendorf tube at -20 °C until DNA extraction. Samples were taken in the beginning of radiotherapy (start; before the fifth fraction; median cumulative dose= 2.16 Gy), halfway therapy (mid; median cumulative dose= 30.24 Gy) and at the end of the treatment (end; median cumulative dose= 66.96 Gy), each time immediately after the daily radiation fraction. After the therapy, an extra sample was taken during the follow-up appointment of the patients (recup; median time= 1 month).

### 7.3.3 Clinical records

At the time of sampling, all patients enrolled for the study consulted a radiotherapist. Their oral cavity was inspected and the severity of mucositis was scored according to the grading scale of the World Health Organization (Table 1-1; Treister and Sonis, 2007)

All patients' characteristics are listed in Table 6-1. The samples of patients who received antibiotics during their treatment were excluded from all analysis.

**Table 7-1: Overview of the patients' clinical characteristics**

Patient ID	Sex	Age (y)	Tumoursite	Treatment	Total dose RT (Gy)	Total nr of RT-fractions	Max mucositis grade
1	m	74	larynx	RT + CT	70.2	30	0
2	m	60	oral cavity	RT + CT	69.12	32	4
3	m	60	CUP	RT + CT	69.12	32	1
4	m	66	oropharynx	RT + CT	69.12	32	3
5	m	58	CUP	RT + CT+AB	66	33	3
6	m	72	oropharynx	RT	70.2	30	2
7	m	60	oropharynx	RT	69.12	32	3
8	f	73	oral cavity	RT+AB	69.12	32	3
9	m	68	larynx	RT	69.12	32	1
10	m	65	oropharynx	RT + CT	69.12	32	1
11	m	60	CUP	RT	69.12	32	2
12	m	64	oropharynx	RT + CT	80.6	30	3
13	m	72	larynx	RT	69.12	32	1
14	m	53	oral cavity	RT	66	33	2
15	m	46	oral cavity	RT	69.12	32	3
16	m	48	oropharynx	RT + CT	80.6	30	3
17	m	67	larynx	RT	66	33	1
18	m	49	oropharynx	RT + CT+AB	69.12	32	2
19	m	61	larynx	RT + CT	69.12	32	1
20	m	56	CUP	RT + CT+AB	69.12	33	2
21	f	55	oropharynx	RT	66	30	2
22	m	69	oropharynx	RT	69.12	32	2
23	m	70	oral cavity	RT + CT+AB	69.12	32	3
24	f	65	oral cavity	RT	66	33	2
25	m	63	hypopharynx	RT+AB	66	33	1

m= male; f= female; CUP= cancer of unknown primary origin; RT= radiotherapy; CT= chemotherapy; AB= antibiotics

### **7.3.4 DNA-extraction**

Total DNA extraction was performed as described earlier in Chapter 6.

### **7.3.5 Illumina sequencing analysis**

DNA samples were sequenced by LGC genomics (Berlin, Germany). 300 bp paired-end reads (Illumina MiSeq V3) of the bacteria 16S DNA were obtained using the primers 341F (3'- CCTACGGGNGGCWGCAG -5') and 785R (3'- GACTACHVGGGTATCTAAKCC - 5'). All samples were demultiplexed using Illumina's CASAVA data analysis software. The Illumina TruSeq™ adapters were clipped and reads with a final length < 100 bases were discarded. The primer and barcodes were clipped and the forward and reverse reads were combined using FLASH 1.2.4 (minimum overlap of 10 bases and a maximum mismatch rate of 25 %). These combined sequences were further processed using Mothur v1.33.3 following the MiSeq SOP ([http://www.mothur.org/wiki/MiSeq\\_SOP](http://www.mothur.org/wiki/MiSeq_SOP)) with the phylotype approach to obtain the OTU-table. The reference alignments were SILVA-based and the RDP trainset v9 was used to classify the sequences.

### **7.3.6 Analysis and statistics**

The diversity indices (Richness, Inverse Simpson and Shannon) were calculated using Mothur v1.33.3. For all other analyses, OTUs present for less than 0.01 % in the whole dataset were excluded. R v3.0.2 was used to draw the rarefaction curves and to perform the principal component analysis (phyloseq package). To investigate the effects of irradiation on the microbiota, only the patients of whom we obtained samples of the 4 time points were considered (buccal: 13 patients, tongue: 16 patients.). To investigate the link with the severity of mucositis all available samples were used. The statistical analyses were performed using SPSS statistics 22. Kruskal Wallis or Mann Whitney U tests were performed to identify significant differences. Bonferroni correction of the p-values was performed where needed. Differences were considered significant when  $p < 0.05$ .

## **7.4. Results**

### **7.4.1 Overall sequencing results**

To normalize the obtained sequence data, we subsampled 7,000 sequences of each sample. At this threshold, rarefaction curves show that the complete richness of the different samples is mostly reached and only 10 % of the samples were lost for further analysis (Figure 7-1). 14 of the 20 eliminated samples originated from swabs taken during the therapy (mid and end), which possibly points to the loss of oral microbiota. In total, 337 different operational taxonomic units (OTU) were observed

in the oral samples. As sample coverages were all above 99 %, sampling of the communities was performed well.

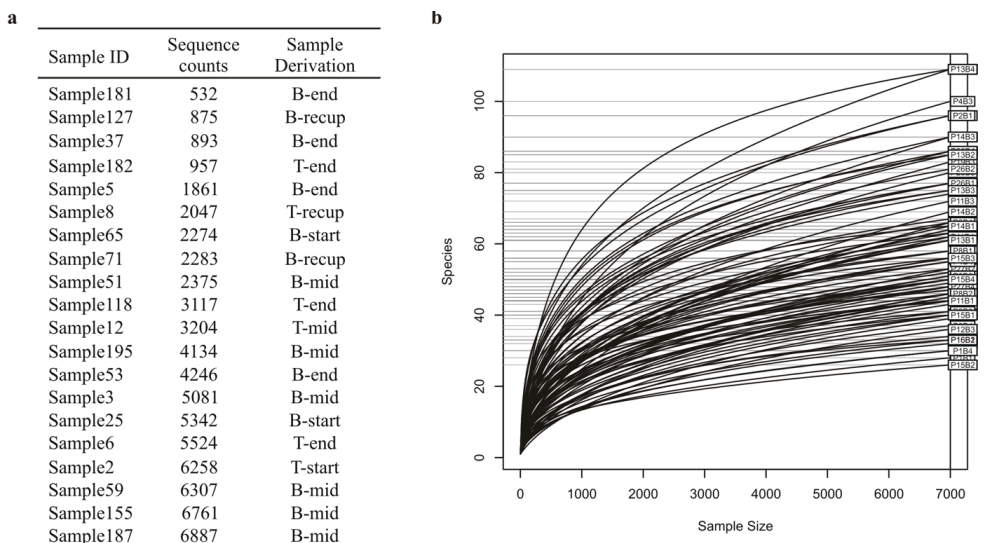


**Figure 7-1 a: Samples with less than 7,000 sequences that were excluded from the study (B= buccal, T= Tongue). b: Rarefraction curves of the samples retained in the study**

The average richness of the different samples was  $58.6 \pm 16.2$  and no significant differences were found when comparing the richness of the buccal samples with those of the tongue at the different time points. Furthermore, no significant differences were found in the richness of the oral community of the buccal or tongue samples during radiotherapy.

Rarefaction analysis of different diversity indices showed the potential of the Shannon and Inverse Simpson index to describe the diversity of our samples (data not shown). The Shannon entropy index is a measure for the evenness of a sample. When all OTUs are equally distributed, the uncertainty to predict which OTU one will pick from a particular community will be higher and thus the Shannon index will be higher. The inverse Simpson index is a measure for proportional abundances. An increase in the inverse Simpson index reflects an increase in the diversity. During the therapy, no significant shifts in the microbial diversity could be observed. The diversity in the tongue samples was found to be higher compared to the buccal samples, which was significant in the first half of the therapy (Shannon:  $p_{\text{start}} = 0.001$ ,  $p_{\text{mid}} = 0.023$ ; Inv. Simpson:  $p_{\text{start}} < 0.001$ ,  $p_{\text{mid}} = 0.007$ ; Table 7-2).

**Table 7-2: Diversity indices of the buccal and tongue samples (n= 17; mean ± stdev)**

	Buccal samples			Tongue samples		
	Richness	Shannon	Inv. Simpson	Richness	Shannon	Inv. Simpson
<b>Start</b>	56.11 ± 3.91	1.39 ± 0.62	2.88 ± 2.26	57.77 ± 10.59	1.89 ± 0.23	4.38 ± 1.10
<b>Mid</b>	52.65 ± 15.68	1.26 ± 0.40	2.24 ± 0.71	60.10 ± 13.76	1.65 ± 0.51	3.80 ± 1.75
<b>End</b>	63.22 ± 19.56	1.51 ± 0.66	3.07 ± 1.44	61.28 ± 17.09	1.69 ± 0.36	3.54 ± 1.13
<b>Recup</b>	62.20 ± 22.45	1.56 ± 0.65	3.36 ± 2.11	55.56 ± 12.30	1.69 ± 0.46	3.91 ± 1.87

**7.4.2 Analysis of the buccal microbiota**

First, principal component analysis (PCA) of the buccal samples was performed to visualize the variation within the data. In the first 2 dimensions, the variance between the samples could be described for 82 %. Here, the presence of OTU1, OTU2, OTU4, OTU6 and OTU12 appeared to be the most important determinants to describe the variance (Figure 7-2). These OTUs represent the *Streptococcus*, *Veillonella*, *Rothia*, *Prevotella* and *Fusobacterium* spp., respectively. However, no clear distinction between different samples depending on the time during therapy or the severity of mucositis was found.

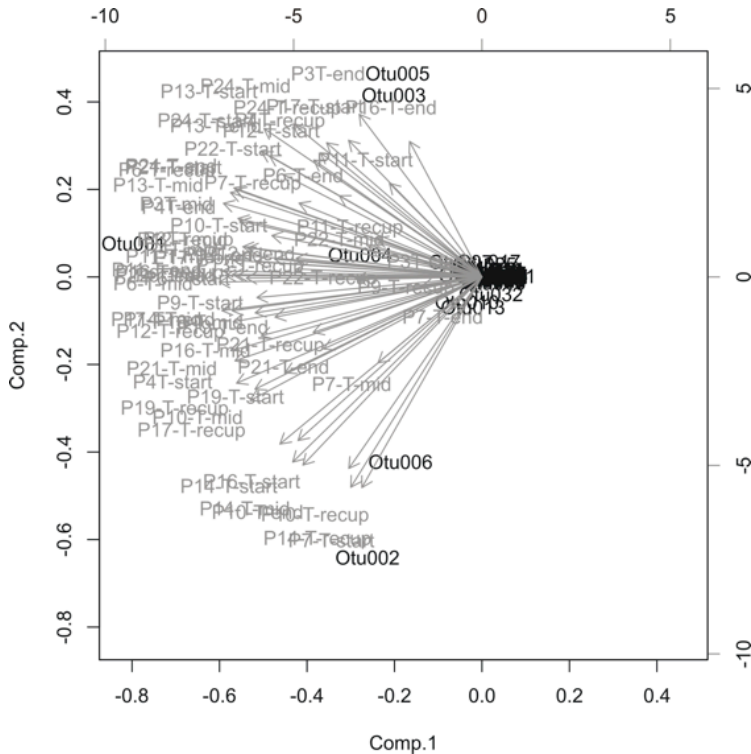


**Figure 7-2: Principal component analysis of the buccal samples**

Within the buccal microbiota, 8 different phyla were found, of which the Firmicutes, Proteobacteria, Actinobacteria, Bacteroidetes and Fusobacteria are the most dominant, counting for 99.24 % of the observed sequences and the Spirochaetes, Tenericutes and TM7 are almost negligible (0.31 %). Due to radiotherapy the relative abundance of Bacteroidetes and Fusobacteria spp. were shown to increase ( $p= 0.059$ ,  $p= 0.159$ , respectively). In contrast, the Actinobacteria tended to decrease at the end of the therapy ( $p= 0.680$ )(Figure 7-3).

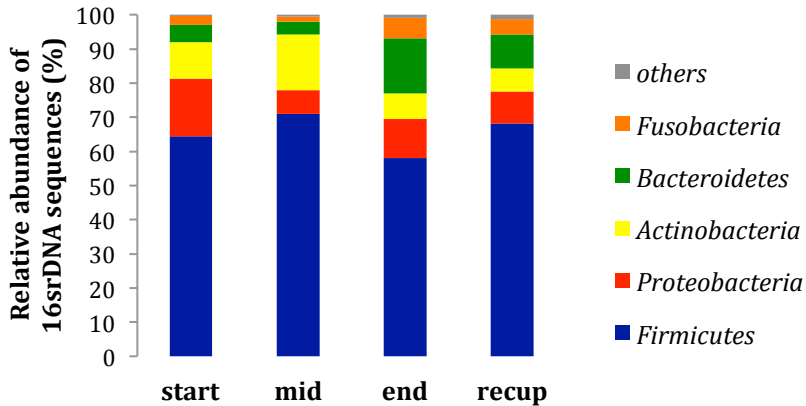


**Figure 7-3: Relative abundance (%) of the predominant phyla of the buccal microbiota at different time points during radiotherapy (n= 13)**

At the genus level, the number of *Abiotrophia* significantly decreased due to radiotherapy ( $p= 0.003$ ,  $p_{\text{start-end}}= 0.018$ ), whereas the abundance of *Lachnospiraceae\_incertae\_sedis* and unclassified *Prevotellaceae* spp. increased towards the end of the therapy (*Lachnospiraceae\_incertae\_sedis*:  $p= 0.016$ ,  $p_{\text{mid-end}}= 0.006$ ; *Prevotellaceae*:  $p= 0.016$ ,  $p_{\text{mid-end}}= 0.024$ ). The abundances of unclassified *Streptococcaceae* were shown to fluctuate during radiotherapy ( $p= 0.031$ ,  $p_{\text{mid-end}}= 0.012$ )(Figure 7-4).

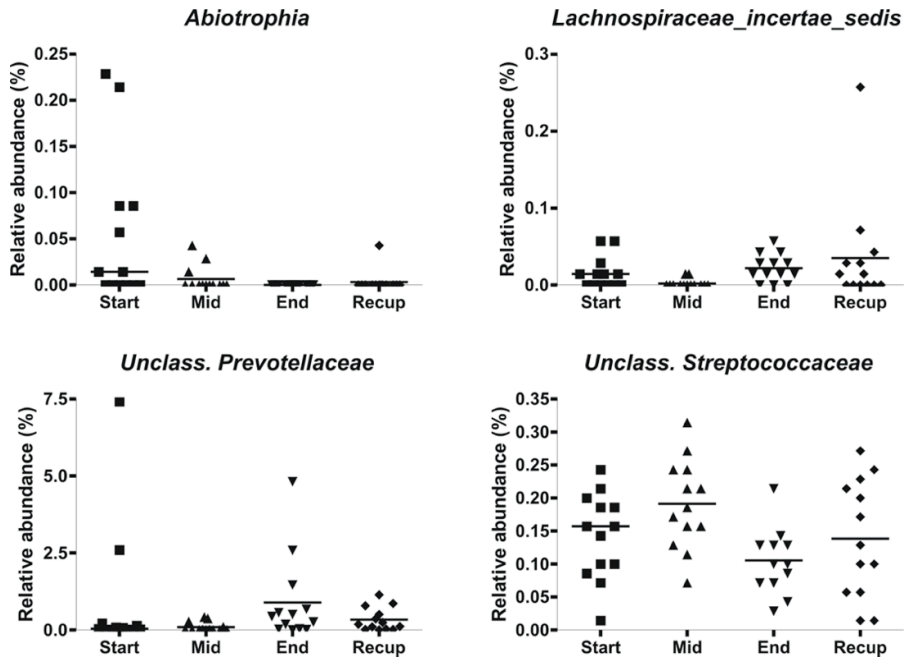


**Figure 7-4: Relative abundance (%) of 4 genera of the buccal microbiota at different time points during radiotherapy. Median values of the different samples are depicted (n= 13)**

As our main goal was to gain more insights in the shifts of the microbial community in the context of oral mucositis, we further tried to identify the differences in the oral microbial composition depending on the mucositis grade. From the oral microbiota present at the start of the therapy, 7 genera were found to be significantly different between the patients suffering from mild mucositis (Grade 0, 1 or 2) and those suffering from severe mucositis (Grade 3 or 4)(Figure 7-5;  $p_{Atopobium}= 0.027$ ;  $p_{Corynebacterium}= 0.037$ ;  $p_{Aggregatibacter}= 0.048$ ;  $p_{Unclass.Lachnospiraceae}= 0.037$ ;  $p_{UnclassTM7}= 0.048$ ;  $p_{Gemella}= 0.027$ ;  $p_{Unclass.Proteobacteria}= 0.048$ ). Of these *Gemella*, *Atopobium* and unclassified *Proteobacteria* are the most interesting. Our data showed that when *Gemella* spp. were present at an abundance of > 2.5 % and *Atopobium* spp. were absent; patients did not suffer from severe mucositis (grade 3 or 4) during their therapy. After the therapy, in the follow-up period, patients that suffered from severe mucositis showed a significantly higher abundance of unclassified *Prevotellaceae* ( $p= 0.027$ ) and no unclassified *Enterobacteriaceae* ( $p= 0.014$ ).

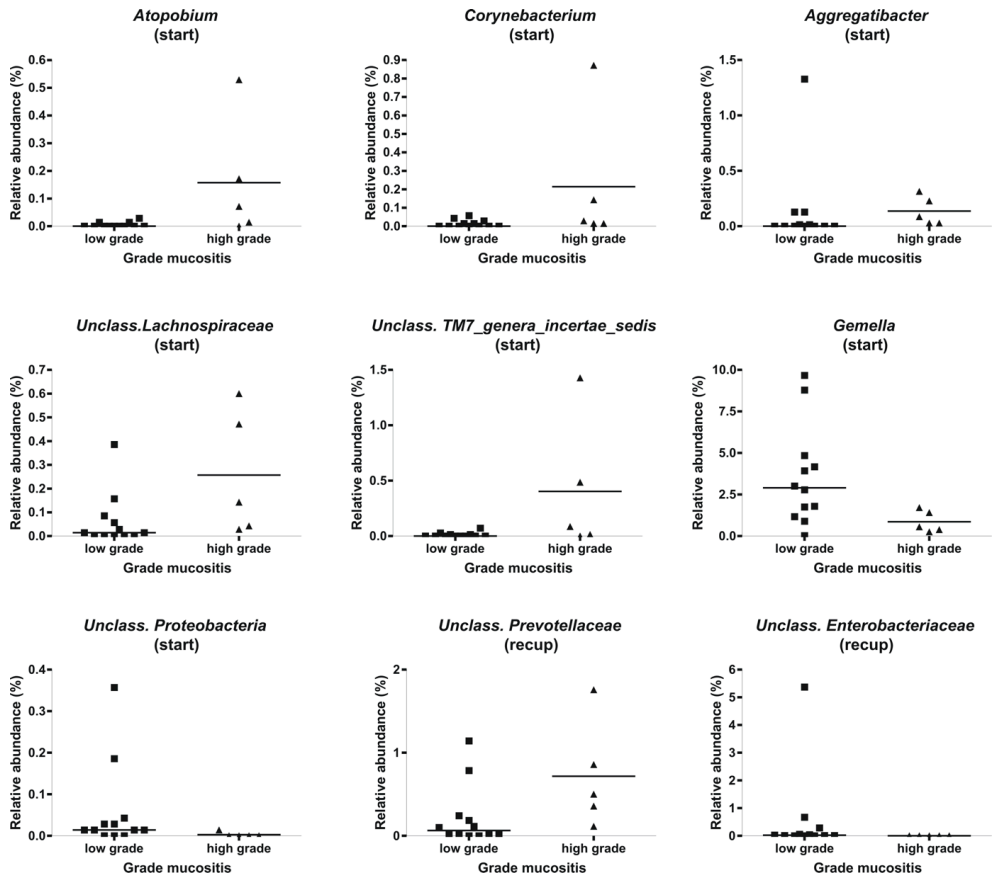


**Figure 7-5: Relative abundance of the buccal microbiota at the start and after radiation therapy (recup) assigned to genus depending on the maximal severity of mucositis scored during treatment (low grade: Gr 0, Gr 1, Gr2; high grade: Gr 3 or Gr 4). Median values of the different samples are depicted (n<sub>low grade</sub>= 12; n<sub>high grade</sub>= 5)**

Next, we evaluated the link between the oral microbial composition during the therapy (mid and end) and the mucositis grade at those specific time points. A significant increase in 13 genera was found (Table 7-3), of which *Bifidobacterium*, *Fusobacterium*, *Peptostreptococcus*, *Porphyromonas* and *Prevotella* spp. are of interest as they increased steadily with the severity of mucositis.



**Table 7-3: Relative abundance of the buccal microbiota during radiotherapy (mid and end) assigned to genus depending on the severity of mucositis, together with the Bonferroni corrected p-values**

Abundance (%) Microbial genus	Severity of mucositis				Bonferroni corrected P-value		
	Gr 0 (n=1)	Gr 1 (n=17)	Gr 2 (n=10)	Gr 3 (n=5)	Gr1-Gr2	Gr1-Gr3	Gr2-Gr3
<i>Bifidobacterium</i>	0.000	0.003	0.053	0.114	0.513	0.006	0.621
<i>Catonella</i>	0.000	0.006	0.071	0.023	0.339	0.021	0.651
<i>Dialister</i>	0.029	0.019	0.411	0.060	0.288	0.015	1.608
<i>Eubacterium</i>	0.014	0.002	0.079	0.031	0.510	0.003	1.161
<i>Filifactor</i>	0.029	0.000	0.207	0.046	0.018	0.024	2.670
<i>Fusobacterium</i>	0.257	0.223	5.067	4.194	0.075	0.012	0.423
<i>Hallella</i>	0.000	0.002	0.100	0.054	0.018	0.003	1.239
<i>Oribacterium</i>	0.014	0.002	0.053	0.063	0.021	0.003	1.968
<i>Peptostreptococcus</i>	0.014	0.002	0.039	0.440	0.021	0.000	0.687
<i>Porphyromonas</i>	0.129	0.138	0.534	1.457	0.096	0.030	0.804
<i>Prevotella</i>	0.214	0.791	6.924	12.846	0.006	0.006	0.981
<i>Treponema</i>	0.100	0.003	0.426	0.069	0.027	0.543	1.557
<i>unclas. Prevotellaceae</i>	0.014	0.352	0.373	0.746	0.108	0.039	1.500
<i>unclass. Fusobacteriaceae</i>	0.000	0.009	0.044	0.069	0.210	0.036	1.143

n= number of samples; Gr= grade

### 7.4.3 Analysis of the tongue microbiota

PCA on the tongue samples showed that the variance between the samples was only described for 64 % in the first 2 dimensions. Similar to the buccal samples, the presence of OTU1, OTU2, OTU3, OTU4, OTU5 and OTU6 will be the most determining for these dimensions (Figure 7-6). This was not surprising since these are the 6 most abundant OTUs in our dataset.

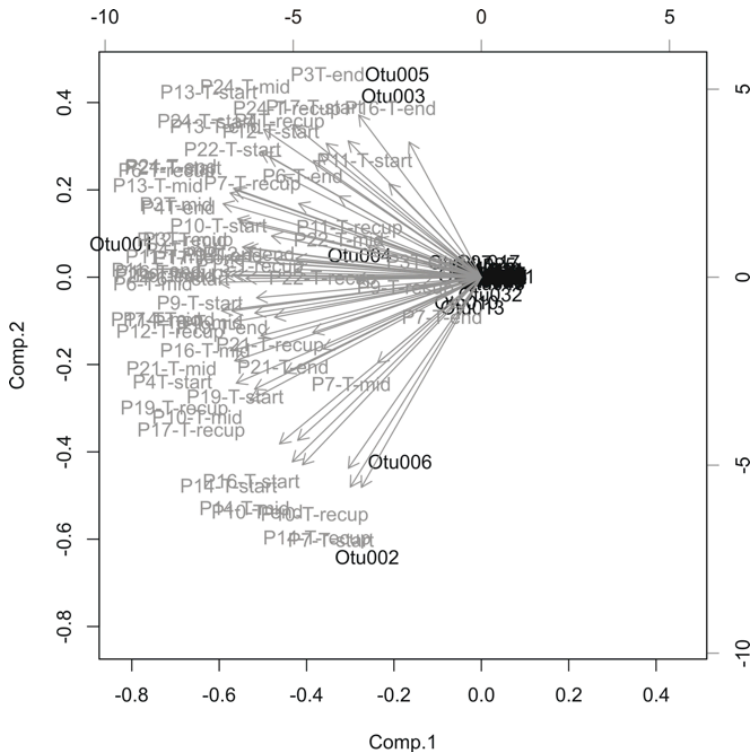


**Figure 7-6: Principal component analysis of the tongue samples**

The microbial community of the tongue consists of 9 different phyla. Of these the *Firmicutes*, *Proteobacteria*, *Actinobacteria*, *Bacteroidetes* and *Fusobacteria* are again the most dominant, counting for 99.45 % of the observed sequences. The other phyla are the *Spirochaetes* (0.06 %), *TM7* (0.03 %), *Tenericutes* (0.03 %) and *Deferribacteres* (0.01 %). Compared to the buccal microbiota, a smaller proportion of *Firmicutes* was found in the microbial community of the tongue samples, mainly in favour of the *Proteobacteria*. After radiotherapy, no clear shifts in abundances could be noticed (Figure 7-7). Also at genus level, no significant shifts were observed due to irradiation.

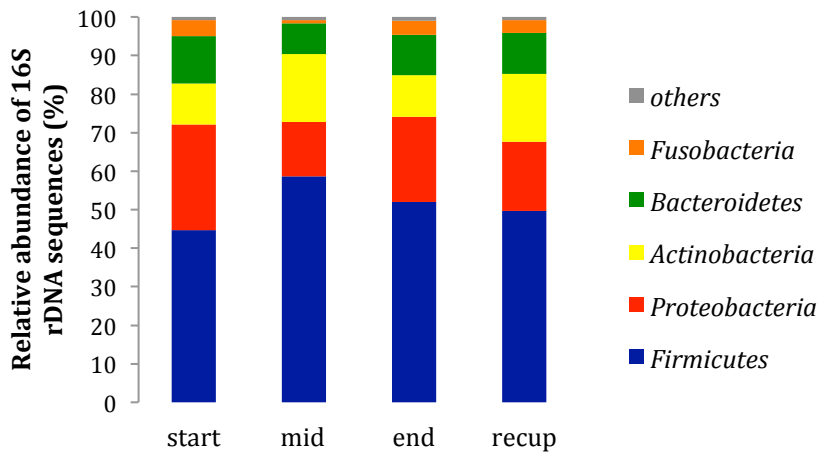


**Figure 7-7: Relative abundance (%) of the predominant phyla of the tongue microbiota at different time points during radiotherapy (n= 16)**

Similar to the buccal analysis, we further tried to identify the shifts in the tongue microbial community in the context of oral mucositis. Patients with higher abundances of *Leptotrichia*, *Atopobium* and an unclassified group of *Lachnospiraceae* at the start of their treatment were more likely to develop severe mucositis (grade 3 or 4) during therapy ( $p_{Leptotrichia} = 0.024$ ,  $p_{Atopobium} = 0.013$ ,  $p_{unclas.Lachnospiraceae} = 0.024$ ). In the follow-up period, *Streptococcus* spp. and unclassified *Pasteurellaceae* were more abundant on the tongue surface of patients that suffered from severe mucositis during radiotherapy ( $p_{streptococcus} = 0.041$ ;  $p_{unclas.pasteurellaceae} = 0.024$ ; Figure 7-8).

During and at the end of the radiotherapy, 7 low abundant genera were significantly linked with the mucositis grade (Table 7-4). Of these the *Parvimonas* and *Peptostreptococcus* spp. are the most interesting as these genera become at least 10 times more abundant when patients suffered from mucositis (Gr 2 or Gr 3).

**Table 7-4: Relative abundance (%) of the tongue microbiota during radiotherapy (mid and end) assigned to genus depending on the severity of mucositis, together with the Bonferroni corrected p-values**

Abundance (%) Microbial genus	Severity of mucositis				Bonferroni corrected P-value		
	Gr 0 (n=2)	Gr 1 (n=18)	Gr 2 (n=10)	Gr 3 (n=5)	Gr1-Gr2	Gr1-Gr3	Gr2-Gr3
<i>Anaeroglobus</i>	0.000	0.018	0.099	0.017	0.009	1.575	0.198
<i>Eubacterium</i>	0.021	0.002	0.039	0.026	0.048	0.039	3.000
<i>Gemella</i>	0.107	3.610	3.691	0.400	2.943	0.063	0.030
<i>Hallella</i>	0.007	0.003	0.017	0.026	0.054	0.015	1.029
<i>Parvimonas</i>	0.029	0.022	0.306	0.491	0.003	0.177	1.167
<i>Peptostreptococcus</i>	0.000	0.007	0.301	0.640	0.009	0.144	2.265
<i>unclas. Bacteroidetes</i>	0.014	0.038	0.194	0.040	0.024	1.629	0.414

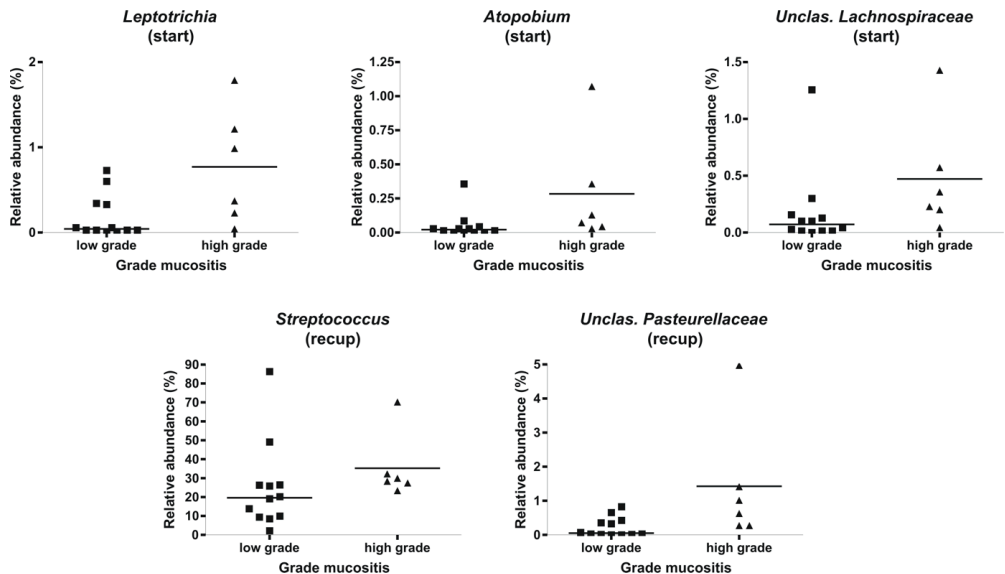


**Figure 7-8: Relative abundance of the tongue microbiota at the start and after radiation therapy (recup) assigned to genus depending on the maximal severity of mucositis scored during treatment (low grade: Gr 0, Gr 1, Gr2; high grade: Gr 3 or Gr 4). Median values of the different samples are depicted (n<sub>low grade</sub>= 12; n<sub>high grade</sub>= 6)**

## 7.5. Discussion

The oral cavity provides good habitats for a wide diversity of microbiota. By use of Illumina sequencing analysis we were able to identify the microbiota present on the buccal and tongue mucosa of 25 head and neck cancer patients. In total 9 phyla were found, of which the most abundant were *Firmicutes*, *Proteobacteria*, *Actinobacteria*, *Bacteroidetes* and *Fusobacteria*. *Spirochaetes* and *TM7* were less abundant in the samples and the low abundant *Tenericutes* and *Deferribacteres* were only found on the tongue surface. The presence of these phyla in the oral cavity has already been described (Aas et al., 2005; Keijsers et al., 2008; Bik et al., 2010; Dewhirst et al., 2010; Hu et al., 2013a). However, in our study, the *Firmicutes* was by far the most abundant phylum, whereas previous studies showed an equal abundance of the *Proteobacteria* and *Firmicutes*, followed by the *Bacteroidetes* and *Actinobacteria* (Bik et al., 2010; Hu et al., 2013a). This difference can be explained by the use of pooled samples of the oral cavity or plaque samples in those studies instead of the individual buccal or tongue swabs in our analysis (Segata et al., 2012).

In contrast to the study of Hu et al. (2013), the richness of the samples in our study was not affected by irradiation. This might be explained by the fact that most of the samples that were excluded from our study due to the low sequence count were all

samples taken at the end of the therapy, which is likely to result in a distorted view when analysing the microbial richness of the samples during radiotherapy. Furthermore, it is very likely that new microbial niches arise due to radiotherapy, allowing other microbiota to come into play.

The buccal mucosa and dorsal tongue surface are two different habitats in the oral cavity, each with their specific microbial niches (Mager et al., 2003; Aas et al., 2005). Remarkably, the tongue microbiota in our study were unaffected by irradiation in contrast to the buccal microbiota. Before, it has been shown that a higher evenness favours functional resistance (Wittebolle et al., 2009) and here we provide further evidence that a higher evenness also results in a higher community resistance.

Previous studies reported an increase of oral *Lactobacillus* spp. following irradiation (Tong et al., 2003; Almståhl et al., 2008; Guobis et al., 2011). A similar increase was also observed in our study, although shifts were not significant (data not shown). Within the buccal microbiota we did find a significant decrease in the number of *Abiotrophia*, whereas the abundance of *Lachnospiraceae\_incertae\_sedis* and unclassified *Prevotellaceae* spp. increased towards the end of the therapy. In the oral cavity, *Abiotrophia defectiva* is reported to be beneficial in relation to caries (Aas et al., 2008) and its presence has been linked with halitosis (Haraszthy et al., 2012). Nevertheless in literature, clinical samples of *Abiotrophia* are mainly correlated with bacterial infectious endocarditis and bacteraemia (Christensen and Facklam, 2001). Therefore, care should be taken to avoid *Abiotrophia* spp. to enter the blood stream, as they inherit the risk to develop into serious infections as a side effect of severe mucositis. The microbial family of the *Prevotellaceae* is considered as a periodontal pathogen (Reyes and Dalmacio, 2012). Presumably, the shifts observed in our study due to radiotherapy can be linked with irradiation-induced xerostomia and/or caries. The decrease of *Abiotrophia* and increase of *Lachnospiraceae* was previously also reported following a chemotherapeutic treatment (Napeñas et al., 2010; Montassier et al., 2014).

During therapy, we were able to identify certain genera on the buccal and tongue mucosa of which the abundance increased with the severity of mucositis. Likely, some of these genera, like *Bifidobacterium*, are taking advantage of the anaerobic circumstances created by other microbiota that come into play. Yet, some of these genera, like *Prevotella*, *Porphyromonas* and *Parvimonas* have previously been correlated with caries or periodontitis (Rawlinson et al., 1993; Aas et al., 2008; Ahmed et al., 2012; Hsiao et al., 2012; Reyes and Dalmacio, 2012; Hu et al., 2013a). Even *Bifidobacterium* spp., which are mainly known as beneficial bacteria in the gut environment can be found in dental caries and plaque (Aas et al., 2008; Beighton et al., 2010; Dewhirst et al., 2010). The *Fusobacterium* spp. are important in the biofilm formation and are thus also associated with periodontal diseases (Hsiao et al., 2012),

although Aas et al. (2008) reported a decrease in *Fusobacterium nucleatum* in the plaque of patients with severe caries. Apart from dental caries and periodontitis, increased abundances of *Porphyromonas* and *Prevotella* spp. were also found in subgingival samples after brace placement (Naranjo et al., 2006). Although these studies are all concerning samples of denture plaque and not of the buccal and tongue mucosa, Han et al. (2000) showed the ability of e.g. *Fusobacterium nucleatum* to adhere to and invade in oral epithelial cells, marking the potential importance of these dental microbiota in the context of mucositis. Recently, microbiota of the *Prevotellaceae* family were also shown to be more abundant in the gut of mice suffering from severe colitis (Littman and Pamer, 2011) and in the study of Marchini et al. (2007) the *Prevotella* spp. were only found in samples of recurrent aphthous lesions. Laheij et al. (2012) reported *Porphyromonas gingivalis*, *Parvimonas micra* and *Fusobacterium nucleatum* as explanatory species for the development of oral ulcerations in hematopoietic stem cell transplants. Finally, Peptostreptococci and *Fusobacteria* were also shown to be upregulated in tube-fed patients (Takeshita et al., 2011). As patients with severe oral mucositis suffer from aphthous lesions and oral ulcerations and are often relied on tube feeding, altogether these studies are able to confirm our observed shifts due to irradiation.

In the follow-up period, we found higher abundances of *Pasteurellaceae*, *Prevotella* and *Streptococcus* spp. in patients who suffered from severe mucositis during therapy. This is probably a remaining consequence of the infectious lesions in the oral cavity or the need for tube feeding. Indeed, tube-fed patients were found to have higher abundances of *Pasteurellaceae* (Takeshita et al., 2011). However, as streptococci and *Prevotellaceae* have also been described as early colonizers of the oral cavity, a higher abundance of those families might point to the restoration of the oral microbiota after the therapy (Könönen et al., 1999; Avila et al., 2009).

Interestingly, we were also able to identify genera at start of the therapy of which the abundance differed significantly between the patients who eventually developed low-grade mucositis and those who suffered from severe mucositis. These genera included *Gemella*, *Leptotrichia* and *Atopobium*, all part of the normal oral microbiome (Aas et al., 2005; Keijser et al., 2008; Bik et al., 2010). In our study, *Gemella* species were less abundant in patients who developed severe mucositis. Similarly, Aas et al. (2008) reported a lower abundance of *Gemella morbillorum* on the enamel of patients with caries, suggesting a beneficial role of the genus. Nevertheless, this species has also been described as an opportunistic pathogen, for example causing a septic shock (Vasishtha et al., 1996). Also *Leptotrichia* spp. were previously reported in the context of serious infections and bacteraemia, especially in an immune-compromised host (Morgenstein et al., 1980; Bhally et al., 2005; Eribe and Olsen, 2008). The *Atopobium* spp. were found to be significantly higher in the patients that would develop severe

mucositis both on the buccal as on the tongue mucosa, making them particularly interesting. Previously this genus was associated with halitosis, caries progression, endodontic infections, bacterial vaginosis and uterine endometritis (Kazor et al., 2003; Aas et al., 2008; Copeland et al., 2009; Yamagishi et al., 2011; Haraszthy et al., 2012; Hsiao et al., 2012). However, we are the first to describe this genus, together with the *Gemella* and *Leptotrichia* as a potential marker for the development of severe mucositis. Nevertheless, the high diversity within the high mucositis group points to the complexity of oral mucositis in which a plenitude of risk factors will all contribute to the development of severe mucositis.

In conclusion, the buccal microbiota were shown to shift due to radiotherapy, which could be related with known radiotherapy-induced side effects like xerostomia and caries. Furthermore, severe mucositis was correlated with higher abundances of other genera like *Prevotella*, *Porphyromonas* and *Parvimonas*. Of particular interest are the *Gemella*, *Leptotrichia* and *Atopobium* spp. as their abundance at start of the therapy was indicative for the severity of mucositis the patients would develop during the therapy. Further research is needed to obtain better insights in the individual roles of all these genera in the context of mucositis, which may lead to new therapeutic targets in the combat against mucositis.

## 8. E-CADHERIN AS SALIVARY BIOMARKER OF MUCOSITIS

---

### 8.1. Abstract

Oral mucositis is an important toxicity of cancer therapy, for which different risk factors are proposed. Nevertheless at this timepoint it is not possible to predict which patients are at high risk of developing severe ulcerative mucositis. Therefore, we investigated the potential of E-cadherin as a salivary marker of mucositis and determined the concentrations of the soluble fragment of E-cadherin in the saliva of head and neck cancer patients treated with radiotherapy. A significant decrease in salivary E-cadherin concentrations was found after 2 weeks of irradiation, the time point at which most of the patients were diagnosed with first signs mucositis. Furthermore, in oropharynxcarcinoma patients the relative soluble E-cadherin concentration after 1 week of therapy was shown to be a potential marker for the severity of oral mucositis. Further research is needed to understand the role of E-cadherin in the pathobiology of mucositis and to determine the value of this predictive marker in search for effective treatment strategies for patients at high risk for severe mucositis.

### 8.2. Introduction

Oral mucositis is a severe inflammatory side effect, which occurs in 91 % of the patients treated with radio- and/or chemotherapy (Elting et al., 2007). It is associated with oral pain, malnutrition and in a worst-case scenario interruption of the therapy is needed. Moreover, Elting et al., (2007) estimated an incremental cost of \$1700 – \$6000, depending on the severity of mucositis. Different risk factors for the development of severe mucositis have been proposed, including therapy- and patient-related factors (Barasch and Peterson, 2003). These include the choice of treatment and schedule. Intensity-modulated radiotherapy (IMRT), for example, is shown to be a helpful technique to reduce the prevalence of mucositis (Lambrecht et al., 2013), but when radiotherapy is combined with chemotherapy the risk increases with 13 % (Elting et al., 2007). Moreover, also the site of the primary tumour is very important. Patients with a primary tumour in the oral cavity or oropharynx are at higher risk to develop oral mucositis compared to patients with tumours in the larynx or



hypopharynx (Elting et al., 2007). Patient-related variables embrace age and gender, nutritional status, oral microbiota, oral health, salivary flow rate and neutrophil counts (Barasch and Peterson, 2003). As all these risk factors are not equally distributed, it is up to date still impossible to predict which patients are at high risk to develop severe mucositis. Therefore it would be useful to have a biological marker that indicates which patients are at high risk.

Due to irradiation the epithelial layers of the oral mucosa are damaged, eventually leading to oral ulcerations. E-cadherin is known as the major protein in epithelial cellular junctions. It provides cell-cell adhesion through Ca<sup>2+</sup>-dependent, homophilic binding between E-cadherin molecules on adjacent epithelial cells (Takeichi, 1990; Angst et al., 2001; Bryant and Stow, 2004). When cells are apoptotic, the E-cadherin molecules are cleaved and a soluble 84 kDa fragment is released (Steinhusen et al., 2001). Furthermore, the E-cadherin/catenin complex is a well-known invasion suppressor involved in the epithelial-mesenchymal transition (Weinberg, 2007). Cleavage of the ectodomain by matrix metalloproteinases and thus the release of soluble E-cadherin fragments in the environment was shown to induce cellular invasion (Noë et al., 2000). Moreover, the matrix metalloproteinases are proposed to be key regulators of chemotherapy-induced mucositis (Al-Dasooqi et al., 2009). Therefore, we hypothesized the involvement of E-cadherin in radiotherapy-induced oral mucositis. For this study, we investigated the presence of the soluble E-cadherin fragment in the saliva of head and neck cancer patients treated with radiotherapy in search for a new biological marker for mucositis.

### **8.3. Patients, material and methods**

#### **8.3.1 Patients**

Twenty-five patients treated with radiotherapy for head and neck cancer were enrolled in this study. Three of the included patients were female and the age of the patients ranged from 46-74 y, with a median of 63 y. All patients were treated with radiotherapy at the department of Radiotherapy at Ghent University Hospital, Belgium (2011-2012). Eleven patients received concurrent chemotherapy. All patients received the best possible treatment for their illness and therefore they all had different treatment regimens.

The study was approved by the Medical Ethical Committee (Ghent University hospital, B670201110552) and all patients provided their written informed consent prior to the study.

### 8.3.2 Saliva samples

Before sampling, the oral cavity of the patients was flushed with drinking water. Unstimulated whole saliva samples were collected in sterile tubes and stored at -20 °C. After thawing, samples were centrifuged and the supernatant was collected for further analysis.

Saliva samples were collected at the beginning of radiotherapy (before the fifth fraction) and weekly during treatment (immediately after irradiation) until the end of the therapy. After treatment, an extra sample was taken within the first 2 months after the therapy (follow-up appointment).

### 8.3.3 Clinical records

Weekly, all patients enrolled for the study consulted a radiotherapist. Their oral cavity and oropharynx was inspected and the severity of mucositis was scored according to the grading scale of the World Health Organization (Table 1-1; Treister and Sonis, 2007).

All patients' characteristics are listed in Table 8-1.

**Table 8-1: Overview of the patients' clinical characteristics**

Patient ID	Sex	Age (y)	Tumoursite	Treatment	Max mucositis grade
1	m	74	larynx	RT + CT	0
2	m	60	oral cavity	RT + CT	4
3	m	66	oropharynx	RT + CT	3
4	m	58	CUP	RT + CT	3
5	m	72	oropharynx	RT	2
6	m	60	oropharynx	RT	3
7	m	49	hypopharynx	RT	1
8	f	73	oral cavity	RT	3
9	m	68	larynx	RT	1
10	m	65	oropharynx	RT + CT	1
11	m	60	CUP	RT	2
12	m	64	oropharynx	RT + CT	3
13	m	72	larynx	RT	1
14	m	53	oral cavity	RT	2
15	m	46	oral cavity	RT	3
16	m	48	oropharynx	RT + CT	3
17	m	67	larynx	RT	1
18	m	49	oropharynx	RT + CT	2
19	m	61	larynx	RT + CT	1
20	m	56	CUP	RT + CT	2
21	f	55	oropharynx	RT	2
22	m	69	oropharynx	RT	2
23	m	70	oral cavity	RT + CT	3
24	f	65	oral cavity	RT	2
25	m	63	hypopharynx	RT	1

m= male; f= female; CUP= cancer of unknown primary origin;  
RT= radiotherapy; CT= chemotherapy; AB= antibiotics

### **8.3.4 Western blot analysis**

For western blot analysis, 20  $\mu\text{L}$  of the saliva was mixed with 5  $\mu\text{L}$  of sample buffer (Laemmli 4 $\times$ , 5 % bromophenol blue and 5 %  $\beta$ - mercaptoethanol) and boiled for 5 min at 95  $^{\circ}\text{C}$  and 900 rpm. Proteins were separated on a 10 % polyacrylamide gel and transferred to a nitrocellulose membrane (GE Healthcare, Diegem, Belgium). For immunostaining, the HECD-1 human anti-E-cadherin antibody (Takara, Shiga, Japan) was diluted in milk solution (Nestlé, Brussels, Belgium) to a final concentration of 0.1  $\mu\text{g}/\text{mL}$ . As a secondary antibody, the horseradish peroxidase-labelled secondary anti-mouse (GE Healthcare, Diegem, Belgium) was used at a 1:3000 dilution in milk.

### **8.3.5 Enzyme-linked immunosorbent assay (ELISA)**

ELISA was performed using the Human E-cadherin duoset ELISA kit (R&D systems, Abingdon, UK), following the manufacturers protocol. Briefly, a 96-well microplate was coated with 50  $\mu\text{L}$  of the capture antibody during an overnight incubation step at room temperature. After washing, plates were blocked for 1 h using the reagent diluent (1 % BSA-V in PBS, pH 7.2-7.4). Then, 100  $\mu\text{L}$  of the standard or a 1/10 dilution of the saliva sample was allowed to react for 2 h at room temperature. The plates were washed and 50  $\mu\text{L}$  of the detection antibody was added to each well. After 2 h of incubation, the washing step was repeated and 50  $\mu\text{L}$  of the streptavidin-HRP solution was brought in the wells and plates were incubated for 20 min protected from light. Next, the plates were washed to remove unbound streptavidin and 50  $\mu\text{L}$  of the substrate solution was added to each well. After a 20 min incubation step at room temperature protected from light, 25  $\mu\text{L}$  of the stop solution was added and the optical density was measured at 450 nm.

All samples of one patient were analysed on the same plate in duplicate. A standard and quality control samples were included on each plate.

### **8.3.6 Statistics**

Statistical analyses were performed in SPSS statistics 22. Normality of the data was checked using the Shapiro-Wilk assay, after which the student's T-test or the paired sample T-test was applied in search for significant differences ( $p < 0.05$ ). Cluster analysis was performed in R v3.0.2 (kml package).

## **8.4. Results and discussion**

By use of ELISA, the concentration of the soluble extracellular fragment of E-cadherin (sE-cadherin) was measured in the saliva of patients with head and neck cancer treated with radiotherapy. Our data show that salivary sE-cadherin concentrations

decrease during therapy ( $p_{\text{mid-start}}= 0.016$ ;  $p_{\text{end-start}}= 0.005$ ;  $p_{\text{recup-start}}= 0.009$ ; Figure 8-1). Only one outlier was observed with a steep increase halfway therapy (Figure 8-1 - light blue), however this was the only sample of that patient with such high sE-cadherin level.

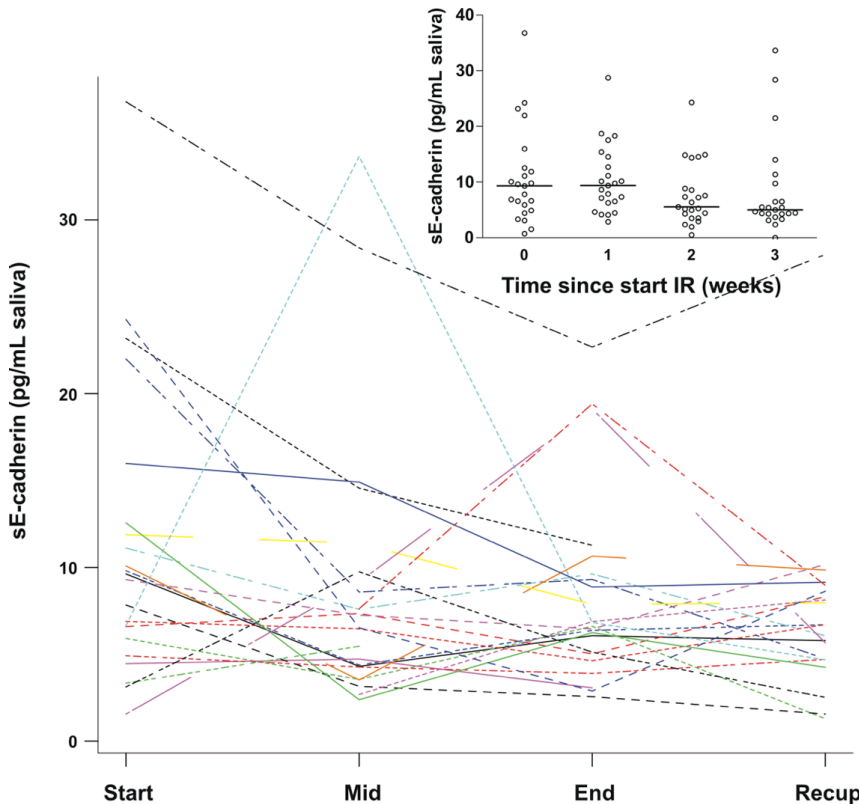


**Figure 8-1: Absolute sE-cadherin concentrations detected in the unstimulated saliva of patients treated with radiotherapy in the beginning (start), halfway (mid), at the end and after (recup) the therapy. Insert: dotplot of sE-cadherin concentrations (including median value) during the first 3 weeks of the therapy (n= 25)**

Although ELISA is a powerful technique, when analysing proteins in a complex solution such as saliva, validation of the assay by means of additional techniques is required. Therefore a small set of samples were analysed by both Western blot and ELISA (Figure 8-2). On Western blot, we were able to detect the soluble extracellular fragment of E-cadherin (sE-cadherin) at its corresponding molecular weight (84 kD). With both Western blot and ELISA, a decrease in sE-cadherin concentration was noticed, approving the use of the high throughput, quantitative ELISA-technique to determine the sE-cadherin concentrations in the saliva of the patients.

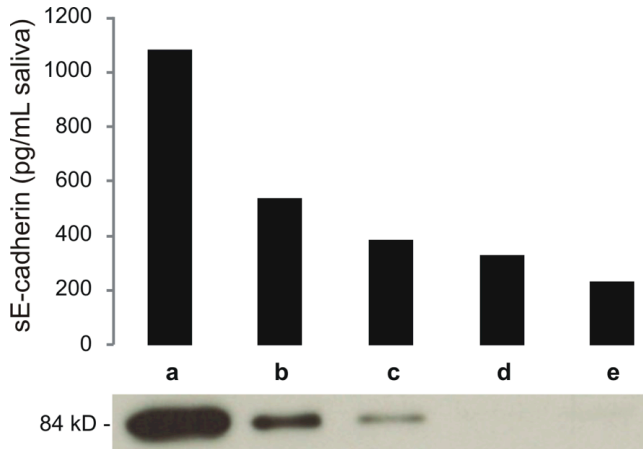


**Figure 8-2: Validation of the ELISA results using Western blot. The same samples were tested both on Western blot (blot) and with ELISA (graph)**

In general, the decrease in sE-cadherin could already be observed within the first half of the therapy (median cumulative dose of 30.24 Gy), we analysed the data obtained during the first 3 weeks of irradiation more in detail (insert in Figure 8-1). Our analysis shows that after 2 weeks of irradiation (median cumulative dose of 23.76 Gy) a significant decrease in sE-cadherin concentrations could be seen compared to the levels at start of the therapy ( $p= 0.002$ ). This was also the time point at which most of the patients (55 %) were diagnosed with first signs of mucositis. First ulcerations are indeed described to appear after a cumulative dose of 20 Gy (2 weeks of irradiation), while the ulcerative phase was mainly situated after a cumulative dose of 30 Gy dose (end of the 3<sup>th</sup> week of irradiation) (Van der Schueren et al., 1990; Treister and Sonis, 2007). However, Sonis (2007) already reported first adverse mucosal changes at a cumulative dose of 10 Gy (1 week of irradiation).

As the sE-cadherin concentrations at start of the therapy were highly variable in absolute values, the relative sE-cadherin concentrations were used to evaluate if sE-cadherin salivary levels could be used as a biomarker for severe mucositis. Grade 1 and 2 mucositis are considered to be mild or moderate (low grade), whereas grade 3 and 4 are more severe (high grade) (Treister and Sonis, 2007). Cluster analyses of the relative sE-cadherin concentrations were performed and were found to be interesting in case of the oropharynxcarcinoma patients. In this group, 2 clusters could be identified namely the patients suffering from severe mucositis (red lines in Figure 8-3a) versus the ones with low grade of mucositis during therapy (blue lines in Figure 8-3a).

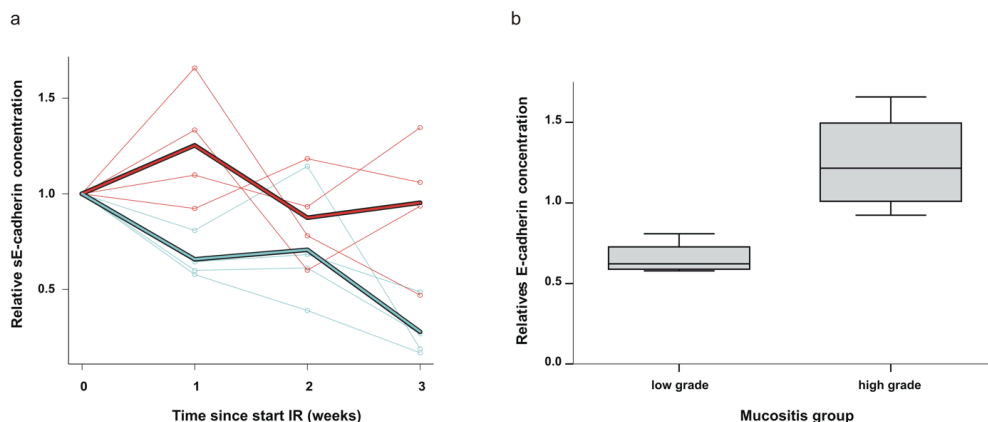


**Figure 8-3 a: Cluster analysis of the samples obtained from the oropharynxcarcinoma patients (n= 8). Consensus profile of both clusters are marked (thick lines) b: Boxplot presentation of the relative sE-cadherin concentrations in the saliva of the oropharynxcarcinoma patients after 1 week of irradiation in function of the mucositis score (low grade= grade 1 or 2; high grade= grade 3)**

After one week of irradiation, there was already a remarkable difference between both clusters. In patients that would develop severe mucositis during therapy (red cluster in Figure 8-3a), the sE-cadherin concentrations were shown to increase after one week, whereas the sE-cadherin levels decreased in the group of patients with mild mucositis (blue cluster in Figure 8-3a) This indicates that for this particular group of patients, the salivary levels of sE-cadherin are predictive for the mucositis grade. Indeed, the relative salivary sE-cadherin concentration after one week of treatment appeared to be significantly higher in patients that would develop severe mucositis during therapy compared to the ones that would only suffer from a low grade of mucositis ( $p= 0.012$ ; Figure 8-3b). As the oropharynxcarcinoma patients are likely to develop oral mucositis (Elting et al., 2007), the measurement of salivary sE-cadherin concentrations is an easy, non-invasive way to predict their risk of developing severe mucositis, which would allow adjuvant treatments or more frequent follow-up.

A biomarker of severe mucositis would allow adaptive radiotherapy for patients at high risk. Adaptive radiotherapy for head and neck cancer was already described before in the context of IMRT (Castadot et al., 2010). As changes in the patients anatomy, like alterations in the muscle mass and fat distribution can induce major changes in the location, shape, and size of the tumour and organs at risk, it is important that the sharp dose gradients given during IMRT are adapted when needed, for example by using image-guided radiotherapy. Although this technique is fairly intuitive, the implementation into the clinic is difficult as this technique is time consuming and requires a shift in the infrastructure towards a feedback controlled system. Until now, this technique is thus mainly used in the context of clinical studies

and is not part of the standard treatment (Castadot et al., 2010; Yan, 2010; Schwartz and Dong, 2011; Schwartz, 2012). The probability that adaptive radiotherapy will ultimately be implemented to diminish the mucosal toxicity is so far very limited, as this could go against the main goal of the radiotherapist, which is to kill all tumour cells. Therefore, more focus should go to the development of effective preventive measurements for patients at high risk for developing severe mucositis. Also, more research should be done on the role of E-cadherin in the pathobiology of mucositis, which might lead to new fundamental insights or to new therapeutic interventions.

## 9. E-CADHERIN AS THERAPEUTIC TARGET

---

*Modified from: De Ryck T, Van Impe A, Vanhoecke B, Heyerick A, Vakaet L, De Neve W, Müller D, Schmidt M, Dörr W\*, Bracke M\* (2015). 8-prenylningenin and tamoxifen inhibit the shedding of irradiated epithelial cells and increase the latency period of radiation-induced oral mucositis. Strahlentherapie und onkologie 191(5), 429-436 (\*Equally contributing).*

### 9.1. Abstract

The major component in the pathogenesis of oropharyngeal radiation-induced mucositis is progressive epithelial hypoplasia and eventual ulceration. Irradiation inhibits cell proliferation, while cell loss at the surface continues. We conceived to slow down this desquamation by increasing intercellular adhesion, regulated by the E-cadherin/catenin complex. We investigated if 8-prenylningenin or tamoxifen decrease the shedding of irradiated human oropharyngeal epithelial cells *in vitro* and thus delay the ulcerative phase of radiation-induced mucositis *in vivo*. 8-PN or TAM were shown to prevent the volume reduction of the irradiated cell aggregates during the incubation period. This was the result of a higher residual cell number in the treated *versus* the untreated irradiated aggregates. In a well-established murine oral mucositis model, topical treatment with 8-PN or TAM significantly increased the latency of mucositis from 10.9 to 12.1 and 12.4 days, respectively, while the ulcer incidence was unchanged. This suggests a role for these compounds for the amelioration of radiation-induced mucositis in the treatment of head and neck tumours.

### 9.2. Introduction

Radiation-induced mucositis is a severe and often dose-limiting side effect of radiotherapy for tumours in the head and neck region (Trotti et al., 2003; Sonis, 2009; Raber-Durlacher et al., 2013). One mechanism contributing to the pathogenesis of radiation-induced mucositis is progressive hypoplasia and eventually ulceration of the multi-layered epithelium, at about 9 days after cumulative radiation doses of 20 Gy (Van der Schueren et al., 1990; Dörr et al., 2002). Irradiation indeed inhibits cell



production in the proliferative epithelial compartments, while cell loss at the surface continues independently of the treatment. A variety of attempts to interfere with these processes have been described, including radioprotective or pro-proliferative approaches (Rosenthal and Trotti, 2009; Worthington et al., 2011). Maier et al. (2014b) recently highlighted the current strategies to prevent or reduce damage to normal cells. Radioprotectors can be subdivided in 3 groups: scavengers of free radicals, suppressors of apoptosis pathways and inducers of cell cycle arrest. Amifostine is an important, clinically approved, scavenger of OH radicals, which is highly accumulated in normal tissue cells. Although this substance is clinically applied during radiotherapy of head and neck cancer patients, more well-designed clinical trials are needed to define clinical guidelines due to the major Hadorn flaws in the current available studies (Nicolatou-Galitis et al., 2013; Maier et al., 2014b). Also the application of, for example, the keratinocyte growth factor Palifermin raises important issues, since it is not always devoid of the risk of stimulating tumour growth as well.

We conceived a different approach, namely increasing the cell-cell adhesion in order to reduce desquamation of the superficial layers. The E-cadherin/catenin complex at the membrane of normal epithelial cells is instrumental in maintaining cell-cell adhesion as this complex is part of the adherent junctions (Lewis et al., 1995; Baum and Georgiou, 2011). *In vitro* studies have shown that the activity of this complex can be increased by a number of compounds, some of which interact with the estrogen receptors, e.g. 8-prenylnaringenin (8-PN) (Rong et al., 2001) and tamoxifen (TAM) (Bracke et al., 1994). We aimed to test the effect of these compounds on cell-cell adhesion of mucosal epithelial cells. Therefore, we present an *in vitro* model using aggregates of human TR146 epithelial cells derived from buccal mucosa (Rupniak et al., 1985), which express both E-cadherin and the oestrogen receptor- $\beta$ . After irradiation, the volume of these aggregates progressively decreases while cultured in suspension for 11 days. Since histological analysis confirmed that the number of TR146 cells is a measurement for the volume of the aggregate, we could assume that cell shedding was responsible for the volume decrease of the irradiated aggregates. By adding 8-PN or TAM to the culture medium, we investigated the potential of these compounds to reduce cell shedding. Using mouse tongue epithelium, a well-established murine oral mucositis model (Dörr et al., 2001, 2005a), effects of 8-PN and TAM on the incidence of mucosal ulceration as well as on the time course, i.e. latency period and duration of the ulceration phase, were explored *in vivo*.

## **9.3. Material and methods**

### **9.3.1 Cell culture**

TR146 cells (a kind gift from Dr. Bridget Hill, Clare Hall Laboratories, London, UK) are derived from a lymph node metastasis of a human buccal carcinoma, and display an epithelial morphology on tissue culture plastic. The cells were cultured in Dulbecco's modified Eagle's medium (DMEM; Gibco, Belgium), supplemented with 0.05 % L-glutamine (w/v), 100 µg/ml streptomycin (Gibco), 250 IU/ml penicillin (Gibco), 2.5 µg/ml fungizone (Bristol-Myer Squibb, Belgium) and 10 % foetal bovine serum (FBS; Gibco) at 37 °C in a 100 % humidified atmosphere of 10 % CO<sub>2</sub> and 90 % air. The cells were regularly confirmed to be mycoplasma-free. In a particular set-up, cells were treated for 24 h with 2 µg/ml MB2, a murine monoclonal antibody selected for functional inhibition of human E-cadherin (Bracke et al., 1993) in tissue culture plastic flasks.

### **9.3.2 Cell aggregate treatments**

For obtaining spheroid aggregates, cell suspensions of  $1 \times 10^6$  cells in 6 ml of culture medium in 50 ml Erlenmeyer flasks were kept at 37°C in an atmosphere of 10 % CO<sub>2</sub> on a gyrotory shaker (New Brunswick Scientific Company, New Jersey) at 70 rpm for 24 h.

TR146 cell aggregates with a diameter of about 0.3 mm were transferred individually to 5 ml Erlenmeyer flasks for further incubation in 2.5 ml medium at 120 rpm for 11 days (as described in Bracke et al. (2001)) (Figure 9-1). During this incubation period, the aggregates were treated with 5 µM 8-PN (extracted from hops, Milligan et al. 2002), 5 µM TAM (Astra Zeneca, United kingdom) or with 0.1 % ethanol, the common solvent of these compounds. Culture media and drugs were refreshed after 5 days of incubation. The aggregates were irradiated with 5 MeV photons by means of a linear accelerator (Philips, The Netherlands) at a distance of 100 cm. A single dose of 15 Gy (after 1 day of incubation) or a hypofractionated dose of  $2 \times 10$  Gy (after 1 and 6 days of incubation) was applied at a dose rate of 350 MU/min.

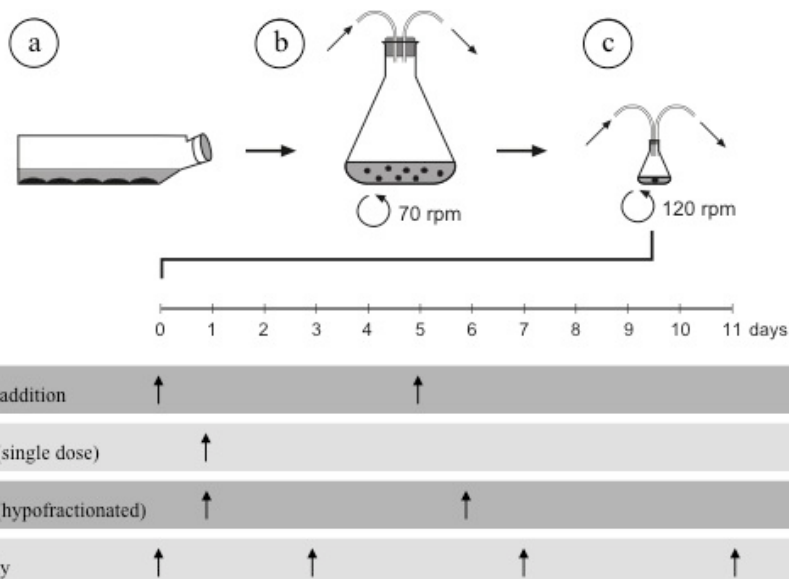


**Figure 9-1: Schematic representation of the experimental set-up for the *in vitro* experiments.** Static cultures (a) of TR146 cells are trypsinized for further transfer from the suspension into a 50 ml Erlenmeyer flask (b). Suspension culture on a gyrotory shaker at 70 rpm yields cell aggregates, which are transferred individually to 5 ml Erlenmeyer flasks (c) for further incubation at 120 rpm during 11 days. Tubes piercing the rubber caps of the flasks allow the in- and outlets of the gas supply (10 % CO<sub>2</sub> in 90 % air). Addition of fresh compounds (8PN, TAM or ethanol solvent), irradiation fractions (1 fraction of 15 Gy or 2 fractions of 10 Gy) and photography of the aggregates are indicated with arrows on the time axis of the incubation period.

### 9.3.3 Cell aggregate analyses

The cell aggregates were photographed with a phase-contrast microscope (DMI 3000B, Leica) at the start of the treatment and after 3, 7 and 11 days of incubation. On the micrographs, the larger (a) and the smaller (b) diameter was measured, and volumes ( $V$ ) were measured in accordance with the formula  $V = 0.4 \times a \times b^2$  (Attia and Weiss, 1966). At the start and at the end of the incubation period, a number of cell aggregates were fixed with Bouin-Hollande's solution, embedded in paraffin blocks, and 8- $\mu\text{m}$ -thin sections were stained with haematoxylin-eosin for histological analysis.

### 9.3.4 Immunodetection of E-cadherin

Immunocytochemistry was performed on TR146 cells grown on glass cover slips as described earlier (De Ryck et al., 2014). The primary mouse monoclonal anti-human E-cadherin antibody HECD-1 (Takara, Japan) was applied at a concentration of 0.1  $\mu\text{g}/\text{mL}$  and the secondary goat anti-mouse IgG 594 nm (Molecular probes, Belgium) at a dilution of 1/1000, mixed with a 1/100 dilution of DAPI. Western blotting was

performed on TR146 cell lysates. The same primary antibody as for immunocytochemistry was applied. The primary antibody against tubulin used for loading control was the mouse monoclonal anti- $\alpha$ -tubulin (Sigma, Belgium). As secondary antibody HRP-labelled anti-mouse antibody (GE Healthcare, Belgium) was used. Quantification of the bands was performed with the 'Quantity one' software of Biorad.

### **9.3.5 *In vivo* mouse oral mucositis model**

Inbred C3H/Neu mice from the Dresden breeding colony were housed under specified pathogen-free conditions, with controlled temperature (21-24 °C) and humidity (30-50 %). An automated light program regulated a 12/12-h light/dark rhythm. Maximally ten animals were kept in size 3 Macrolon® cages on saw dust bedding with free access to standard mouse diet and water.

Local irradiation of a test area at the lower tongue surface was performed as described previously (Dörr et al., 2001, 2005b; Gehrisch and Dörr, 2007). In brief, the animals were anesthetized by pentobarbitone sodium (60 mg/kg i.p.) and placed in the central bore of an aluminium block in a supine position. The tongue was pulled through a hole in the roof of the block by means of a forceps and fixed by adhesive tape, thus exposing the lower tongue surface. A 3 mm<sup>2</sup> window in a 1 mm thick aluminium plate was used to define the central irradiation field. An YXLON MG325 device (Yxlon International X-ray GmbH, Hamburg, Germany) was operated at 25 kV with a tube current of 20 mA. The beam filter of 0.3 mm aluminium resulted in a dose rate of ca. 4 Gy/min at a focus-to-surface distance of 15 cm. Graded single doses were applied (5 dose groups, 10 animals each) in order to generate complete dose-effect curves. The tongues were scored daily from the onset of first signs of a radiation response.

Drug treatment was administered from day -3 before irradiation (day 0) until diagnosis of ulceration; animals without ulceration received the drug until no further ulcerations occurred in the respective experiment. The test drug solutions were applied repeatedly (6×10  $\mu$ l, 10 min intervals) over 1 h, locally to the lower tongue surface, under pentobarbitone sodium anaesthesia. On the day of irradiation, the drugs were applied over 1 h immediately before irradiation.

8-PN and TAM were dissolved in DMSO at concentrations of 3.4 and 3.7 mg/ml (stock solutions), respectively. For administration, the stock solutions were further dissolved with sterile water to final concentrations of 3.4 and 3.7  $\mu$ g/ml. DMSO plus water was used as the solvent control. The experiments were performed in a blinded design.

Mucosal ulceration, corresponding to confluent mucositis grade 3 of the established classification protocols of the RTOG/EORTC classification (Radiation Therapy

Oncology Group/European Organization for Research and Treatment of Cancer), was analysed as the clinically relevant, primary endpoint. Secondary endpoints were the time course parameters, i.e. time to onset after irradiation (latency) and ulcer duration.

### **9.3.6 Statistical Procedures**

Statistical analysis of the *in vitro* data was performed in SPSS Statistics 21 (IBM, NY, USA). After normality check (Shapiro-Wilk), ANOVA analyses, Kruskal-Wallis or Mann-Whitney U analyses were performed (post-hoc analysis with Bonferroni correction).

Grouped linear regression with covariance analysis after linearity assumption check (StatsDirect Ltd, UK) was used to compare the volume evolution curves between treated and control groups during incubation.

For statistical analyses of the *in vivo* results, the Statistical Analysis System (SAS) version 9.2 (SAS Institute Inc., USA) was used. Probit analyses were performed to establish dose-effect relationships, assuming a log-normal distribution (logit analysis), revealing ED50-values (doses, where a positive reaction is expected in 50 % of the animals) and their standard deviation (SD). For the comparison of dose-effect relationships, a likelihood ratio test was used, based on the logit model, without assumption of a threshold dose.

Mean latent time and ulcer duration were calculated for all animals developing ulcers within the individual experiments. For comparison between treatments, Kruskal-Wallis analyses and Mann-Whitney U tests were applied.

Differences were considered significant at the  $p < 0.05$  levels.

## **9.4. Results**

### **9.4.1 E-cadherin expression in TR146 cells**

Immunocytochemistry of E-cadherin in TR146 cells grown on a glass coverslips showed a typical honeycomb pattern, confirming its homogeneous expression and presence at the cell-cell contact sites (Figure 9-2a). E-cadherin was involved in cell-cell adhesion, as treatment of cells with the MB2 monoclonal antibody against human E-cadherin inhibited the formation of normal intercellular junctions, as evidenced by refringent cell-cell borders (arrowheads) and the appearance of a number of fibroblast-like cells (arrows in Figure 9-2b). Furthermore, formation of aggregates was completely abolished in presence of MB2. Western blot analysis, revealed an increase in E-cadherin expression (120 kD) of 26 and 48 %, compared to their solvent (EtOH) treated counterparts when TR146 cells were treated with 5  $\mu$ M 8-PN or TAM respectively, for 48 h. This increase in E-cadherin expression levels due to 8-PN or

TAM was not altered by irradiation of the cells (10Gy; 24h pre-treatment and 24h post-treatment with the test drugs; Figure 9-2c).

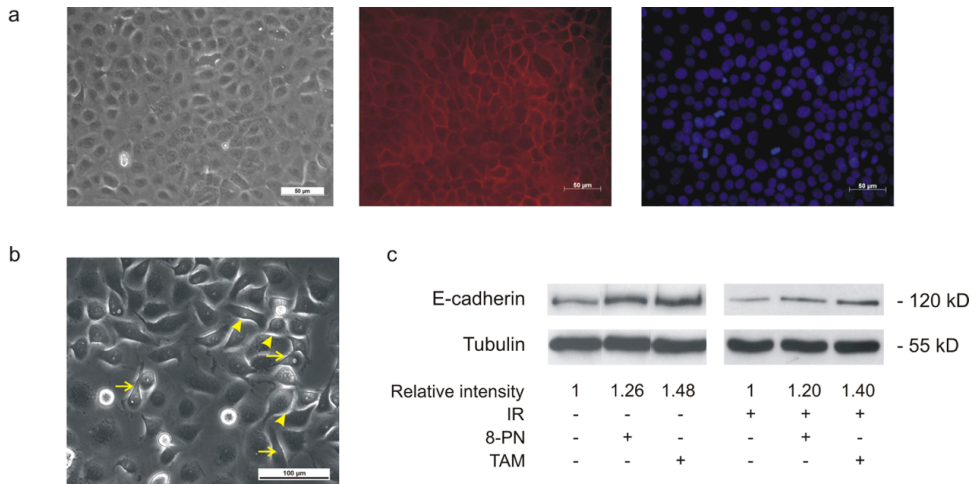


**Figure 9-2 a:** TR146 cells display an epithelioid morphology as evidenced from phase contrast micrographs. Immunostaining of E-cadherin showed a typical honeycomb pattern. DAPI staining was used to visualize the cell nuclei. **b:** Blocking of E-cadherin with MB2 monoclonal antibody against E-cadherin resulted in abnormal intercellular junctions (arrowheads) and aberrant morphology of the cells (arrows) as evidenced from phase-contrast micrographs. **c:** Western blots of E-cadherin from cells treated with 8-PN or TAM for 48 h, showed more intense bands than solvent controls, which were not altered by irradiation (10 Gy, 24 h). The relative band signal intensity is indicated after correction for sample loading (via tubulin immunostaining)

#### 9.4.2 8-PN and TAM inhibit shedding of irradiated TR146 cells

After one single irradiation with a dose of 15 Gy, the mean volume of the TR146 aggregates decreased during the incubation period to 49 % of its initial value due to cell shedding (Figure 9-3a). Treatment of the irradiated aggregates with 5  $\mu$ M 8-PN or TAM retained, respectively, 56 and 75 % of the initial volume. However, no significant differences ( $p_{D3}= 0.636$ ;  $p_{D7}= 0.495$ ;  $p_{D11}= 0.396$ ) were found (Figure 9-3b). Prior check of the volume curves sustained linearity assumption, and allowed application of grouped linear regression with covariance analysis for 8-PN, TAM and solvent treatments (Figure 9-3c). The differences between the slopes of the curves (-4.14, -3.68 and -1.94 from solvent, 8-PN and TAM respectively) were also not significant ( $p= 0.333$ ).

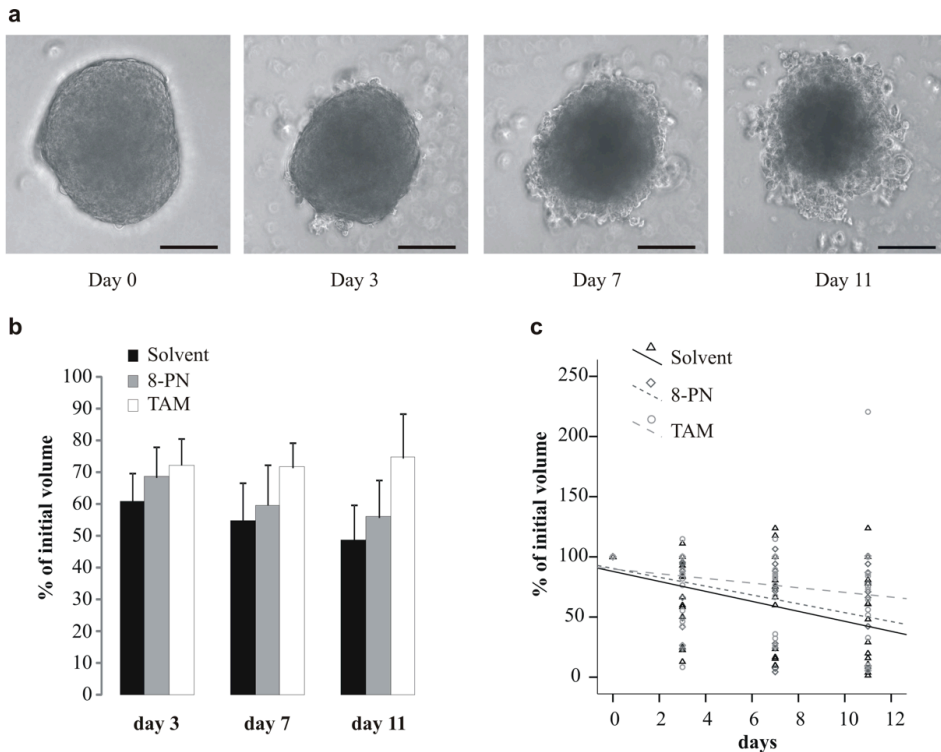


**Figure 9-3 a: Mean volume evolution of irradiated TR146 cell aggregates. All aggregates were irradiated with 15 Gy after 1 day of incubation in suspension culture and treated with 8-PN, TAM or solvent. A volume decrease of the aggregates due to cell shedding was seen after irradiation (scale bar = 100  $\mu$ m). b: Volume calculations after 3, 7 and 11 days of incubation relative to the start point (n= 10-14; mean + SE) are shown. c: Grouped linear regression curves of individual aggregate volumes expressed as percentages of the initial volumes**

Hypo-fractionated irradiation of the TR146 aggregates (2 fractions of 10 Gy) reduced the mean volume of the aggregates to 71 %. Treatment with 5  $\mu$ M 8-PN or TAM prevented this volume decrease, and the mean volumes after 11 days were 113 and 90 % of the initial mean ones, respectively (Figure 9-4a). At day 7, the mean volumes of the treated aggregates were significantly higher than those of the solvent treated ones ( $p= 0.002$  for 8-PN and  $0.006$  for TAM). Also here, the linearity assumption was sustained and allowed application of grouped linear regression with covariance analysis for 8-PN, TAM en solvent treatments (Figure 9-4b). The slopes of the solvent, the 8-PN and the TAM treatments were -2.95, +1.20 and -0.17 respectively. The slope of the 8-PN treatment was significantly higher than the slope of the solvent treatment ( $p= 0.0062$ ). No significance was found when comparing the slopes of solvent and TAM ( $p= 0.0912$ ) and 8-PN and TAM treatments ( $p= 0.4139$ ). Histology of the TR146

aggregates showed that their volume differences were the result of differences in cell numbers (data not shown).

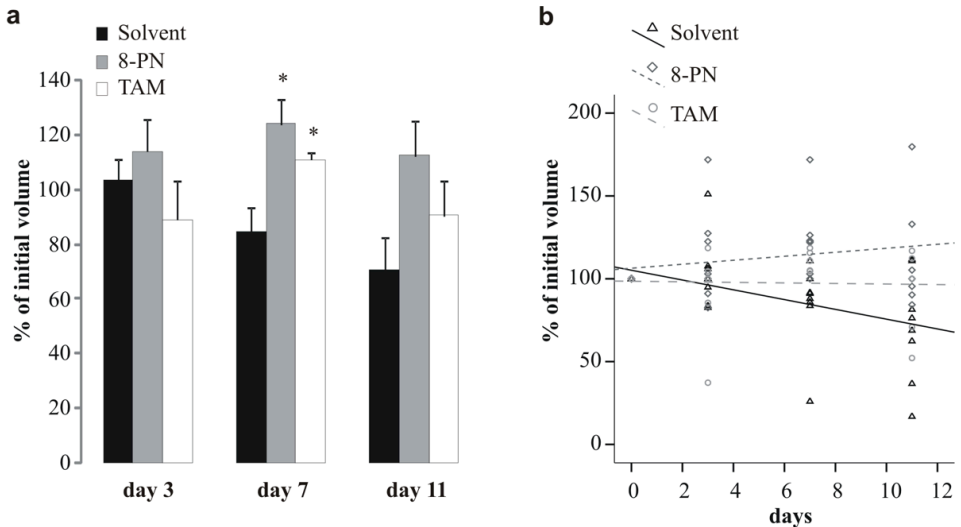


**Figure 9-4 a:** Mean volume evolution of irradiated TR146 cell aggregates. All aggregates were irradiated with 10 Gy after 1 and 6 days of incubation in suspension culture and treated with 8-PN, TAM or solvent. Volume calculations after 3, 7 and 11 days of incubation relative to the start point (n= 5-8; mean + SE) are shown. Asterisks indicate results significantly different from the solvent control ( $p < 0.05$ ). **b:** Grouped linear regression curves of individual aggregate volumes expressed as percentages of the initial volumes

#### 9.4.3 Oral application of 8-PN and TAM increase latency period of oral mucositis *in vivo* after single dose irradiation

The dose-response curves for ulcer induction were well defined (data not shown), but no significant effect of either 8-PN or TAM on the incidence of mucositis was observed; the corresponding ED50 values ( $\pm$  SD) were  $15.5 \pm 0.9$  Gy for solvent alone,  $14.9 \pm 0.1$  Gy for 8-PN ( $p = 0.2258$ ) and  $14.8 \pm 1.0$  Gy for TAM ( $p = 0.3416$ ). However, mice treated with 8-PN or TAM displayed a significantly delayed onset of mucositis. The mean latency periods ( $\pm$  SD) were  $10.9 \pm 1.3$  days for placebo,  $12.1 \pm 0.9$  d for 8-PN ( $p = 0.015$ ) and  $12.3 \pm 1.0$  d for TAM ( $p = 0.006$ ). Also ulcer duration tended to shorten after treatment with 8-PN, although no significant differences were found ( $p = 0.124$ ; Table 9-1).



**Table 9-1: Latency periods and ulcer durations of mice developing mucositis on the tongue after single irradiation (n<sub>placebo</sub>= 11; n<sub>8-PN</sub>= 17; n<sub>TAM</sub>= 15). Results significantly different from the placebo control are indicated**

	Latent time (d)			Ulcer duration (d)		
	Mean	SD	95% C.I.	Mean	SD	95% C.I.
Placebo	10.91	1.30	10.04; 11.78	4.00	0.78	3.48; 4.52
8-PN	12.12 *	0.86	11.68; 12.56	3.24	1.03	2.70; 3.77
TAM	12.33 *	0.98	11.79; 12.87	3.80	1.15	3.17; 4.43

8-PN= 8-prenylnaringenin; TAM= tamoxifen; \*p< 0.05

## 9.5. Discussion

Oral mucositis is a frequent, severe and often dose-limiting side effect of radiotherapy for advanced head-and-neck cancer as well as of the conditioning treatment before stem cell transplantation in patients with malignant haematological diseases. Although, new irradiation techniques like intensity-modulated radiotherapy significantly improve the late toxicities in patients (Lambrecht et al., 2013), mucositis still has a major impact on the patients' clinical status and quality of life (Trotti et al., 2003; Sonis, 2009; Raber-Durlacher et al., 2013). Despite a variety of novel, partly also biology-based, prophylactic or interventional approaches tested pre-clinically and/or clinically, so far only very few strategies have been introduced into clinical routine (Maier et al., 2014b). To our knowledge, we are the first to describe a potential role for 8-PN and TAM in the delayed onset of oral mucositis by stabilizing the cell-cell adhesion in the mucosal layers. Prolonged protection against microbial invasion of the submucosal layers will probably reduce patient's complaints and allow cancer treatment schedules to be maintained. In normal epithelia the E-cadherin/catenin complex offers a master molecular mechanism that organizes cell-cell adhesion junctions and conditional overexpression of E-cadherin can lead to multi-layering of the murine intestinal epithelium (Hermiston and Gordon, 1995). The TR146 cells used in the *in vitro* model are derived from a human buccal carcinoma (Rupniak et al., 1985). Despite their tumoural origin, TR146 cells express E-cadherin at their cell surface and show an epithelial morphology on tissue culture plastic and glass substrates (De Ryck et al., 2014). This morphology is determined by an intact E-cadherin function, since a monoclonal antibody against the E-cadherin ectodomain disrupted cell-cell contacts. The functionality of their E-cadherin/catenin complex renders TR146 cells a *bona fide* model for our radiation-induced mucositis study. The ability of 8-PN and TAM to stimulate the cell-cell adhesive and invasion suppressor functions of the E-cadherin/catenin complex was shown earlier with

human MCF-7/6 breast adenocarcinoma cells (Bracke et al., 1994; Rong et al., 2001). In our assay for cell shedding from irradiated aggregates provoked by liquid shear forces, 8-PN significantly protected the volume of the aggregates, eventually resulting in larger aggregates with a higher cell number than the solvent treated ones. Based on our encouraging findings *in vitro* we developed formulations of 8-PN and TAM for topical application on the tongue mucosa. The feasibility of maintaining a multilayered epithelium by topical application of hop-derived phytoestrogens has already been shown with a vaginal gel that prevented postmenopausal atrophy (Morali et al., 2006). In the established mouse model used (Dörr et al., 2001, 2005a; Gehrisch and Dörr, 2007), we found a clear increase of the latency period in mucositis after treatment with 8-PN or TAM towards 12 days. The latency period, ranging from 3 - 14 days in patients with head and neck cancer, was reported to be inversely correlated with the accumulated dose per week (Wygoda et al., 2013). This study supported our choice for the simplified single dose irradiation model to investigate effects of TAM or 8-PN on the latency period. In contrast to the increased latency period, no significant effect was found on ulcer incidence when compared to treatment with solvent alone. However, compared to earlier studies in this model (Dörr et al., 2001, 2005b; Gehrisch and Dörr, 2007; Kiliç et al., 2007), which resulted in ED50 values in the range of 11-13 Gy, the dose effect curves in all present experimental arms were clearly shifted to higher doses, indicating a reduced radiation sensitivity of the tongue epithelium. This may be attributed to the repeated application of the solutions, daily over a significant time interval. Repeated mouthwashes in patients have also demonstrated a beneficial effect, largely independent of the ingredients in the solutions, in head and neck patients and are hence recommended in the respective guidelines (Lalla et al., 2014).

The compounds tested in the present study are preferable, compared to most other drugs, as they act on the terminal differentiation processes rather than on cancer (stem) cell proliferation. Moreover, TAM is already accepted as anticancer treatment (Osborne, 1998) and new beneficial effects are still being discovered (Morad et al., 2013), while 8-PN is marketed as nutritional supplement and recently described in the prevention of disuse muscle atrophy (Mukai et al., 2012).

We have proven the potential to significantly prolong the latency period of oral mucositis by stimulating cell-cell contacts in the oral epithelium. This may lead to a new treatment strategy for radio(chemo)therapy patients at risk of developing oral mucositis and potentially for radiation effects in other squamous epithelia.



## 10. GENERAL DISCUSSION

---

Oral mucositis is a serious and frequent side effect of radiotherapy in head and neck cancer patients resulting in a decreased quality of life, hospitalization and in the worst-case, interruption of the anticancer therapy. Oral mucositis is still largely considered as an inflammatory reaction of the mucosal tissues in the mouth, but the involvement of the oral microbiota in the pathobiology of the disease is largely underexplored. The general aim of this dissertation was therefore to focus on the host-microbe interactions in the context of radiotherapy-induced mucositis.

### 10.1. Research objectives

First of all, we ***developed a new in vitro model that enables gaining new insights in the microbe-epithelial interactions.*** Research on microbe-epithelial interactions *in vitro* is complicated due to cytotoxicity of microbiota towards cell cultures, limiting the exposure time to maximally 4 h. However, this is too short to obtain a representative host and microbial metabolism (Marzorati et al., 2011). Our new model overcomes this issue by physically separating microbiota and epithelium by means of a porous membrane, which enables exposure times up to 72 h in absence of direct microbe-epithelial contact (Chapter 2; De Ryck et al., 2014a). Moreover, through its modular set-up the model allows the study of characteristics of the biofilm, the mucosa and the co-culture medium separately.

Using this model, we found that an *in vitro* reconstituted biofilm derived from an oral swab and monocultures of *Klebsiella oxytoca* and *Lactobacillus salivarius* significantly reduced the wound healing capacity of epithelial cells. Interestingly, monocultures of *Streptococcus mitis* and *Streptococcus oralis* enhanced wound healing. Further mechanistic work showed that this inhibition was possibly due to the release of quorum sensing molecules during wound healing (Chapter 3; De Ryck et al., 2015a).

When the model was used in a radiotherapy setting applying a single dose of 10 Gy, we were able to demonstrate that the effect of irradiation on epithelial wound healing largely depended on the microbial composition of the inoculum. 454-pyrosequencing analyses pointed to a slight increase in abundance of *Rothia*, *Granulicatella* and *Gemella* in our reconstituted oral biofilm cultured in the model after irradiation (Chapter 4; De Ryck et al., 2015b). Irradiation experiments using monocultures further showed that biofilm formation and virulence of microbiota can be affected by

single dose irradiation (10 Gy) as was shown for *K. oxytoca* (Chapter 5; Vanhoecke et al., 2015).

Altogether, these results highlight the effects of low dose irradiation on the composition and functional behaviour of resident microbiota, which might be linked to a general negative impact on epithelial wound healing in the context of radiation-induced mucositis.

As our results *in vitro* showed that irradiation could generate shifts in the microbial community, we were interested in **assessing potential shifts in the oral microbial community of head and neck cancer patients due to radiotherapy and tried to link the shifts with the severity of mucositis they developed**. Denaturing gradient gel electrophoresis of samples of 10 patients indeed showed that shifts in the oral microbial community of the buccal and tongue mucosa occurred during radiotherapy after the first 2-3 weeks of treatment. We further showed a significant correlation between the shifts in the buccal microbial community and the patients' normal oral functioning (pain, nutrition) (Chapter 6; De Ryck et al., 2015c). Illumina sequencing analysis of buccal and tongue swabs taken from 25 patients with head and neck cancer at different time points during therapy revealed increased abundances of *Lachnospiraceae\_incertae\_sedis* and unclassified *Prevotellaceae* spp., while the number of *Abiotrophia* decreased following radiotherapy. Higher abundances of genera like *Prevotella*, *Porphyromonas* and *Parvimonas* could be linked with the severity of mucositis and for example the *Atopobium* spp. could play a role as predictive marker for the development of severe mucositis. Patients with an abundance of *Atopobium* > 0.02 % are at high risk to develop severe mucositis (Chapter 7). This genus is part of the normal oral microbiota and can be regarded as an opportunistic pathogen as it was previously associated with halitosis, caries progression and endodontic infections (Kazor et al., 2003; Aas et al., 2008; Copeland et al., 2009; Haraszthy et al., 2012; Hsiao et al., 2012). Further research is needed to obtain better insights in the individual roles of the oral microbial species in the context of mucositis. Up to date, the guidelines for the management of mucositis advise against the treatment of antimicrobial agents (Lalla et al., 2014). Nevertheless, more specific therapies like bacteriophage therapy (Sulakvelidze et al., 2001), can overcome the problems seen with antibiotics. In that way, further identification of microbial species causative for the development of severe mucositis, together with the search for highly specific phages for those particular species can lead to new antimicrobial approaches for the management of oral mucositis.

When developing mucositis, the epithelial barrier is interrupted, allowing microbiota to invade underlying tissues. The E-cadherin/catenin complex at the membrane of normal epithelial cells is instrumental in maintaining cell-cell adhesion as this complex is part of the adherent junctions (Lewis et al., 1995; Baum and Georgiou, 2011). Therefore, ***the potential use of soluble E-cadherin (sE-cadherin) as a salivary marker of mucositis or as a therapeutic target was evaluated.*** As the risk factors to develop oral mucositis are versatile and compromise both therapy-related and patient-related variables (Barasch and Peterson, 2003), a clinical biomarker for developing severe mucositis would be very useful. Our results showed that salivary sE-cadherin levels decreased during radiotherapy. After two weeks of treatment, the time point at which first signs of mucositis appear, this decrease in sE-cadherin was already significant. Furthermore, in the oropharynxcarcinoma patients, the level of salivary sE-cadherin after the first week of treatment can be used as a predictive marker of severe oral mucositis (Chapter 8). Although the probability that the implementation of adaptive radiotherapy for diminishing the mucosal toxicity, is so far very limited, this new biomarker can identify those patients that are in the need for adjuvant therapies or more frequent follow-up.

Regarding the use of E-cadherin as a therapeutic target for mucositis, two drugs, 8-prenylnaringenin (8-PN) and tamoxifen were investigated in the context of oral mucositis (De Ryck et al., 2014b; Chapter 9). These drugs have been shown to increase the activity of the E-cadherin/catenin complex (Bracke et al., 1994; Rong et al., 2001). Interestingly, we found that 8-PN and tamoxifen delayed the onset of radiation-induced oral mucositis in an established mouse model for oral radiotherapy-induced mucositis (Dörr et al., 2001). We hypothesize that 8-PN stabilizes the E-cadherin mediated cell-cell adhesion in the mucosal layers, thereby delaying further damage (ulcer formation) and protecting the mucosa from microbial translocation. Apart from the effects on E-cadherin, 8-PN is known as one of the most potent phytoestrogens. A multitude of health benefits including a lowered risk of osteoporosis and the relief of menopausal symptoms are frequently attributed to phytoestrogens (Patisaul and Jefferson, 2010). Therefore, it would be interesting to use this molecule in a clinical trial as a preventive measure for radiotherapy-induced mucositis to further explore our results. Nevertheless, as phytoestrogens are also considered as endocrine disruptors (Patisaul and Jefferson, 2010), care should be taken to determine the best dose to use in a clinical setting.

## 10.2. Validation of the model in the context of radiotherapy-induced oral mucositis

To further validate the model for its use in the context of radiotherapy-induced mucositis, it is important that the microbial shifts found *in vitro* following irradiation correlate with what is recorded in patients treated with radiotherapy. The core oral microbiome of head and neck cancer patients consists of 11 genera: *Streptococcus*, *Actinomyces*, *Veillonella*, *Capnocytophaga*, *Derrxia*, *Neisseria*, *Rothia*, *Prevotella*, *Granulicatella*, *Luteococcus*, and *Gemella*, which were shown to vary in relative abundance during radiotherapy (Hu et al., 2013a). Of these the *Streptococcus*, *Veillonella*, *Rothia*, *Granulicatella* and *Gemella* were also found in our reconstructed oral biofilm, while the *Actinomyces*, *Neisseria*, *Prevotella* and *Luteococcus* spp. were lost. The *Capnocytophaga* and *Derrxia* spp. were not detected in the oral swab used for our *in vitro* model. As it has been shown that the oral microbiota can differ between tumour and non-tumour tissues (Pushalkar et al., 2012), it would be interesting to apply an oral swab derived from a cancer patient instead of a healthy donor in our *in vitro* model.

In our patient study, radiotherapy resulted in a significant decrease in *Abiotrophia* spp. and an increase in *Lachnospiraceae\_incertain\_sedis* and unclassified *Prevotellaceae* spp. Of these, only the *Abiotrophia* spp. could be found in our *in vitro* model and no differences were seen between the irradiated and non-irradiated conditions. *In vitro*, we did detect an increased abundance of *Actinobacillus*, *Fusobacterium*, *Gemella*, *Granulicatella*, *Neisseria*, *Rothia*, unclassified *Pasteurellaceae* and *Veillonella* following irradiation, whereas the abundance of streptococci decreased. Interestingly, Hu et al. (2013b) previously also reported increased abundances of *Veillonella* and *Fusobacterium* after 10 Gy irradiation dose in head and neck cancer patients. At a later stage during the therapy, also the abundance of *Rothia* and *Gemella* spp. increased (Hu et al., 2013b). In our cohort study, the abundance of streptococci, *Neisseria* and *Granulicatella* spp. decreased, whereas *Veillonella* and *Gemella* spp. increased towards the end of the therapy. In case of the *Rothia*, *Fusobacterium* and unclassified *Pasteurellaceae* spp. the observed shifts differed between patients. Therefore, it would be interesting to study the microbial changes of different patient-derived oral microbial communities *in vitro* and compare these with the shifts observed in the patients' oral cavity. One could also consider supplementing certain (pathogenic) microbes in the apical compartment at certain time points during the experiment.

As oral mucositis is an inflammatory reaction, it will result in the release of different cytokines and chemokines in the oral cavity. As many chemokines possess an inherent antimicrobial activity (Dürr and Peschel, 2002; Ganz, 2003; Yang et al., 2003), it would be interesting to include inflammatory cells, for example macrophages, in the *in vitro*

model. Therefore, the model needs to be expanded with an extra compartment as described by Zoumpopoulou et al. (2009) for the co-culture of epithelial cells with dendritic cells. Nevertheless, by including another cell line, the model becomes even more complex potentially leading to increased variability in the results. Moreover, the final interpretation of the results may become far too complex. A better solution would be to dissolve the cytokines, which are normally produced by the macrophages, in the collagen layer. In the context of mucositis, it would for example be interesting to add TNF- $\alpha$ , IL-1 $\beta$  and IL-6 (Logan et al., 2007).

The pathobiology of oral mucositis can be subdivided into different phases as described by Sonis (2007), which are simulated all at once in our *in vitro* model. In particular research settings it would be interesting to apply our *in vitro* model to mimic those phases separately. For the **initiation phase**, the presence of reactive oxygen species could be analysed in the co-culture medium short term after low dose irradiation, together with rapid shifts in the microbial or epithelial metabolism. Furthermore, the **up- or downregulation** of certain genes, like those involved in the NF- $\kappa$ B and mitogen-activated protein kinase signalling pathways (Sonis, 2007), in the epithelial cells could be analysed using qPCR. For the **ulceration phase and healing phase**, a wound healing set-up can be applied as was shown in this dissertation. *In vitro*, we showed that the inhibitory effect of microbiota on epithelial wound healing was altered due to radiotherapy, depending on the microbial inoculum. Similarly, in our patient study, we were able to identify some genera like *Atopobium* present at start that are predictive for the development of severe mucositis.

To mimic the ulceration phase, one could also consider the use of Transwell® membranes with larger pore sizes (3 or 8  $\mu$ m) to allow migration of the microbiota across the agar/mucin to infect the epithelial layer. Nevertheless, in that case the experimental time will again be limited due to the cytotoxicity of the microbiota towards the epithelial cells.

Apart from the microbial inoculum, the radiotherapeutic dose should also be optimized. In our experiments, we applied a single dose of 10 Gy, similar to the dose a patient receives on average during the first week of treatment. Nevertheless, the biological effects between fractionated doses and a single dose will differ significantly. The early effects of the single dose irradiation (10 Gy) can be determined using model calculations (Hall and Giaccia, 2006), and appeared to be similar to the early effect of 8 fractions of 2.15 Gy. As the first mucosal effects arise after a cumulative dose of 10 Gy in patients, with first ulcerations appearing after a cumulative dose of 20 Gy (Van der Schueren et al., 1990; Sonis, 2007; Treister and Sonis, 2007), a single dose of 10 Gy is a good intermediate dose to study the early onset of the ulceration phase.

In conclusion, our model has a lot of potential to be used as a model for radiotherapy-induced mucositis, nevertheless further optimization and validation is needed. First,



as oral mucositis is an inflammatory reaction, one should include an immunologic component in the model. Furthermore, the microbial inoculum and growth should be investigated in parallel with patient studies to ensure that all microbiota found to be important in patients, are represented *in vitro*. Afterwards, the model will be useful to investigate the host-microbe interactions in a radiotherapeutic setting and to search for new therapies and treatment strategies for oral mucositis.

### **10.3. Oral radiotherapy-induced mucositis: taking into account the oral microbiota**

Due to radiotherapy a plethora of processes is activated in the oral mucosa. Sonis (2004b, 2007) described the pathobiology of mucositis, although no role for the oral microbiota was included. Van Vliet et al. (2010) pointed to the role of the intestinal microbiota in the development and severity of chemotherapy-induced mucositis. Similarly, the host-microbe interactions in the oral cavity can be important in the context of radiotherapy-induced mucositis.

Irradiation for head and neck tumours was shown to alter the oral microbial composition, with an increase in the number of lactobacilli and Gram-negative species during or after radiotherapy (Tong et al., 2003; Almståhl et al., 2008; Guobis et al., 2011; Sonalika et al., 2012a). Moreover, in our study we also identified some low abundant genera that were significantly affected by irradiation. Shifts in the oral microbiome during therapy could be linked with the severity of oral mucositis. Previously, some of these shifts have been described in the context of radiation-induced xerostomia and caries, which points to a potential correlation between mucositis and other radiotherapy-induced side effects (Brown et al., 1975; Aas et al., 2008; Almståhl et al., 2008). Indeed, the correlation between different toxicities was already described in the gut environment (Aprile et al., 2008). Further research is needed to elucidate if the microbial shifts are a cause or a consequence of the different toxicities.

In our patient study, certain genera of the oral microbial community were found to be particularly interesting, as their abundance at the start of the radiotherapy was predictive for the severity of oral mucositis. Most probably, these genera are more sensitive towards irradiation and trigger the epithelium in an aberrant way compared to the other oral microbiota. Indeed, using our model, we confirmed the variable effects that different microbial species have towards epithelial wound healing (De Ryck et al., 2015a), which has been described in other studies as well (de Bentzmann et al., 2000; Stephens et al., 2003). Various microbial compounds or metabolites are known to influence the epithelial migration. For example low concentrations of LPS or SCFA were shown to stimulate the epithelial wound healing, while higher

concentrations inhibit the wound healing due to cytotoxicity (Wilson and Gibson, 1997; Koff et al., 2006). Our study pointed to the potential inhibitory role of the microbial quorum sensing molecules in the epithelial wound healing process, a hypothesis that was supported by recent reviews of quorum sensing molecules in the context of interkingdom signalling (Hughes and Sperandio, 2008; Pacheco and Sperandio, 2009). Recently, a new cell-cell communication signal was described in *Pseudomonas aeruginosa* (Lee et al., 2013), which was shown to be activated by phosphate limitation. As this molecule will induce the production of quorum sensing molecules e.g. N-butanoylhomoserine lactone, environmental stress conditions will thus result in an increased production of quorum sensing molecules. Most probably, similar systems exist that will induce quorum sensing molecules in other stress conditions, for example after low-dose irradiation of the microbiota. Quorum sensing molecules will at their turn regulate a diverse array of physiological activities, like virulence (Miller and Bassler, 2001). This hypothesis was strengthened by our results, which showed an increased pathogenicity of *Klebsiella oxytoca* after single dose irradiation.

At last, E-cadherin was found to be a salivary marker for severe mucositis in oropharynxcarcinoma patients. Apart from its role as cell-cell adhesion molecules, E-cadherin is also involved in host-microbe interactions. It can serve as a receptor for internalin of *Listeria monocytogenes* and FadA of *Fusobacterium nucleatum* (Mengaud et al., 1996; Rubinstein et al., 2013). Moreover, microbiota like *Bacteroides fragilis*, *Phorphyromonas gingivalis* and *Candida albicans* were shown to degrade the E-cadherin molecule, allowing their passage to the underlying tissues (Wu et al., 1998; Katz et al., 2000; Villar et al., 2007). In our patient study, a higher abundance of *Phorphyromonas* spp. was related with severe mucositis. The increased abundance of soluble E-cadherin in the saliva is thus possibly not only the result of the irradiation damage of the mucosa but is most possibly also induced by microbial degradation. Due to this loss of cell-cell adhesion molecules, the epithelial barrier will be disturbed, which results in a port of entry for (opportunistic) pathogens.

These data point to the potential roles of the oral microbiota in the context of mucositis. Yet, more research is needed to further explore our preliminary findings.



## 11. GENERAL CONCLUSION

---

Recently, awareness of the impact of microbiota in both health and disease is growing. Using our new *in vitro* oral mucosa model, we have proven the importance of the host-microbe interactions in a wound healing set-up. The microbial quorum sensing molecules might play an important role in this interaction, pointing to the emerging importance of interkingdom signalling in human health and disease. As many different quorum sensing molecules exist, further research should elaborate on the direct effects of these molecules on the host cells. Moreover, new strategies to interfere with the quorum sensing molecules, may lead to new therapies for a variety of diseases.

Until now, research on radiotherapy-induced oral mucositis mainly focussed on the effects of irradiation on the human cells. Nevertheless, we showed an important impact of therapeutic irradiation doses on the functional behaviour and pathogenicity of oral microbiota. Furthermore, microbial shifts in the oral cavity of head and neck cancer patients were observed during radiotherapy. In the future, the radiosensitivity of different oral microbiota, both as pure cultures and in a complex biofilm, should be investigated to identify potential harmful species present in the oral cavity during radiotherapy.

Moreover, the abundance of certain microbiota, like *Prevotella*, were shown to increase steadily with the severity of oral mucositis and thus have potential to be used as a bio-indicator. Interestingly, the abundance of specific microbiota, like *Atopobium* spp., at start of the therapy was shown to be predictive for severe oral mucositis. Those genera should be investigated more in detail both *in vitro* and in patients, as they provide potentially new therapeutic targets in the combat against mucositis. As our patient population was rather small, there is an urgent need to further characterize the oral microbial composition at start and during the therapy of more patients at risk of developing oral mucositis. This research strategy can lead to more specific information concerning the role of the oral microbiota, which will probably help the clinicians to prevent or treat oral mucositis in an effective way.

The new biomarkers proposed in this dissertation, like the presence of certain oral microbial species and the salivary levels of E-cadherin, can be applied to select those patients at high risk for developing mucositis. Unfortunately, the probability of the implementation of adaptive radiotherapy for diminishing the mucosal toxicity is so far very limited. Nevertheless, further research should investigate if the biomarker can identify those patients that would benefit from the existing preventive and

therapeutic measures that are nowadays not applied in clinic due to conflicting results. In that way, some simple tests could make a huge difference for the head and neck cancer patients.

## REFERENCES

---

- Aas, J.A., Paster, B.J., Stokes, L.N., Olsen, I., and Dewhirst, F.E. (2005). Defining the Normal Bacterial Flora of the Oral Cavity. *J Clin Microbiol* 43, 5721–5732.
- Aas, J.A., Griffen, A.L., Dardis, S.R., Lee, A.M., Olsen, I., Dewhirst, F.E., et al. (2008). Bacteria of dental caries in primary and permanent teeth in children and young adults. *J Clin Microbiol* 46, 1407–1417.
- Van den Abbeele, P., Grootaert, C., Possemiers, S., Verstraete, W., Verbeken, K., and Van de Wiele, T. (2009). In vitro model to study the modulation of the mucin-adhered bacterial community. *Appl Microbiol Biotechnol* 83, 349–359.
- Aepfelbacher, M., Essler, M., Huber, E., Sugai, M., and Weber, P.C. (1997). Bacterial Toxins Block Endothelial Wound Repair: Evidence That Rho GTPases Control Cytoskeletal Rearrangements in Migrating Endothelial Cells. *Arterioscler. Thromb. Vasc. Biol.* 17, 1623–1629.
- Aguirre, J.S., Rodríguez, M.R., and García de Fernando, G.D. (2011). Effects of electron beam irradiation on the variability in survivor number and duration of lag phase of four food-borne organisms. *Int. J. Food Microbiol.* 149, 236–246.
- Ahmed, A., Liu, J., Moosa, Y., Tang, L., Zang, S., and Xin, Y. (2012). Microbial profiling of dental caries and periodontitis patients using denaturing gradient gel electrophoresis. *African J. Microbiol. Res.* 6, 2559–2566.
- Ahn, J., Chen, C.Y., and Hayes, R.B. (2012). Oral microbiome and oral and gastrointestinal cancer risk. *Cancer Causes Control* 23, 399–404.
- Al-Dasooqi, N., Gibson, R.J., Bowen, J.M., and Keefe, D.M. (2009). Matrix metalloproteinases: key regulators in the pathogenesis of chemotherapy-induced mucositis? *Cancer Chemother. Pharmacol.* 64, 1–9.
- Al-Nawas, B., and Grötz, K. a (2006). Prospective study of the long term change of the oral flora after radiation therapy. *Support. Care Cancer* 14, 291–296.
- Alander, M., De Smet, I., Nollet, L., Verstraete, W., von Wright, A., and Mattila-Sandholm, T. (1999). The effect of probiotic strains on the microbiota of the Simulator of the Human Intestinal Microbial Ecosystem (SHIME). *Int J Food Microbiol* 46, 71–79.
- Allen, A., and Flemström, G. (2005). Gastroduodenal mucus bicarbonate barrier: protection against acid and pepsin. *Am. J. Physiol. Cell Physiol.* 288, C1–C19.
- Almståhl, a, Wikström, M., and Fagerberg-Mohlin, B. (2008). Microflora in oral ecosystems in subjects with radiation-induced hyposalivation. *Oral Dis.* 14, 541–549.
- Amado, F., Lobo, M.J.C., Domingues, P., Duarte, J.A., and Vitorino, R. (2010). Salivary peptidomics. *Expert Rev. Proteomics* 7, 709–721.
- Andrieu-Abadie, N., Gouazé, V., Salvayre, R., and Levade, T. (2001). Ceramide in apoptosis signaling: relationship with oxidative stress. *Free Radic. Biol. Med.* 31, 717–728.
- Angst, B.D., Marozzi, C., and Magee, A.I. (2001). The cadherin superfamily. *J. Cell Sci.* 114, 625–626.

- Aprile, G., Ramoni, M., Keefe, D., and Sonis, S. (2008). Application of distance matrices to define associations between acute toxicities in colorectal cancer patients receiving chemotherapy. *Cancer* 112, 284–292.
- Attia, M.A.M., and Weiss, D.W. (1966). Immunology of Spontaneous Mammary Carcinomas in Mice : V . Acquired Tumor Resistance and Enhancement in Strain A Mice Infected with Mammary Tumor Virus. *Cancer Res.* 26, 1787–1800.
- Avila, M., Ojcius, D.M., and Yilmaz, O. (2009). The oral microbiota: living with a permanent guest. *DNA Cell Biol.* 28, 405–411.
- Bagg, J., Sweeney, M.P., Wood, K.H., and Wiggins, A. (1995). Possible Role of *Staphylococcus aureus* in Severe Oral Mucositis among Elderly Dehydrated Patients. *Microb. Ecol. Health Dis.* 8, 51–56.
- Bahri, R., Saidane-Mosbahi, D., and Rouabhia, M. (2010a). *Candida famata* modulates toll-like receptor, beta-defensin, and proinflammatory cytokine expression by normal human epithelial cells. *J. Cell. Physiol.* 222, 209–218.
- Bahri, R., Curt, S., Saidane-Mosbahi, D., and Rouabhia, M. (2010b). Normal human gingival epithelial cells sense *C. parapsilosis* by toll-like receptors and module its pathogenesis through antimicrobial peptides and proinflammatory cytokines. *Mediators Inflamm.* 2010, 940383.
- Bakke, I., De Schryver, P., Boon, N., and Vadstein, O. (2011). PCR-based community structure studies of bacteria associated with eukaryotic organisms: a simple PCR strategy to avoid co-amplification of eukaryotic DNA. *J. Microbiol. Methods* 84, 349–351.
- Bansal, T., Alaniz, R.C., Wood, T.K., and Jayaraman, A. (2010). The bacterial signal indole increases epithelial-cell tight-junction resistance and attenuates indicators of inflammation. *Proc. Natl. Acad. Sci. U. S. A.* 107, 228–233.
- Bansal, T., Alaniz, R., and Jayaraman, A. (2012). Role for the Bacterial Signal Indole in Promoting Epithelial Cell Barrier Function. *J. Epithel. Biol. Pharmacol.* 5, 32–38.
- Barasch, A., and Peterson, D.E. (2003). Risk factors for ulcerative oral mucositis in cancer patients: unanswered questions. *Oral Oncol.* 39, 91–100.
- Barham, D., and Trinder, P. (1972). An improved colour reagent for the determination of blood glucose by the oxidase system. *Analyst* 97, 142–145.
- Barnard, J.A. (1993). Butyrate Rapidly Induces Differentiation in HT-29 Growth Cells ' Inhibition and. 4, 495–501.
- Baum, B., and Georgiou, M. (2011). Dynamics of adherens junctions in epithelial establishment, maintenance, and remodeling. *J. Cell Biol.* 192, 907–917.
- Beighton, D., Al-Haboubi, M., Mantzourani, M., Gilbert, S.C., Clark, D., Zoitopoulos, L., and Gallagher, J.E. (2010). Oral Bifidobacteria: caries-associated bacteria in older adults. *J. Dent. Res.* 89, 970–974.
- Beklen, A., Sorsa, T., and Konttinen, Y.T. (2009). Toll-like receptors 2 and 5 in human gingival epithelial cells co-operate with T-cell cytokine interleukin-17. *Oral Microbiol. Immunol.* 24, 38–42.
- Belazi, M., Velegraki, A., Koussidou-Eremondi, T., Andreadis, D., Hini, S., Arsenis, G., et al. (2004). Oral *Candida* isolates in patients undergoing radiotherapy for head and neck cancer: prevalence , azole susceptibility profiles and response to antifungal treatment. *Oral Microbiol. Immunol.* 19, 347–351.
- Belgian Cancer Registry (2012). Cancer incidence in Belgium. ([www.kankerregister.org](http://www.kankerregister.org) - Dec 2014).

- Belgian Cancer Registry (2015). Belgian Cancer Registry: personal communication (Jan 2015).
- De Bentzmann, S., Polette, M., Zahm, J.-M., Hinrasky, J., Kileztky, C., Bajolet, O., et al. (2000). Airway Epithelial Wound Repair by Altering the Actin Cytoskeleton and Inducing Overactivation of Epithelial Matrix Metalloproteinase – 2. *Lab. Investig.* *80*, 209–219.
- Bergin, D., Reeves, E.P., Renwick, J., Frans, B., Kavanagh, K., and Wientjes, F.B. (2005). Superoxide Production in *Galleria mellonella* Hemocytes: Identification of Proteins Homologous to the NADPH Oxidase Complex of Human Neutrophils Superoxide Production in *Galleria mellonella* Hemocytes: Identification of Proteins Homologous to the NADPH Ox. *73*, 4161–4170.
- Bhally, H.S., Lema, C., Romagnoli, M., Borek, A., Wakefield, T., and Carroll, K.C. (2005). *Leptotrichia buccalis* bacteremia in two patients with acute myelogenous leukemia. *Anaerobe* *11*, 350–353.
- Bik, E.M. (2009). Composition and function of the human-associated microbiota. *Nutr. Rev.* *67 Suppl 2*, S164–S171.
- Bik, E.M., Long, C.D., Armitage, G.C., Loomer, P., Emerson, J., Mongodin, E.F., et al. (2010). Bacterial diversity in the oral cavity of 10 healthy individuals. *ISME J* *4*, 962–974.
- Blais, J.-F., and Lavoie, M.C. (1990). Effect of Dietary Components on the Indigenous Oral Bacterial Flora of BALB/c Mice. *J. Dent. Res.* *69*, 868–873.
- De Boever, P., Deplancke, B., and Verstraete, W. (2000). Fermentation by gut microbiota cultured in a simulator of the human intestinal microbial ecosystem is improved by supplementing a soygerm powder. *J Nutr* *130*, 2599–2606.
- Bonuccelli, G., Tsirigos, A., Whitaker-Menezes, D., Pavlides, S., Pestell, R.G., Chiavarina, B., et al. (2010). Ketones and lactate “fuel” tumor growth and metastasis: Evidence that epithelial cancer cells use oxidative mitochondrial metabolism. *Cell Cycle* *9*, 3506–3514.
- Boukamp, P., Petrussevska, R.T., Breitkreutz, D., Hornung, J., Markham, A., and Fusenig, N.E. (1988). Normal Keratinization in a Spontaneously Immortalized aneuploid Human Keratinocyte cell line. *J. Cell Biol.* *106*, 761–771.
- Bracke, M.E., Vyncke, B.M., Bruyneel, E. a, Vermeulen, S.J., De Bruyne, G.K., Van Larebeke, N. a, et al. (1993). Insulin-like growth factor I activates the invasion suppressor function of E-cadherin in MCF-7 human mammary carcinoma cells in vitro. *Br. J. Cancer* *68*, 282–289.
- Bracke, M.E., Charlier, C., Bruyneel, E.A., Labit, C., Mareel, M.M., and Castronovo, V. (1994). Tamoxifen Restores the E-Cadherin Function in Human Breast Cancer MCF-7/6 Cells and Suppresses Their Invasive Phenotype. *Cancer Res.* *54*, 4607–4609.
- Bracke, M.E., Boterberg, T., and Mareel, M.M. (2001). Chick heart invasion assay. *Methods Mol. Med.* *58*, 91–102.
- Brandão, R.L., Castro, I.M., Bambirra, E.A., Amaral, S.C., Fietto, L.G., Tropaia, M.J., et al. (1998). Intracellular signal triggered by cholera toxin in *Saccharomyces boulardii* and *Saccharomyces cerevisiae*. *Appl. Environ. Microbiol.* *64*, 564–568.
- Brown, L.R., Dreizen, S., Handler, S., and Johnston, D. a. (1975). Effect of Radiation-Induced Xerostomia on Human Oral Microflora. *J. Dent. Res.* *54*, 740–750.



- Bryant, D.M., and Stow, J.L. (2004). The ins and outs of E-cadherin trafficking. *Trends Cell Biol.* *14*, 427–434.
- Bucknall, T.E. (1980). The effect of local infection upon wound healing: An experimental study. *Br J Surg* *67*, 851–855.
- Burdelya, L.G., Gleiberman, A.S., Toshkov, I., Aygun-Sunar, S., Bapardekar, M., Manderscheid-Kern, P., et al. (2012). Toll-like receptor 5 agonist protects mice from dermatitis and oral mucositis caused by local radiation: implications for head-and-neck cancer radiotherapy. *Int. J. Radiat. Oncol. Biol. Phys.* *83*, 228–234.
- Caillet, S., Millette, M., Dussault, D., Shareck, F., and Lacroix, M. (2008). Effect of gamma radiation on heat shock protein expression of four foodborne pathogens. *J. Appl. Microbiol.* *105*, 1384–1391.
- Callewaert, C., Kerckhof, F.-M., Granitsiotis, M.S., Van Gele, M., Van de Wiele, T., and Boon, N. (2013). Characterization of Staphylococcus and Corynebacterium clusters in the human axillary region. *PLoS One* *8*, e70538.
- Caluwaerts, S., Vandenbroucke, K., Steidler, L., Neiryneck, S., Vanhoenacker, P., Corveleyn, S., et al. (2010). AG013, a mouth rinse formulation of Lactococcus lactis secreting human Trefoil Factor 1, provides a safe and efficacious therapeutic tool for treating oral mucositis. *Oral Oncol.* *46*, 564–570.
- Castadot, P., Lee, J. a, Geets, X., and Grégoire, V. (2010). Adaptive radiotherapy of head and neck cancer. *Semin. Radiat. Oncol.* *20*, 84–93.
- Chen, T., Yu, W.-H., IZard, J., Baranova, O. V, Lakshmanan, A., and Dewhirst, F.E. (2010). The Human Oral Microbiome Database: a web accessible resource for investigating oral microbe taxonomic and genomic information. *Database* baq013.
- Christensen, J.J., and Facklam, R.R. (2001). Granulicatella and Abiotrophia species from human clinical specimens. *J. Clin. Microbiol.* *39*, 3520–3523.
- Clarke, T.B., Davis, K.M., Lysenko, E.S., Zhou, A.Y., Yu, Y., and Weiser, J.N. (2010). Recognition of peptidoglycan from the microbiota by Nod1 enhances systemic innate immunity. *Nat. Med.* *16*, 228–231.
- Collins, L.M., and Dawes, C. (1987). The surface area of the adult human mouth and thickness of the salivary film covering the teeth and oral mucosa. *J. Dent. Res.* *66*, 1300–1302.
- Comalada, M., Bailón, E., de Haro, O., Lara-Villoslada, F., Xaus, J., Zarzuelo, A., and Gálvez, J. (2006). The effects of short-chain fatty acids on colon epithelial proliferation and survival depend on the cellular phenotype. *J. Cancer Res. Clin. Oncol.* *132*, 487–497.
- Copeland, A., Sikorski, J., Lapidus, A., Nolan, M., Del Rio, T.G., Lucas, S., et al. (2009). Complete genome sequence of Atopobium parvulum type strain (IPP 1246). *Stand. Genomic Sci.* *1*, 166–173.
- Costerton, J.W., Cheng, K.J., Geesey, G.G., Ladd, T.I., Nickel, J.C., Dasgupta, M., and Marrie, T.J. (1987). Bacterial biofilms in nature and disease. *Annu Rev Microbiol* *41*, 435–464.
- Costerton, J.W., Lewandowski, Z., Caldwell, D.E., Korber, D.R., and Lappin-Scott, H.M. (1995). Microbial biofilms. *Annu Rev Microbiol* *49*, 711–745.
- Crawford, P. a, and Gordon, J.I. (2005). Microbial regulation of intestinal radiosensitivity. *Proc. Natl. Acad. Sci. U. S. A.* *102*, 13254–13259.

- Cruz, A.D. da, Cogo, K., Bergamaschi, C. de C., Bóscolo, F.N., Groppo, F.C., and Almeida, S.M. de (2010). Oral streptococci growth on aging and non-aging esthetic restorations after radiotherapy. *Braz. Dent. J.* 21, 346–350.
- Czerucka, D., Roux, I., and Rampal, P. (1994). Saccharomyces boulardii inhibits secretagogue-mediated adenosine 3',5'-cyclic monophosphate induction in intestinal cells. *Gastroenterology* 106, 65–72.
- Denham, J.W., and Hauer-jensen, M. (2002). The radiotherapeutic injury – a complex “wound.” *Radiother. Oncol.* 63, 129–145.
- Deplancke, B., and Gaskins, H.R. (2001). Microbial modulation of innate defense: goblet cells and the intestinal mucus layer. *Am. J. Clin. Nutr.* 73, 1131S – 1141S.
- Derrien, M., van Passel, M.W., van de Bovenkamp, J.H., Schipper, R.G., de Vos, W.M., and Dekker, J. (2010). Mucin-bacterial interactions in the human oral cavity and digestive tract. *Gut Microbes* 1, 254–268.
- Dewhirst, F.E., Chen, T., Izard, J., Paster, B.J., Tanner, A.C.R., Yu, W.-H., et al. (2010). The human oral microbiome. *J Bacteriol* 192, 5002–5017.
- Dewson, G., and Kluck, R.M. (2010). Bcl-2 family-regulated apoptosis in health and disease. *Cell Health Cytoskelet.*
- Dongari-Bagtzoglou, A., and Kashleva, H. (2006). Development of a novel three-dimensional in vitro model of oral Candida infection. *Microb Pathog* 40, 271–278.
- Dongari-bagtzoglou, A., and Kashleva, H. (2006). Development of a highly reproducible three-dimensional organotypic model of the oral mucosa. *Nat Protoc* 1, 2012–2018.
- Donnelly, J.P., Bellm, L.A., Epstein, J.B., Sonis, S.T., and Symonds, R.P. (2003). Antimicrobial therapy to prevent or treat oral mucositis. *Lancet* 3, 405–412.
- Donohoe, D.R., Garge, N., Zhang, X., Sun, W., O'Connell, T.M., Bunger, M.K., and Bultman, S.J. (2011). The Microbiome and Butyrate Regulate Energy Metabolism and Autophagy in the Mammalian Colon. *Cell Metab* 13, 517–526.
- Dörr, W., Noack, R., Spekl, K., and Farrell, C.L. (2001). Modification of oral mucositis by keratinocyte growth factor: single radiation exposure. *Int. J. Radiat. Biol.* 77, 341–347.
- Dörr, W., Hamilton, C.S., Boyd, T., Reed, B., and Denham, J.W. (2002). Radiation-induced changes in cellularity and proliferation in human oral mucosa. *Int. J. Radiat. Oncol. Biol. Phys.* 52, 911–917.
- Dörr, W., Reichel, S., and Spekl, K. (2005a). Effects of keratinocyte growth factor (palifermin) administration protocols on oral mucositis (mouse) induced by fractionated irradiation. *Radiother. Oncol.* 75, 99–105.
- Dörr, W., Bässler, S., Reichel, S., and Spekl, K. (2005b). Reduction of radiochemotherapy-induced early oral mucositis by recombinant human keratinocyte growth factor (palifermin): experimental studies in mice. *Int. J. Radiat. Oncol. Biol. Phys.* 62, 881–887.
- Dürr, M., and Peschel, A. (2002). Chemokines Meet Defensins : the Merging Concepts of Chemoattractants and Antimicrobial Peptides in Host Defense. *Infect Immun* 70, 6515–6517.
- Edwards, R., and Harding, K.G. (2004). Bacteria and wound healing. *Curr Opin Infect Dis* 17, 91–96.

- Edwards, U., Rogall, T., Blöcker, H., Emde, M., and Böttger, E.C. (1989). Isolation and direct complete nucleotide determination of entire genes. Characterization of a gene coding for 16S ribosomal RNA. *Nucleic Acids Res* 17, 7843–7853.
- Ellepola, a. N.B., and Samaranyake, L.P. (2000). Oral Candidal Infections and Antimycotics. *Crit. Rev. Oral Biol. Med.* 11, 172–198.
- Elting, L.S., Cooksley, C.D., Chambers, M.S., and Garden, A.S. (2007). Risk, outcomes, and costs of radiation-induced oral mucositis among patients with head-and-neck malignancies. *Int. J. Radiat. Oncol. Biol. Phys.* 68, 1110–1120.
- Emenaker, N.J., and Basson, M.D. (1998). Short chain fatty acids inhibit human (SW1116) colon cancer cell invasion by reducing urokinase plasminogen activator activity and stimulating TIMP-1 and TIMP-2 activities, rather than via MMP modulation. *J. Surg. Res.* 76, 41–46.
- Enoch, S., and Stephens, P. (2009). Scarless healing : oral mucosa as a scientific model. *Wounds UK* 5, 42–48.
- Eribe, E.R.K., and Olsen, I. (2008). *Leptotrichia* species in human infections. *Anaerobe* 14, 131–137.
- Everard, A., and Cani, P.D. (2013). Diabetes, obesity and gut microbiota. *Best Pract. Res. Clin. Gastroenterol.* 27, 73–83.
- Fagundes, C.T., Amaral, F. a, Teixeira, A.L., Souza, D.G., and Teixeira, M.M. (2012). Adapting to environmental stresses: the role of the microbiota in controlling innate immunity and behavioral responses. *Immunol. Rev.* 245, 250–264.
- Farah, C.S., Hong, S., Wanasaengsakul, S., Elahi, S., Pang, G., Gotjamanos, T., et al. (2001). Irradiation-induced oral candidiasis in an experimental murine model. *Oral Microbiol. Immunol.* 16, 358–363.
- Farkas, J. (1998). Irradiation as a method for decontaminating food. *Int. J. Food Microbiol.* 44, 189–204.
- Firth, J.D., Putnins, E.E., Larjava, H., and Uitto, V.J. (1997). Bacterial phospholipase C upregulates matrix metalloproteinase expression by cultured epithelial cells. *Infect. Immun.* 65, 4931–4936.
- Firth, J.D., Putnins, E.E., Larjava, H., and Uitto, V.-J. (2001). Exogenous Phospholipase C Stimulates Epithelial Cell Migration and Integrin Expression in Vitro. *Wound Repair Regen.* 9, 86–94.
- Forstner, J., and Forstner, G. (1994). Gastrointestinal mucus. In *Physiology of the Gastrointestinal Tract.*, L. Johnson, ed. (New York: Raven Press), pp. 1255–1283.
- Fuchs, B.B., and Mylonakis, E. (2006). Using non-mammalian hosts to study fungal virulence and host defense. *Curr. Opin. Microbiol.* 9, 346–351.
- Fuchs, B.B., O'Brien, E., El Khoury, J.B., and Mylonakis, E. (2010). Methods for using *Galleria mellonella* as a model host to study fungal pathogenesis. *Virulence* 1, 475–482.
- Fukuda, S., Toh, H., Hase, K., Oshima, K., Nakanishi, Y., Yoshimura, K., et al. (2011). Bifidobacteria can protect from enteropathogenic infection through production of acetate. *Nature* 469, 543–547.
- Gaetti-Jardim Júnior, E., Nakano, V., Wahasugui, T.C., Cabral, F.C., Gamba, R., and Avila-Campos, M.J. (2008). Occurrence of yeasts, enterococci and other enteric bacteria in subgingival biofilm of HIV-positive patients with chronic gingivitis and necrotizing periodontitis. *Braz. J. Microbiol.* 39, 257–261.

- Gaetti-Jardim Júnior, E., Ciesielski, F.I.N., de Sousa, F.R.N., Nwaokorie, F., Schweitzer, C.M., and Avila-Campos, M.J. (2011). Occurrence of yeast, pseudomonas and enteric bacteria in the oral cavity of patients undergoing head and neck radiotherapy. *Brazilian J. Microbiol.* *42*, 1047–1055.
- Ganz, T. (2003). Defensins: antimicrobial peptides of innate immunity. *Nat Rev Immunol* *3*, 710–720.
- Gaudier, E., Jarry, a, Blottière, H.M., de Coppet, P., Buisine, M.P., Aubert, J.P., et al. (2004). Butyrate specifically modulates MUC gene expression in intestinal epithelial goblet cells deprived of glucose. *Am. J. Physiol. Gastrointest. Liver Physiol.* *287*, G1168–G1174.
- Gehrisch, A., and Dörr, W. (2007). Effects of systemic or topical administration of sodium selenite on early radiation effects in mouse oral mucosa. *Strahlenther. Onkol.* *183*, 36–42.
- Glim, J.E., van Egmond, M., Niessen, F.B., Everts, V., and Beelen, R.H.J. (2013). Detrimental dermal wound healing: what can we learn from the oral mucosa? *Wound Repair Regen.* *21*, 648–660.
- Gloire, G., Legrand-Poels, S., and Piette, J. (2006). NF-kappaB activation by reactive oxygen species: fifteen years later. *Biochem. Pharmacol.* *72*, 1493–1505.
- Gonçalves, M.O., Coutinho-Filho, W.P., Pimenta, F.P., Pereira, G. a, Pereira, J. a a, Mattos-Guaraldi, a L., and Hirata, R. (2007). Periodontal disease as reservoir for multi-resistant and hydrolytic enterobacterial species. *Lett. Appl. Microbiol.* *44*, 488–494.
- Goodson, J.M., Groppo, D., Halem, S., and Carpino, E. (2009). Is obesity an oral bacterial disease? *J. Dent. Res.* *88*, 519–523.
- Grootaert, C., Van de Wiele, T., Van Roosbroeck, I., Possemiers, S., Vercoutter-Edouart, A.-S., Verstraete, W., et al. (2011a). Bacterial monocultures, propionate, butyrate and H<sub>2</sub>O<sub>2</sub> modulate the expression, secretion and structure of the fasting-induced adipose factor in gut epithelial cell lines. *Environ. Microbiol.* *13*, 1778–1789.
- Grootaert, C., Boon, N., Zeka, F., Vanhoecke, B., Bracke, M., Verstraete, W., and Van de Wiele, T. (2011b). Adherence and viability of intestinal bacteria to differentiated Caco-2 cells quantified by flow cytometry. *J Microbiol Methods* *86*, 33–41.
- Guobis, Ž., Kareivienė, V., Basevičienė, N., Paipalienė, P., Niedzelskienė, I., Sabalys, G., et al. (2011). Microflora of the oral cavity in patients with xerostomia. *Medicina (Kaunas).* *47*, 646–651.
- Haimovitz-Friedman, a., Kolesnick, R.N., and Fuks, Z. (1997). Ceramide signaling in apoptosis. *Br. Med. Bull.* *53*, 539–553.
- Häkkinen, L., Uitto, V.J., and Larjava, H. (2000). Cell biology of gingival wound healing. *Periodontol.* *2000* *24*, 127–152.
- Hall, E.J., and Giaccia, A.J. (2006). *Radiobiology for the radiologist* (Lippincott Williams & Wilkins).
- Halper, J., Leshin, L.S., Lewis, S.J., and Li, W.I. (2003). Wound healing and angiogenic properties of supernatants from *Lactobacillus* cultures. *Exp. Biol. Med.* (Maywood). *228*, 1329–1337.

- Hamer, H.M., Jonkers, D., Venema, K., Vanhoutvin, S., Troost, F.J., and Brummer, R.-J. (2008). Review article: the role of butyrate on colonic function. *Aliment. Pharmacol. Ther.* *27*, 104–119.
- Han, Y.W., Shi, W., Huang, G.T., Haake, S.K., Park, N.-H., Kuramitsu, H., and Genco, R.J. (2000). Interactions between Periodontal Bacteria and Human Oral Epithelial Cells : *Fusobacterium nucleatum* Adheres to and Invades Epithelial Cells. *Infect. Immun.*
- Hanstock, T.L., Mallet, P.E., and Clayton, E.H. (2010). Increased plasma d-lactic acid associated with impaired memory in rats. *Physiol. Behav.* *101*, 653–659.
- Haraszthy, V.I., Zambon, J.J., Sreenivasan, P.K., Zambon, M.M., Gerber, D., Rego, R., and Parker, C. (2012). Identification of oral bacterial species associated with halitosis. *Nephrol. Dial. Transplant* *27 Suppl 1*, i1.
- Hashibe, M., Brennan, P., Chuang, S.-C., Boccia, S., Castellsague, X., Chen, C., et al. (2009). Interaction between tobacco and alcohol use and the risk of head and neck cancer: pooled analysis in the International Head and Neck Cancer Epidemiology Consortium. *Cancer Epidemiol. Biomarkers Prev.* *18*, 541–550.
- Hermiston, M.L., and Gordon, J.I. (1995). In vivo analysis of cadherin function in the mouse intestinal epithelium: essential roles in adhesion, maintenance of differentiation, and regulation of programmed cell death. *J. Cell Biol.* *129*, 489–506.
- Hinnebusch, B.F., Meng, S., Wu, J.T., Archer, S.Y., and Hodin, R.A. (2002). Nutrition and Cancer The Effects of Short-Chain Fatty Acids on Human Colon Cancer Cell Phenotype Are Associated with Histone Hyperacetylation. *J. Nutr.* *132*, 1012–1017.
- Hoffmann, J. a (1995). Innate immunity of insects. *Curr. Opin. Immunol.* *7*, 4–10.
- Hold, G.L., Smith, M., Grange, C., Watt, E.R., El-Omar, E.M., and Mukhopadhyaya, I. (2014). Role of the gut microbiota in inflammatory bowel disease pathogenesis: what have we learnt in the past 10 years? *World J. Gastroenterol.* *20*, 1192–1210.
- Hsiao, W.W., Li, K.L., Liu, Z., Jones, C., Fraser-Liggett, C.M., and Fouad, A.F. (2012). Microbial transformation from normal oral microbiota to acute endodontic infections. *BMC Genomics* *13*, 345.
- Hu, Y., Shao, Z., Wang, Q., Jiang, Y., Ma, R., Tang, Z., et al. (2013a). Exploring the dynamic core microbiome of plaque microbiota during head-and-neck radiotherapy using pyrosequencing. *PLoS One* *8*, e56343.
- Hu, Y., Wang, Q., Jiang, Y., Ma, R., Xia, W., Tang, Z., and Liu, Z. (2013b). Characterization of oral bacterial diversity of irradiated patients by high-throughput sequencing. *Int. J. Oral Sci.* *5*, 21–25.
- Hughes, D.T., and Sperandio, V. (2008). Inter-kingdom signalling: communication between bacteria and their hosts. *Nat Rev Microbiol* *6*, 111–120.
- Ichikawa, H., and Sakata, T. (1998). Stimulation of Epithelial Cell Proliferation of Isolated Distal Colon of Rats by Continuous Colonic Infusion of Ammonia or Short-Chain Fatty Acids Is Nonadditive. *J. Nutr.* *128*, 843–847.
- Igarashi, M., Kitada, Y., Yoshiyama, H., Takagi, a, Miwa, T., and Koga, Y. (2001). Ammonia as an accelerator of tumor necrosis factor alpha-induced apoptosis of gastric epithelial cells in *Helicobacter pylori* infection. *Infect. Immun.* *69*, 816–821.

- Imamura, Y., Yanagihara, K., Mizuta, Y., Seki, M., Ohno, H., Higashiyama, Y., et al. (2004). Azithromycin Inhibits MUC5AC Production Induced by the *Pseudomonas aeruginosa* Homoserine Lactone in NCI-H292 Cells. *Antimicrob. Agents Chemother.* *48*, 3457.
- Inan, M.S., Rasoulpour, R.J., Yin, L., Hubbard, a K., Rosenberg, D.W., and Giardina, C. (2000). The luminal short-chain fatty acid butyrate modulates NF-kappaB activity in a human colonic epithelial cell line. *Gastroenterology* *118*, 724–734.
- Jacobsen, J., van Deurs, B., Pedersen, M., and Rassing, M.R. (1995). TR146 cells grown on filters as a model for human buccal epithelium: I. Morphology, growth, barrier properties, and permeability. *Int. J. Pharm.* *125*, 165–184.
- Jeng, J.H., Chan, C.P., Ho, Y.S., Lan, W.H., Hsieh, C.C., and Chang, M.C. (1999). Effects of butyrate and propionate on the adhesion, growth, cell cycle kinetics, and protein synthesis of cultured human gingival fibroblasts. *J. Periodontol.* *70*, 1435–1442.
- Jiao, Y., Darzi, Y., Tawaratsumida, K., Marchesan, J.T., Hasegawa, M., Moon, H., et al. (2013). Induction of Bone Loss by Pathobiont-Mediated Nod1 Signaling in the Oral Cavity. *Cell Host Microbe* *13*, 595–601.
- Katz, J., Sambandam, V., Wu, J.H., Michalek, S.M., and Balkovetz, D.F. (2000). Characterization of *Porphyromonas gingivalis* -Induced Degradation of Epithelial Cell Junctional Complexes. *Infect. Immun.* *68*, 1441–1449.
- Kazor, C.E., Mitchell, P.M., Lee, A.M., Stokes, L.N., Loesche, W.J., Dewhirst, F.E., and Paster, B.J. (2003). Diversity of Bacterial Populations on the Tongue Dorsa of Patients with Halitosis and Healthy Patients. *Society* *41*, 558–563.
- Keene, H.J., and Fleming, T.J. (1987). Prevalence of caries-associated microflora after radiotherapy in patients with cancer of the head and neck. *Oral Surgery, Oral Med. Oral Pathol.* *64*, 421–426.
- Keijser, B.J.F., Zaura, E., Huse, S.M., van der Vossen, J.M.B.M., Schuren, F.H.J., Montijn, R.C., et al. (2008). Pyrosequencing analysis of the Oral Microflora of healthy adults. *J. Dent. Res.* *87*, 1016–1020.
- Kersun, L.S., Propert, K.J., Lautenbach, E., Bunin, N., and Demichele, A. (2005). Early bacteremia in pediatric hematopoietic stem cell transplant patients on oral antibiotic prophylaxis. *Pediatr. Blood Cancer* *45*, 162–169.
- Kesimer, M., Kiliç, N., Mehrotra, R., Thornton, D.J., and Sheehan, J.K. (2009). Identification of salivary mucin MUC7 binding proteins from *Streptococcus gordonii*. *BMC Microbiol.* *9*, 163.
- Khaw, a, Logan, R., Keefe, D., and Bartold, M. (2014). Radiation-induced oral mucositis and periodontitis - proposal for an inter-relationship. *Oral Dis.* *20*, e7–e18.
- Kiliç, Y., Rajewski, K., and Dörr, W. (2007). Effect of post-exposure administration of keratinocyte growth factor (Palifermin) on radiation effects in oral mucosa in mice. *Radiat. Environ. Biophys.* *46*, 13–19.
- Kim, I.-J., and Blanke, S.R. (2012). Remodeling the host environment: modulation of the gastric epithelium by the *Helicobacter pylori* vacuolating toxin (VacA). *Front. Cell. Infect. Microbiol.* *2*, 37.
- Kim, M.H., Kang, S.G., Park, J.H., Yanagisawa, M., and Kim, C.H. (2013). Short-chain fatty acids activate GPR41 and GPR43 on intestinal epithelial cells to promote inflammatory responses in mice. *Gastroenterology* *145*, 396–406.e1–e10.

- Kocgozlu, L., Elkaim, R., Tenenbaum, H., and Werner, S. (2009). Variable cell responses to *P. gingivalis* lipopolysaccharide. *J. Dent. Res.* *88*, 741–745.
- Koff, J.L., Shao, M.X.G., Kim, S., Ueki, I.F., and Nadel, J.A. (2006). *Pseudomonas* Lipopolysaccharide accelerates wound repair via activation of a novel epithelial cell signaling cascade. *J. Immunol.* *177*, 8693–8700.
- Kolenbrander, P.E., Palmer, R.J., Periasamy, S., and Jakubovics, N.S. (2010). Oral multispecies biofilm development and the key role of cell-cell distance. *Nat. Rev. Microbiol.* *8*, 471–480.
- Könönen, E., Kanervo, A., Takala, A., Asikainen, S., and Jousimies-Somer, H. (1999). Establishment of Oral Anaerobes during the First Year of Life. *J Dent Res* *78*, 1634–1639.
- Küchler, S., Wolf, N.B., Heilmann, S., Weindl, G., Helfmann, J., Yahya, M.M., et al. (2010). 3D-wound healing model: influence of morphine and solid lipid nanoparticles. *J Biotechnol* *148*, 24–30.
- Kuehn, M.J., and Kesty, N.C. (2005). Bacterial outer membrane vesicles and the host-pathogen interaction. *Genes Dev.* *19*, 2645–2655.
- Kulp, A., and Kuehn, M.J. (2010). Biological Functions and Biogenesis of secreted bacterial outer membrane vesicles. *Annu Rev Microbiol* *64*, 163–184.
- Kurnatowski, P., Moqbil, S., and Kaczmarczyk, D. (2014). Signs , symptoms and the prevalence of fungi detected from the oral cavity and pharynx of radiotherapy subjects with head and neck tumors , and their susceptibility to chemotherapeutics. *Ann. Parasitol.* *60*, 207–213.
- Laato, M., Niinikoski, J., and Gerdin, B. (1990). The effect of *Staphylococcus aureus* bacteria and its products on wound healing. In *Pathogenesis of Wound and Biomaterial-Associated Infections*, T. Wadström, I. Eliasson, I. Holder, and A. Ljungh, eds. (Springer London), pp. 25–34.
- Laheij, A.M.G. a, de Soet, J.J., von dem Borne, P. a, Kuijper, E.J., Kraneveld, E. a, van Loveren, C., and Raber-Durlacher, J.E. (2012). Oral bacteria and yeasts in relationship to oral ulcerations in hematopoietic stem cell transplant recipients. *Support. Care Cancer* *20*, 3231–3240.
- Laheij, A.M.G. a, de Soet, J.J., Veerman, E.C.I., Bolscher, J.G.M., and van Loveren, C. (2013). The influence of oral bacteria on epithelial cell migration in vitro. *Mediators Inflamm.* *2013*, 154532.
- Lalla, R. V, Bowen, J., Barasch, A., Elting, L., Epstein, J., Keefe, D.M., et al. (2014). MASCC/ISOO clinical practice guidelines for the management of mucositis secondary to cancer therapy. *Cancer* *120*, 1453–1461.
- Lamarque, D., Moran, a P., Szepes, Z., Delchier, J.C., and Whittle, B.J. (2000). Cytotoxicity associated with induction of nitric oxide synthase in rat duodenal epithelial cells in vivo by lipopolysaccharide of *Helicobacter pylori*: inhibition by superoxide dismutase. *Br. J. Pharmacol.* *130*, 1531–1538.
- Lambrecht, M., Nevens, D., and Nuyts, S. (2013). Intensity-modulated radiotherapy vs. parotid-sparing 3D conformal radiotherapy. Effect on outcome and toxicity in locally advanced head and neck cancer. *Strahlenther. Onkol.* *189*, 223–229.
- Latham, T., Mackay, L., Sproul, D., Karim, M., Culley, J., Harrison, D.J., et al. (2012). Lactate, a product of glycolytic metabolism, inhibits histone deacetylase activity and promotes changes in gene expression. *Nucleic Acids Res.* *40*, 4794–4803.

- Lee, J., Wu, J., Deng, Y., Wang, J., Wang, C., Wang, J., et al. (2013). A cell-cell communication signal integrates quorum sensing and stress response. *Nat. Chem. Biol.* *9*, 339–343.
- Letzelter, C., Croute, F., Pianezzi, B., Roques, C., and Soleilhavoup, J.P. (1998). Supernatant cytotoxicity and proteolytic activity of selected oral bacteria against human gingival fibroblasts in vitro. *Arch Oral Biol* *43*, 15–23.
- Lewis, J.E., Jensen, P.J., Johnson, K.R., and Wheelock, M.J. (1995). E-cadherin mediates adherens junction organization through protein kinase C. *J. Cell Sci.* *108*, 3615–3621.
- Li, J., Setiawan, M., Wu, H., Beurman, R.W., and Zhao, P. (2014). Regulation of Toll-like receptor expression in human conjunctival epithelial cells. *Mediators Inflamm.* *2014*, 9.
- Li, L., Hooi, D., Chhabra, S.R., Pritchard, D., and Shaw, P.E. (2004). Bacterial N-acylhomoserine lactone-induced apoptosis in breast carcinoma cells correlated with down-modulation of STAT3. *Oncogene* *23*, 4894–4902.
- Li, X., Kolltveit, K.M., Tronstad, L., and Olsen, I. (2000). Systemic Diseases Caused by Oral Infection. *Clin Microbiol Rev* *13*, 547–558.
- Ligtenberg, A.J., Walgreen-Weterings, E., Veerman, E.C., de Soet, J.J., de Graaff, J., and Amerongen, A. V (1992). Influence of saliva on aggregation and adherence of *Streptococcus gordonii* HG 222. *Infect. Immun.* *60*, 3878–3884.
- Limaye, S.A., Haddad, R.I., Cilli, F., Sonis, S.T., Colevas, a. D., Brennan, M.T., et al. (2013). Phase 1b, multicenter, single blinded, placebo-controlled, sequential dose escalation study to assess the safety and tolerability of topically applied AG013 in subjects with locally advanced head and neck cancer receiving induction chemotherapy. *Cancer* *119*, 4268–4276.
- Linden, D.R. (2014). Hydrogen sulfide signaling in the gastrointestinal tract. *Antioxid. Redox Signal.* *20*, 818–830.
- Lionakis, M.S. (2011). *Drosophila* and *Galleria* insect model hosts: new tools for the study of fungal virulence, pharmacology and immunology. *Virulence* *2*, 521–527.
- Littman, D.R., and Pamer, E.G. (2011). Role of the commensal microbiota in normal and pathogenic host immune responses. *Cell Host Microbe* *10*, 311–323.
- Löe, H. (1981). The role of bacteria in periodontal diseases. *Bull World Heal. Organ* *59*, 821–825.
- Logan, R.M., Stringer, A.M., Bowen, J.M., Yeoh, A.S.-J., Gibson, R.J., Sonis, S.T., and Keefe, D.M.K. (2007). The role of pro-inflammatory cytokines in cancer treatment-induced alimentary tract mucositis: pathobiology, animal models and cytotoxic drugs. *Cancer Treat. Rev.* *33*, 448–460.
- Van Loosdrecht, M.C., Lyklema, J., Norde, W., and Zehnder, A.J. (1990). Influence of interfaces on microbial activity. *Microbiol Rev* *54*, 75–87.
- Louis, P., Hold, G.L., and Flint, H.J. (2014). The gut microbiota, bacterial metabolites and colorectal cancer. *Nat. Rev. Microbiol.* *12*, 661–672.
- Lupton, J.R., and Kurtz, P.P. (1993). Relationship of Colonic Luminal Short-Chain Fatty Acids and pH to In Vivo Cell Proliferation in Rats. *J. Nutr.* *123*, 1522–1530.
- MacNeil, S., Shepherd, J., and Smith, L. (2011). Production of tissue-engineered skin and oral mucosa for clinical and experimental use. *Methods Mol Biol* *695*, 129–153.



- Mager, D.L., Ximenez-fyvie, L.A., Haffajee, A.D., and Socransky, S.S. (2003). Distribution of selected bacterial species on intraoral surfaces. *J Clin Periodontol* 30, 644–654.
- Maier, I., Berry, D.M., and Schiestl, R.H. (2014a). Intestinal microbiota reduces genotoxic endpoints induced by high-energy protons. *Radiat. Res.* 181, 45–53.
- Maier, P., Wenz, F., and Herskind, C. (2014b). Radioprotection of normal tissue cells. *Strahlenther. Onkol.* 190, 745–752.
- Marchini, L., Campos, M.S., Silva, a M., Paulino, L.C., and Nobrega, F.G. (2007). Bacterial diversity in aphthous ulcers. *Oral Microbiol. Immunol.* 22, 225–231.
- Marsh, P., and Martin, M. V (1999). *Oral microbiology* (London, United Kingdom: Chapman & Hall).
- Marzorati, M., Wittebolle, L., Boon, N., Daffonchio, D., and Verstraete, W. (2008). How to get more out of molecular fingerprints: practical tools for microbial ecology. *Environ. Microbiol.* 10, 1571–1581.
- Marzorati, M., Abbeele, P., Possemiers, S., Benner, J., Verstraete, W., and Wiele, T. (2011). Studying the host-microbiota interaction in the human gastrointestinal tract: basic concepts and in vitro approaches. *Ann. Microbiol.* 61, 709–715.
- Marzorati, M., Van den Abbeele, P., Grootaert, C., De Weirtdt, R., Marcos, C.A., Vermeiren, J., and Van de Wiele, T. (2014). Chapter 7: Models of the human microbiota and microbiome in vitro. In *The Human Microbiota and Microbiome.*, J.R. Marchesi, ed. (CABI Publishing).
- Matsuki, T., Pédrón, T., Regnault, B., Mulet, C., Hara, T., and Sansonetti, P.J. (2013). Epithelial cell proliferation arrest induced by lactate and acetate from *Lactobacillus casei* and *Bifidobacterium breve*. *PLoS One* 8, e63053.
- Mayer, M.L., Sheridan, J. a, Blohmke, C.J., Turvey, S.E., and Hancock, R.E.W. (2011). The *Pseudomonas aeruginosa* autoinducer 3O-C12 homoserine lactone provokes hyperinflammatory responses from cystic fibrosis airway epithelial cells. *PLoS One* 6, e16246.
- McAuley, J.L., Linden, S.K., Png, C.W., King, R.M., Pennington, H.L., Gendler, S.J., et al. (2007). MUC1 cell surface mucin is a critical element of the mucosal barrier to infection. *J. Clin. Invest.* 117, 2313–2324.
- McBain, J.A., Eastman, A., Nobel, C.S., and Mueller, G.C. (1997). Apoptotic Death in Adenocarcinoma Cell Lines Induced by Butyrate and Other Histone Deacetylase Inhibitors. *Biochem. Pharmacol.* 53, 1357–1368.
- McDermott, a M., Kern, T.S., and Murphy, C.J. (1998). The effect of elevated extracellular glucose on migration, adhesion and proliferation of SV40 transformed human corneal epithelial cells. *Curr. Eye Res.* 17, 924–932.
- McGee, D.W., Elson, C.O., and McGhee, J.R. (1993). Enhancing effect of cholera toxin on interleukin-6 secretion by IEC-6 intestinal epithelial cells: mode of action and augmenting effect of inflammatory cytokines. *Infect. Immun.* 61, 4637–4644.
- Mcleod, J.W., and Gordon, J. (1922). Production of hydrogen peroxide by bacteria. *Biochem J* 16, 499–506.
- Meca, L.B., Souza, F.R.N. de, Tanimoto, H.M., Castro, A.L. de, and Gaetti-Jardim Júnior, E. (2009). Influence of preventive dental treatment on mutans streptococci counts in patients undergoing head and neck radiotherapy. *J. Appl. Oral Sci.* 17, 5–12.

- Megraud, F., Neman-simha, V., and Brugmann, D. (1992). Further Evidence of the Toxic Effect of Ammonia Produced by *Helicobacter pylori* Urease on Human Epithelial Cells. *Infect. Immun.* *60*, 1858–1863.
- Mempel, M., Schnopp, C., Hojka, M., Fesq, H., Weidinger, S., Schaller, M., et al. (2002). Invasion of human keratinocytes by *Staphylococcus aureus* and intracellular bacterial persistence represent haemolysin-independent virulence mechanisms that are followed by features of necrotic and apoptotic keratinocyte cell death. *Br J Dermatol* *146*, 943–951.
- Mengaud, J., Ohayon, H., Gounon, P., Mège, R.-M., and Cossart, P. (1996). E-Cadherin Is the Receptor for Internalin, a Surface Protein Required for Entry of *L. monocytogenes* into Epithelial Cells. *Cell* *84*, 923–932.
- Miller, M.B., and Bassler, B.L. (2001). Quorum Sensing in Bacteria. *Annu. Rev. Microbiol.* *55*, 165–199.
- Milligan, S., Kalita, J., Pocock, V., Heyerick, a, De Cooman, L., Rong, H., and De Keukeleire, D. (2002). Oestrogenic activity of the hop phyto-oestrogen, 8-prenylnaringenin. *Reproduction* *123*, 235–242.
- Milovic, V., Teller, I.C., Turchanowa, L., Caspary, W.F., and Stein, J. (2000). Effect of structural analogues of propionate and butyrate on colon cancer cell growth. *Int. J. Colorectal Dis.* *15*, 264–270.
- Mitchell, J. (2011). *Streptococcus mitis*: walking the line between commensalism and pathogenesis. *Mol. Oral Microbiol.* *26*, 89–98.
- Mitchell, H.L., Dashper, S.G., Catmull, D. V, Paolini, R. a, Cleal, S.M., Slakeski, N., et al. (2010). *Treponema denticola* biofilm-induced expression of a bacteriophage, toxin-antitoxin systems and transposases. *Microbiology* *156*, 774–788.
- Mitsuyama, M., Ohara, R., Amako, K., Nomoto, K., and Yokokura, T. (1986). Ontogeny of macrophage function to release superoxide anion in conventional and germfree mice. *Infect. Immun.* *52*, 236–239.
- Moharamzadeh, K., Brook, I.M., Noort, R. Van, Scutt, A.M., and Thornhill, M.H. (2007). Tissue-engineered Oral Mucosa : a Review of the Scientific Literature. *J Dent Res* *86*, 115–124.
- Moharamzadeh, K., Brook, I.M., Scutt, A.M., Thornhill, M.H., and Van Noort, R. (2008a). Mucotoxicity of dental composite resins on a tissue-engineered human oral mucosal model. *J Dent* *36*, 331–336.
- Moharamzadeh, K., Brook, I.M., Van Noort, R., Scutt, a M., Smith, K.G., and Thornhill, M.H. (2008b). Development, optimization and characterization of a full-thickness tissue engineered human oral mucosal model for biological assessment of dental biomaterials. *J. Mater. Sci. Mater. Med.* *19*, 1793–1801.
- Moharamzadeh, K., Colley, H., Murdoch, C., Hearnden, V., Chai, W.L., Brook, I.M., et al. (2012). Tissue-engineered Oral Mucosa. *J. Dent. Res.* *91*, 642–650.
- Mohr, N., and Budzikiewicz, H. (1982). Tilivalline, a new pyrrolo[2,1-c][1,4]benzodiazepine metabolite from *Klebsiella*. *Tetrahedron* *38*, 147–152.
- Momose, Y., Hirayama, K., and Itoh, K. (2008). Competition for proline between indigenous *Escherichia coli* and *E. coli* O157:H7 in gnotobiotic mice associated with infant intestinal microbiota and its contribution to the colonization resistance against *E. coli* O157:H7. *Antonie Van Leeuwenhoek* *94*, 165–171.
- Montassier, E., Batard, E., Massart, S., Gastinne, T., Carton, T., Caillon, J., et al. (2014). 16S rRNA gene pyrosequencing reveals shift in patient faecal microbiota during

- high-dose chemotherapy as conditioning regimen for bone marrow transplantation. *Microb. Ecol.* 67, 690–699.
- Morad, S.A., Levin, J.C., Tan, S.-F., Fox, T.E., Feith, D.J., and Cabot, M.C. (2013). Novel off-target effect of tamoxifen - Inhibition of acid ceramidase activity in cancer cells. *Biochim. Biophys. Acta* 1831, 1657–1664.
- Morali, G., Polatti, F., Metelitsa, E.N., Mascarucci, P., Magnani, P., and Marrè, G.B. (2006). Open, non-controlled clinical studies to assess the efficacy and safety of a medical device in form of gel topically and intravaginally used in postmenopausal women with genital atrophy. *Arzneimittelforschung.* 56, 230–238.
- Moreno-Indias, I., Cardona, F., Tinahones, F.J., and Queipo-Ortuño, M.I. (2014). Impact of the gut microbiota on the development of obesity and type 2 diabetes mellitus. *Front. Microbiol.* 5, 1–10.
- Morgenstein, A.A., Citron, D.M., Orisek, B., and Finegold, S.M. (1980). Serious Infection with *Leptotrichia buccalis*: Report of a Case and Review of the Literature. *Am. J. Med.* 68, 782–785.
- Mosmann, T. (1983). Rapid colorimetric assay for cellular growth and survival: Application to proliferation and cytotoxicity assays. *J Immunol Methods* 65, 55–63.
- Mukai, R., Horikawa, H., Fujikura, Y., Kawamura, T., Nemoto, H., Nikawa, T., and Terao, J. (2012). Prevention of disuse muscle atrophy by dietary ingestion of 8-prenylnaringenin in denervated mice. *PLoS One* 7, e45048.
- Mukherjee, K., Altincicek, B., Hain, T., Domann, E., Vilcinskas, A., and Chakraborty, T. (2010). *Galleria mellonella* as a model system for studying *Listeria* pathogenesis. *Appl. Environ. Microbiol.* 76, 310–317.
- Napeñas, J.J., Brennan, M.T., Bahrani-Mougeot, F.K., Fox, P.C., and Lockhart, P.B. (2007). Relationship between mucositis and changes in oral microflora during cancer chemotherapy. *Oral Surg. Oral Med. Oral Pathol. Oral Radiol. Endod.* 103, 48–59.
- Napeñas, J.J., Brennan, M.T., Coleman, S., Kent, M.L., Noll, J., Frenette, G., et al. (2010). Molecular methodology to assess the impact of cancer chemotherapy on the oral bacterial flora: a pilot study. *Oral Surg. Oral Med. Oral Pathol. Oral Radiol. Endod.* 109, 554–560.
- Naranjo, A.A., Triviño, M.L., Jaramillo, A., Betancourth, M., and Botero, J.E. (2006). Changes in the subgingival microbiota and periodontal parameters before and 3 months after bracket placement. *Am. J. Orthod. Dentofacial Orthop.* 130, 275.e17–e22.
- Navarro-Velasco, G.Y., Prados-Rosales, R.C., Ortíz-Urquiza, A., Quesada-Moraga, E., and Di Pietro, A. (2011). *Galleria mellonella* as model host for the trans-kingdom pathogen *Fusarium oxysporum*. *Fungal Genet. Biol.* 48, 1124–1129.
- Nepelska, M., Cultrone, A., Béguet-Crespel, F., Le Roux, K., Doré, J., Arulampalam, V., and Blotière, H.M. (2012). Butyrate produced by commensal bacteria potentiates phorbol esters induced AP-1 response in human intestinal epithelial cells. *PLoS One* 7, e52869.
- Nicolatou-Galitis, O., Sarri, T., Bowen, J., Di Palma, M., Kouloulis, V.E., Niscola, P., et al. (2013). Systematic review of amifostine for the management of oral mucositis in cancer patients. *Support. Care Cancer* 21, 357–364.

- Nishimura, A., Fujimoto, M., Oguchi, S., Fusunyan, R.D., MacDermott, R.P., and Sanderson, I.R. (1998). Short-chain fatty acids regulate IGF-binding protein secretion by intestinal epithelial cells. *Am. J. Physiol.* 275, E55–E63.
- Noë, V., Fingleton, B., Jacobs, K., Crawford, H.C., Vermeulen, S., Steelant, W., et al. (2000). Release of an invasion promoter E-cadherin fragment by matrilysin and stromelysin-1. *J. Cell Sci.*
- Nusrat, a, Sitaraman, S. V, and Neish, a (2001a). Interaction of bacteria and bacterial toxins with intestinal epithelial cells. *Curr. Gastroenterol. Rep.* 3, 392–398.
- Nusrat, A., von Eichel-Streiber, C., Turner, J.R., Verkade, P., Madara, L., and Parkos, C.A. (2001b). Clostridium difficile Toxins Disrupt Epithelial Barrier Function by Altering Membrane Microdomain Localization of Tight Junction Proteins. *Infect Immun* 69, 1329.
- Nutting, C.M., Morden, J.P., Harrington, K.J., Urbano, T.G., Bhide, S. a, Clark, C., et al. (2011). Parotid-sparing intensity modulated versus conventional radiotherapy in head and neck cancer (PARSPORT): a phase 3 multicentre randomised controlled trial. *Lancet. Oncol.* 12, 127–136.
- Nyvad, B., and Kilian, M. (1987). Microbiology of the early colonization of human enamel and root surfaces in vivo. *Scand. J. Dent. Res.* 95, 369–380.
- Ohata, A., Usami, M., and Miyoshi, M. (2005). Short-chain fatty acids alter tight junction permeability in intestinal monolayer cells via lipoxigenase activation. *Nutrition* 21, 838–847.
- Ohkubo, T., Tsuda, M., Tamura, M., and Yamamura, M. (1990). Impaired Superoxide Production in Peripheral Blood Neutrophils of Germ-Free Rats. *Scand. J. Immunol.* 32, 727–729.
- Okada, M. (1994). The influence of intestinal flora on wound healing in mice. *Surg. Today* 24, 347–355.
- Okahashi, N., Sumitomo, T., Nakata, M., Sakurai, A., Kuwata, H., and Kawabata, S. (2014). Hydrogen peroxide contributes to the epithelial cell death induced by the oral mitis group of streptococci. *PLoS One* 9, e88136.
- Olczak-Kowalczyk, D., Daszkiewicz, M., Krasuska-Sławińska, Dembowska-Bagińska, B., Gozdowski, D., Daszkiewicz, P., et al. (2012). Bacteria and Candida yeasts in inflammations of the oral mucosa in children with secondary immunodeficiency. *J. Oral Pathol. Med.* 41, 568–576.
- Oliveira, M.J., Van Damme, J., Lauwaet, T., De Corte, V., De Bruyne, G., Verschraegen, G., et al. (2003). B-casein-derived peptides , produced by bacteria , stimulate cancer cell invasion and motility. *EMBO J.* 22, 6161–6173.
- Osborne, C.K. (1998). Tamoxifen in the treatment of breast cancer. *N. Engl. J. Med.* 339, 1609–1618.
- Ovington, L. (2003). Bacterial toxins and wound healing. *Ostomy. Wound. Manage.* 49, 8–12.
- Pacheco, A.R., and Sperandio, V. (2009). Inter-kingdom signaling: chemical language between bacteria and host. *Curr. Opin. Microbiol.* 12, 192–198.
- Paju, S., and Scannapieco, F.A. (2007). Oral biofilms, periodontitis, and pulmonary infections. *Oral Dis* 13, 508–512.
- Panghal, M., Kaushal, V., Kadayam, S., and Yadav, J.P. (2012). Incidence and risk factors for infection in oral cancer patients undergoing different treatments protocols. *BMC Oral Health* 12, 22.

- Parikka, M., Hammarén, M.M., Harjula, S.-K.E., Halfpenny, N.J. a, Oksanen, K.E., Lahtinen, M.J., et al. (2012). Mycobacterium marinum causes a latent infection that can be reactivated by gamma irradiation in adult zebrafish. *PLoS Pathog.* *8*, e1002944.
- Patisaul, H.B., and Jefferson, W. (2010). The pros and cons of phytoestrogens. *Front Neuroendocr.* *31*, 400–419.
- Peng, L., He, Z., Chen, W., Holzman, I.R., and Lin, J. (2007). Effects of butyrate on intestinal barrier function in a Caco-2 cell monolayer model of intestinal barrier. *Pediatr. Res.* *61*, 37–41.
- Peng, L., Li, Z.-R., Green, R.S., Holzman, I.R., and Lin, J. (2009). Butyrate enhances the intestinal barrier by facilitating tight junction assembly via activation of AMP-activated protein kinase in Caco-2 cell monolayers. *J. Nutr.* *139*, 1619–1625.
- Pereira, C.A., Toledo, B.C., Santos, C.T., Pereira Costa, A.C.B., Back-Brito, G.N., Kaminagakura, E., and Jorge, A.O.C. (2013). Opportunistic microorganisms in individuals with lesions of denture stomatitis. *Diagn. Microbiol. Infect. Dis.* *76*, 419–424.
- Phillips, J.R., Tripp, T.J., Regelman, W.E., Schlievert, P.M., and Wangenstein, O.D. (2006). Staphylococcal alpha-toxin causes increased tracheal epithelial permeability. *Pediatr. Pulmonol.* *41*, 1146–1152.
- Pico, J.-L., Avila-Garavito, A., and Naccache, P. (1998). Mucositis: Its Occurrence, Consequences, and Treatment in the Oncology Setting. *Oncologist* *3*, 446–451.
- Podschun, R., and Ullmann, U. (1998). Klebsiella spp. as nosocomial pathogens: epidemiology, taxonomy, typing methods, and pathogenicity factors. *Clin. Microbiol. Rev.* *11*, 589–603.
- Pothoulakis, C. (2000). Effects of Clostridium difficile Toxins on epithelial cell barrier. *Ann N Y Acad Sci* *915*, 347–356.
- Pushalkar, S., Ji, X., Li, Y., Estilo, C., Yegnanarayana, R., Singh, B., et al. (2012). Comparison of oral microbiota in tumor and non-tumor tissues of patients with oral squamous cell carcinoma. *BMC Microbiol.* *12*, 144.
- Raber-Durlacher, J.E., von Bültzingslöwen, I., Logan, R.M., Bowen, J., Al-Azri, A.R., Everaus, H., et al. (2013). Systematic review of cytokines and growth factors for the management of oral mucositis in cancer patients. *Support. Care Cancer* *21*, 343–355.
- Ramanan, P., Barreto, J.N., Osmon, D.R., and Tosh, P.K. (2014). Rothia bacteremia: a 10-year experience at mayo clinic, Rochester, Minnesota. *J. Clin. Microbiol.* *52*, 3184–3189.
- Rand, K.H., Kramer, B., and Johnson, A.C. (1982). Cancer chemotherapy associated symptomatic stomatitis: role of Herpes simplex virus (HSV). *Cancer* *50*, 1262–1265.
- Rautava, J., Pöllänen, M., Laine, M. a, Willberg, J., Lukkarinen, H., and Soukka, T. (2012). Effects of tacrolimus on an organotypic raft-culture model mimicking oral mucosa. *Clin. Exp. Dermatol.* *37*, 897–903.
- Rawlinson, A., Duerden, B.I., and Goodwin, L. (1993). New findings on the microbial flora associated with adult periodontitis. *J. Dent.* *21*, 179–184.
- Ren, H., Musch, M.W., Kojima, K., Boone, D., Ma, A., and Chang, E.B. (2001). Short-chain fatty acids induce intestinal epithelial heat shock protein 25 expression in rats and IEC 18 cells. *Gastroenterology* *121*, 631–639.

- Reyes, C.P.A., and Dalmacio, L.M.M. (2012). Bacterial Diversity in the Saliva and Plaque of Caries-free and Caries-active Filipino Adults. *Philipp. J. Sci.* *141*, 217–227.
- Rheinwald, J.G., and Green, H. (1975). Serial Cultivation of Strains of Human Epidermal Keratinocytes: the Formation of Keratinizing Colonies from Single Cells. *Cell* *6*, 331–344.
- Ricci, V., Sommi, P., Fiocca, R., Cova, E., Figura, N., Romano, M., et al. (1993). Cytotoxicity of *Helicobacter pylori* on human gastric epithelial cells in vitro: role of cytotoxin(s) and ammonia. *Eur. J. Gastroenterol. Hepatol.* *5*, 687–694.
- Rickard, K.L., Gibson, P.R., Wilson, N.J., Mariadason, J.M., and Phillips, W.A. (2000). Short-Chain Fatty Acids Reduce Expression of Specific Protein Kinase C Isoforms in Human Colon Epithelial Cells. *J. Cell. Physiol.* *182*, 222–231.
- Rodrigues, C.F., Silva, S., and Henriques, M. (2014). *Candida glabrata*: a review of its features and resistance. *Eur. J. Clin. Microbiol. Infect. Dis.* *33*, 673–688.
- Rodriguez, V., and Bodey, G.P. (1973). Bacterial infections in immunosuppressed patients: diagnosis and management. *Transplant. Proc.* *5*, 1249–1254.
- Rong, H., Boterberg, T., Maubach, J., Stove, C., Depypere, H., Van Slambrouck, S., et al. (2001). 8-Prenylnaringenin, the phytoestrogen in hops and beer, upregulates the function of the E-cadherin/catenin complex in human mammary carcinoma cells. *Eur. J. Cell Biol.* *80*, 580–585.
- Rosenthal, D.I., and Trotti, A. (2009). Strategies for managing radiation-induced mucositis in head and neck cancer. *Semin. Radiat. Oncol.* *19*, 29–34.
- Ross, G. (1999). Induction of cell death by radiotherapy. *Endocr. Relat. Cancer* *6*, 41–44.
- Rowe, W. a, Blackmon, D.L., and Montrose, M.H. (1993). Propionate activates multiple ion transport mechanisms in the HT29-18-C1 human colon cell line. *Am. J. Physiol.* *265*, G564–G571.
- Rubenstein, E.B., Peterson, D.E., Schubert, M., Keefe, D., McGuire, D., Epstein, J., et al. (2004). Clinical practice guidelines for the prevention and treatment of cancer therapy-induced oral and gastrointestinal mucositis. *Cancer* *100*, 2026–2046.
- Rubinstein, M.R., Wang, X., Liu, W., Hao, Y., Cai, G., and Han, Y.W. (2013). *Fusobacterium nucleatum* Promotes Colorectal Carcinogenesis by Modulating E-Cadherin/ $\beta$ -Catenin Signaling via its FadA Adhesin. *Cell Host Microbe* *14*, 195–206.
- Rupniak, H.T., Rowlatt, C., Lane, E.B., Steele, J.G., Trejdosiewicz, L.K., Laskiewicz, B., et al. (1985). Characteristics of four new human cell lines derived from squamous cell carcinomas of the head and neck. *J. Natl. Cancer Inst.* *75*, 621–635.
- De Ryck, T., Grootaert, C., Jaspaert, L., Kerckhof, F.-M., Van Gele, M., De Schrijver, J., et al. (2014). Development of an oral mucosa model to study host-microbiome interactions during wound healing. *Appl. Microbiol. Biotechnol.* *98*, 6831–6846.
- De Ryck, T., Vanlancker, E., Grootaert, C., Roman, B.I., De Coen, L.M., Vandenberghe, I., et al. (2015a). Microbial inhibition of oral epithelial wound recovery: potential role for quorum sensing molecules? *AMB Express* *5*, 1–12.
- De Ryck, T., Boterberg, T., Kerckhof, F., De Schrijver, J., Bracke, M., Van de Wiele, T., and Vanhoecke, B. (2015b). Effects of Irradiation on Epithelial Wound Healing and Microbial Diversity in an in-vitro Oral Mucosa Model. *J. Nucl. Med. Radiat. Ther.* *6*, 1–4.

- De Ryck, T., Duprez, F., Bracke, M., Van de Wiele, T., and Vanhoecke, B. (2015c). Dynamic Shifts in the Oral Microbiome during Radiotherapy. *Clin. Res. Infect. Dis.* *2*, 1013.
- De Ryck, T., Van Impe, A., Vanhoecke, B.W., Heyerick, A., Vakaet, L., De Neve, W., et al. (2015d). 8-prenylningerin and tamoxifen inhibit the shedding of irradiated epithelial cells and increase the latency period of radiation-induced oral mucositis. *Strahlentherapie Und Onkol.* *191*, 429–436.
- Sahly, H., and Podschun, R. (1997). Clinical, Bacteriological, and Serological Aspects of Klebsiella Infections and Their Spondylarthropathic Sequelae. *Clin. Diagn. Lab. Immunol.* *4*, 393–399.
- Sakurazawa, T., and Ohkusa, T. (2005). Cytotoxicity of organic acids produced by anaerobic intestinal bacteria on cultured epithelial cells. *J. Gastroenterol.* *40*, 600–609.
- Saleh, a, Figarella, C., Kammouni, W., Marchand-Pinatel, S., Lazdunski, a, Tubul, a, et al. (1999). Pseudomonas aeruginosa quorum-sensing signal molecule N-(3-oxododecanoyl)-L-homoserine lactone inhibits expression of P2Y receptors in cystic fibrosis tracheal gland cells. *Infect. Immun.* *67*, 5076–5082.
- Saunders, D.P., Epstein, J.B., Elad, S., Allemano, J., Bossi, P., van de Wetering, M.D., et al. (2013). Systematic review of antimicrobials, mucosal coating agents, anesthetics, and analgesics for the management of oral mucositis in cancer patients. *Support. Care Cancer* *21*, 3191–3207.
- Scannapieco, F.A. (1999). Role of oral bacteria in respiratory infection. *J Periodontol* *70*, 793–802.
- Scheppach, W. (1994). Effects of short chain fatty acids on gut morphology and function. *Gut* *35*, S35–S38.
- Scheppach, W., Bartram, P., Richter, A., Richter, F., Liepold, H., Dusel, G., et al. (1992). Effect of short-chain fatty acids on the human colonic mucosa in vitro. *J. Parenter. Enter. Nutr.* *16*, 43–48.
- Scheppach, W., Bartram, H.P., and Richter, F. (1995). Role of short-chain fatty acids in the prevention of colorectal cancer. *Eur. J. Cancer* *31A*, 1077–1080.
- Schneditz, G., Rentner, J., Roier, S., Pletz, J., Herzog, K. a. T., Bucker, R., et al. (2014). Enterotoxicity of a nonribosomal peptide causes antibiotic-associated colitis. *Proc. Natl. Acad. Sci.* *111*, 13181–13186.
- Van der Schueren, E., Van den Bogaert, W., Vanuytsel, L., and Van Limbergen, E. (1990). Radiotherapy by multiple fractions per day (MFD) in head and neck cancer: acute reactions of skin and mucosa. *Int J Radiat. Oncol. Biol Phys* *19*, 301–311.
- Schütze, S., Wiegmann, K., Machleidt, T., and Krönke, M. (1995). TNF-induced activation of NF-kappa B. *Immunobiology* *193*, 193–203.
- Schwartz, D.L. (2012). Current progress in adaptive radiation therapy for head and neck cancer. *Curr. Oncol. Rep.* *14*, 139–147.
- Schwartz, D.L., and Dong, L. (2011). Adaptive radiation therapy for head and neck cancer-can an old goal evolve into a new standard? *J. Oncol.* *2011*, 1–14.
- Scully, C., El-Kabir, M., and Samaranyake, L.P. (1994). Candida and Oral candidosis: A review. *Crit. Rev. Oral Biol. Med.* *5*, 125–157.

- Segata, N., Haake, S.K., Mannon, P., Lemon, K.P., Waldron, L., Gevers, D., et al. (2012). Composition of the adult digestive tract bacterial microbiome based on seven mouth surfaces, tonsils, throat and stool samples. *Genome Biol* 13, R42.
- Servin, A.L. (2004). Antagonistic activities of lactobacilli and bifidobacteria against microbial pathogens. *FEMS Microbiol. Rev.* 28, 405–440.
- Servin, A.L., and Coconnier, M.-H. (2003). Adhesion of probiotic strains to the intestinal mucosa and interaction with pathogens. *Best Pract. Res. Clin. Gastroenterol.* 17, 741–754.
- Shao, Z.-Y., Tang, Z.-S., Yan, C., Jiang, Y.-T., Ma, R., Liu, Z., and Huang, Z.-W. (2011). Effects of Intensity-modulated Radiotherapy on Human Oral Microflora. *J. Radiat. Res.* 52, 834–839.
- Shapiro, H., Thaiss, C. a, Levy, M., and Elinav, E. (2014). The cross talk between microbiota and the immune system: metabolites take center stage. *Curr. Opin. Immunol.* 30C, 54–62.
- Sharma, A., Rath, G.K., Chaudhary, S.P., Thakar, A., Mohanti, B.K., and Bahadur, S. (2012). Lactobacillus brevis CD2 lozenges reduce radiation- and chemotherapy-induced mucositis in patients with head and neck cancer: a randomized double-blind placebo-controlled study. *Eur. J. Cancer* 48, 875–881.
- Shepherd, J., Douglas, I., Rimmer, S., Swanson, L., and MacNeil, S. (2009). Development of Three-Dimensional Tissue-Engineered Models of Bacterial Infected Human Skin Wounds. *Tissue Eng Part C Methods* 15, 475–484.
- Simard, E.P., Torre, L. a, and Jemal, A. (2014). International trends in head and neck cancer incidence rates: differences by country, sex and anatomic site. *Oral Oncol.* 50, 387–403.
- Simiantonaki, N., Taxeidis, M., Jayasinghe, C., Kurzik-Dumke, U., and Kirkpatrick, C.J. (2008). Hypoxia-inducible factor 1 alpha expression increases during colorectal carcinogenesis and tumor progression. *BMC Cancer* 8, 320.
- Singh, A., Verma, R., Murari, A., and Agrawal, A. (2014). Oral candidiasis: An overview. *J. Oral Maxillofac. Pathol.* 18, S81–S85.
- Smith, A.J., Robertson, D., Tang, M.K., Jackson, M.S., MacKenzie, D., and Bagg, J. (2003). Staphylococcus aureus in the oral cavity: a three-year retrospective analysis of clinical laboratory data. *Br. Dent. J.* 195, 701–703.
- Smith, R.S., Fedyk, E.R., Springer, T. a., Mukaida, N., Iglewski, B.H., and Phipps, R.P. (2001). IL-8 Production in Human Lung Fibroblasts and Epithelial Cells Activated by the Pseudomonas Autoinducer N-3-Oxododecanoyl Homoserine Lactone Is Transcriptionally Regulated by NF- $\kappa$ B and Activator Protein-2. *J. Immunol.* 167, 366–374.
- Smoot, D.T., Mobley, H.L., Chippendale, G.R., Lewison, J.F., and Resau, J.H. (1990). Helicobacter Pylori Urease Activity Is Toxic to Human Gastric Epithelial Cells. *Infect. Immun.* 58, 1992–1994.
- Soares, A.F., de Aquino, A.R.L., de Carvalho, Cyntia Helena Pereira Nonaka, C.F.W., Almeida, D., and Pereira Pinto, L. (2011). Frequency of Oral Mucositis and Microbiological Analysis in Children with Acute Lymphoblastic Leukemia Treated with. *Braz Dent J* 22, 312–316.
- Sonalika, W.G., Amsavardani Tayaar, S., Bhat, K.G., Patil, B.R., and Muddapur, M. V (2012a). Oral microbial carriage in oral squamous cell carcinoma patients at



- the time of diagnosis and during radiotherapy - a comparative study. *Oral Oncol.* *48*, 881–886.
- Sonalika, W.G., Amsavardani Tayaar, S., Bhat, K.G., Patil, B.R., and Muddapur, M. V (2012b). Oral microbial carriage in oral squamous cell carcinoma patients at the time of diagnosis and during radiotherapy - a comparative study. *Oral Oncol.* *48*, 881–886.
- Sonis, S.T. (2004). The pathobiology of mucositis. *Nat. Rev. Cancer* *4*, 277–284.
- Sonis, S.T. (2007). Pathobiology of Oral Mucositis : novel insights and opportunities. *J Support Oncol* *5*, 3–11.
- Sonis, S.T. (2009). Mucositis: The impact, biology and therapeutic opportunities of oral mucositis. *Oral Oncol.* *45*, 1015–1020.
- Sonis, S.T. (2010). New thoughts on the initiation of mucositis. *Oral Dis.* *16*, 597–600.
- Sonis, S.T., O'Donnell, K.E., Popat, R., Bragdon, C., Phelan, S., Cocks, D., and Epstein, J.B. (2004). The relationship between mucosal cyclooxygenase-2 (COX-2) expression and experimental radiation-induced mucositis. *Oral Oncol.* *40*, 170–176.
- De Spiegeleer, B., Verbeke, F., D'Hondt, M., Hendrix, A., Van de Wiele, C., Burvenich, C., et al. (2015). Quorum sensing peptides promote angiogenesis and invasion of breast cancer cells. Submitted.
- Starling, J.R., and Balish, E. (1981). Lysosomal enzyme activity in pulmonary alveolar macrophages from conventional, germfree, monoassociated, and conventionalized rats. *J. Reticuloendothel. Soc.* *30*, 497–505.
- Steinhusen, U., Weiske, J., Badock, V., Tauber, R., Bommert, K., and Huber, O. (2001). Cleavage and shedding of E-cadherin after induction of apoptosis. *J. Biol. Chem.* *276*, 4972–4980.
- Stephens, P., Wall, I.B., Wilson, M.J., Hill, K.E., Davies, C.E., Hill, C.M., et al. (2003). Anaerobic cocci populating the deep tissues of chronic wounds impair cellular wound healing responses in vitro. *Br. J. Dermatol.* *148*, 456–466.
- Stewart, P.S., and Costerton, J.W. (2001). Antibiotic resistance of bacteria in biofilms. *Lancet* *358*, 135–138.
- Stringer, A.M., Gibson, R.J., Bowen, J.M., Logan, R.M., Ashton, K., Yeoh, A.S.J., et al. (2009a). Irinotecan-induced mucositis manifesting as diarrhoea corresponds with an amended intestinal flora and mucin profile. *Int. J. Exp. Pathol.* *90*, 489–499.
- Stringer, A.M., Gibson, R.J., Logan, R.M., Bowen, J.M., Yeoh, A.S.J., Hamilton, J., and Keefe, D.M.K. (2009b). Gastrointestinal microflora and mucins may play a critical role in the development of 5-Fluorouracil-induced gastrointestinal mucositis. *Exp. Biol. Med. (Maywood)*. *234*, 430–441.
- Stringer, A.M., Gibson, R.J., Logan, R.M., Bowen, J.M., Yeoh, A.S.J., Laurence, J., and Keefe, D.M.K. (2009c). Irinotecan-induced mucositis is associated with changes in intestinal mucins. *Cancer Chemother. Pharmacol.* *64*, 123–132.
- Strous, G.J., and Dekker, J. (1992). Mucin-type glycoproteins. *Crit. Rev. Biochem. Mol. Biol.* *27*, 57–92.
- Strus, M., Janczyk, A., Gonet-Surowka, A., Brzychczy-Wloch, M., Stochel, G., Kochan, P., and Heczko, P.B. (2009). Effect of hydrogen peroxide of bacterial origin on apoptosis and necrosis of gut mucosa epithelial cells as possible

- pathomechanism of inflammatory bowel disease and cancer. *J. Physiol. Pharmacol.* *60*, 55–60.
- Su, N., Marek, C.L., Ching, V., and Grushka, M. (2011). Caries Prevention for Patients with Dry Mouth. *J Can Dent Assoc.*
- Sulakvelidze, A., Alavidze, Z., and Morris, J.G. (2001). Bacteriophage Therapy. *Antimicrob. Agents Chemother.* *45*, 649–659.
- Takeichi, M. (1990). Cadherins: a molecular family important in selective cell-cell adhesion. *Annu. Rev. Biochem.* *59*, 237–252.
- Takeshita, T., Yasui, M., Tomioka, M., Nakano, Y., Shimazaki, Y., and Yamashita, Y. (2011). Enteral tube feeding alters the oral indigenous microbiota in elderly adults. *Appl. Environ. Microbiol.* *77*, 6739–6745.
- Tao, Y., Zhou, Y., Ouyang, Y., and Lin, H. (2013). Dynamics of oral microbial community profiling during severe early childhood caries development monitored by PCR-DGGE. *Arch. Oral Biol.* *58*, 1129–1138.
- Taylor-Papadimitriou, J., Purkis, P., and Fentiman, I.S. (1980). Cholera toxin and analogues of cyclic AMP stimulate the growth of cultured human mammary epithelial cells. *J. Cell. Physiol.* *102*, 317–321.
- Thomson, P.J., Potten, C.S., and Appleton, D.R. (1999). Mapping dynamic epithelial cell proliferative activity within the oral cavity of man: a new insight into carcinogenesis? *Br. J. Oral Maxillofac. Surg.* *37*, 377–383.
- Thornton, D.J., and Sheehan, J.K. (2004). From mucins to mucus: toward a more coherent understanding of this essential barrier. *Proc. Am. Thorac. Soc.* *1*, 54–61.
- Thornton, D.J., Khan, N., Mehrotra, R., Howard, M., Veerman, E., Packer, N.H., and Sheehan, J.K. (1999). Salivary mucin MG1 is comprised almost entirely of different glycosylated forms of the MUC5B gene product. *Glycobiology* *9*, 293–302.
- Thorpe, D.W., Stringer, A.M., and Gibson, R.J. (2013). Chemotherapy-induced mucositis: the role of the gastrointestinal microbiome and toll-like receptors. *Exp. Biol. Med. (Maywood)*. *238*, 1–6.
- Titball, R.W. (1993). Bacterial phospholipases C. *Microbiol. Rev.* *57*, 347–366.
- Tong, H.C., Gao, X.J., and Dong, X.Z. (2003). Non-Mutans Streptococci in Patients Receiving Radiotherapy in the Head and Neck Area. *Caries Res.* *37*, 261–266.
- Treister, N., and Sonis, S. (2007). Mucositis: biology and management. *Curr. Opin. Otolaryngol. Head Neck Surg.* *15*, 123–129.
- Tribius, S., Sommer, J., Prosch, C., Bajrovic, A., Muenscher, A., Blessmann, M., et al. (2013). Xerostomia after radiotherapy. What matters—mean total dose or dose to each parotid gland? *Strahlenther. Onkol.* *189*, 216–222.
- Trotti, A., Bellm, L. a, Epstein, J.B., Frame, D., Fuchs, H.J., Gwede, C.K., et al. (2003). Mucositis incidence, severity and associated outcomes in patients with head and neck cancer receiving radiotherapy with or without chemotherapy: a systematic literature review. *Radiother. Oncol.* *66*, 253–262.
- Trudeau, K., Vu, K.D., Shareck, F., and Lacroix, M. (2012). Capillary electrophoresis separation of protein composition of  $\gamma$ -irradiated food pathogens *Listeria monocytogenes* and *Staphylococcus aureus*. *PLoS One* *7*, e32488.
- Tucker, K.D., Carrig, P.E., and Wilkins, T.D. (1990). Toxin A of *Clostridium difficile* is a potent cytotoxin. *J. Clin. Microbiol.* *28*, 869–871.

- Uchida, H., Kiyokawa, N., Taguchi, T., Horie, H., Fujimoto, J., and Takeda, T. (1999). Shiga toxins induce apoptosis in pulmonary epithelium-derived cells. *J. Infect. Dis.* *180*, 1902–1911.
- Vanhoecke, B., De Ryck, T., De boel, K., Boterberg, T., Wiles, S., Van de Wiele, T., and Swift, S. (2015a). Effects of low dose irradiation on function behavior of oral microbiota in the context of mucositis. *Accept. Publ. Exp. Biol. Med.*
- Vanhoecke, B., De Ryck, T., Stringer, A., Van de Wiele, T., and Keefe, D. (2015b). Microbiota and their role in the pathogenesis of oral mucositis. *Oral Dis.* *21*, 17–30.
- Vasishtha, S., Isenberg, H.D., and Sood, S.K. (1996). *Gemella morbillorum* as a Cause of Septic Shock. *Clin. Infect. Dis.* *22*, 1084–1086.
- Vergeer, M.R., Doornaert, P. a H., Rietveld, D.H.F., Leemans, C.R., Slotman, B.J., and Langendijk, J. a. (2009). Intensity-Modulated Radiotherapy Reduces Radiation-Induced Morbidity and Improves Health-Related Quality of Life: Results of a Nonrandomized Prospective Study Using a Standardized Follow-Up Program. *Int. J. Radiat. Oncol. Biol. Phys.* *74*, 1–8.
- Vichai, V., and Kirtikara, K. (2006). Sulforhodamine B colorimetric assay for cytotoxicity screening. *Nat. Protoc.* *1*, 1112–1116.
- Vikström, E., Tafazoli, F., and Magnusson, K.-E. (2006). *Pseudomonas aeruginosa* quorum sensing molecule N-(3 oxododecanoyl)-l-homoserine lactone disrupts epithelial barrier integrity of Caco-2 cells. *FEBS Lett.* *580*, 6921–6928.
- Villar, C.C., Kashleva, H., Nobile, C.J., Mitchell, a P., and Dongari-Bagtzoglou, a (2007). Mucosal tissue invasion by *Candida albicans* is associated with E-cadherin degradation, mediated by transcription factor Rim101p and protease Sap5p. *Infect. Immun.* *75*, 2126–2135.
- Van Vliet, M.J., Tissing, W.J.E., Dun, C. a J., Meessen, N.E.L., Kamps, W. a, de Bont, E.S.J.M., and Harmsen, H.J.M. (2009). Chemotherapy treatment in pediatric patients with acute myeloid leukemia receiving antimicrobial prophylaxis leads to a relative increase of colonization with potentially pathogenic bacteria in the gut. *Clin. Infect. Dis.* *49*, 262–270.
- Van Vliet, M.J., Harmsen, H.J.M., de Bont, E.S.J.M., and Tissing, W.J.E. (2010). The role of intestinal microbiota in the development and severity of chemotherapy-induced mucositis. *PLoS Pathog.* *6*, e1000879.
- Voltan, S., Martines, D., Elli, M., Brun, P., Longo, S., Porzionato, A., et al. (2008). *Lactobacillus crispatus* M247-derived H2O2 acts as a signal transducing molecule activating peroxisome proliferator activated receptor-gamma in the intestinal mucosa. *Gastroenterology* *135*, 1216–1227.
- Waldecker, M., Kautenburger, T., Daumann, H., Busch, C., and Schrenk, D. (2008). Inhibition of histone-deacetylase activity by short-chain fatty acids and some polyphenol metabolites formed in the colon. *J. Nutr. Biochem.* *19*, 587–593.
- Wang, H., Cai, T., Weng, M., Zhou, J., Cao, H., Zhong, Z., and Zhu, J. (2006). Conditional production of acyl-homoserine lactone-type quorum-sensing signals in clinical isolates of enterobacteria. *J. Med. Microbiol.* *55*, 1751–1753.
- Wei, G.-X., Campagna, A.N., and Bobek, L. a (2006). Effect of MUC7 peptides on the growth of bacteria and on *Streptococcus mutans* biofilm. *J. Antimicrob. Chemother.* *57*, 1100–1109.
- Weinberg, R.A. (2007). *The biology of cancer* (Garland Science, Abingdon, UK).

- Weisburg, W.G., Barns, S.M., Pelletier, D. a, and Lane, D.J. (1991). 16S ribosomal DNA amplification for phylogenetic study. *J. Bacteriol.* *173*, 697–703.
- Wells, M.T., Gaffin, S.L., and Jordaan, J.P. (1987). Radiation induced gram negative bacteremia and endotoxemia in rabbits: modification by anti-lipopolysaccharide hyperimmune equine plasma. *Life Sci.* *40*, 2543–2550.
- Werner, S., Krieg, T., and Smola, H. (2007). Keratinocyte-fibroblast interactions in wound healing. *J. Invest. Dermatol.* *127*, 998–1008.
- Whitlock, J.P., Augustine, R., and Schulman, H. (1980). Calcium-dependent phosphorylation of histone H3 in butyrate-treated HeLa cells. *Nature* *287*, 74–76.
- Wickström, C., and Svensäter, G. (2008). Salivary gel-forming mucin MUC5B – a nutrient for dental plaque bacteria. *Oral Microbiol. Immunol.* *23*, 177–182.
- Wiegand, C., Abel, M., Ruth, P., and Hipler, U.-C. (2009). HaCaT keratinocytes in co-culture with *Staphylococcus aureus* can be protected from bacterial damage by polihexanide. *Wound Repair Regen.* *17*, 730–738.
- Wilson, A.J., and Gibson, P.R. (1997). Short-chain fatty acids promote the migration of colonic epithelial cells in vitro. *Gastroenterology* *113*, 487–496.
- Windey, K., De Preter, V., and Verbeke, K. (2012). Relevance of protein fermentation to gut health. *Mol. Nutr. Food Res.* *56*, 184–196.
- Wittebolle, L., Marzorati, M., Clement, L., Balloi, A., Daffonchio, D., Heylen, K., et al. (2009). Initial community evenness favours functionality under selective stress. *Nature* *458*, 623–626.
- Worthington, H., Clarkson, J., Bryan, G., Furness, S., Glenny, A., Littlewood, A., et al. (2011). Interventions for preventing oral mucositis for patients with cancer receiving treatment (Review). In *The Cochrane Library*, p. 293.
- Wu, S., Lim, K.-C., Huang, J., Saidi, R.F., and Sears, C.L. (1998). *Bacteroides fragilis* enterotoxin cleaves the zonula adherens protein , E-cadherin. *Proc. Natl. Acad. Sci. USA* *95*, 14979–14984.
- Wygoda, a, Skłodowski, K., Rutkowski, T., Hutnik, M., Goleń, M., Pilecki, B., et al. (2012). Acute mucosal radiation reactions in patients with head and neck cancer. Patterns of mucosal healing on the basis of daily examinations. *Strahlenther. Onkol.* *188*, 686–691.
- Wygoda, a, Rutkowski, T., Hutnik, M., Skłodowski, K., Goleń, M., and Pilecki, B. (2013). Acute mucosal reactions in patients with head and neck cancer. Three patterns of mucositis observed during radiotherapy. *Strahlenther. Onkol.* *189*, 547–551.
- Wynendaele, E., Pauwels, E., Van de Wiele, C., Burvenich, C., and De Spiegeleer, B. (2012). The potential role of quorum-sensing peptides in oncology. *Med. Hypotheses* *78*, 814–817.
- Yamagishi, Y., Mikamo, H., Tanaka, K., and Watanabe, K. (2011). A case of uterine endometritis caused by *Atopobium vaginae*. *J. Infect. Chemother.* *17*, 119–121.
- Yan, D. (2010). Adaptive radiotherapy: merging principle into clinical practice. *Semin. Radiat. Oncol.* *20*, 79–83.
- Yang, D., Chen, Q., Hoover, D.M., Staley, P., Tucker, K.D., Lubkowski, J., and Oppenheim, J.J. (2003). Many chemokines including CCL20/ MIP-3 $\alpha$  display antimicrobial activity. *J Leukoc Biol* *74*, 448–455.

- Yin, L., Laevsky, G., and Giardina, C. (2001). Butyrate suppression of colonocyte NF-kappa B activation and cellular proteasome activity. *J. Biol. Chem.* 276, 44641–44646.
- Yin, W.-F., Purmal, K., Chin, S., Chan, X.-Y., Koh, C.-L., Sam, C.-K., and Chan, K.-G. (2012). N-acyl homoserine lactone production by *Klebsiella pneumoniae* isolated from human tongue surface. *Sensors (Basel)*. 12, 3472–3483.
- Zack, M.B., Stottmeier, K., Berg, G., and Kazemi, H. (1974). The effect of Radiation on Microbiologic Characteristics of M Tuberculosis. *Chest* 66, 240–243.
- Zambon, J.J., Reynolds, H.S., and Genco, R.J. (1990). Studies of the subgingival microflora in patient with acquired Immunodeficiency syndrome. *J Periodontol* 61, 699–704.
- Zaura, E., Keijsers, B.J.F., Huse, S.M., and Crielaard, W. (2009). Defining the healthy “core microbiome” of oral microbial communities. *BMC Microbiol.* 9, 259.
- Zoumpopoulou, G., Tsakalidou, E., Dewulf, J., Pot, B., and Grangette, C. (2009). Differential crosstalk between epithelial cells, dendritic cells and bacteria in a co-culture model. *Int J Food Microbiol* 131, 40–51.
- Zumbrun, S.D., Melton-Celsa, A.R., Smith, M.A., Gilbreath, J.J., Merrell, D.S., and O’Brien, A.D. (2013). Dietary choice affects Shiga toxin-producing *Escherichia coli* (STEC) O157 : H7 colonization and disease. *PNAS* 110, E2126–E2133.

## ADDENDUM 1

---

*Supplementary information of Chapter 2: De Ryck T, Grootaert C, Jaspert L, Kerckhof FM, Van Gele M, De Schrijver J, Van den Abbeele P, Swift S, Bracke M, Van de Wiele T, Vanhoecke B (2014). Development of an oral mucosa model to study host-microbiome interactions during wound healing. Applied microbiology and biotechnology 98 (15), 6831-6846.*

### **A1.1. Material and methods**

#### **A1.1.1. Pyrosequencing**

Amplicon pyrosequencing was performed on the total DNA extracted from 9 specific individual samples. Barcoded amplicons were prepared with the primers pA (Edwards et al., 1989) and BKL1 (5' gtattaccgcgctgctggca 3'), priming on respectively nucleotides 8-27 and 536-516 thus effectively amplifying a 489 bp DNA fragment encompassing the V1, V2 and part of the V3 regions of the 16S rRNA gene, extended with amplicon fusion primers with respective Lib-A adaptor, key sequence and multiplex identifiers (MID) on the forward primer. Amplicons were generated by using FastStart High Fidelity Taq DNA Polymerase kit (Roche, Belgium) under the following conditions: Each PCR reaction (25  $\mu$ L) contained 1 $\times$ PCR buffer, 0.72  $\mu$ L MgCl<sub>2</sub>, 0.05  $\mu$ L dNTPs, 1 % dimethyl sulphoxide (DMSO), 0.625 mU Taq polymerase, 0.32 mg ml<sup>-1</sup> Bovine Serum Albumin (BSA), 0.3 mM of each MID-primer and 0,5  $\mu$ l of template DNA. PCR was performed using the following cycle conditions: an initial denaturation step at 98 °C for 30 s, followed by 30 cycles of denaturation at 98 °C for 5 s, annealing at 53 °C for 20 s, elongation at 72 °C for 20 s, and then a final elongation step at 72 °C for 5 min. Amplicons were purified with the High Pure PCR Product Purification Kit (Roche, Belgium) and pooled equimolarly as determined by picogreen DNA concentration measurement. The purity and quality of the PCR products was verified on an agarose gel. Emulsion PCR, emulsion breaking and sequencing were performed applying the GS FLX Titanium chemistry protocols and using a 454 GS FLX pyrosequencer (Roche, Belgium) as recommended by the manufacturer. For this study, 9 amplicons were sequenced in a pool of 30 mixed amplicons on 1/2nd of an FLX picotitre plate. The other samples contained bacterial sequences and primers from a comparable set-up. Quality filtering of the pyrosequencing reads was performed using the automatic amplicon pipeline of the GS Run Processor (Roche,

Belgium), with a modification of the valley filter (vfScanAll- Flows false instead of TiOnly) to extract sequences.

#### **A1.1.2. Pyrosequencing data analysis**

The raw flowgrams were processed and analyzed in an in-house Mothur (<http://www.mothur.org>, version 1.28.0) and R (<http://www.r-project.org/version> 2.15.1)/Sweave pipeline. Sequencing error was reduced using the Mothur implementation of the SeqNoise algorithm, alignment with the SILVA 16S reference alignment was performed and sequences were trimmed to overlap in the same alignment space. Chimeric sequences were removed using Uchime. A Bayesian classifier was used with the RDP training set of RDP release 9 (<http://rdp.cme.msu.edu/>) to classify the sequences after clustering at 97% sequence identity in OTUs.

## A1.2. Figures and tables

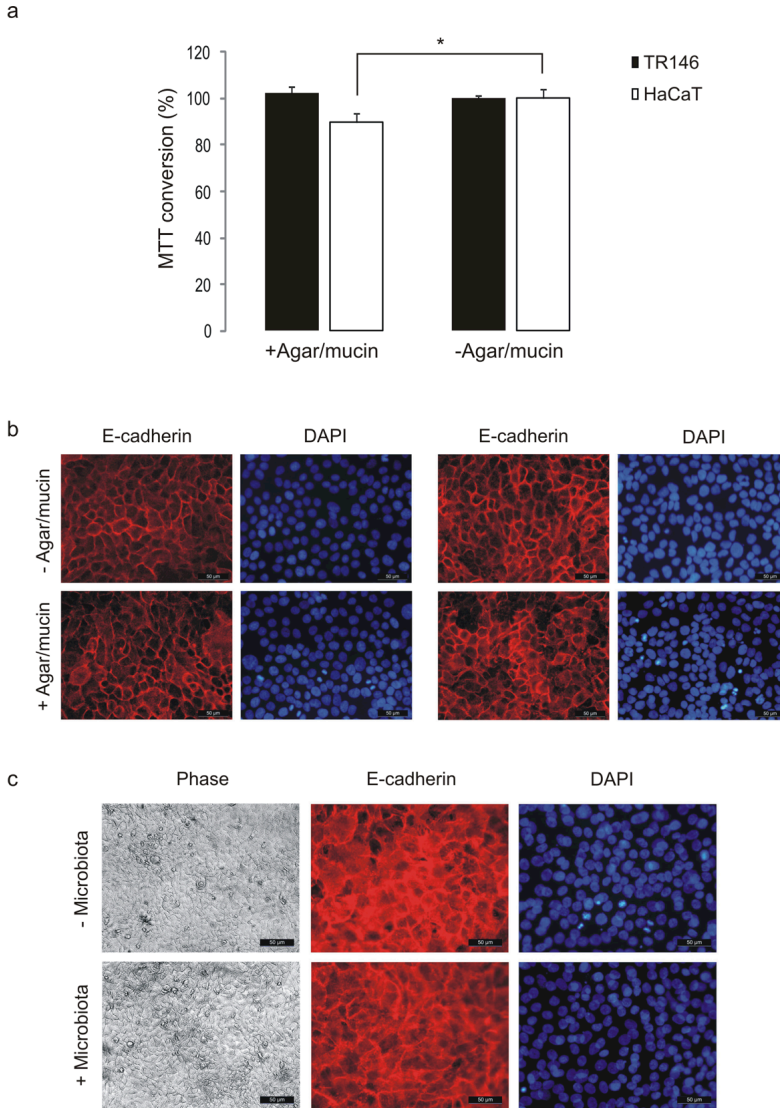


**Figure A1-1 a:** Effect of the agar/mucin insert on the MTT conversion of TR146 and HaCaT cells ( $n = 6$ ; mean + SD; \*  $p < 0.05$ ). **b:** E-cadherin and DAPI staining of TR146 cells after 24 h in presence or absence of an agar/mucin insert without microbiota. **c:** phase-contrast microscopy, immunostaining of E-cadherin and DAPI staining of the monolayer of TR146 cells after 24 h in presence or absence of an oral biofilm cultured on an agar/mucin insert



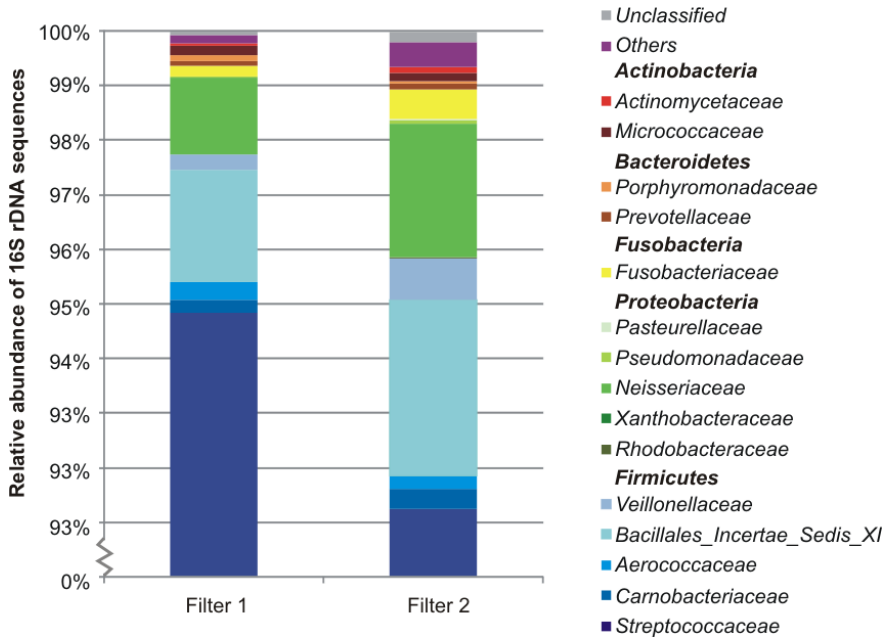


**Figure A1-1: Variation in relative abundance of microbiota from duplicate filters at 0 h. 454 pyrosequencing results of 16S rDNA assigned to family, grouped in the different phyla are shown**

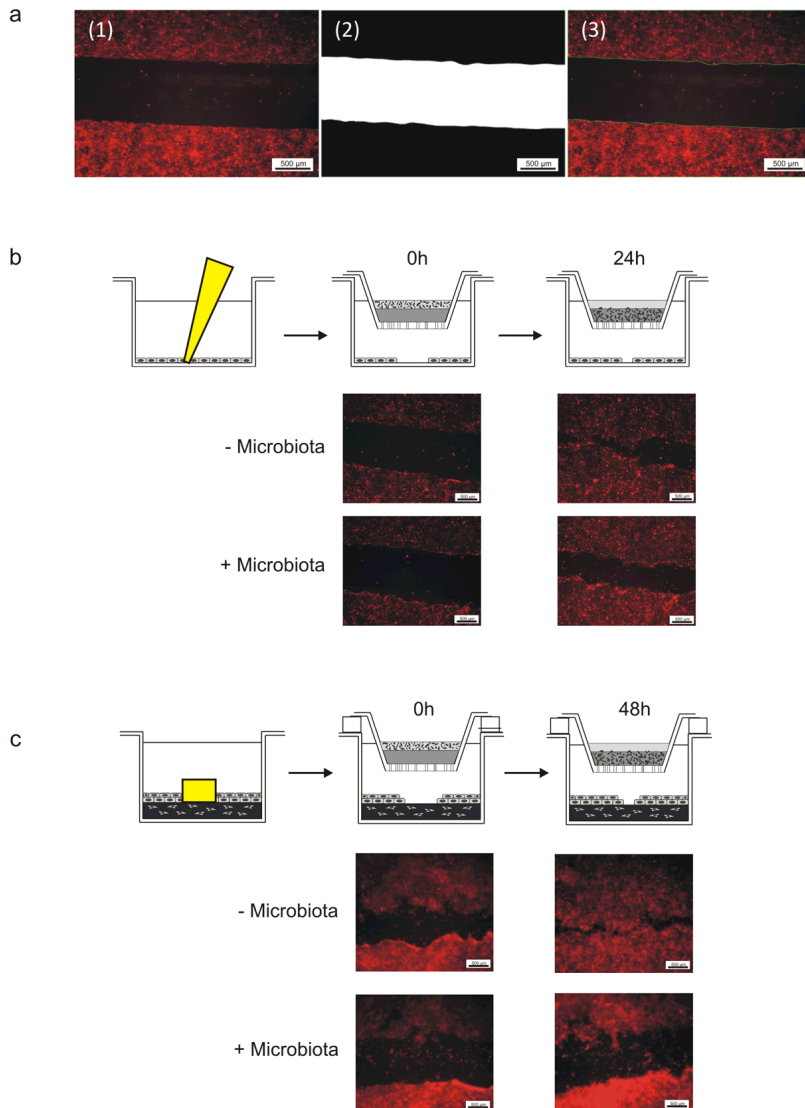


**Figure A1-2: a: (1) fluorescence image of wounded TR146 monolayers. (2) ImageJ black-white pictures were generated to calculate the wound area. (3) ImageJ-generated overlay pictures used for quality check. Green lines represent the edges of the wound region, which are used in the calculation process. b: A schematic overview of the wound scratch assay in the simplified model is shown together with some representative examples of the micrographs at 0 and 24 h. c: A schematic overview of the wound scratch assay in the complex model is depicted. Representative micrographs of the wound healing on collagen are also included**

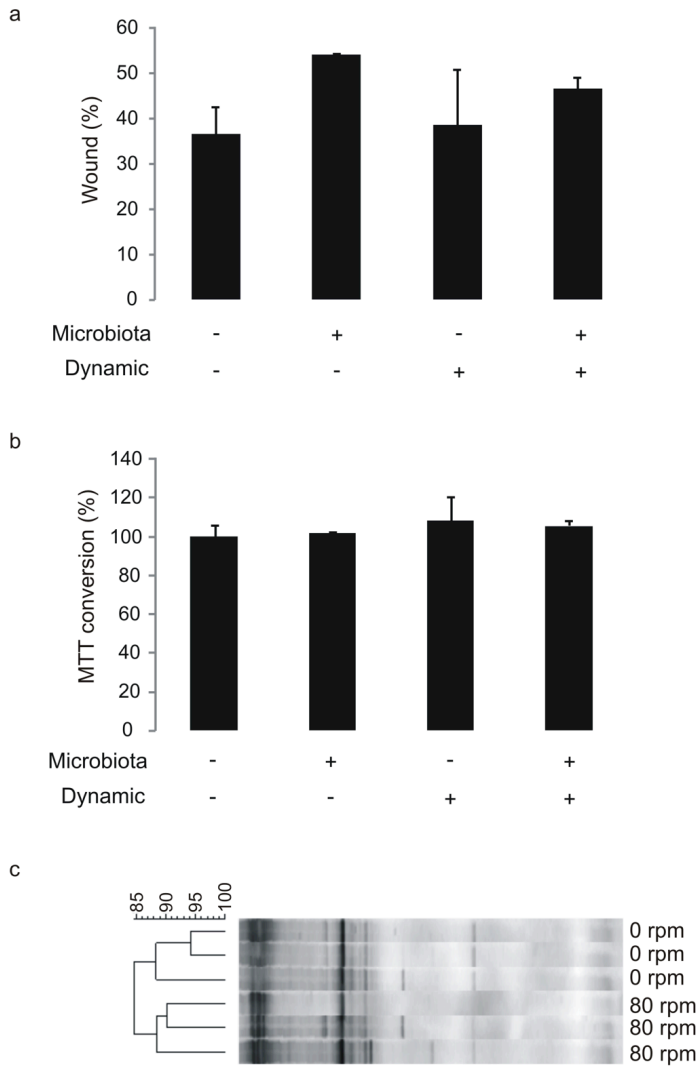


**Figure A1-3 a: Wound healing and b: MTT assay of TR146 cells in presence or absence of microbiota in dynamic (80 rpm) or static (0 rpm) conditions (n= 3; mean + SD; \* p< 0.05). c: DGGE profiling and cluster analysis of the apical part of the model in a dynamic or static set-up**

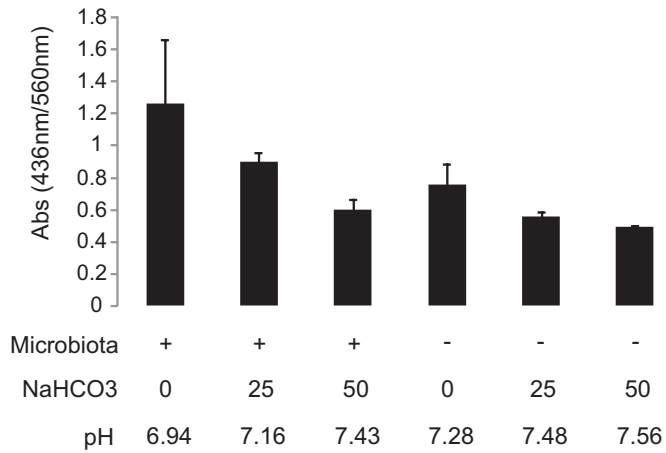


**Figure A1-4: Absorbance ratios (OD 436 nm/OD 560 nm) of the co-culture medium in presence or absence of oral microbiota, buffered with NaHCO<sub>3</sub>, together with their respective pH values (n= 4; mean + SD)**

**Table A1-1: Number of reads generated by 454 pyrosequencing for each sample.**

Sample	n° of reads
0h	4789
Agar 24h	9273
Agar/Mucin 24h	16763
Simple 24h	12472
Complex 24h	22481
Agar 48h	11585
Agar/Mucin 48h	6466
Simple 48h	12421
Complex 48h	14787

**Table A1-2: Analysis of the microbiota cultured for 0, 24 or 48 h on an insert with agar or with agar/mucin without cells, in presence of a monolayer of FFR146 cells (simple) or with cells cultured on a collagen type I matrix (complex), 454 pyrosequencing results of 16S rDNA assigned to genus are shown (N.D. = not detected)**

	Agar/mucin 0h	Agar 24h	Agar/Mucin 24h	Simple 24h	Complex 24h	Agar 48h	Agar/Mucin 48h	Simple 48h	Complex 48h
Abiotrophia	0.334	N.D.	0.012	0.104	0.004	0.043	N.D.	N.D.	N.D.
Actinobacillus	N.D.	N.D.	N.D.	N.D.	0.009	N.D.	N.D.	N.D.	0.041
Actinomyces	0.063	N.D.	N.D.	N.D.	N.D.	0.009	N.D.	N.D.	N.D.
Acrobacter	N.D.	N.D.	N.D.	0.024	0.004	0.026	N.D.	N.D.	N.D.
Burkholderia	0.021	N.D.	N.D.	0.008	N.D.	N.D.	N.D.	N.D.	N.D.
Chryseobacterium	0.042	N.D.	N.D.	N.D.	N.D.	N.D.	N.D.	N.D.	N.D.
Corynebacterium	0.042	N.D.	N.D.	N.D.	N.D.	N.D.	N.D.	N.D.	N.D.
Fusobacterium	0.209	N.D.	N.D.	N.D.	N.D.	N.D.	N.D.	N.D.	N.D.
Gemella	2.067	N.D.	0.022	0.008	0.004	N.D.	N.D.	N.D.	N.D.
Granulicatella	0.230	0.162	0.233	0.345	0.489	0.820	0.433	0.145	5.167
Hydrogenophaga	0.021	N.D.	N.D.	N.D.	N.D.	N.D.	N.D.	0.024	0.041
Hyphomicrobium	N.D.	0.011	N.D.	N.D.	N.D.	N.D.	N.D.	N.D.	N.D.
Humatobacter	N.D.	N.D.	0.006	N.D.	N.D.	N.D.	N.D.	N.D.	N.D.
Kingella	0.021	N.D.	N.D.	N.D.	N.D.	N.D.	N.D.	N.D.	N.D.
Marikta	N.D.	N.D.	0.006	N.D.	N.D.	N.D.	N.D.	N.D.	N.D.
Myroides	N.D.	N.D.	N.D.	N.D.	N.D.	N.D.	N.D.	0.016	N.D.
Neisseria	1.378	N.D.	N.D.	N.D.	0.004	N.D.	N.D.	N.D.	N.D.
Paratococcus	N.D.	N.D.	0.006	N.D.	N.D.	N.D.	N.D.	N.D.	0.007
Porphyromonas	0.104	N.D.	N.D.	N.D.	N.D.	N.D.	N.D.	N.D.	N.D.
Prevotella	0.084	N.D.	N.D.	N.D.	N.D.	N.D.	N.D.	N.D.	N.D.
Pseudomonas	N.D.	0.140	0.036	0.008	N.D.	N.D.	N.D.	N.D.	N.D.
Rhodanobacter	N.D.	0.011	N.D.	N.D.	N.D.	N.D.	N.D.	N.D.	N.D.
Rhodobacter	N.D.	N.D.	N.D.	N.D.	N.D.	N.D.	N.D.	N.D.	N.D.
Rhodococcus	N.D.	N.D.	N.D.	N.D.	N.D.	N.D.	N.D.	0.008	N.D.
Rothia	0.167	0.011	0.012	0.016	0.009	N.D.	N.D.	0.024	N.D.
Schlegella	0.021	N.D.	N.D.	N.D.	N.D.	N.D.	N.D.	N.D.	N.D.
Selenomonas	0.021	N.D.	N.D.	N.D.	N.D.	N.D.	N.D.	N.D.	N.D.
Serpens	0.021	N.D.	N.D.	0.008	N.D.	N.D.	N.D.	N.D.	N.D.
Sphingomonas	N.D.	0.011	N.D.	N.D.	N.D.	N.D.	N.D.	N.D.	N.D.
Staphylococcus	N.D.	N.D.	N.D.	N.D.	0.004	N.D.	0.031	N.D.	N.D.
Stenotrophomonas	N.D.	N.D.	N.D.	0.008	N.D.	0.009	N.D.	N.D.	N.D.
Streptococcus	94.842	99.623	99.623	99.439	99.386	98.282	99.536	99.718	94.671
Thermomonas	N.D.	N.D.	N.D.	N.D.	N.D.	N.D.	N.D.	0.008	N.D.
Velloneella	0.251	N.D.	N.D.	0.024	0.018	N.D.	N.D.	0.047	N.D.
Wolinella	N.D.	N.D.	N.D.	N.D.	N.D.	N.D.	N.D.	0.008	N.D.
Xanthobacter	N.D.	N.D.	N.D.	N.D.	N.D.	0.691	N.D.	0.024	N.D.
Unclassified	0.063	0.011	0.006	0.008	0.067	0.121	N.D.	0.016	0.027

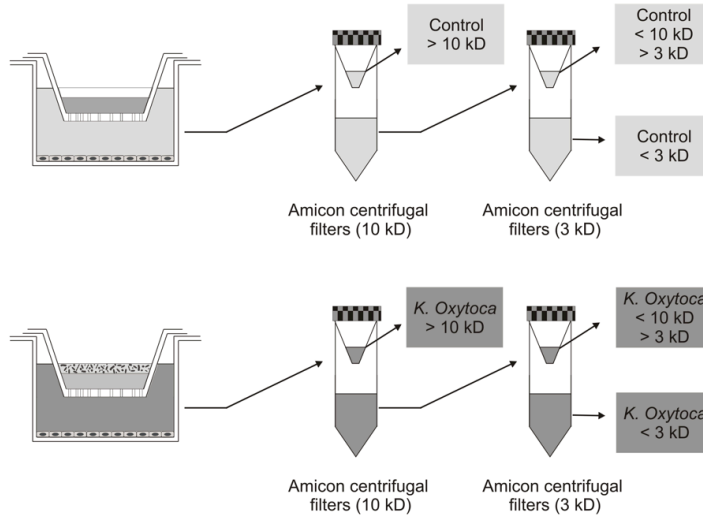
## ADDENDUM 2

---

*Supplementary information of Chapter 3: De Ryck T, Vanlancker E, Grootaert C, Roman B, De Coen LM, Vandenberghe I, Stevens CV, Bracke M, Van de Wiele T, Vanhoecke B (2015). Microbial inhibition of oral epithelial wound recovery: potential role for quorum sensing molecules? AMB Express 5:27.*

## A2.1. Figures and tables

a



b

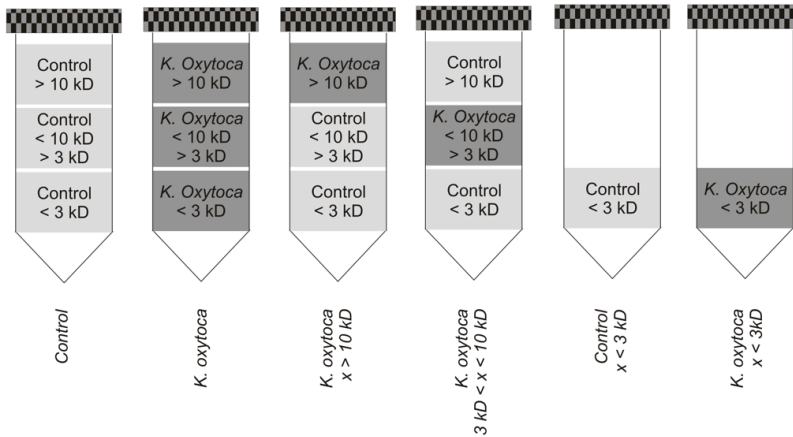


**Figure A2-1 a:** Schematic overview of the fractionation of the control- and *K. oxytoca*-conditioned medium by use of Amicon centrifugal filters (3kD, 10kD; Merck Millipore, Overijse, Belgium). **b:** Replacement strategy of particular fractions in the control conditioned medium (light grey) with the same fractions of the conditioned medium of *K. oxytoca*-exposed cells (dark grey), in order to analyse the effect of different medium fractions on wound recovery

**Table A2-1 a: p-Values of the ANOVA-analysis with Bonferroni correction of the wound healing assays, comparing data generated for the control cells (TR146 cells exposed to an insert without microbiota) with data obtained for the TR146 cells that were co-cultured with different oral microbial species. b: Microbial counts of the different oral species present on the insert at time 0 and after 24 h of co-culture with TR146 epithelial cells (mean  $\pm$  SD; N.D. = not detected). Data shown from experiments performed with and without a 4 h pre-incubation step of the microbial inserts prior to confrontation with TR146 cells**

a	<b>P-values</b>		
	<b>wound healing after 24 h</b>	<b>Pre-incubation</b>	
		<b>0 h</b>	<b>4 h</b>
	<i>S. salivarius</i>	0.587	< 0.001
	<i>S. oralis</i>	0.022	0.029
	<i>S. mitis</i>	0.054	0.081
	<i>S. pyogenes</i>	1.000	0.200
	<i>L. salivarius</i>	0.070	< 0.001
	<i>L. oralis</i>	0.933	0.206
	<i>L. plantarum</i>	0.003	0.206
	<i>N. mucosa</i>	0.517	0.580
	<i>K. oxytoca</i>	0.007	0.001

b	<b>Bacterial counts</b>		
	<b>after 24 h (log CFU/filter)</b>	<b>Pre-incubation</b>	
		<b>0 h</b>	<b>4 h</b>
	<i>S. salivarius</i>	1.63 $\pm$ 0.92	6.27 $\pm$ 0.41
	<i>S. oralis</i>	1.79 $\pm$ 0.05	3.45 $\pm$ 0.03
	<i>S. mitis</i>	1.69 $\pm$ 0.30	3.08 $\pm$ 0.42
	<i>S. pyogenes</i>	N.D.	3.80 $\pm$ 0.62
	<i>L. salivarius</i>	7.34 $\pm$ 0.06	7.67 $\pm$ 0.12
	<i>L. oralis</i>	5.74 $\pm$ 0.05	5.69 $\pm$ 0.08
	<i>L. plantarum</i>	7.67 $\pm$ 0.08	7.65 $\pm$ 0.11
	<i>N. mucosa</i>	4.13 $\pm$ 0.46	5.09 $\pm$ 0.55
	<i>K. oxytoca</i>	8.66 $\pm$ 0.14	8.72 $\pm$ 0.13



**Table A2-2: Concentrations of IL-1 $\beta$ , IL-6, TNF- $\alpha$  and Rantes present in the co-culture medium of TR146 cells exposed to different oral microbial species (with a 4 h pre-incubation step for the microbiota). p-Values of the ANOVA analysis with Bonferroni correction for comparison of the data generated for control cells (TR146 cells exposed to an insert without microbiota) and the data obtained from TR146 cells that were co-cultured with different oral microbial species.**

	TNF- $\alpha$ (pg/mL)		IL-1 $\beta$ (pg/mL)		IL-6 (pg/mL)		Rantes (pg/mL)	
	mean $\pm$ SD	p-value	mean $\pm$ SD	p-value	mean $\pm$ SD	p-value	mean $\pm$ SD	p-value
<i>Control</i>	0.390 $\pm$ 0.184		4.450 $\pm$ 0.820		179.380 $\pm$ 22.882		61.720 $\pm$ 5.572	
<i>K. oxytoca</i>	0.435 $\pm$ 0.120	1.000	5.390 $\pm$ 0.240	1.000	133.745 $\pm$ 21.786	0.726	32.950 $\pm$ 6.590	0.070
<i>N. mucosa</i>	0.717 $\pm$ 0.046	0.065	5.853 $\pm$ 1.515	1.000	243.530 $\pm$ 30.689	0.192	65.370 $\pm$ 5.284	1.000
<i>S. salivarius</i>	0.460 $\pm$ 0.052	1.000	3.497 $\pm$ 0.823	1.000	114.287 $\pm$ 21.783	0.182	45.523 $\pm$ 11.336	0.416
<i>Control</i>	0.573 $\pm$ 0.215		5.570 $\pm$ 1.889		144.247 $\pm$ 35.721		83.333 $\pm$ 17.594	
<i>S. mitis</i>	0.530 $\pm$ 0.105	1.000	7.927 $\pm$ 1.033	0.187	88.623 $\pm$ 12.271	0.093	44.363 $\pm$ 9.016	0.020
<i>S. pyogenes</i>	0.257 $\pm$ 0.150	0.165	2.363 $\pm$ 0.387	0.063	179.157 $\pm$ 18.484	0.386	42.807 $\pm$ 4.516	0.016
<i>Control</i>	0.200 $\pm$ 0.089		4.800 $\pm$ 1.457		83.793 $\pm$ 9.326		59.413 $\pm$ 3.804	
<i>L. oralis</i>	0.347 $\pm$ 0.085	0.428	3.820 $\pm$ 0.339	1.000	78.247 $\pm$ 3.974	1.000	56.193 $\pm$ 3.563	1.000
<i>L. pyogenes</i>	0.200 $\pm$ 0.137	1.000	4.503 $\pm$ 0.811	1.000	87.053 $\pm$ 15.780	1.000	60.237 $\pm$ 7.383	1.000
<i>Control</i>	0.300 $\pm$ 0.220		6.200 $\pm$ 1.429		150.237 $\pm$ 33.858		69.740 $\pm$ 6.914	
<i>S. oralis</i>	0.317 $\pm$ 0.067	0.906	10.480 $\pm$ 0.469	0.008	126.847 $\pm$ 16.603	0.343	53.070 $\pm$ 2.363	0.017
<i>Control</i>	0.157 $\pm$ 0.023		1.843 $\pm$ 0.257		92.993 $\pm$ 19.647		48.657 $\pm$ 1.000	
<i>L. salivarius</i>	0.215 $\pm$ 0.064	0.407	2.673 $\pm$ 0.682	0.120	80.493 $\pm$ 10.583	0.387	32.373 $\pm$ 8.381	0.076

**Table A2-3: Results of the MALDI-TOF-analysis of the conditioned medium fraction < 3 kD of control cells (TR146 cells exposed to an insert without microbiota) and *K. oxytoca*-exposed cells. Presence (large peak: +; small peak: (+); absence (-)) of different peptides is shown together with the fraction in which these were found. One peptide was more abundant in the eluate of the *K. oxytoca*-conditioned medium (\*).**

Peptide	Control	Fraction	<i>K. Oxytoca</i>	Fraction
970.4	+	Drain	+	Drain
993	+	Washing step 50% MeOH	+	Washing step 50% MeOH Eluate
996.5	+	Eluate	(+)	Drain
1051	(+)	Eluate	-	
1158	+	Washing step 50% MeOH	+	Eluate
1165.6	+	Eluate	-	
1186.6	+	Drain	+	Drain
1208.5	+	Washing step 10% MeOH	+	Washing step 10% MeOH
1236.6	+	Washing step 10% MeOH Washing step 50% MeOH	+	Washing step 10% MeOH Eluate
1257.5	+	Washing step 50% MeOH	+	Washing step 50% MeOH Eluate
1279.6	(+)	Eluate	-	
1534.6	+	Washing step 50% MeOH	+	Eluate
* 1605.6	(+)	Washing step 50% MeOH Eluate	+	Eluate
1732	+	Washing step 50% MeOH	+	Washing step 50% MeOH



## CURRICULUM VITAE

---

Tine De Ryck was born on April 4, 1987 in Sint-Niklaas (Belgium). In 2005, she started a bioscience engineering education, where she received a Master's degree *Magna cum laude* in 2010, specialized in cell and gene biotechnology. During her education, she successfully performed an internship at ILVO (unit Plant), where she obtained practical experience in *in vitro* azalea plant cultures. For her master's thesis, she was involved in the search for new anti-invasive compounds, which resulted in several patented molecules. As this research is still ongoing, she further collaborated on this topic during her PhD. In 2010, she received the IE-price for one of the best master dissertations from young graduated engineering students.

In July 2010, she started her PhD (FWO-project) in search for the potential role of oral microbiota in the context of radiotherapy-induced oral mucositis at the Laboratory of Experimental Cancer Research. She presented her work on different national and international conferences and received the MASCC/ISOO Young investigator award in 2014. Furthermore, she guided 8 master students on different research topics. The results of this dissertation, together with the results from different collaborations are or will be published in peer reviewed international journals. In 2015, she also received the certificate of completing the Doctoral Training Programme at the Doctoral School of Life sciences and Medicine.



# SCIENTIFIC CURRICULUM VITAE

---

## Publications

- Vanhoecke B, De Ryck T, De boel K, Boterberg T, Wiles Siouxsie, Van de Wiele T, Swift S (2015). Effects of low dose irradiation on function behaviour of oral microbiota in the context of mucositis. *Accepted for publication in Experimental Biology and Medicine*.
- De Ryck T, Vanlancker E, Grootaert C, Roman B, De Coen LM, Vandenberghe I, Stevens CV, Bracke M, Van de Wiele T, Vanhoecke B (2015). Microbial inhibition of oral epithelial wound recovery: potential role for quorum sensing molecules? *AMB express* 5: 27.
- De Ryck T, Duprez F, Bracke M, Vanhoecke B, Van de Wiele T (2015). Dynamic shifts in the oral microbiome during radiotherapy. *Clinical research in infectious diseases* 2(1): 1013.
- De Ryck T, Boterberg T, Kerckhof FM, De Schrijver J, Bracke M, Van de Wiele T, Vanhoecke B (2015). Effects of irradiation on epithelial wound healing and microbial diversity in an in vitro oral mucosa model. *Journal of Nuclear Medicine & Radiation Therapy* 6: 218.
- Roman B, De Ryck T, Verhasselt S, Bracke ME, Stevens CV (2015). Further studies on anti-invasive chemotypes: an excursion from chalcones to curcuminoids. *Bioorganic & Medicinal Chemistry Letters* 25(5), 1027-1031.
- De Ryck T, Van Impe A, Vanhoecke BW, Heyerick A, Vakaet L, De Neve W, Müller D, Schmidt M, Dörr W, Bracke M (2015). 8-prenylnaringenin and tamoxifen inhibit the shedding of irradiated epithelial cells and increase the latency period of radiation-induced oral mucositis. *Strahlentherapie und Onkologie* 191 (5), 429-436.
- Vanhoecke B, De Ryck T, Stringer A, Van de Wiele T, Keefe D (2015). Microbiota and their role in the pathogenesis of oral mucositis. *Oral diseases* 21 (1), 17-30.
- Alava P, Du Laing G, Tack F, De Ryck T, Van de Wiele T (2015). Westernized diets lower arsenic gastrointestinal bioaccessibility but increase microbial arsenic speciation changes in the colon. *Chemosphere* 199, 757-762.
- De Ryck T, Grootaert C, Jaspert L, Kerckhof FM, Van Gele M, De Schrijver J, Van den Abbeele P, Swift S, Bracke M, Van de Wiele T, Vanhoecke B (2014). Development of an oral mucosa model to study host-microbiome interactions during wound healing. *Applied microbiology and Biotechnology* 98(15), 6831-6846.

- Marzorati M, Vanhoecke B, De Ryck T, Sadabad MS, Pinheiro S, Possemiers S, Van den Abbeele P, Derecke L, Bracke M, Pieters J, Hennebel T, Harmsen H, Verstraete W, Van de Wiele T (2014). The HMI module: a new tool to study the Host-Microbiota Interaction in the human gastrointestinal tract in vitro *BMC microbiology* 14, 133.
- Roman B, De Coen L, Mortier S, De Ryck T, Vanhoecke B, Katritzky A, Bracke M, Stevens C (2013). Design, synthesis and structure–activity relationships of some novel, highly potent anti-invasive (E)- and (Z)-stilbenes. *Bioorganic & medicinal chemistry* 21(17), 5054-5063.
- Roman B, De Ryck T, Dierickx L, Vanhoecke B, Katritzky A, Bracke M, Stevens C (2012). Exploration of the SAR of anti-invasive chalcones: Synthesis and biological evaluation of conformationally restricted analogues. *Bioorganic & medicinal chemistry* 20(15), 4812-4819.

## Posters & presentations

- Bacterial profiling of the oral community of head and neck cancer patient treated with radiotherapy (2014). De Ryck T, Duprez F, Bracke M, Van de Wiele T, Vanhoecke B. MASCC/ISOO International symposium on supportive care in cancer, Miami, USA.
- Host-microbioma crosstalk in cancer therapy (2014). De Ryck T, Vanlancker E, Boterberg T, Bracke M, Van de Wiele T, Vanhoecke B. MASCC/ISOO International symposium on supportive care in cancer, Miami, USA.
- Microbe-epithelial crosstalk in cancer therapy (2014). De Ryck T, Vanlancker E, Boterberg T, Bracke M, Van de Wiele T, Vanhoecke B. Knowledge for growth, Ghent, Belgium.
- Microbe-epithelial crosstalk in cancer therapy (2014). De Ryck T, Vanlancker E, Boterberg T, Bracke M, Van de Wiele T, Vanhoecke B. Oncopoint, Ghent, Belgium.
- Microbe-epithelial crosstalk in cancer therapy (2014). De Ryck T, Vanlancker E, Boterberg T, Bracke M, Van de Wiele T, Vanhoecke B. BACR (Belgian association for cancer research) Annual meeting, Zwijnaarde, Belgium.
- E-cadherin as a potential target in the fight against mucositis (2014). De Ryck T, Van Impe A, De Neve W, Vanhoecke B, Bracke M. BACR (Belgian association for cancer research) Annual meeting, Zwijnaarde, Belgium.
- Development of a multidisciplinary platform for the screening of new preventive and therapeutic drugs against mucositis (2013). Vanhoecke B, De Ryck T, Vanlancker E, Bowen J, Van de Wiele T, Keefe D. MASCC/ISOO International symposium on supportive care in cancer, Berlin, Germany.

Development of an *in vitro* model to study host-microbiome interactions in the oral cavity (2012). De Ryck T, Grootaert C, Bracke M, Van de Wiele T, Vanhoecke B. 17<sup>th</sup> symposium on applied biological sciences, Leuven, Belgium.

In vitro en in vivo studie van een nieuwe anti-invasieve component C16 tegen borstkanker (2010). De Ryck T. IE-prijzen 25 november 2010, Brussel, Belgium.



Oral mucositis is an important inflammatory side effect of radiotherapy in head and neck cancer patients resulting in a decreased quality of life, hospitalization and at worst in the interruption of the anticancer therapy. While the pathobiology of mucositis has already been extensively described, research on the potential role of the oral microbiota is still limited. This dissertation therefore focused on the host-microbe interactions in the context of oral mucositis by investigating the influence of irradiation on the microbiota both *in vitro* and in patients.